EFFECT OF METEOROLOGY AND TRANSPORT ON PARTICLE CONCENTRATIONS AND SIZE DISTRIBUTION IN EASTERN MEDITERRANEAN ATMOSPHERE

A THESIS SUBMITTED TO
THE GRADUATE SCHOOL OF NATURAL AND APPLIED SCIENCES
OF
MIDDLE EAST TECHNICAL UNIVERSITY

BY

ELİF SENA UZUNPINAR

IN PARTIAL FULFILLMENT OF THE REQUIREMENTS
FOR
THE DEGREE OF DOCTOR OF PHILOSOPHY
IN
ENVIRONMENTAL ENGINEERING

MARCH 2022

Approval of the thesis:

EFFECT OF METEOROLOGY AND TRANSPORT ON PARTICLE CONCENTRATIONS AND SIZE DISTRIBUTION IN EASTERN MEDITERRANEAN ATMOSPHERE

submitted by **ELİF SENA UZUNPINAR** in partial fulfillment of the requirements for the degree of **Doctor of Philosophy** i**n Environmental Engineering, Middle East Technical University** by,

Prof. Dr. Halil Kalıpçılar
Dean, Graduate School of **Natural and Applied Sciences** _____

Prof. Dr. Bülent İçgen
Head of the Department, **Environmental Engineering** _____

Prof. Dr. Gürdal Tuncel
Supervisor, **Environmental Engineering, METU** _____

Prof. Dr. İpek İmamoğlu
Co-Supervisor, **Environmental Engineering, METU** _____

Examining Committee Members:

Prof. Dr. Ayşegül Aksoy
Environmental Engineering, METU _____

Prof. Dr. Gürdal Tuncel
Environmental Engineering, METU _____

Prof. Dr. Gülen Güllü
Environmental Engineering, Hacettepe University _____

Assoc. Prof. Dr. Sema Yurdakul
Environmental Engineering, Süleyman Demirel University _____

Assist. Prof. Dr. Zöhre Kurt
Environmental Engineering, METU _____

Date: 25.03.2022

I hereby declare that all information in this document has been obtained and presented in accordance with academic rules and ethical conduct. I also declare that, as required by these rules and conduct, I have fully cited and referenced all material and results that are not original to this work.

Name Last name : Elif Sena Uzunpınar

Signature :

ABSTRACT

EFFECT OF METEOROLOGY AND TRANSPORT ON PARTICLE CONCENTRATIONS AND SIZE DISTRIBUTION IN EASTERN MEDITERRANEAN ATMOSPHERE

Uzunpınar, Elif Sena
Doctor of Philosophy, Environmental Engineering
Supervisor: Prof. Dr. Gürdal Tuncel
Co-Supervisor: Prof. Dr. İpek İmamoğlu

March 2022, 226 pages

This study aims to examine the relationship between particle sizes and processes in the atmosphere and the effect of dust transport on particle size distribution. Number (0.2 μm to 32 μm) and mass (PM_1, $PM_{2.5}$, and PM_{10}) concentrations were collected at rural (Mediterranean coast - Marmaris) and suburban (Central Anatolia - Ankara) stations between April 1, 2017, and October 31, 2018. The coarse particles were more dominant in the Ankara while the Marmaris contained relatively smaller-sized particles. The local source contribution was dominant at the suburban station and the effect of transported particles on the concentrations was masked. The effect of Eastern dust was observed at the suburban station. The seasonality shift in the Saharan dust episodes was observed as they occurred dominantly in winter. The rain events were only effective above $PM_{2.5}$, showing that they did not lower the effect of PM on human health. PMF analysis of rural station revealed five factors: sea salt, crustal, local anthropogenic, oil combustion, and regional combustion. Coarse particles were dominated by lithophile and chalcophile elements. Secondary inorganic ions, crustal material, and sea salt formed approximately 75% of PM_{10} mass. North African dust accounted for 55% - 76% of concentrations of lithophile elements, but only 26% of PM_{10} mass, due to sea salt and secondary ion contribution.

Keywords: Eastern Mediterranean, Size Distribution, Long-range Transport, Number Concentration, Trace Elements

ÖZ

DOĞU AKDENİZ ATMOSFERİNDE METEOROLOJİ VE TAŞINIMIN PARÇACIK KONSANTRASYONU VE BOYUT DAĞILIMI ÜZERİNE ETKİSİ

Uzunpınar, Elif Sena
Doktora, Çevre Mühendisliği
Tez Yöneticisi: Prof. Dr. Gürdal Tuncel
Ortak Tez Yöneticisi: Prof. Dr. İpek İmamoğlu

Mart 2022, 226 sayfa

Bu çalışma, partikül madde boyutları ile atmosferik prosesler arasındaki ilişkiyi ve toz taşınımının partikül madde boyutu dağılımı üzerindeki etkisini incelemeyi amaçlamaktadır. Sayısal (0.2 µm ile 32 µm arası) ve kütlesel (PM_1, $PM_{2.5}$ ve PM_{10}) PM konsantrasyonları, 1 Nisan 2017 ve 31 Ekim 2018 tarihleri arasında kırsal (Türkiye'nin Akdeniz kıyısı) ve banliyö (İç Anadolu) olmak üzere iki farklı istasyonda eş zamanlı olarak toplanmıştır. Ankara'da kaba parçacıklar daha baskınken, Marmaris nispeten daha küçük boyutlu parçacıklardan oluşmaktadır. Banliyö istasyonundaki yerel kaynak katkısının baskınlığı nedeniyle taşınan partiküllerin konsantrasyonlar üzerindeki etkisi maskelenmiştir. Banliyö istasyonunda Doğu yönlerden gelen tozunun etkisi gözlenmiştir. Ağırlıklı olarak yaz mevsiminde meydana gelen Sahra tozu olaylarında mevsimsel kayma gözlenmiş ve kış mevsimi baskın olmuştur. Yağmur olaylarının sadece $PM_{2.5}$ üzerinde etkili olduğu ve dolayısıyla PM'nin insan sağlığı üzerindeki olumsuz etkisini azaltmadığı gözlenmiştir. Kırsal istasyonun PMF analizi deniz tuzu, toprak, yerel antropojenik, petrol yanması ve bölgesel yanma olmak üzere beş faktörün varlığını ortaya koymuştur. Kaba partiküllere litofil ve kalkofil elementler hakimdir. İkincil

inorganik iyonlar, toprak elementleri ve deniz tuzu, PM_{10} kütlesinin yaklaşık %75'ini oluşturmaktadır. Kuzey Afrika tozu litofil elementlerinin konsantrasyonlarının %55-%76'sını oluştururken, deniz tuzu ve ikincil iyon katkısı nedeniyle, PM_{10} kütlesinin yalnızca %26'sını oluşturmaktadır.

Anahtar Kelimeler: Doğu Akdeniz, Boyut Dağılımı, Uzun Menzilli Taşınım, Sayısal Konsantrasyon, Eser Elementler

“A place where someone still thinks about you is a place you can call home.”

Jiraiya

ACKNOWLEDGMENTS

I wish to express my deepest gratitude to my supervisor Prof. Dr. Gürdal Tuncel and co-supervisor Prof. Dr. İpek İmamoğlu for their guidance, advice, criticism, encouragement, and insight throughout the research.

The technical and theoretical contributions of Mr. Amir Rahmani, Mr. Ömer Ateş, Assist. Prof. Dr. İlker Balcılar and Ms. Gizem Yücel at various stages of this research are gratefully acknowledged.

I would like to thank all my friends who went through this journey with me, supported me, and helped me in various and unexpected ways. As Itachi said, “However strong you become, never seek to bear everything alone. If you do, failure is certain”.

This work is partially funded by the Scientific and Technological Research Council of Turkey under grant number TUBİTAK 115Y252.

TABLE OF CONTENTS

ABSTRACT……..v

ÖZ vii

ACKNOWLEDGMENTS x

TABLE OF CONTENTS..... xi

LIST OF TABLES xv

LIST OF FIGURES xvi

LIST OF ABBREVIATIONS.....xix

CHAPTERS

1 INTRODUCTION 1

2 LITERATURE REVIEW 5

2.1 Definitions and Classifications of Atmospheric Aerosols 5

2.2 Impacts of Atmospheric Aerosols.....6

2.2.1 Human Health 6

2.2.2 Atmosphere and Climate.....7

2.3 Characteristic Properties of Atmospheric Aerosols 8

2.3.1 Chemical Composition.....8

2.3.2 Size and Size Distribution 10

2.4 Sources of Particulate Matter.....14

2.4.1 Natural Sources 14

2.4.2 Anthropogenic Sources 16

2.5 Removal Mechanisms.....17

2.6 Long-Range Transport.....18

2.6.1 Mediterranean Region and Dust Events.....19

3 MATERIALS AND METHODS 23
3.1 Experimental studies 23
3.1.1 Ankara and Marmaris Sampling Stations 23
3.1.2 Other Sampling Stations 25
3.1.3 Sample Collection and Measurements 27
3.2 Data Analysis 29
3.2.1 Data Quality Assurance/Quality Control (QA/QC) 29
3.2.2 Comparison of Ankara Laser Spectrometer Results with National Air Quality Measurement Network Result 35
3.3 Flow Climatology and Back trajectory Calculations 39
3.4 Cluster Analysis 42
3.5 Potential Source Contribution Function (PSCF) 43
3.6 Source Apportionment 44
3.6.1 Positive Matrix Factorization (PMF) 44
4 FACTORS AFFECTING PARTICLE NUMBER SIZE DISTRIBUTIONS AT AN URBAN AND A HIGH-ALTITUDE RURAL SITE AT THE ANATOLIAN PLATEAU 47
4.1 Introduction 47
4.2 Materials and Methods 50
4.2.1 Stations 50
4.2.2 Instrumentation 51
4.2.3 Quality Assurance / Quality Control (QA / QC) 51
4.3 Results and Discussions 56
4.3.1 Comparison of Particle Size Distribution in Both Stations 58
4.3.2 Flow Climatology 60

4.4 Conclusions 74

5 MODIFICATION OF SAHARAN DUST SIZE DISTRIBUTION DURING ITS TRANSPORT OVER THE ANATOLIAN PLATEAU 77

5.1 Introduction 77

5.2 Materials and Methods 79

5.2.1 Stations 79

5.2.2 Instrumentation and Data Validation 80

5.3 Results and Discussion 81

5.3.1 Data 81

5.3.2 Cluster Analysis 83

5.3.3 Dust Dynamics 91

5.3.4 Dust Climatology 97

5.3.5 Contribution of episodes on annual average PM_{10}, $PM_{2.5}$, and PM_1 concentrations 101

5.3.6 Variation of Particle Size Distribution During Transport 103

5.3.7 Effect of meteorology (rain and wind) on the number size distribution of particles 107

5.4 Conclusions 110

6 CHEMICAL COMPOSITION OF FINE AND COARSE PARTICLES AT AN HIGH-ALTITUDE STATION IN EASTERN MEDITERRANEAN: ASSESSMENT OF AEROSOL COMPONENTS AND THEIR SOURCE REGIONS 113

6.1 Introduction 113

6.2 Materials and Methods 117

6.2.1 Sampling 117

6.2.2 Analysis of Collected Samples 118
6.2.3 Quality Assurance / Quality Control (QA/QC) 119
6.3 Results and Discussion 120
6.3.1 Data 120
6.3.2 Coarse-to-Fine Ratio 121
6.3.3 Comparison with Literature 127
6.3.4 Flow Climatology 128
6.3.5 Cluster Analysis 130
6.3.6 Seasonal Variations 135
6.3.7 Positive Matrix Factorization 137
6.4 Conclusions 143
7 CONCLUSIONS 147
8 OVERVIEW 151
9 RECOMMENDATIONS 155
REFERENCES 157
APPENDICES
A. Factors Affecting Particle Number Size Distributions at An Urban and A High-Altitude Rural Site at The Anatolian Plateau 201
B. Modification of Saharan Dust Size Distribution during Its Transport over the Anatolian Plateau 212
C. Chemical Composition of Fine And Coarse Particles at An High-Altitude Station In Eastern Mediterranean: Assessment Aerosol Components and Their Source Regions. 218
D. Summary Statistics of the Measured Data 223
CURRICULUM VITAE 225

LIST OF TABLES

TABLES

Table 2.1 Characteristic elemental composition of atmospheric PM with respect to its emission sources 10
Table 3.1 MDL and Blank sample concentrations for ED–XRF analysis 30
Table 3.2 Average PM_1, $PM_{2.5}$, and PM_{10} concentrations with different devices (µg m^{-3}) 33
Table 3.3 Mean and Median concentrations measured at Suburban, Bahçelievler, and Sıhhıye stations 38
Table 4.1 Average PM_{10} and $PM_{2.5}$ concentrations measured at regulatory stations and Ankara station used in this study. 54
Table 4.2 Summary statistics for PM fractions (µg m^{-3}), Al, and Si (ng m^{-3}) at Marmaris and Ankara stations 57
Table 5.1 Summary statistics of PM_1, $PM_{2.5}$, PM_{10}, Al, and Si concentrations 83
Table 5.2 Median concentrations of particle mass fractions in each cluster. 90
Table 5.3 Average PM_{10}, $PM_{2.5}$, and PM_1 concentrations at Ankara and Marmaris stations during dust and non-dust periods. Concentrations are in (µg m^{-3}) 94
Table 5.4 Monthly distribution of episodes and their durations. 100
Table 5.5 Contribution of episodes to PM_{10}, $PM_{2.5}$, and PM_{10} average concentrations 103
Table 5.6 Dates and durations of common episodes observed in both stations 104
Table 6.1 Summary statistics for coarse, fine, and PM_{10} data. Numbers in parenthesis are median concentrations of elements. Concentrations are in ng m^{-3}. 120
Table 6.2 Coarse-to-fine concentration ratios and enrichments of elements in coarse and fine fractions relative to soil composition 122
Table 6.3 Median PM_{10} concentrations of elements in each cluster (concentrations of elements are in ng m^{-3}, except for mass which is in µg m^{-3}) 134

LIST OF FIGURES

FIGURES

Figure 2.1 Modal particle size distribution (Araujo & Nel, 2009) 12
Figure 2.2. Typical number and volume distributions of atmospheric particles as a function of different modes (Seinfeld & Pandis, 2006). 13
Figure 3.1 Map showing suburban sampling station at METU Department of Environmental Engineering. 24
Figure 3.2 Map of rural sampling station at Marmaris. 25
Figure 3.3 Map of Ankara national air quality monitoring stations (red markers) in relation to the suburban station at Ankara (yellow marker). 26
Figure 3.4 Map of Marmaris meteorological stations in relation to the rural station at Marmaris. 27
Figure 3.5 Comparison of number concentrations measured by two laser spectrometers used in the study. 32
Figure 3.6 Comparison of sampling efficiency of different devices 34
Figure 3.7 Comparison of METU station measurements with Bahçelievler and Sıhhiye stations 36
Figure 3.8 The correlation between PM_{10} and $PM_{2.5}$ concentrations measured at Suburban station and Dikmen and Demetevler national stations 39
Figure 3.9 Study area for residence time analysis 41
Figure 4.1 Map showing locations of suburban and rural stations 51
Figure 4.2 Median number size distributions measured in both station 59
Figure 4.3 Residence times of back trajectories in each $1^o x 1^o$ grid in the study region computed for rural and suburban stations. Trajectory segments from trajectories with all starting altitudes were combined. 62
Figure 4.4 Summer – winter difference in residence times of air masses in the study domain at Marmaris station. (a) for 100 m starting altitude, (b) for 500 m starting altitude, and (c) for 1500 m starting altitude. 64
Figure 4.5 Binary correlations between hourly PM size fractions at both stations 65

Figure 4.6 1-min, 1-hour, and 24-hour averaged PM_{10} concentrations at Marmaris and Ankara stations, in April 2018. 68
Figure 4.7 Monthly variations of particle size fractions at Marmaris and Ankara stations. 70
Figure 4.8 Diurnal variation in number and mass concentrations at different size fractions in both stations. PM_1, $PM_{2.5}$ and PM_{10} concentrations in Figures (a) and (c) are mass concentrations. The particle concentrations in different size bins in Figures (b) and (d) are number concentrations in (# L^{-1}). 72
Figure 5.1 Locations of stations. 80
Figure 5.2 Cluster centroids at (a) suburban (Ankara) and (b) rural (Marmaris) stations 86
Figure 5.3 Average median particle mass size distributions in each cluster at (a) suburban (Ankara) and (b) rural (Marmaris) stations. Inner graphs are same plots prepared in logarithmic y-scale 88
Figure 5.4 Variation of PM_{10}-to-PM_1 ratio with PM_{10} concentration in both stations. 95
Figure 5.5 Particle number size distributions for dust and non-dust days at the suburban (Ankara) and the rural (Marmaris) stations 97
Figure 5.6 (a) DREAM model, (b) Back-trajectories, and (c) AOD for a common episode (June 28, 2018) as an example 105
Figure 5.7 Particle number size distributions measured at rural and suburban stations in each of the common dust episodes (a-f) 108
Figure 5.8 Effect of rain on the number size distribution of particles at the rural (Marmaris) and the suburban (Ankara) stations 109
Figure 5.9 Effect of wind speed on the number size distribution of particles at the rural (Marmaris) and the suburban (Ankara) stations 110
Figure 6.1 EF_c – Al diagrams for selected elements 126
Figure 6.2 Concentrations of elements measured in this work and other locations in Turkey 127

Figure 6.3 Annual and seasonal air mass flow frequencies from each wind sector 129
Figure 6.4 Centroids of back trajectory clusters arriving at Marmaris station. Trajectories calculated for the entire study period are used in cluster analysis 130
Figure 6.5 Distribution of trajectory segments with z < 500 m 133
Figure 6.6 Monthly median concentrations of selected elements at Marmaris station 136
Figure 6.7 Factor composition, fractions of elements explained by each factor crustal enrichment factors of elements in factor, monthly average factor scores and distribution of PSCF values for Factor 3 139
Figure 6.8 Factor composition, fractions of elements explained by each factor crustal enrichment factors of elements in factor, monthly average factor scores and distribution of PSCF values for Factor 5. 142

LIST OF ABBREVIATIONS

AI: Aerosol Index

ANAEM: Ankara Atomic Research and Training Center

AOD: Aerosol Optical Depth

AQM: Air Quality Monitoring Network Stations

ASL: Above Sea Level

CCN: Cloud Condensation Nuclei

CLRTAP: Convention on Long-range Transboundary Air Pollution

ED-XRF: Energy Dispersive X-ray Fluorescence

EFc: Enrichment Factors

GBD: Global Burden of Disease

HYSPLIT: Hybrid Single-Particle Lagrangian Integrated Trajectory

IPCC: Intergovernmental Panel on Climate Change

MDL: Method Detection Limit

METU: Middle East Technical University

MGM: Turkish State Meteorological Services

MODIS: Moderate Resolution Imaging Spectroradiometer

MoEUCC: Ministry of Environment, Urbanization and Climate Change

NIST: National Institute of Standards and Technology

NOAA: U.S. National Oceanic and Atmospheric Administration

PM: Particulate Matter

PMF: Positive Matrix Factorization

PSCF: Potential Source Contribution Function

QA/QC: Quality Assurance/Quality Control

SFU: Stack Filter Unit

SOA: Secondary Organic Aerosols

SRM: Standard Reference Materials

TRMSD: Total Root Means Square Deviation

TSP: Total Suspended Particles

WHO: World Health Organization

CHAPTER 1

INTRODUCTION

Earth's atmosphere is a complex mixture consisting not only of permanent gases but also of water vapor, solid and liquid phase components. Aerosols are defined as suspended particles together with the gases surrounding them, while particulate matter (PM) refers only to the suspended solid or liquid matter. PM naturally exists in the environment as a result of rock and soil erosion, sand carried by the wind, volcanic fumes, and smoke from naturally occurring forest fires (Gatti & Montanari, 2015). Anthropogenic PM became part of the atmosphere mainly as a result of advancements in combustion processes. The use of fuel for industrial and domestic energy needs, non-industrial fugitive sources, and transportation are currently the major anthropogenic PM sources (Seinfeld & Pandis, 2006).

PM is associated with increases in morbidity and mortality rates, as well as with many factors that impair and reduce environmental quality, such as visibility degradation and acid rain. The particle size of PM is a critical physical property in terms of visibility, Earth's radiation, and energy balance. With increasing concentrations, aerosols pose a serious health hazard to humans as well. It has been shown in many studies that the health effects of submicron particles ($D_p < 1.0$ μm) are much greater than those of larger particles (K.-H. Kim et al., 2013; Oberdorster et al., 1994; Zwozdziak et al., 2016).

Pollutants, including PM, can travel hundreds to thousands of kilometers away from their sources and contribute to pollution at their final destination. Improved understanding of the transboundary movement of pollutants in the atmosphere led to the creation of the Convention on Long-range Transboundary Air Pollution (CLRTAP) in 1979. This treaty requires effective monitoring of pollutants. An integrated monitoring network contributes to building a broad body of knowledge

for the identification of pollutant sources and, perhaps more importantly, for a thorough understanding of the physical and chemical properties of pollutants. This, eventually, can lead to the enactment of proper regional and international policies.

Current regulatory standards are based on the mass concentration of particles. In recent years, it has been argued that standards based on numerical concentrations of particles are more appropriate because they represent submicron particles better (Manigrasso et al., 2019; Pacitto et al., 2020). The Mediterranean region is important in terms of atmospheric aerosol studies as it is influenced by air masses carrying both anthropogenic and natural particle emissions. The basin is subject to high anthropogenic particle loading from metropolitan cities in Europe, Turkey, and the Middle East, desert dust from the Sahara and the Middle East in the eastern part of the basin, and marine particles from the Mediterranean (Güllü et al., 2000; Mustafa Koçak et al., 2009; Koulouri et al., 2008; Moatti & Thiébault, 2016; J. Pey et al., 2013). Studying the region for the chemical and physical composition of PM has created a database for Mediterranean particle composition. However, it is observed that the particles are transformed in terms of not just their concentrations but also their size and composition during their journey taking hundreds to thousands of kilometers. Therefore, a comprehensive understanding of sources, composition, size, and transformation of particles is essential.

This is the first study in Turkey that focuses on particle number concentration measurements. Particle number concentrations will be measured at 32 different size channels along with mass measurements of PM_{10}, $PM_{2.5}$, and PM_1 at two different stations with rural (Marmaris) and suburban (Ankara) characteristics. Measurement of trace element concentrations and apportionment of sources in this work at Ankara will allow an assessment of the long-term variation in both concentrations of elements and their sources. Knowing the sources and their locations at Marmaris will also be very informative about long-term variation in concentrations of these parameters. Atmospheric concentrations of anthropogenic elements and ions are decreasing in most of Europe (Beloconi & Vounatsou, 2021; Colette & Ineris, 2020). Although emission reduction policies will continue to decrease $PM_{2.5}$ concentrations,

future scenarios showed that Mediterranean PM_{10} will not decrease since it is dominated by dust and salt concentrations (Cholakian et al., 2019). Studies in the literature also suggest that, depending on the future land-use scenarios, dust concentrations in the region can decrease or increase (Cholakian et al., 2019; Tegen et al., 2004; Woodward et al., 2005). In the previous studies, a similar decrease was not demonstrated in the Eastern Mediterranean atmosphere.

Overall, the high-resolution data set generated in this study will (i) be the first data generated at a high-altitude station in Eastern Mediterranean, (ii) show if the decreasing trend has started in Eastern Mediterranean as well, (iii) contribute greatly to deposition and transportation studies, (iv) provide valuable data on the trace element measurements in the PM_1 size range, and (v) reduce the uncertainties in the understanding of the changes in the particle concentrations with atmospheric processes.

This study aims to:

1. Examine the particle concentrations and size distributions in the Eastern Mediterranean region
2. Examine the flow climatology of the Eastern Mediterranean region
3. Demonstrate how the size distributions of particles change during dust transport
4. Examine the relationship between particle size and wind speed and rain
5. Determine the sources and/or source regions contributing to PM_{10} concentrations at the rural station

This dissertation is organized as a collection of manuscripts of which portions have been submitted for publication, or are prepared to be submitted for publication. Apart from these, the dissertation also includes a literature review, a methodology presenting in detail the methods used for the collection and analysis of PM samples,

and the analysis to understand the changes in the characteristics and behaviors of the measured PM, concluded by an overview and recommendations chapters. Please note that some repetition may appear between the introduction and methodology sections of relevant chapters.

CHAPTER 2

LITERATURE REVIEW

2.1 Definitions and Classifications of Atmospheric Aerosols

Atmospheric aerosols are small-sized liquid or solid particles that are found suspended in the air. Aerosol particles vary significantly in size, source, chemical composition, amount, and distribution in space and time, and in terms of how long they survive in the atmosphere. In general, aerosols can be grouped into three size ranges as Aitken (0.01 – 0.1 μm), accumulation mode (0.1 – 1 μm), and coarse mode (> 1 μm) (Araujo & Nel, 2009). Aitken and accumulation mode particles can be grouped as fine particulate matter (PM).

The chemical composition of atmospheric aerosols is dependent on the source of emission and mostly includes elemental (black) carbon, organic carbon, inorganic ionic species such as NH_4^+, SO_4^{2-}, and NO_3^-, and trace elements. Sources of atmospheric aerosols are generally divided into two as natural and anthropogenic (man-made) sources. These sources can be further grouped based on their geographical location as marine and continental sources. Last but not least, formation mechanisms (primary and secondary) of aerosols are used as a classification method as well. Primary aerosols are directly injected into the atmosphere from their sources, while secondary aerosols are formed in the atmosphere from primary aerosols via gas-to-particle conversion mechanisms (U.S. EPA, 2014).

2.2 Impacts of Atmospheric Aerosols

2.2.1 Human Health

According to the air pollution model results of the World Health Organization (WHO), 92% of the world's population lives under air quality which poses health risks because WHO limit values are exceeded (WHO, 2016). Atmospheric aerosols are listed among the priority pollutants that have adverse impacts on human health due to their association with various cardiovascular diseases. Global Burden of Disease (GBD) study estimates showed that ambient air pollution was the cause of 4.2 million deaths in 2015 (Landrigan et al., 2017). In the GBD report, it is also stated that the $PM_{2.5}$ related deaths showed a 20% increase (from 3.5 million to 4.2 million) between 1990 and 2015. Future mortality predictions estimated a 50% increase in death between 2015 and 2050 with 6.6 million deaths if no new pollution control measures are applied (Landrigan et al., 2017).

The most important property of PM while defining and dealing with its health effects is the aerodynamic diameter of the particle. The deposition of PM in the human respiratory tract is highly dependent on the size of particulates. Particles that are larger than 10 μm are scavenged from the atmosphere easily through wet and/or dry deposition. They are also captured in the upper respiratory system, so, their health impacts are considerably low. On the other hand, particles in the 2.5 μm size fraction (fine particles) can deposit in the tracheal and bronchial region, be transported, and reach the gastrointestinal tract (Elmes & Gasparon, 2017). These fine particles can also reach the alveolar region and interact with lung fluids (Asgharian et al., 2001). Particles in the 0.1 μm size fraction (ultrafine particles) can even reach the bloodstream due to their capacity to pass the alveolar epithelium (Oberdörster et al., 2005). Awareness of the impacts of these ultrafine particles has increased as their enhanced inflammatory potential and higher deposition efficiency within the pulmonary system are discovered (Elmes & Gasparon, 2017).

Short and long-term exposure to PM has proven to cause allergies, respiratory and cardiovascular diseases, and premature mortality (Agudelo-Castañeda et al., 2017). In addition to the size of the PM, the chemical composition is also important for health effects. Heavy metals, such as Pb, Hg, Cd, and As, that are found in PM emissions can cause various health problems. For example, Pb can cause neurological diseases, anemia, and kidney failure while As can cause skin, liver, and lung cancer, and irritation in the upper respiratory tract (Çelik, 2014). Moreover, several studies have linked V, Fe, Zn, Ni, Mn, and Cu metals to several health problems such as cardiovascular diseases, non-fatal heart attacks, aggravated asthma, and lung cancer.

2.2.2 Atmosphere and Climate

Atmospheric aerosols with different chemical compositions scatter and absorb light rays and cause a reduction in visibility. Such scattering and absorption of light are called the direct effect of aerosols on the atmosphere. Visibility degradation is one of the most prominent impacts of PM on the atmosphere. As the concentration of aerosols increases in the atmosphere, the level of reduction in visibility increases as well (Liu et al., 2013). Fine PM is considered the primary cause of visibility degradation (Malm, 1999; H. Zhao et al., 2013).

The indirect effect of aerosols is observed when the increase in aerosol number concentrations from anthropogenic sources increases the concentrations of cloud condensation nuclei (CCN). As CCN increases, the formation of clouds with larger number concentrations of droplets that have smaller radii is enhanced. This, as a result, leads to higher cloud albedos (Seinfeld & Pandis, 2006). The cloud albedo represents the portion of solar radiation reflected back to space by clouds. It has a significant role in the energy budget of the Earth and changes in the cloud albedo effect can have a major impact on the regional and global climate (Müller et al., 2011). Although the overall effect of clouds on the climate system is uncertain, it is

known that increase in the cloud albedo results in negative forcing, hence a cooling effect on the climate (P. M. Forster et al., 2021).

2.3 Characteristic Properties of Atmospheric Aerosols

2.3.1 Chemical Composition

The chemical composition of PM is highly dependent on the geographical location (i.e., marine, continental, rural, industrial, polar, desert, etc.) and the sources present in those regions. Determination of chemical composition is used during source apportionment studies where the major sources of measured PM concentrations and their contributions are determined through source or receptor-based methodologies (Argyropoulos et al., 2012; Tecer et al., 2012; Titos et al., 2014; Viana et al., 2008; Yao et al., 2016).

Trace metals, or elements, are among the most characteristic chemical species associated with PM emissions. Most trace elements are emitted into the atmosphere from their sources (natural or anthropogenic) on PM and remain on the particles during their transport to remote areas. Because of this conservative behavior of trace elements, they can be measured at any size fractions (Kulkarni et al., 2007) and used as natural tracers to identify sources of pollution (Güllü et al., 2000; Valotto et al., 2014; Yatin et al., 2000). Depending on the ratio of each trace element in aerosols, they can be attributed to their natural or anthropogenic origins.

Natural mineral dust also shows differences in composition depending on the location of emission sources. Mineral dust mostly consists of Fe (iron), Al (aluminum), Si (silicon), Ca (calcium), K (potassium), and Mg (magnesium) elements (I. F. Al-Momani et al., 2008; Argyropoulos et al., 2012; Çelik, 2014; Saltzman, 2013). These elements are enriched in coarse size mode (Saltzman, 2013). The composition of marine PM (sea salt) emissions generally includes Na, Cl, Mg,

K, Ca, Br, and SO_4^{2-} ions (Çelik, 2014; Choi et al., 2011; Heintzenberg et al., 2000; Saltzman, 2013).

Natural forest fires include different types of gases and PM. However, the content of emissions mostly includes organic carbon and black carbon, and incomplete combustion products (Çelik, 2014; Hobbs, 2000). Finally, volcanic dust particles are rich in Fe (iron) and Mg (magnesium) ions in terms of PM. SO_2 is also released as gas from volcanoes. Therefore, S (sulfur) is another important element originating from volcanic emissions.

Motor vehicle emissions consist mostly of black carbon soot. Nitrogen oxides and hydrocarbons and carbon monoxide from incomplete combustion are other important emissions of motor vehicles. Depending on the fuel type (i.e., diesel or gasoline), the number of particulate emissions shows variations. Diesel fuels are found to be releasing more PM compared to other fuel types (Calvo et al., 2013; Kittelson, 1998). Table 2.1 lists the natural and anthropogenic sources of aerosols and their characteristic elemental emissions. Road transport can be grouped under different categories as direct emissions from fuel combustion (Br, Pb, Ba) (Morawska and Zhang, 2002), diesel fuel (Al, Ca, Cu, Fe, Mg, Mn, V, Zn) (Sanderson et al., 2014), and other emissions resulting from wearing in breaks (Cr, Fe, Cu, Zn, Zr, Mo, Sn, Sb, Ba, Pb) (Harrison et al., 2021; Wåhlin et al., 2006), and tires and road (Al, Si, K, Ca, Ti, Mn, Fe, Zn, Sr) (Wåhlin et al., 2006). Resuspension of road dust can also be considered as a separate source and its composition includes EC (elemental carbon), Mg, Ca, Si, Al, Fe, Ti, and Mg trace elements (Harrison et al., 2021; Morawska and Zhang, 2002).

The composition of emissions from industrial facilities might show huge variations depending on the type of industry. For example, coal combustion facilities emit elements such as Se, As, Cr, Co, Cu, Al, S, Pa and Ca (Morawska and Zhang, 2002). Iron and steel manufacturing plants emit Fe, S, Na (coke-making), K and Pb (sintering), S, Fe, Na, K and Ni (cold forming), and Zn (all processes) (Tsai et al.,

2007), while oil-fired power plants emit Ni and V in the majority (Morawska and Zhang, 2002).

Table 2.1 Characteristic elemental composition of atmospheric PM with respect to its emission sources

Emission Source	Characteristic Elemental Emissions	Reference
Motor Vehicle Emission	Br, Pb, Ba	Morawska and Zhang (2002)
Diesel Fuel	Al, Ca, Cu, Fe, Mg, Mn, V, Zn	Sanderson et al. (2014)
Fuel Oil	V, Ni	Morawska and Zhang (2002); Park and Kim (2005)
Break Wear	Cr, Fe, Cu, Zn, Zr, Mo, Sn, Sb, Ba, Pb	Harrison et al. (2021); Wåhlin et al. (2006)
Road and Tire	Al, Si, K, Ca, Ti, Mn, Fe, Zn, Sr	Wåhlin et al. (2006)
Resuspension	Mg, Ca, Si, Al, Fe, Ti, Mg, EC	Harrison et al. (2021); Morawska and Zhang (2002)
Crustal Elements	Mg, Ca, Al, K, Sc, Fe, Mn	Morawska and Zhang (2002); Waheed et al. (2011)
Incinerators	Zn, Sb, Cu, Cd, Hg, K, Pb, Mn, K	Morawska and Zhang (2002); Park and Kim (2005)
Coal Combustion	Se, As, Cr, Co, Cu, Al, S, Pa, Ca	Morawska and Zhang (2002)
Iron and Steel Plants	Fe, S, Na, K, Pb, Ca, Ni	Tsai et al. (2007)
Sea Spray	Na, Cl, S, K	Morawska and Zhang (2002)

2.3.2 Size and Size Distribution

The size of particles in the atmosphere is one of the most important parameters that determine the chemical composition, optical properties, deposition, and inhalation

of particles (Mihalis Lazaridis & Drossinos, 2014). PM can be found in different sizes in the atmosphere ranging between 0.001 μm and 100 μm in diameter (Hinds, 1999; Mihalis Lazaridis & Drossinos, 2014). As PM can be found in many different shapes in the atmosphere as well, these sizes represent the aerodynamic diameter. The aerodynamic diameter is the diameter of the spherical body with a density of 1 gr cm^{-3} and has the same equivalent velocity of settling as the real particle under consideration (Hinds, 1999).

PM in the atmosphere can be classified based on their size under three major categories (Mihalis Lazaridis & Drossinos, 2014):

- modal distribution
- 50% cut-off diameter of the measurement instrument
- dosimetric variables related to human exposure studies

These classifications are application-specific. The second and third categories are self-explanatory as one is based on the specifications of the measurement device, while the other is based on the effect on human health. In the first category, some sub-categories, as shown in Figure 2.1, can be defined (Lazaridis & Drossinos, 2014):

- *Nucleation mode:* This category includes particles with a diameter less than 0.1 μm which are formed by nucleation processes.
- *Aitken mode:* This mode includes particles with a size range of 0.01 μm – 0.1 μm. Particles are formed by either vapor nucleation or the growth of preexisting particles as a result of condensation.
- *Accumulation mode:* This mode includes particles with a size range of 0.1 μm – 1 to 3 μm. The mechanisms that are taking place are coagulation of smaller particles or condensation of vapor constituents.
- *Ultrafine:* A combination of Aitken and nucleation mode particles forms this category.

- *Fine:* In this sub-category, particles with diameters less than 2 μm are present.
- *Coarse:* In this sub-category, particles with diameters greater than 2 μm are present.

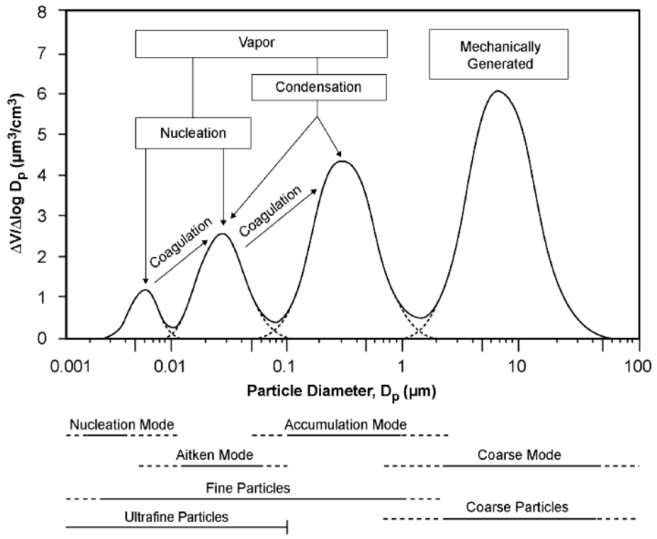

Figure 2.1 Modal particle size distribution (Araujo & Nel, 2009)

Size distribution of particulates can provide valuable information related to their sources, formation mechanisms, and behavior. Atmospheric particle size distributions generally follow a lognormal distribution. If we look at the relationship between the size distribution and formation mechanisms, it can be seen that fine size range is mostly formed from gases via chemical reactions, nucleation, condensation, and coagulation. Therefore, Aitken and accumulation mode particles are secondary particles. The formation of coarse particles, on the other hand, is due to mechanical disruption and suspension of dust, hence they are primary particles (Wilson & Suh, 1997). As the size of the particulate increases, its residence time in the atmosphere decreases. Although these coarse particles are more effective in light scattering, due to their short residence time, they are rapidly removed from the atmosphere (Raes et al., 2000). The particles in the Aitken mode (dp < 0.01 μm) also have a very short

residence time in the atmosphere. The rapid coagulation potential of the particles in this size range enables rapid removal from the atmosphere.

Nitrates, sulfates, ammonia, and inorganic and organic carbon are abundant in the $PM_{2.5}$ fraction. Trace elements that are predominantly found in fine and ultrafine size ranges are V, Cr, Mn, Zn, Se, Pb, Ni, Cd, Pt, Pd, and Rd (Spurny, 2000). In the coarse mode, particles are formed via mechanical processes, and soil dust, sea salt, fly ash, tire wear particles, and pollen are abundant (Lazaridis & Drossinos, 2014; Seinfeld & Pandis, 2006).

If the focus is shifted to the number and volume (or mass) distributions, different modes of distribution are obtained (Figure 2.2). The upper part of Figure 2.2 demonstrates the size distribution based on the number of particles in each size range. The number of particles becomes insignificant for particle sizes greater than 0.1 μm. However, as it can be seen from the lower part of the figure, this size range is very dominant when the distribution is based on the volume (or mass) of particles.

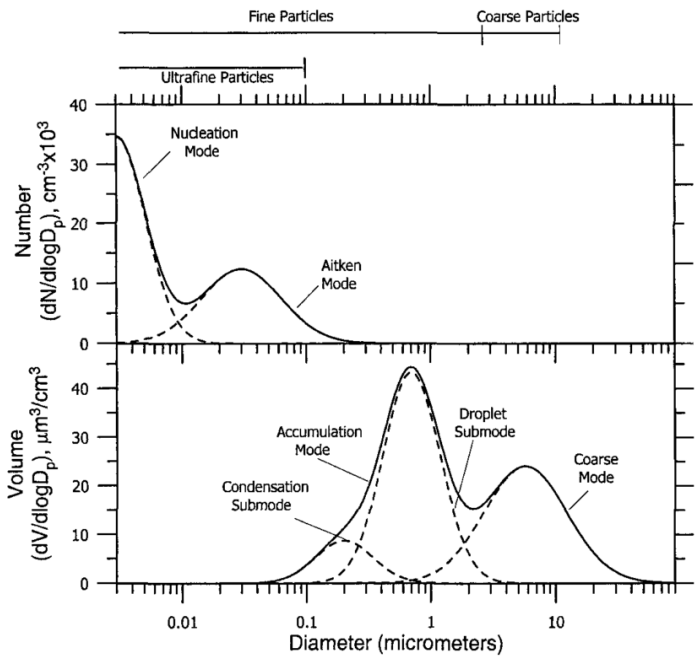

Figure 2.2. Typical number and volume distributions of atmospheric particles as a function of different modes (Seinfeld & Pandis, 2006).

Particle size (diameter) determines the impact of these particles on human health as well. In general, the health impacts of particles increase as their sizes get smaller. Since smaller particles have more chance to pass the upper respiratory tract and reach the lungs compared to larger particles, they are more hazardous to health (Guevara, 2016; Spurny, 2000). As the size has an impact on the composition of the particles, it also has an impact on their toxicity and health impacts. Lastly, visibility and energy budget issues are all size-dependent and the effects of PM on health, visibility degradation, and the energy budget of the Earth will be discussed in the following sections in more detail.

2.4 Sources of Particulate Matter

PM found in the atmosphere can be originating from both natural and anthropogenic sources. Various physical, chemical, and biological processes take place during the formation of these compounds. Source types can also be further divided as primary (directly emitted into the atmosphere as liquids or solids) and secondary sources (formed in the atmosphere). Dust released from roads and elemental and/or black carbon released during combustion processes (mostly coarse particles) are examples of primary particles (U.S. EPA, 2011). The formation of sulfate from sulfur dioxide emissions and nitrates from nitrogen oxides are examples of secondary particles (U.S. EPA, 2011). During the formation of particles in the atmosphere (secondary) following mechanisms can take place: nucleation, condensation of gases (gas-to-particle conversion), and reactions of dissolved substances in cloud droplets (Lazaridis & Drossinos, 2014).

2.4.1 Natural Sources

The primary natural sources of PM are soil (mineral dust), sea salt, natural forest fires, and volcanoes (Çelik, 2014; Vallius, 2005). These sources are also examples of primary natural emission sources. Mineral dust is mostly emitted from arid and

semi-arid regions through soil erosions, dust storms, and resuspension of soil particles (İ. Balcılar, 2018; EEA, 2012). Sahara-Sahel region from northern Africa is considered as the largest global source of dust emissions while central Asia is the second (Seinfeld & Pandis, 2006).

Mineral dust forms a significant portion of naturally emitted particles. According to Zender et al. (2004), almost half of the total global emissions are formed by mineral dust. However, mineral dust can also include an anthropogenic portion due to changes in land surface usage (overgrazing, deforestation, unpaved roads, etc.), human-induced droughts, and climate variability (Choobari et al., 2014). Although it is not possible to determine the anthropogenic contribution exactly, it is estimated to be around 25% of total dust emissions (Ginoux et al., 2012).

Sea salt, or sea-spray aerosols, is the second type of natural particulate source. Almost 1000 to 5000 Tg of aerosols are produced annually by the oceans (Hobbs, 2000). This type of aerosol is formed through bubble-bursting of the sea sprays and tearing of the waves by winds.

Natural forest fires are becoming a serious global threat to air quality due to various types of emissions such as carbon and black carbon, smoke, gaseous emissions, and fine and coarse particulate matter (Sannigrahi et al., 2022). Natural forest fires typically occur due to climate change and factors related to that such as dry spells, lack of soil moisture, and rising temperatures. Such fires are generally induced by lightning and can have short and long-range impacts through atmospheric transport processes (Lazaridis et al., 2008). Almost 200 to 450 Tg of aerosols are injected into the atmosphere annually through this source (Hobbs, 2000).

Volcanic dust particles are the final form of natural sources of aerosol emissions. Volcanoes both emit gases and particles into the atmosphere. Although larger particles are easily removed from the atmosphere, small ones can be transported around the globe as they may reach the stratosphere depending on the emission rate (Hobbs, 2000). Similarly, gases can be converted into particles via nucleation and

condensation processes (Lazaridis & Drossinos, 2014) once they are injected into the atmosphere.

2.4.2 Anthropogenic Sources

The introduction of human-made aerosols into the atmosphere constitutes almost 25% of emissions from natural sources (Ginoux et al., 2012). Emissions from anthropogenic sources are mainly the result of activities such as fuel combustion, industrial processes (cement production, construction, use of blast furnaces, etc.), non-industrial fugitive sources (roadway dust from paved and unpaved roads, wind erosion of cropland, construction, etc.) and transportation (Seinfeld & Pandis, 2006). Domestic activities in developing countries are a significant contributor to aerosol emissions. Intentional stubble burning can also be grouped under this category. It forms almost 25% of the total biomass emissions (forest fires included) globally (Abdurrahman et al., 2020). According to Karagulian et al. (2015), the contribution of different sources to urban $PM_{2.5}$ emissions globally are as follows: traffic (25%), industrial activities (15%), domestic fuel burning (20%), unspecified sources of human origin (22%) and natural dust and salt (18%).

Emissions from road traffic can be categorized as exhaust pipe emissions and non-exhaust pipe emissions. These categories have almost equal contributions to traffic-related PM emissions (Querol et al., 2004; Thorpe & Harrison, 2008). Emissions from the exhaust pipe of vehicles are the main source of aerosols from traffic in urban areas (Calvo et al., 2013). The composition and the number of aerosols released from exhaust emissions vary based on the fuel type, whether it is diesel or gasoline. Non-exhaust emissions include tire and brake wear, abrasion on the road surface, and resuspension of road dust (Calvo et al., 2013; Thorpe & Harrison, 2008).

Numerous different industrial activities release atmospheric particles or precursor gases. Industrial activities are a major source of PM in the atmosphere. Main contributors to industrial PM emissions can be listed as manufacturing (automotive,

steel, and metal-making included), aerospace, agriculture, chemical, construction, and energy (Taiwo et al., 2014).

Domestic fuel burning includes both cooking and residential heating activities. During such activities, the combustion of wood, coal, and gas results in the emission of PM.

2.5 Removal Mechanisms

Removal of dust particles from the atmosphere occurs through dry and wet deposition processes. Dry deposition refers to the removal of the particles from the atmosphere via non-precipitation mechanisms such as gravitational settling, molecular and turbulent diffusion, impaction, and interception. Wet deposition, on the other hand, requires the presence of a type of precipitation, snow, or rain, and includes in-cloud and sub-cloud scavenging processes (Y. Wu et al., 2018).

Gravitational settling, as the name implies, mainly occurs due to the action of gravity on PM. Larger particles are influenced more by this mechanism. Impaction occurs when a particle cannot follow the air stream and hits an obstacle. Interception, on the other hand, happens when a particle cannot move along with the gas stream due to the presence of an object which is not directly in the path of the particle (Lagzi et al., 2013).

Wet deposition is the removal of atmospheric constituents (gas and particle) through events such as rain, snow, and fog. When the components are incorporated into water droplets in the cloud, this process is called rainout. If incorporation occurs sub-cloud, where the precipitation occurs and removes the pollutants along the way, this process is addressed as a washout (Vallero, 2014).

Both of the removal mechanisms result in the deposition of atmospheric constituents onto soils, water, vegetation, or non-biotic structures. Although both wet and dry deposition is equally important for PM removal, the flux of deposition is dependent

on different parameters such as PM concentration, size distribution, surface conditions, and meteorology (Tai et al., 2017).

2.6 Long-Range Transport

Measured ambient aerosol concentrations are dependent on the location of the source of origin, and the transport and deposition processes. Depending on these parameters, the aerosol residence time in the atmosphere can change from hours to weeks (Bagtasa et al., 2019). Long-range transport of locally produced atmospheric pollutants occurs when they are mobilized and transported away from their source of origin through the wind. During dust transport, 100-200 μm diameter particles are lifted off with strong winds closer to the surface. The lifted particles can tear down due to collisions and eject smaller particles (< 50 μm), which are eventually transported to the boundary layer and travel long distances (Mahowald et al., 2014). Pollutants, including PM, can travel hundreds to thousands of kilometers away from their source and contribute to pollution at their final destination. Typically, the size of the particles that are transported more than 100 km from their origin has a diameter of less than 20 μm (Shepherd, 2016). However, mineral dust particles, with sizes reaching above 60 μm, are found thousands of kilometers away from their source of origin (Shepherd, 2016).

More than 50% of all global atmospheric aerosols come from mineral aerosols in deserts and their surrounding areas (Andreae, 1995; Nenes et al., 2014). The journey and transformation of mineral dust have been the subject of many studies in an attempt to understand the effects of long-range transport. The transport of mineral particles from desert areas around the world across the Atlantic and Pacific oceans is well documented (Benedetti et al., 2019; Benkhalifa et al., 2019; Kaskaoutis et al., 2019; Querol, Pérez, et al., 2019). The most active dust source areas in Northern Hemisphere are the Saharan Desert in North Africa, particularly the Bodele depression in the Republic of Chad, deserts in Asia (particularly the Taklamakan

Desert in China), and deserts in the Middle East and Arabic peninsula (Shepherd, 2016).

Asian dust dominantly occurs in spring from Gobi and Taklamakan, Mongolia, China, and Kazakhstan regions and has a major impact on east Asia. However, it can also affect the air quality in Korea, Japan, and North America (Benedetti et al. 2019). As it is stated by Park et al. (2010), according to the 2007 report of the Intergovernmental Panel on Climate Change (IPCC), almost 70% of annually emitted 800 T g of Asian dust undergoes regional and long-range transport, while 30% is removed near the source. The influence of Asian dust on other regions such as the North Pacific is also studied and documented (Husar et al., 2001; Su and Toon, 2009). The effect of Asian dust is becoming more serious as the concentrations of anthropogenic emissions from Asia are observed to be increased. An increase in industrialization and desertification are described as the major causes of higher dust emissions in Asia (J. W. Kim, 2006).

The Saharan region has been intensively studied in terms of long-range transport as it is the largest source of dust globally. It is found that Saharan dust is a huge contributor to the measured PM concentrations in Europe and the Atlantic Ocean (Gini et al., 2022; Nava et al., 2012; Wanger et al., 2000). Saharan dust is transported via four main transport routes around the globe: towards the Gulf of Guinea, the Ivory Coast, and Ghana (southwestward route), towards North America and South America over the North Atlantic (westward route), towards Southern Europe and Scandinavia over the Mediterranean region (northward route) and towards Middle East and Himalayas and Asia over the Mediterranean region (eastward route) (Goudie and Middleton, 2006).

2.6.1 Mediterranean Region and Dust Events

The Eastern Mediterranean region has been studied extensively in terms of composition, source, and transport mechanisms of aerosols into the region. Studies

showed that the region is under the influence of both natural (i.e., soil, wildfires, and sea salt) (Ozdemir et al., 2020; Reicher et al., 2019) and anthropogenic (i.e., urban and industrial) sources (Kallos et al., 2007; Pateraki et al., 2014). The high anthropogenic particle loading comes from metropolitan cities in Europe, Turkey, and the Middle East. The desert dust comes from the Sahara and the Middle East in the eastern part of the basin, and marine particles come from the Mediterranean (Güllü et al., 2000; Mustafa Koçak et al., 2009; Koulouri et al., 2008; Moatti & Thiébault, 2016; J. Pey et al., 2013). Although it is difficult to estimate the anthropogenic emission contribution to the PM concentrations with high certainty, this is estimated to be 25% of the total dust emissions of the region (Ginoux et al., 2012). Anthropogenic sources are mostly located in the North and the Northwest of the region, while natural dust sources are located more towards the South (Güllü et al., 1998). Atmospheric conditions of the region favor the formation of secondary pollutants such as ozone (O_3), non-sea-salt sulfate (nss-SO_4^{2-}), and secondary organic aerosols (SOA) (Kallos et al., 2007).

When the influence and transport pattern of dust into the region is investigated, three-time scales for maximum influence emerge (1) Spring (between March and May), (2) Summer (June and July), and (3) Autumn (August and September) (Israelevich et al., 2012). While the impact of dust is at its maximum during summer in Central Europe, Western and Eastern Europe are dominated by dust emissions during Spring and Autumn.

According to Prospero (1996), approximately 70% of resuspended dust crosses the Atlantic Ocean and reaches South and North America and 10% is transported to the Mediterranean. Although the majority of the resuspended Saharan dust is transported across the Atlantic Ocean, dust concentrations and deposition rates are higher in the Mediterranean due to its closer proximity to the source region. Saharan dust deposition rate in the Caribbean is approximately 1 mg m^{-2} yr^{-1} (J.M. Prospero, 1996), whereas deposition rates around 8 mg m^{-2} yr^{-1} and 10 mg m^{-2} yr^{-1} were reported for the Western (Gi. Bergametti et al., 1989; Molinaroli et al., 1993) and 16 mg m^{-2} yr^{-1} was reported for the Eastern Mediterranean (Herut et al., 2001).

Although emission reduction policies will continue to decrease $PM_{2.5}$ concentrations, future scenarios showed that Mediterranean PM_{10} will not decrease since it is dominated by dust and salt concentrations (Cholakian et al., 2019). The studies in the literature also suggest that, depending on the future land-use scenarios, the dust concentrations in the region can decrease or increase (Cholakian et al., 2019; Tegen et al., 2004; Woodward et al., 2005). However, there is uncertainty regarding dust flux due to the lack of long-term monitoring data, particularly in the Mediterranean region (Varga, 2020).

It is also observed that the particles are transformed in terms of not just their concentrations but also their size and composition during their hundreds to thousands of kilometers journey. As the atmospheric height increases, the mean diameter of suspended dust shows an exponential decrease (Friese et al., 2016). Similarly, as the transport distance increases, the mean particle size also decreases horizontally due to gravitational settling (Friese et al., 2016; Tsoar and PYE, 1987).

Considering the uncertainties in the dust flux and the importance of understanding the effect of atmospheric processes on the particle characteristics during the long-range transport, comprehensive monitoring of sources, composition, size, and transformation of particles is essential. Although the current regulatory standards are based on the mass concentration of particles, in recent years it has been argued that standards based on numerical concentrations of particles are more appropriate because they represent submicron particles better (Manigrasso et al., 2019; Pacitto et al., 2020). For this purpose, the use of mass and number concentrations together is critical.

CHAPTER 3

MATERIALS AND METHODS

In this chapter, the methodology followed throughout the study is explained. The sampling station, equipment used in the sampling and measurement, the sampling methodology, quality assurance, quality control procedures, and the data analysis methods are explained in detail.

3.1 Experimental studies

3.1.1 Ankara and Marmaris Sampling Stations

In this study, two stations, namely, suburban and rural were established. Suburban station is located at Middle East Technical University, Department of Environmental Engineering, Ankara (39°53'13" N, 32°46'59" E). Ankara station has an altitude of 950 m above sea level and it is located far away from major pollution sources (Figure 3.1). Major roads that are surrounding the campus are located 2.5 km (Eskişehir road) and 2.4 km (Konya Road) away from this sampling location. There are no other major pollution sources around the department other than these potential traffic sources. During semester breaks, the traffic inside the campus drops to a minimum. This station was chosen as it is not under the influence of heavy emissions yet enables us to see the effect of both anthropogenic and natural sources at the same time. Moreover, the station was well-established and has been in use for many years. Therefore, ease of operation was another major factor in the selection of the Ankara station as the suburban station.



Figure 3.1 Map showing suburban sampling station at METU Department of Environmental Engineering.

The rural station is located around Marmaris on the Mediterranean coast (36°53'8.88" N, 28°19'57.00" E). The selected station is located at the radar station of Turkish State Meteorological Services, 10 km north of Marmaris, and 935 m above sea level (Figure 3.2). The station is situated in a pine forest in the Taurus mountains, and there is neither a settlement nor an industrial activity around it. The nearest road, Marmaris – Muğla road, passes 5 km away from the station. Therefore, Marmaris station is not affected by any anthropogenic sources. The fact that this high-altitude station is located away from all primary anthropogenic emission sources enables the identification of the dust events more accurately.

Moreover, the station on the Eastern Mediterranean coast is located on the pathway of air masses coming from both the Sahara region and Europe and the Middle East. This location was selected for the sampling as it is both away from any anthropogenic intrusions and on the pathway of the air masses coming from both dust regions and the source regions such as Europe.



Figure 3.2 Map of rural sampling station at Marmaris.

3.1.2 Other Sampling Stations

Ankara sampling station is expected to receive both anthropogenic and natural particulate matter emissions. Therefore, its atmospheric composition is expected to be more complex compared to the Marmaris station composition as the latter is mostly affected by dust movement. Differentiation between anthropogenic and natural contributions to concentrations measured in Ankara station is necessary. For this purpose, data obtained from national air quality monitoring network stations (AQM) operated by the Ministry of Environment, Urbanization and Climate Change (MoEUCC) are used along with measured data (Figure 3.3). Seven AQM stations are located within a 5 – 25 km range of our suburban station. These stations are located in Bahçelievler, Cebeci, Demetevler, Dikmen, Keçiören, Sıhhiye, and Sincan in Ankara. Hourly PM_{10}, $PM_{2.5}$, SO_2, NO, and NO_2 data from these stations are downloaded from the website of the Ministry.

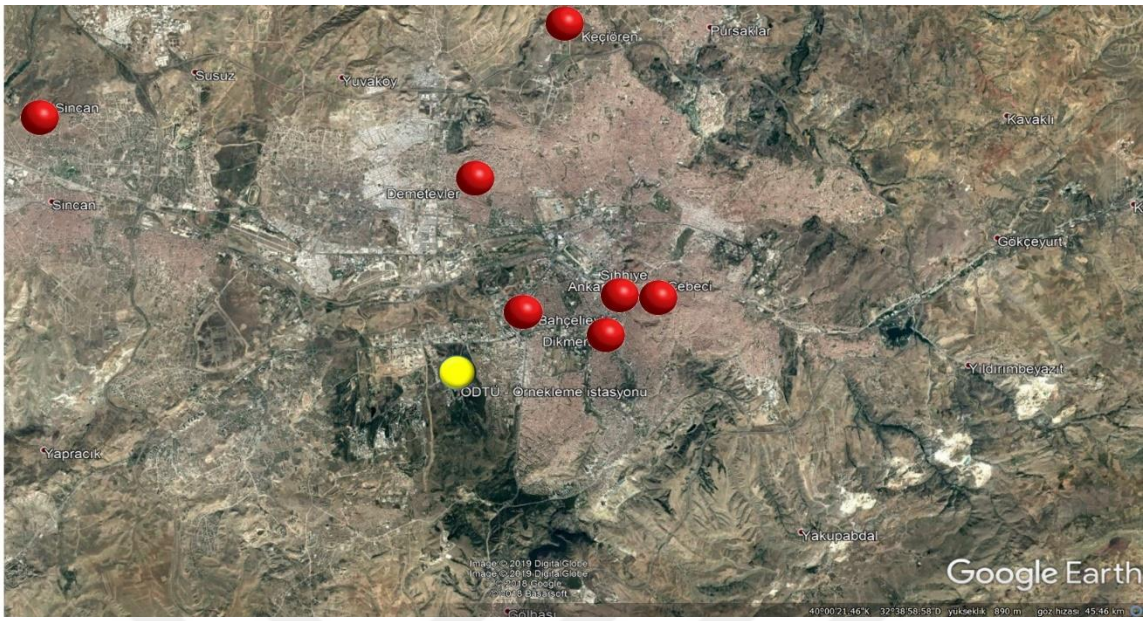

Figure 3.3 Map of Ankara national air quality monitoring stations (red markers) in relation to the suburban station at Ankara (yellow marker).

Marmaris sampling station is located at the radar station of Turkish State Meteorological Services (MGM). There is no air quality measurement on the radar, but there are five meteorological stations operated by MGM around the radar (Figure 3.4). Those stations are Çetibeli (36°59'36.45" N, 28°18'21.14" E), Ula Kavakçalı (37°06'10.30" N, 28°38'12.64" E), Ula Helicopter (37°07'41.65" E), Köyceğiz Zeytinalanı 36°57'14.42" N, 28°45"5.76"), and Marmaris (36°20'21.20" N, 28°14'41.70" E). The distances between these stations and the radar station vary from 9 km to 38 km. Although none of these stations are close enough to the sampling station, data from these stations are used as there are no other meteorological stations in the vicinity of the radar.

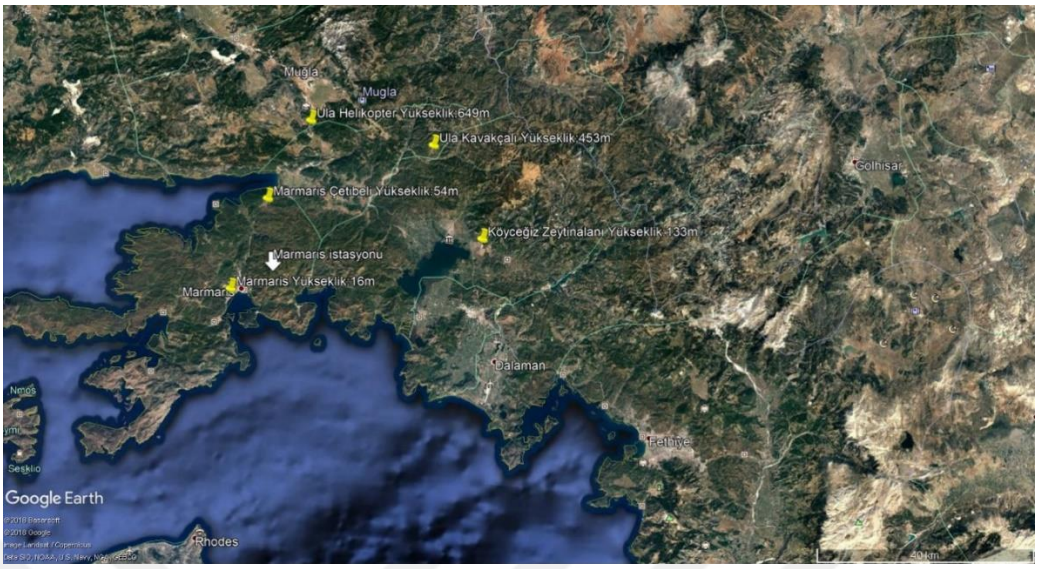

Figure 3.4 Map of Marmaris meteorological stations in relation to the rural station at Marmaris.

3.1.3 Sample Collection and Measurements

3.1.3.1 Mass Concentration Measurements and Trace Element Analysis

Sampling was started in March 2014 and completed in January 2018. It was not continuous, there were several interruptions due to instrument malfunctions and lack of adequate funding. Trace element samples were collected as 24-hour samples at both stations for PM_1, $PM_{2.5}$, and PM_{10} size ranges. For the collection of PM_1 samples along with $PM_{2.5}$ and PM_{10}, the PM_1 sampling unit has been designed and put together within our group, specifically for this purpose. Sampling has started as $PM_{2.5}$ and PM_{10} sampling at Marmaris station and PM_1, $PM_{2.5}$, and PM_{10} sampling at Ankara station.

Stack filter unit samplers (SFU) were used with nucleopore filters at Marmaris station. Fine and coarse fraction samples were separately collected on polycarbonate (Nuclepore Co.) filters using SFU. The SFU was developed at Gent University, Belgium (Maenhaut et al., 1993) and is frequently used to collect fine and coarse particles (Alves et al., 2020; Humairoh et al., 2020; Santoso et al, 2020). Satisfactory

particle cut-off characteristics and collection efficiency of SFU were reported in the literature (Hopke et al., 1997). Teflon filters were used at Ankara station with the assembled low-volume sampler (16.7 L air/min). Although the sampling device with the PM_1 sampling head was relocated to Marmaris station for PM_1 measurements, sampling had to be stopped due to technical problems and the possible risk of a forest fire at the station. Therefore, PM_1 samples could not be obtained from the Marmaris station.

Collected samples, nucleopore, and Teflon filters are analyzed at the Ankara Atomic Research and Training Center (ANAEM) of the Turkish Atomic Energy Authority (TAEK). Analysis was done with Energy Dispersive X-ray Fluorescence (ED-XRF) using an Oxford, ED-2000 energy dispersive X-Ray Fluorescence Spectrometer. Sample preparation included only the weighing of filters before and after sampling. For this, filters were left in a homemade constant-humidity and constant-temperature chamber for 24 hours and weighed, to the nearest 1 μg, using a Sartorius model MC-5 microbalance.

In ED– XRF, all of the elements in the sample are excited simultaneously, and an energy dispersive detector in combination with a multi-channel analyzer is used to simultaneously collect the fluorescence radiation emitted from the sample and then separate the different energies of the characteristic radiation from each of the different sample elements. Therefore, possible sources of uncertainty and contamination have been lowered significantly. Fifteen elements, including Al, Si, Ca, Na, Mg, K, Ti, V, Mn. Ni, As, Cu, Pb, S, and Zn, were determined in collected samples.

3.1.3.2 Number Concentration Measurements

Number concentrations were measured with laser spectrometers at both stations. In this study, the Grimm Aerosol Spectrometer was used for the number concentration and size distributions by measuring the number of particles per unit volume

(particles/cm^3) through light scattering technology. The size range of the device is between 0.25 μm and 32.0 μm particle diameters. The measurement frequency is measurement per minute. The data generated with this measurement frequency were used to calculate hourly and daily size distributions. Hourly average size distributions were used during correlation with mass concentrations. Similarly, daily average size distributions were used during the correlation with trace element analysis. The number concentrations that are measured at 32 different size channels were converted to relevant size ranges (PM_1, $PM_{2.5}$, and PM_{10}) during correlation studies.

3.2 Data Analysis

3.2.1 Data Quality Assurance/Quality Control (QA/QC)

3.2.1.1 Method Detection Limit (MDL)

The method detection limit of the ED–XRF for each target element has been determined. For this purpose, two empty filters were analyzed ten times by ED – XRF. Standard deviations of analysis results were multiplied by three. Concentrations that are corresponding to resulting values are determined and accepted as method detection limits. The final values are given in Table 3.1.

3.2.1.2 Blank Analysis

Since blank samples have significant effects on uncertainty in sampling and measurements, field blanks were analyzed. Field blanks were prepared the same way sample filters were prepared. They were conditioned for 24 hours, weighed, numbered, and sent to the field. Field blanks were one of the sample filters, which were loaded to the sampler and then removed after one-minute sampling. After this step, field blanks were treated as sample filters, and the same processes were applied.

Twenty of the collected field blanks and numerous laboratory blanks were analyzed to assess and minimize sample contamination. Sample-to-blank ratios of elements varied between 1.1 for Zn and 150 for S. Concentrations of elements, V, Cu, Zn, As, and Pb in blank filters were between 16% to 40% of their concentrations in sample filters. High blank subtraction for these elements is reflected in their frequency of observances. Blank subtraction was < 10% for the remaining elements.

MDL and blank sample concentrations were also compared with measured sample concentrations. Average concentrations obtained from analyzed samples are also presented in Table 3.1. Sample to MDL ratios (Sample/MDL) range between 3 (Zn) and 3000 (Ca). The average of these ratios for all elements is calculated as almost 500. Similarly, blank sample concentrations were also lower than sample concentrations, and analysis results are acceptable.

Table 3.1 MDL and Blank sample concentrations for ED–XRF analysis

	MDL ng cm^{-2}	**Blank concentrations ng cm^{-3}**	**Average sample concentrations ng cm^{-2}**
Al	0.58	2.40	452
As	0.09	0.82	7.6
Ca	0.58	4.28	1844
Cu	7.05	22.94	57.9
Fe	44	62	1560
K	0.42	4.09	326
Mg	0.42	1.33	123
Mn	7.95	14.29	80
Na	1.42	4.16	176
Ni	0.80	1.30	26.7
Pb	2.67	4.68	15.4
S	1.48	5.13	1369
Si	2.01	11.81	1186
Ti	2.78	8.55	63.8
V	2.18	4.62	10.9
Zn	24.1	28.68	69.8

3.2.1.3 Standard Reference Materials (SRM) Analysis

To test the accuracy of the analyses, Standard Reference Materials (SRMs) were analyzed, and measured trace element levels of the SRMs were compared with their certified levels. National Institute of Standards and Technology (NIST) reference filters (SRM 2783) were used to determine the accuracy of the ED-XRF analysis. This reference filter is analyzed along with the sample filters under the same ED-XRF conditions. SRM 2783 filters were counted at the beginning of each analysis day to monitor variations in the sensitivity of the instrument. If the difference between certified and measured values of an element is > ± 10%, the instrument was recalibrated before resuming analysis.

3.2.1.4 Repeated Sample Analysis

As a QA/QC protocol, 5% of the previously counted samples were resent to XRF laboratory with every sample batch, without informing laboratory personnel, to assess variation of repeatability in time. Samples that were sent for reanalysis were randomly selected. This way, the precision of the analytical system was calculated. Relative standard deviation values varied between 3.3% for Ca and Ti and 10% for Pb.

3.2.1.5 Validation of Laser Spectrometer Sampling

GRIMM Laser Spectrometers that were used in this study were operated simultaneously before the beginning of the sampling period. After reaching the same analysis results from both spectrometers, the sampling period at both stations was started. Both devices were operated simultaneously for a month. Ratios of averages of measured concentrations and average concentrations for each size range are provided in Figure 3.5. The average ratio of number concentrations measured at each size bin by two spectrometers varied between 0.47 and 1.5, with an average value of

1.1. Student t-test showed that two data sets at each size bin are statistically similar within a 99% confidence interval [p(r, n)<0.01].

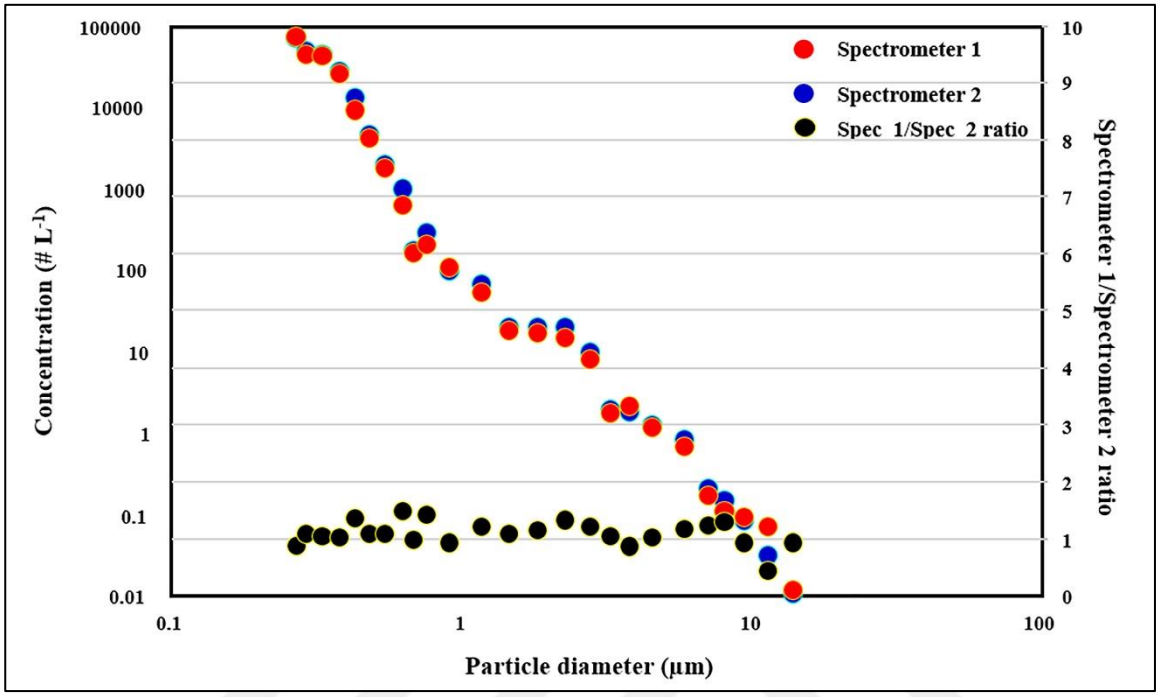

Figure 3.5 Comparison of number concentrations measured by two laser spectrometers used in the study.

In the second phase of the validation process, one of the laser spectrometers was run side-by-side with a stack filter unit (SFU) (Hopke et al., 1997), a home-made, low volume sampler, with cyclone-based PM_{10}, $PM_{2.5}$, and PM_1 size cut points (Ates, 2019) and two high-volume samplers equipped with $PM_{2.5}$ preimpactor. All devices were operated for a month at Ankara station. 24-hour samples of PM_{10} and $PM_{2.5}$ were collected with both devices. PM_1 measurements were done with a laser spectrometer and the cyclone sampler only. All size cut-points were not available in all instruments. PM_{10} data were generated with SFU, cyclone sampler, and a laser spectrometer. $PM_{2.5}$ data were generated by SFU, cyclone sampler two high volume samplers, and a spectrometer. Only the spectrometer and cyclone sampler had a PM_1 cut-point and PM_1 data were generated with these two instruments. Although high-

volume samplers were not used in this study, the use of these devices during calibration increases the reliability of the results.

The results of the calibration study are provided in Figure 3.6 and average concentrations and standard deviations measured by the devices are summarized in Table 3.2 as well. As can be seen, the concentrations measured by the different instruments are very close to each other among $PM_{10,}$ $PM_{2.5,}$ and PM_1 measurements. The difference between $PM_{2.5}$ and PM_1 concentrations measured with spectrometer and other gravimetric samplers are <10%. Data generated with laser spectrometer, cyclone sampler, SFU, and high-volume samplers are statistically the same with >95% confidence. The difference between average PM_{10} concentrations measured with spectrometer and SFU and cyclone sampler were 18% and 15%, respectively. The correlation between the devices was tested with the Student t-test and confirmed with 95% confidence that the results are correlated. As in number size distributions, mass size fractions measured by two spectrometers (PM_{10}, $PM_{2.5}$, PM_1) are similar with 95% statistical significance [P(r,n)<0.05]

Table 3.2 Average PM_1, $PM_{2.5}$, and PM_{10} concentrations with different devices ($\mu g\ m^{-3}$)

PM_{10}	
SFU	21 ± 10
Cyclone	22 ± 9 (24)
GRIMM 164	26 ± 11 (27)
$PM_{2.5}$	
SFU	11 ± 4 (11)
Cyclone	12 ± 4 (12)
GRIMM 164	13 ± 4 (13)
Hi-Vol 1	14 ± 4 (14)
Hi-Vol 2	13 ± 4 (12)
PM_1	
Cyclone	9 ± 3 (7)
GRIMM 164	10 ± 4 (10)

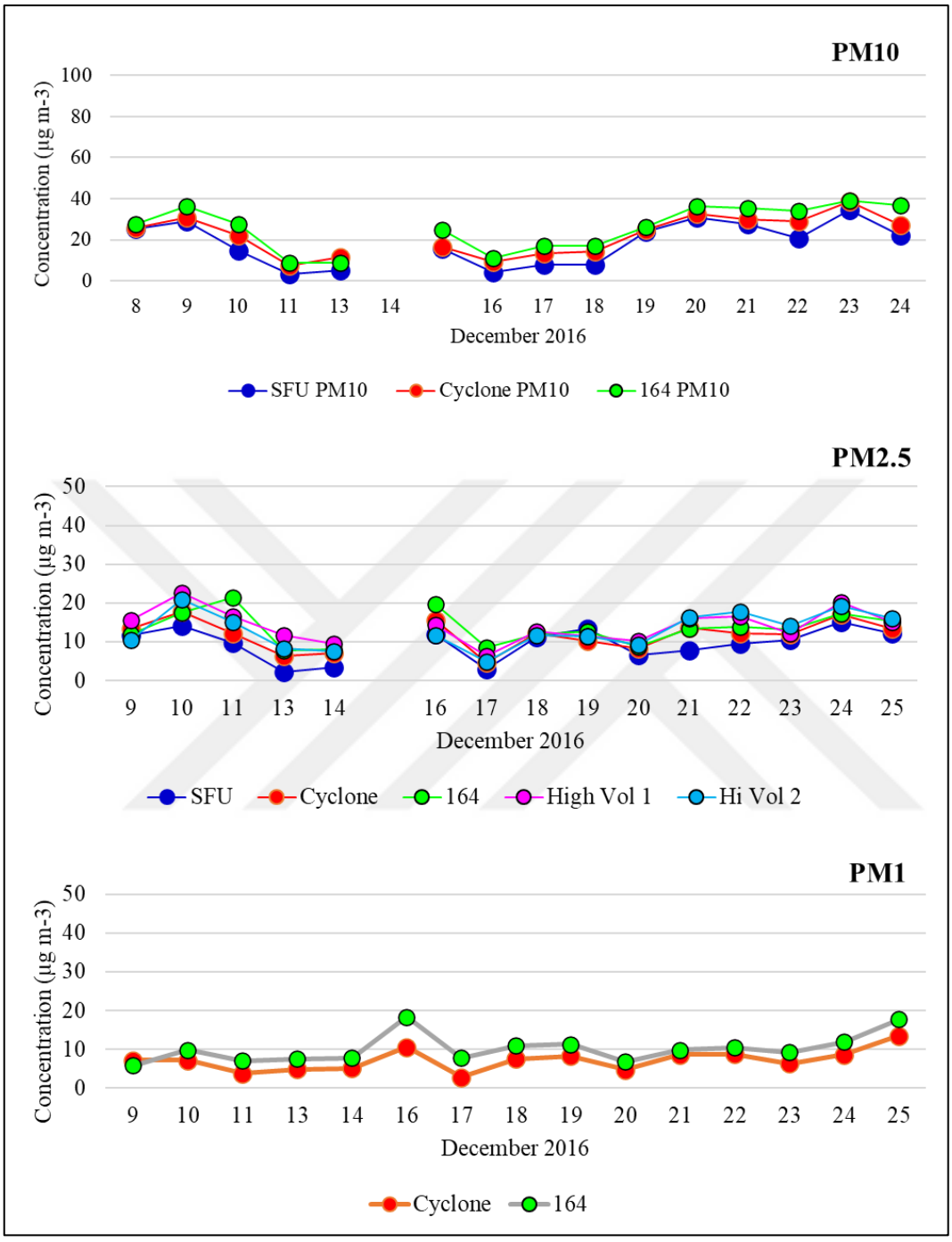

Figure 3.6 Comparison of sampling efficiency of different devices

3.2.2 Comparison of Ankara Laser Spectrometer Results with National Air Quality Measurement Network Result

PM_{10} and $PM_{2.5}$ mass concentrations generated by the laser spectrometer at our suburban station were compared with corresponding concentrations from AQM stations operated by the MoEUCC, for the period between April 1, 2017, and October 31, 2018. Those stations are Bahçelievler, Cebeci, Demetevler, Dikmen, Keçiören, Sıhhıye and Sincan stations. One-to-one agreement between concentrations measured at our suburban site and those reported for AQM stations should not be expected, as instruments in AQM stations are not co-located with our spectrometer. The data was investigated for general agreement between mean concentrations, the simultaneous occurrence of dust episodes, and correlations between them, which may indicate co-variance of data, even if the concentrations are not the same. Figure 3.7 demonstrates the comparison results for Bahçelievler and Sıhhıye sampling stations. Statistical comparison can be seen in Table 3.3 as well.

Both Figure 3.7 and Table 3.3 show that METU measurement results are very close to national network station measurements except for the Sıhhiye station. Sıhhıye station concentrations are significantly high compared to other stations. This is because Sıhhıye station is located in a very polluted location of the city in terms of PM emissions. For other stations, as yearly wind speed is pretty low in Ankara (2 m s^{-1}), the concentrations are distributed homogenously around the city, and measured concentrations are very close to each other.

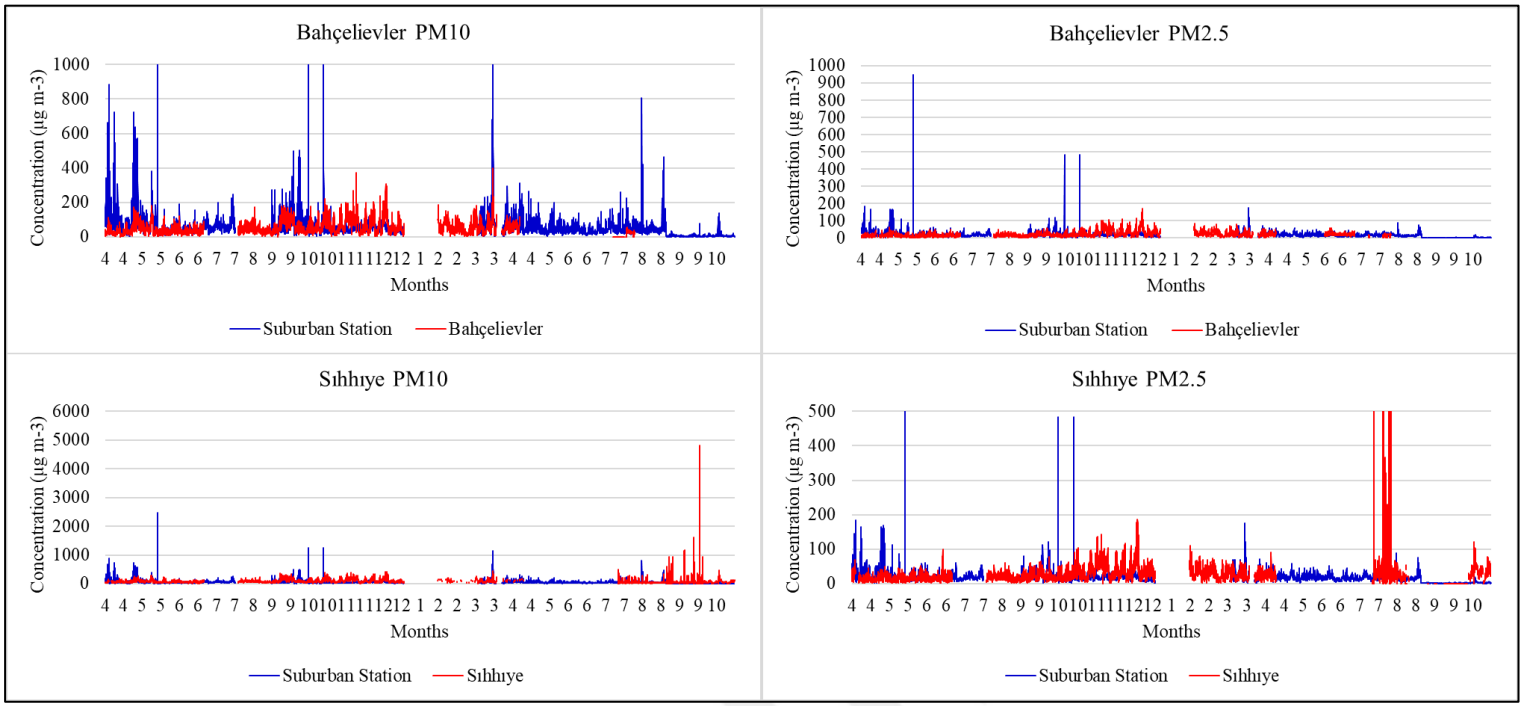

Figure 3.7 Comparison of METU station measurements with Bahçelievler and Sıhhiye stations

PM_{10} concentrations range between 50 and 60 µg/m³ at all stations except for Sıhhıye. April 2017 – October 2018 average PM_{10} concentration at the suburban station is 52 ± 66 µg m^{-3} whereas they range between 52 and 84 µg m^{-3} at AQM stations. Similar observations can be made for $PM_{2.5}$ concentrations as well. The average $PM_{2.5}$ concentration at the suburban station is 18 ± 20 µg m^{-3} and varies between 18 and 27 µg m^{-3} in AQM stations. Measured PM_{10} and $PM_{2.5}$ concentrations in seven AQM stations in Ankara are close to each other. The similarity of concentrations of criteria pollutants measured in AQM stations in Ankara was noted in earlier studies in the city (Genc et al., 2010) and attributed to the very low average wind speed in Ankara. Ankara is not an industrial city and the measured pollutants originate mostly from space heating and traffic (Yatin et al., 2000; Genc et al., 2010), both of which are homogeneously distributed over the city. This results in the homogenous spatial distribution of pollutant concentrations, particularly when it is coupled with a very low average wind speed over the city (annual average wind speed is 2.0 m s^{-1}).

Table 3.3 Mean and Median concentrations measured at Suburban, Bahçelievler, and Sıhhıye stations

	Mean ± σ **µg m^{-3}**	**Median** **µg m^{-3}**
Suburban PM_{10}	52.7 ± 66.2	38.8
Suburban $PM_{2.5}$	18.2 ± 19.9	15.6
	PM_{10}	
Bahçelievler	53.8 ± 41.1	43
Cebeci	57.5 ± 56.4	44
Demetevler	65.4 ± 68.0	49
Dikmen	65.4 ± 82.2	52
Keçiören	62.2 ± 72.6	50
Sıhhıye	84.2 ± 84.8	66
Sincan	69.8 ± 118.3	47
	$PM_{2.5}$	
Bahçelievler	23.0 ± 16.9	19
Cebeci	26.7 ± 22.2	21
Demetevler	27.1 ± 23.7	21
Dikmen	18.4 ± 14.9	15
Keçiören	18.0 ± 15.0	14
Sıhhıye	26.5 ± 34.4	21
Sincan	20.8 ± 24.4	12

To determine whether a meaningful relationship could be obtained between measurements from our stations and national network stations, a regression analysis was done. Scatter plots are given in

Figure 3.8. The relation between PM_{10} and $PM_{2.5}$ data generated in our Ankara station and AQM stations are statistically significant at 95% confidence interval ($p[r,n] < 0.05$). The observed statistical significance is due to very large data sets used in regression analysis (N = 11200 at our station and varied between 7400 and 11200 at AQM stations). R^2 values are very low indicating no relation between the two sets of parameters.

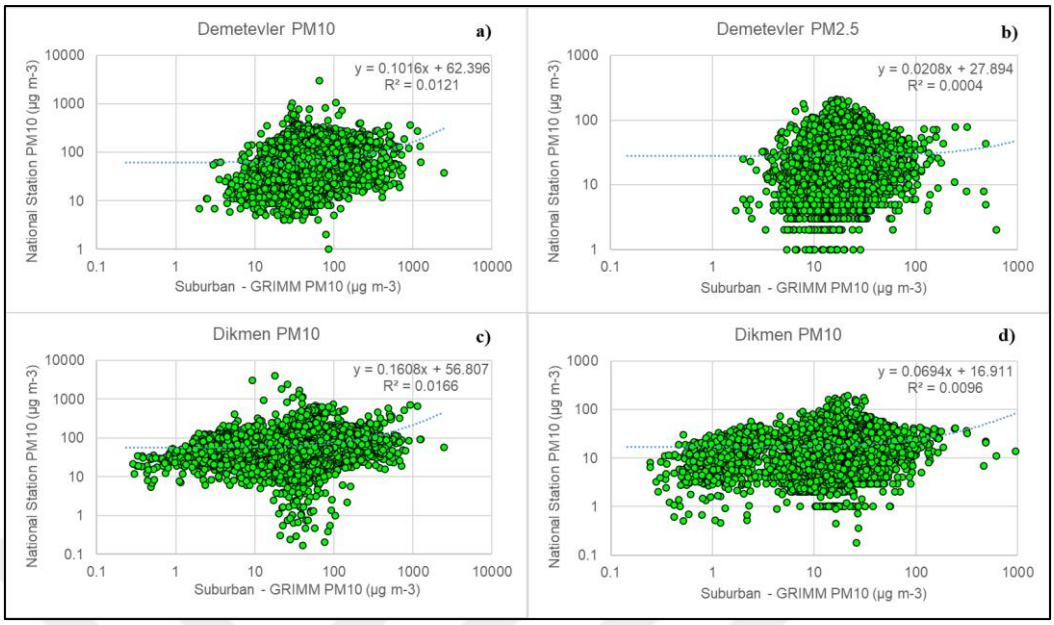

Figure 3.8 The correlation between PM_{10} and $PM_{2.5}$ concentrations measured at Suburban station and Dikmen and Demetevler national stations

3.3 Flow Climatology and Back trajectory Calculations

Flow climatology is defined as the study of the characterization of the source areas of the pollutants through the application of trajectory statistics methods (İ. Balcılar, 2018; Eneroth et al., 2003; Moody et al., 2013). Through the application of flow climatology, the origin and the frequency of air masses that reach a receptor can be determined. Air movement around the stations gives information about the source regions that affect measured pollutant concentrations and the transportation of dust. Therefore, the upper atmosphere movements have been investigated to better understand the sources affecting the sampling stations as they provide information on the remote pollution sources (İ. Balcılar, 2018; Brankov et al., 1998).

In this study, the frequency of air masses coming from different directions is shown in two different methods, i.e. residence time analysis and the calculation of time spent by air masses in each wind sector (İ. Balcılar, 2018; Yücel, 2019). Both methods are based on back trajectory calculations. Back trajectories are calculated for each day, starting from the beginning of the sampling period until the final day

of sampling. The location of the sampling station is the starting point for back trajectory calculations. Air masses located at 100m, 500m, and 1500m above ground level are traced back for five days for each day starting from the sampling location (Dimitrau and Kassomenas, 2019; Stein et al., 2015; Rolph et al., 2017). In this way, the locations the air masses have passed before they reach the sampling station could be determined.

Hybrid Single-Particle Lagrangian Integrated Trajectory (HYSPLIT) model developed by U.S. National Oceanic and Atmospheric Administration (NOAA) is used for back trajectory calculations. HYSPLIT model can be operated online through the webpage of the model (NOAA, 2019). The model was operated five days backward, starting from each sampling day. The reason for choosing a five-day back trajectory method was 1) the horizontal uncertainty of the model outputs increases as the time frame is extended, and 2) five days is enough for air masses to reach Turkey from the western edge of the study area (Ozturk et al., 2012). The study area is defined as the Western edge of England on the West, the east coast of the Caspian Sea on the East, the Northern edge of the Scandinavian peninsula on the North, and the Equator on the South (Figure 3.9). Model outputs are the x, y, and z coordinates of the air masses at each hour. Each point defined by these coordinates is identified as a "back trajectory segment." Therefore, each back trajectory comprised 105 segments (24 hours and five days). For three different heights and 2-year of data, almost 228000 segments are used during calculations.

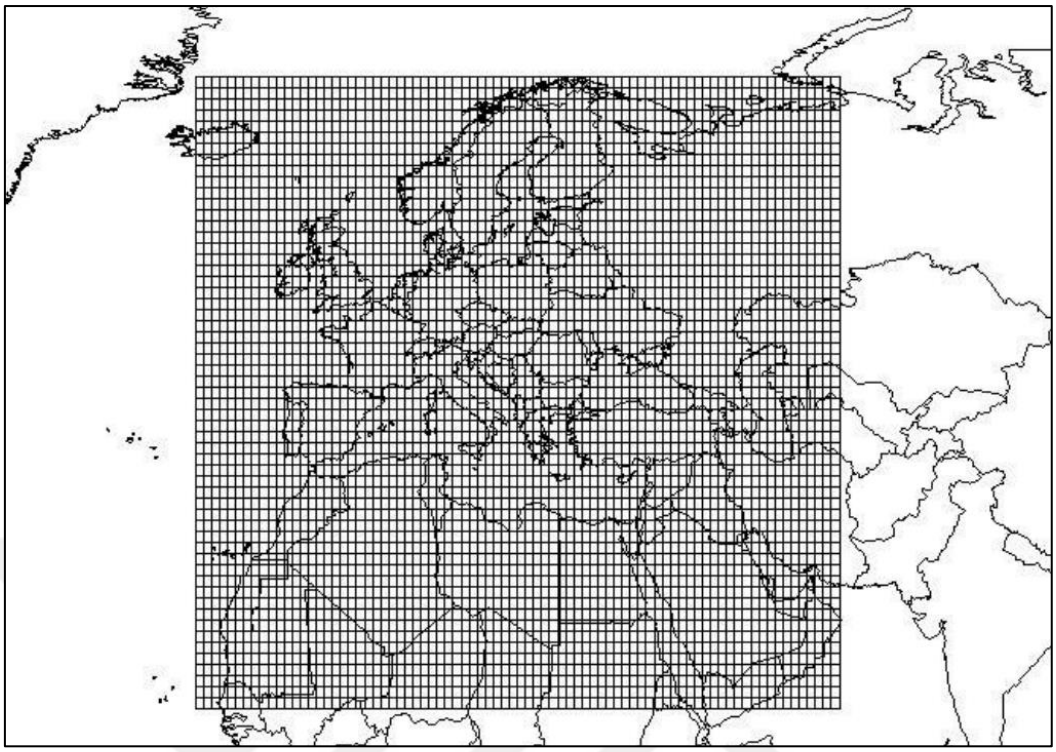

Figure 3.9 Study area for residence time analysis

After the determination of segments, the study area was split into 1° x 1° (100 km x 100 km) sized grids, and segments in each grid are counted. As each segment represents a one-hour back trajectory, the number of segments in each grid shows how long air masses spend at each grid. Finally, the segment numbers are converted into a distribution map by MapInfo software.

During the calculation of summer and winter back trajectories, April, May, June, July, August, and September months are accepted as summer months, while November to March is accepted as winter months. This categorization is based on the rain patterns of the region as precipitation is an important parameter that affects the regional pollutant concentrations. In the Mediterranean region, 80% of precipitation occurs during months that were depicted as winter months. Therefore, only 20% of precipitation occurs between April and September (summer months).

This categorization enables the determination of temporal variation of pollutants (anthropogenic and natural, dust, and gas) to be easier.

3.4 Cluster Analysis

The dynamics of dust transportation in the region were investigated using cluster analysis via the calculated back trajectories. Cluster analysis is a statistical technique that distinguishes the back trajectories based on their physical properties such as direction and length (Wang et al., 2006). Results of cluster analysis provide very important information on the relationship between the source and the receptor (Baklanov et al., 2011; İ. Balcılar et al., 2014a; Byčenkiene et al., 2014; Karaca & Camci, 2010; Piñero-García et al., 2015; Szkop et al., 2016).

As a first step in the cluster analysis, the number of clusters is determined. Back trajectories were grouped based on the length (transport speed) and curvature using cluster analysis (TrajStat software). The optimum number of clusters was determined by investigating variation in total root means square deviation (TRMSD) with increasing the number of clusters (Brankov et al., 1998). To achieve this, the cluster number is changed between 2 and 20, and for each cluster number, TRMSD is calculated. The last cluster number where a 5% or more difference is observed between two consecutive TRMSD values is chosen (Brankov et al., 1998).

During the process of understanding the relationship between particle sources and trajectory clusters, the distributions of trajectory segments below 500m in each cluster were investigated. These low-lying segments were assumed to be the ones that have a higher probability of picking up particles from source regions. Therefore, they were chosen as better indicators of source areas affecting the receptor sites at Marmaris and Ankara.

.

3.5 Potential Source Contribution Function (PSCF)

Potential Source Contribution Function (PSCF) calculates the geographical location of the sources that might be contributing to the measured pollutant concentrations at the sampling stations. For the PSCF analysis, the study area is divided into 1º x 1º (100 km x 100 km) sized grids. The study area is defined as the Western edge of England on the West, the coast of the Caspian Sea on the East, the Northern edge of the Scandinavian peninsula on the North, and the Equator on the South (Figure 3.9).

For the analysis, the back trajectories that were calculated previously were divided into hourly segments. These segments were assigned to the grids based on their coordinates and the number of segments in each grid was counted (n_{ij}). The segments with the back trajectories that are assigned to the highest 30% are also counted separately (m_{ij}). The PSCF values are calculated according to Equation 3.1 and the MAPINFO program is used for the PSCF analysis.

$$PSCF_{ij} = \frac{m_{ij}}{n_{ij}} \quad (3\text{-}1)$$

The PSCF values range between 0 and 1, and as the value approaches 1, the chance of that grid being a potential source region increases (İ. Balcılar, 2018). The weighting method, developed by Zhao and Hopke (2006), was used to minimize the effect of grids with only a few trajectory segments in them at the edges of the study area. In addition to this, trajectory segments were also weighted depending on their altitude, to increase the significance of segments that are close to the surface, assuming that those segments have a higher probability of picking up particles from sources at the surface than segments at high altitudes (Malkaz, 2014; Yıkmaz, 2010). For this, segments with altitudes < 500 m are multiplied by 1.0, segments between 500 and 1000 m are weighted by 0.5, and segments with z > 1000 m are weighted by 0.3 (Malkaz, 2014).

3.6 Source Apportionment

Positive Matrix Factorization (PMF) and PSCF methodologies were used for source apportionment. Each is described briefly below.

3.6.1 Positive Matrix Factorization (PMF)

PMF model is used to determine the sources contributing to the measured PM concentrations at Ankara and Marmaris stations. The PMF model calculates the source profiles and contributions, and the uncertainties related to these source profiles based on user-provided species concentrations. It aims to minimize the weighted difference between the observed and predicted concentrations (Equation 3.2) while attempting to solve Equation 3.3. The terms *x*, *g*, *f*, and *e* represent the concentration of species, contribution, fraction, and residual, respectively. The terms *i*, *j*, and *k* represent the sample, species, and factor, respectively. Hence, x_{ij} represents the concentration of jth species in the ith sample; g_{ik} represents the contribution of the kth factor to the ith sample; f_{kj} represents the fraction of the jth species in the kth factor, and e_{ij} represents the residual part of the jth species in the ith sample.

$$Q = \sum_{i=1}^{n}\sum_{j=1}^{m}\left(\frac{e_{ij}}{s_{ij}}\right)^2 \tag{3-2}$$

$$x_{ij} = \sum_{k=1}^{p}\left(g_{ik}f_{kj} + e_{ij}\right) \tag{3-3}$$

The latest version of the PMF model, EPA PMF 5.0, was used to determine the source profiles. As the data provided to the model should be complete, the missing data is filled with the geometric mean of the related species (Reff et al., 2007). For measurements below the detection limit (DL), missing data is replaced with half of

the detection limit for that species. The uncertainty for each species in each sample is calculated based on the following methodology (Norris et al., 2014; Reff et al., 2007):

$$\sigma_{ij} = \begin{cases} Real\ concentration: & x_{ij} * 0.05 + \dfrac{DL}{2} \\ Below\ detection\ limit: & \dfrac{5}{6} * DL \\ Missing\ data: & 4 * Geometric\ mean \end{cases} \quad (3\text{-}4)$$

Based on Equation 3.2, Q_{robust} and Q_{true} values are calculated by the model several times during the determination of the number of factors. Q_{robust} is calculated with data remaining after the elimination of the data points with the uncertainty-scaled residuals greater than +4 and less than -4 (İ. Balcılar, 2018). Q_{true} is calculated with all the data points. The theoretical *Q* value is also calculated according to Equation 3.5 and compared with $Q_{true.}$ In Equation 3.5, *k* represents the number of elements, *m* represents the number of days and *t* represents the number of factors (Yücel, 2019). According to Norris et al. (2014), the ratio of $Q_{true}/Q_{theoretical}$ should be no more than 2.

$$Q_{theoretical} = (k * m) - t * (k + m) \quad (3\text{-}5)$$

For each species, distributions of the *eij/sij* ratios are obtained and checked for normal distribution. Data points that do not show a normal distribution are either removed from the dataset or the number of factors is increased and the feasibility of the PMF solution is checked again (İ. Balcılar, 2018).

Scatter plots for measured concentrations and predicted (modeled) concentrations are also reviewed. Species that lack a strong correlation between measured and predicted concentrations were categorized as “weak” and down-weighted.

By examining the factor profiles (F-loadings) and factor contributions (G-Score) of each source, and adjusting the *F-peak* values and scaled residuals, the number of factors is determined. Additional modeling uncertainty was assigned a value of 0 since Q_{robust} and Q_{true} values were sufficiently close without using it. Factor composition, fractions of elements explained by each factor, crustal enrichment factors of elements in each factor, monthly average factor scores, and PSCF value distributions for each factor are plotted and examined. The robustness of the factor solution was tested using the bootstrapping capability of the PMF model with 100 iterations.

The data used in the aforementioned analysis techniques are provided in Appendix D. The summary statistics of PM measurements with average, median, maximum, and minimum concentrations along with the number of samples are given for both stations. Moreover, the results of the trace element analysis for 15 elements are also provided for the Marmaris station. Only Al and Si analysis results are provided for the Ankara station for comparison purposes.

CHAPTER 4

FACTORS AFFECTING PARTICLE NUMBER SIZE DISTRIBUTIONS AT AN URBAN AND A HIGH-ALTITUDE RURAL SITE AT THE ANATOLIAN PLATEAU

4.1 Introduction

Atmospheric aerosols have been studied extensively due to their effects on human health (Caggiano et al., 2019; Doyi et al., 2020), visibility (Pope, 2016), energy budget of the Earth (Jiang et al., 2020; Lu & Sokolik, 2018; Rasch et al., 2008), and the cloud formation (Morawska et al., 1999; Spurny, 2000). Although all size fractions contribute to these effects to a certain extent, the magnitude of effects depends strongly on particle diameter (d_p). Monitoring of atmospheric particles changed with changes in our understanding of the health effects of particles. Regulatory monitoring of atmospheric particles started in 1971 with the measurement of total PM and shifted to PM_{10} in 1987. In 1997 monitoring of $PM_{2.5}$ was implemented in monitoring programs, because there was convincing evidence that $PM_{2.5}$ is a better health indicator than PM_{10} (Cao et al., 2013). With the current decrease in sizes of regulated particles, one wonders if there will be a standard for PM_1 particles in the future. The issue was discussed and ruled out because changing the fine fraction cut point from 2.5 μm to 1 μm would make only a minor change in fine fraction mass concentration (Cao et al., 2013; Chow, 1995).

Submicron particle fractions, particularly ultrafine particles (particles with diameter < 0.1 μm), which is the low end of the particle size spectrum, have more important health effects compared to larger particle fractions (Aguilera et al., 2021; Baccini et al., 2015; Cheriyan et al., 2021). The majority of particles in this size fraction originate from traffic and biomass burning (Bonnefoy et al., 2017; Nicolás et al., 2020; Rajput et al., 2019; Sparks et al., 2014). Measurement of particle number rather than its mass gained importance recently when it is realized that number

concentration is a better indicator for submicron particles, which has a strong impact on human health (Aalto et al., 2005; Greig, 2000; Kivekäs et al., 2007; Reche et al., 2011; Rodriguez et al., 2008). Particle mass concentration is not a proper indicator for submicron particles, because particles in this size range do not contribute to particle mass concentration significantly. Monitoring of particle number instead of particle mass was suggested for ultrafine particles originating from traffic and combustion (Reche et al., 2011).

The transport of mineral particles from desert areas around the world across the Atlantic and Pacific oceans is well documented (Benedetti et al., 2019; Benkhalifa et al., 2019; Kaskaoutis et al., 2019; Querol et al., 2019). More than 50% of total suspended particles (TSP) (Andreae, 1995; Nenes et al., 2014) and more than 35% of particles with aerodynamic diameters smaller than 10 μm (PM_{10}) (Boucher et al., 2013) are accounted for by mineral aerosol. Each year 1536 Tg of crustal material is resuspended from deserts around the world and transported long distances in the atmosphere. Source areas for desert dust, which is known as the "dust belt" extends from the West Coast of North Africa, the Middle East, and central Asia (Goudie & Middleton, 2006; Shepherd, 2016). Although there are some dust activities in the Southern Hemisphere as well (particularly in Australia), it is not as vigorous as the dust activity observed in Northern Hemisphere (Shepherd, 2016). The most active dust source areas in Northern Hemisphere are the Saharan Desert in North Africa, particularly the Bodele depression in the Republic of Chad, deserts in Asia (particularly the Taklamakan Desert in China), and deserts in the Middle East and Arabic peninsula (Shepherd, 2016).

Among dust source regions Sahara is by far the most important one, emitting 800 Tg crustal material each year, which accounts for 70% - 80% of global dust emissions (Huneeus et al., 2011). Approximately 70% of the resuspended dust crosses the Atlantic Ocean and reaches South and North America (Prospero, 1996). Ten percent of the dust is transported to the Mediterranean (Prospero, 1996). Although the majority of the resuspended Saharan dust is transported across the Atlantic Ocean, dust concentrations and deposition rates are higher in the Mediterranean due to its

closer proximity to the source region. Saharan dust deposition rate in the Caribbean is approximately 1 mg m^{-2} yr^{-1} (Prospero, 1996) whereas deposition rates around 8 mg m^{-2} yr^{-1} and 10 mg m^{-2} yr^{-1} were reported for western (Bergametti et al., 1989; Molinaroli et al., 1993) and 16 mg m^{-2} yr^{-1} was reported for the Eastern Mediterranean (Herut et al., 2001). However, the uncertainty of dust flux, due to the lack of long-term monitoring data, particularly in the Mediterranean region is highlighted (Varga, 2020).

The Eastern Mediterranean region has been studied extensively in terms of composition, source, and transport mechanisms of aerosols into the region. Studies showed that the region is under the influence of both natural (dust, wildfires, and sea salt) (Ozdemir et al., 2020; Reicher et al., 2019) and anthropogenic (urban and industrial) sources (Kallos et al., 2007; Pateraki et al., 2014). Anthropogenic sources are mostly located in the North and the Northwest of the region, while natural dust sources are located more towards the South (Güllü et al., 1998). Atmospheric conditions of the region favor the formation of secondary pollutants such as ozone (O_3), non-sea-salt sulfate (nss-SO_4^2), and secondary organic aerosols (SOA) (Kallos et al., 2007).

In this study, PM_1, $PM_{2.5}$, and PM_{10} mass concentrations and number concentrations in 30 size bins between 0.26 – 34 μm of atmospheric aerosol were measured at two stations. One of the stations was a rural station on the Mediterranean coast (Marmaris) and the other one was a suburban station on the Anatolian Plateau (Ankara). This is one of the two manuscripts prepared for publication. Factors affecting variability in particle concentrations and number distributions at two locations, and modification of size distributions due to anthropogenic sources are discussed here and dust climatology in this part of the Mediterranean basin, modification of particle size distribution during transport of dust plume from the Mediterranean coast to Central Anatolia are discussed in the second manuscript.

4.2 Materials and Methods

4.2.1 Stations

Data were generated in one suburban and one rural station, between April 1, 2017, and October 31, 2018. Locations of stations are given in Figure 4.1. The suburban station was located at the Middle East Technical University campus in Ankara (39°53'13" N, 32°46'59" E). There are no significant pollution sources around the station as the nearest major road is located 2.5 km away from the sampling point and the campus is a restricted area. Ankara station has an altitude of 950 m above sea level. The rural station (36°53'8.88" N, 28°19'57.00" E) is located approximately 10 km to the Northeast of Marmaris, which is a holiday resort on the Mediterranean coast of Turkey. The station is situated in a pine forest in the Taurus mountains and has an altitude of 935 m above sea level. There is no settlement or industrial activity around the station.

At Ankara, PM_{10} and $PM_{2.5}$ mass concentration data were also obtained from seven stations operating in a national air quality monitoring network to supplement differentiation between dust and anthropogenic episodes. A similar approach was not used at Marmaris station, because the nearest air quality monitoring station was 10 km away and at a lower altitude. However, meteorological data from five automated meteorological stations around our station (with distances varying between 5 and 20 km) were used to relate measured concentrations with meteorological parameters.

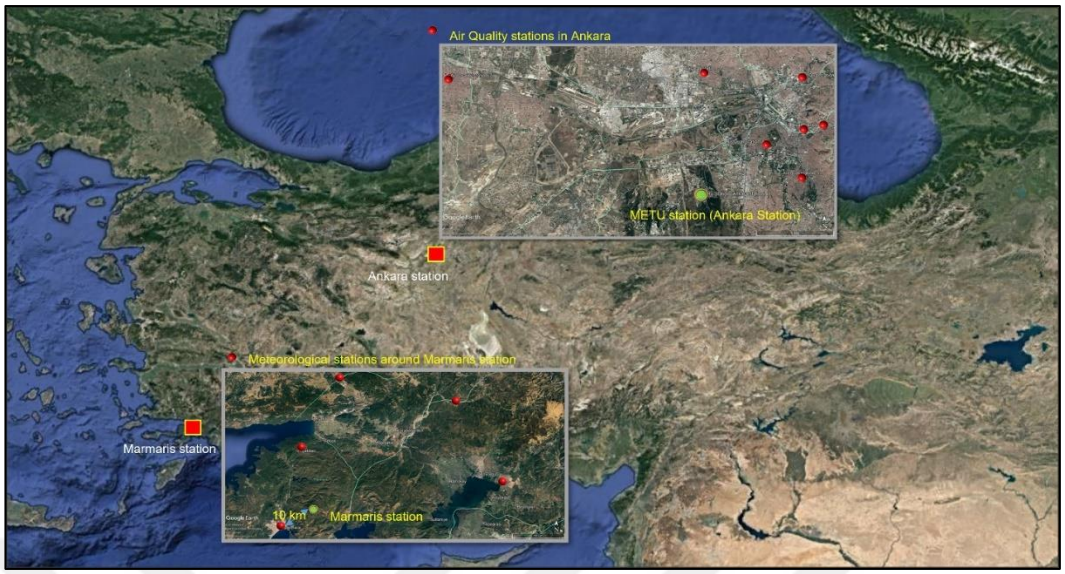

Figure 4.1 Map showing locations of suburban and rural stations

4.2.2 Instrumentation

PM_{10}, $PM_{2.5,}$ and PM_1 mass concentrations and number size distributions were measured using GRIMM Model 164 (in Marmaris) laser spectrometers. GRIMM Laser spectrometers measure particle number concentrations in 31 size bins between 0.265 µm and 34.0 µm particle diameters with a 1-min integration time. Hourly and daily size distributions were generated from this data. PM_{10}, $PM_{2.5,}$ and PM_1 mass concentrations were calculated by an algorithm developed by the manufacturer.

4.2.3 Quality Assurance / Quality Control (QA / QC)

4.2.3.1 Validation of Size Distribution and Mass Concentration Measurements

Data validation was performed for two purposes; (1) we wanted to ensure that two spectrometers that will be operating in two stations generate identical mass and number concentrations when they are placed side-by-side. (2) Since mass

concentrations are calculated from measured number concentrations, we wanted to ensure that these calculated numbers are comparable with mass concentrations measured with conventional gravimetric methods. For this purpose, the first two spectrometers were operated side-by-side at Ankara station for one month. The average number concentrations measured by each device at each size bin and ratios of these concentrations are given in Figure A1 in the supplementary material. The average ratio of number concentrations measured at each size bin by two spectrometers varied between 0.47 and 1.5, with an average value of 1.1. Student t-test showed that two data sets at each size bin are statistically similar within a 99% confidence interval [$p(r, n)<0.01$].

PM_{10}, $PM_{2.5,}$ and PM_1 mass concentrations measured by co-located spectrometers are given in Table A1 in the supplementary material. As in number size distributions, mass size fractions measured by two spectrometers (PM_{10}, $PM_{2,5}$, PM_1) were similar with 95% statistical significance [$P(r,n)<0.05$]. In the second phase of the validation process, one of the laser spectrometers was run side-by-side with a stack filter unit (SFU), a homemade, low volume sampler, with cyclone-based PM_{10}, $PM_{2.5,}$ and PM_1 size cut points, and two high-volume samplers equipped with $PM_{2.5}$ preimpactor. All samplers were operated at Ankara station for one month. Although high-volume samplers were not used in this study, they were used during calibration to increase the reliability of the results. Stack filter sampler and three-channel cyclone sampler were used to collect aerosol samples for trace element analysis in both stations. However, those results are beyond the scope of our discussion in this manuscript.

Results obtained (PM_{10}, $PM_{2.5,}$ and PM_1 mass concentrations) from parallel measurements are given in Table A2 in the supplementary material. Please note that all size cut-points were not available in all instruments. PM_{10} data were generated with SFU, cyclone sampler, and a laser spectrometer. $PM_{2.5}$ data were generated by SFU, cyclone sampler, two high-volume samplers, and spectrometers. Only spectrometers and cyclone sampler had PM_1 cut-point and PM_1 data were generated with these two instruments. The difference between $PM_{2.5}$ and PM_1 concentrations measured with spectrometer and other gravimetric samplers are <10%. Data

generated with laser spectrometer, cyclone sampler, SFU, and high-volume samplers are statistically the same with >95% confidence. The difference between average PM_{10} concentrations measured with spectrometer and SFU and cyclone sampler were 18% and 15%, respectively. Although the difference between PM_{10} data generated by the laser spectrometer and gravimetric methods is larger than the corresponding differences in $PM_{2.5}$ and PM_1 size fractions, the student's t-test demonstrated that these three data populations are not different with a 95% statistical confidence interval.

4.2.3.2 Comparison with Data from National Air Quality Stations

PM_{10} and $PM_{2.5}$ mass concentrations generated by the laser spectrometer at our suburban station were compared with corresponding concentrations from air quality monitoring (AQM) stations operated by the Ministry of Environment and Urbanization (MoEU), for the period between April 1, 2017, and October 31, 2018. Mean concentrations are presented in Table 4.1. There are seven AQM stations, which are located within a 5 – 25 km range of our suburban station. One-to-one agreement between concentrations measured at our suburban site and those reported for AQM stations should not be expected, as instruments in AQM stations are not co-located with our spectrometer. In this case, we looked for general agreement between mean concentrations, the simultaneous occurrence of dust episodes, and correlations between them, which may indicate co-variance of data, even if concentrations are not the same.

Table 4.1 Average PM_{10} and $PM_{2.5}$ concentrations measured at regulatory stations and Ankara station used in this study.

	Average ± σ	**Median**
	µg/m³	**µg/m³**
ODTU PM10	52.7 ± 66.2	38.8
ODTU PM2.5	18.2 ± 19.9	15.6
	PM_{10}	
Bahçelievler	53.8 ± 41.1	43
Cebeci	57.5 ± 56.4	44
Demetevler	65.4 ± 68.0	49
Dikmen	65.4 ± 82.2	52
Keçiören	62.2 ± 72.6	50
Sıhhıye	84.2 ± 84.8	66
Sincan	69.8 ± 118.3	47
	$PM_{2.5}$	
Bahçelievler	23.0 ± 16.9	19
Cebeci	26.7 ± 22.2	21
Demetevler	27.1 ± 23.7	21
Dikmen	18.4 ± 14.9	15
Keçiören	18.0 ± 15.0	14
Sıhhıye	26.5 ± 34.4	21
Sincan	20.8 ± 24.4	12

PM_{10} and $PM_{2.5}$ measurements for the suburban station and AQM stations show a general agreement. April 2017 – October 2018 average PM_{10} concentration at the suburban station is 52 ± 66 µg m^{-3} whereas they range between 52 and 84 µg m^{-3} at AQM stations. Similar observations can be made for $PM_{2.5}$ concentrations as well, i.e., the average at the suburban station is 18 ± 20 µg m^{-3}, and varies between 18 and 27 µg m^{-3} in AQM stations. It is interesting to note that PM_{10} and $PM_{2.5}$ concentrations in seven AQM stations in Ankara are close to each other. The similarity of concentrations of criteria pollutants measured in AQM stations in Ankara was noted in earlier studies in the city (Genc et al., 2010) and attributed to the very low average wind speed in Ankara. Ankara is not an industrial city.

Pollutants measured in the Ankara air shed originate mostly from space heating and traffic (Genc et al., 2010; Yatin et al., 2000), both of which are homogeneously distributed over the city. This results in the homogenous spatial distribution of pollutant concentrations, particularly when it is coupled with a very low average wind speed over the city (annual average wind speed is 2.0 m s^{-1}).

Apart from this comparison, regression analysis was performed between network stations and suburban stations using PM_{10} and $PM_{2.5}$ concentrations. Scatterplots for selected AQM stations (Dikmen and Demetevler) are given in Figure A2 in the supplementary material. The relation between PM_{10} and $PM_{2.5}$ data generated in our Ankara station and AQM stations are statistically significant at 95% confidence interval ($p[r,n] < 0.05$). The observed statistical significance is due to very large data sets used in regression analysis (N = 11200 at our station and varied between 7400 and 11200 at AQM stations). R^2 values are very low indicating only marginal relation between two sets of parameters.

4.2.3.3 Flow Climatology

Upper atmospheric movements were investigated to determine the path followed by the air masses before they arrive at sampling stations. A trajectory-based GIS approach was used to quantify frequencies (flow climatology). Five-day-long back trajectories, with 100 m, 500 m, and 1500 m starting altitudes were computed using HYSPLIT 3D isentropic model (Dimitriou & Kassomenos, 2019; Rolph et al., 2017; Stein et al., 2015) for each day during the entire sampling period. The study area was defined as the Western edge of England in the West, the east coast of the Caspian Sea in the East, the Northern edge of the Scandinavian peninsula in the North, and the Equator in the South. Back-trajectories were computed for five days, because, the horizontal uncertainty of the model outputs increases as the time frame is extended, and five days is enough for air masses to reach Turkey from the western edge of the study area (Öztürk et al., 2012). The study area has been split into 1° x 1° (100 km x 100 km) sized grids, and trajectory segments (X, Y, Z coordinates of

air mass at every hour) in each grid were counted to give the hours spent by air masses in that grid during the study period.

4.3 Results and Discussions

Summary statistics for PM_{10}, PM_1 and $PM_{2.5}$ concentrations measured at suburban and rural stations are given in Table 4.2. Average and median concentrations of all PM fractions are higher in the suburban station compared to the rural one. The observed difference in the concentrations is higher in the PM_{10} size fraction than in $PM_{2.5}$. PM_1 concentrations measured in the two stations are not significantly different from each other.

Median PM_{10} concentrations measured at suburban and rural stations are 38 and 17 $\mu g\ m^{-3}$, respectively. The rural station is under the stronger influence of dust from North Africa due to its closer proximity to source areas. PM_{10} concentration can reach very high levels during episodes. The maximum hourly PM_{10} concentration at the rural station, given in Table 2 is 3400 $\mu g\ m^{-3}$, which is higher than the maximum PM_{10} concentration measured at the suburban station (2460 $\mu g\ m^{-3}$). PM_{10} concentration during dust episodes can reach more dramatic values at shorter integration times. For example, the maximum PM_{10} concentration with a 1-min integration time was >6000 $\mu g\ m^{-3}$ at the rural station. However, 25 dust episodes were recorded at a rural station in one year between April 1, 2017, and April 1, 2018 (31 episodes were observed in 19 months-long measurement period). On the other hand, non-Saharan, man-made PM_{10} sources, such as soil resuspended by human activities, traffic, and incomplete combustion of fossil fuels, which are more influential at a suburban station, were active throughout the year. Finally, the rural station is located in the middle of the forest where local soil resuspension is at a minimum. All of these factors play a role in higher PM_{10} concentrations measured at the suburban station.

Table 4.2 Summary statistics for PM fractions (μg m^{-3}), Al, and Si (ng m^{-3}) at Marmaris and Ankara stations

	Avg ± STD	Median	Max	Min	N
Marmaris					
PM_{10}	37 ± 136	17	3410	0.005	12232
$PM_{2.5}$	14 ± 13	12	237	0.003	12232
PM_1	10 ± 6	9	48	0.002	12230
PM_{10} Al	127 ± 177	72	1610	1.8	299
$PM_{2.5}$ Al	36 ± 94	7.9	902	0.08	307
$PM_{2.5}$ Si	403 ± 490	258	3891	3.44	223
PM_1 Si	110 ± 257	29	2167	0.54	232
Ankara					
PM_{10}	53 ± 66	38	2460	0.23	11248
$PM_{2.5}$	18 ± 18	16	948	0.14	11248
PM_1	12 ± 13	10	611	0.1	11248
PM_{10} Al	792 ± 903	454	6642	10	255
$PM_{2.5}$ Al	340 ± 494	172	4996	3.04	258
PM_1 Al	88.6 ± 151	36	1188	0.51	258
PM_{10} Si	2137 ± 2298	1304	15886	28.1	255
$PM_{2.5}$ Si	852 ± 1168	453	11642	8.1	258
PM_1 Si	223 ± 365	94	2712	0.9	254

$PM_{2.5}$ concentrations are higher in the suburban station. This is not surprising, because a large fraction of $PM_{2.5}$ particles come from anthropogenic sources, whose influence is at a minimum at our rural station. However, please note that all $PM_{2.5}$ particles are not necessarily anthropogenic. As will be discussed later in the manuscript, the mass concentration of $PM_{2.5}$ size fraction increases during dust episodes at our rural station, which indicates that a fraction of $PM_{2.5}$ aerosol at Marmaris may be litophilic in nature.

Unlike PM_{10} and $PM_{2.5}$, PM_1 concentrations are not significantly different in the two stations. Sources of PM_1 aerosols are not as well defined as $PM_{2.5}$ and PM_{10} size

fractions (Bougiatioti et al., 2013). The presence of submicron particles is generally attributed to anthropogenic sources in urban studies (Caggiano et al., 2010; Konishi et al., 2018; Lin, Y., 2017). However, secondary particle formation may contribute significantly to submicron particle mass in the rural atmosphere (Chen et al., 2018; Rai et al., 2016). The similarity of PM_1 mass concentrations in suburban and urban stations can be due to the contribution of secondary particle formation to submicron particle concentrations at the rural station, which is probably masked by anthropogenic primary PM_1 sources at the suburban station.

Calculations with the data from Table 4.2 showed that at the rural station, $PM_{2.5}$ and PM_1 accounted for 38% and 27% of the measured PM_{10} concentration, respectively, indicating that majority of fine particle mass is accounted for by PM_1 size fraction (PM_1 made up 71% of $PM_{2.5}$). A similar pattern was also observed in the suburban station, where $PM_{2.5}$ and PM_1 particles accounted for 33% and 22% of PM_{10} mass concentration, respectively.

4.3.1 Comparison of Particle Size Distribution in Both Stations

Median number size distributions calculated for the study period in both stations are given in Figure 4.2. Distributions were prepared by calculating median values from almost 11000 hourly measurements at each station for each size channel. Number size distributions in both stations were dominated by particles with 0.26 – 1.0 μm diameter. Five modes were observed in both stations. The first mode is not directly observed, but a decrease between 0.26 – 0.6 μm size range implies that there should be a maximum at $D < 0.26$ μm which is the lower limit of our measurement system. Two small modes were observed at 0.67 μm and 2.7 μm. The fourth mode, which is the most pronounced, was at 5.7 μm. There was also a fifth small mode at $D>10$ μm.

Although size distributions measured in rural and suburban stations resemble each other, there are significant differences as well. The differences can be better seen using size profiles given in Figure A3 in the supplementary material. Size profiles

are generated by calculating the contribution of each channel to the total particle number. Submicron particles (D<1.0 µm) have a similar contribution to the total particle number in both stations, 99.3% in the rural station and 99.5% in the suburban station. The contribution of particles in size range between 1 µm and 2.5 µm to total particle number is also not significantly different in the two stations. This particle size range accounts for 0.46% of particle number in rural and 0.37% of total particle number in Suburban stations. However, there is clear difference in contributions of coarse particles (2.5 µm < D < 10 µm) and very large particles (D > 10 µm). Coarse particles account for 0.22% of particle numbers in a rural site, whereas they account for 0.13% of particle numbers in a suburban site. Similarly, 2.5 – 10 µm particles account for 56% of total particle mass in the rural station and 34% of particle mass in the suburban station. The higher contribution of particles in this size range to total particle number and mass may be due to the interception of stronger dust plumes at our rural site on the Mediterranean coast, due to its closer proximity to dust source areas.

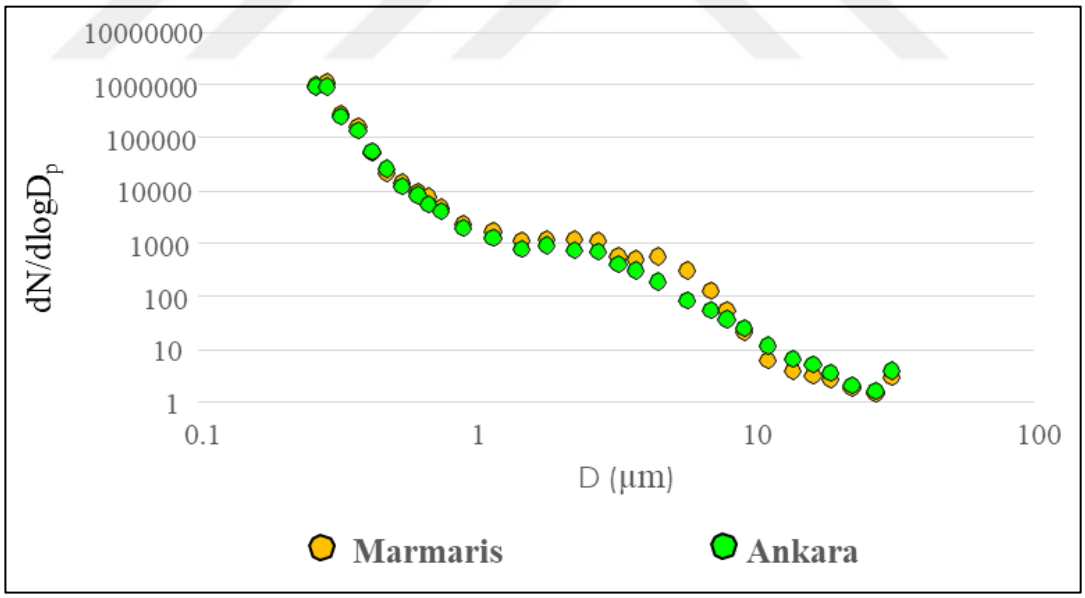

Figure 4.2 Median number size distributions measured in both station

Contributions of very large particles (D>10 μm) to total particle number and mass are also different in the two stations. Unlike coarse particles, which are discussed in the previous paragraph, very large particles account for larger fractions of number and mass concentration at the suburban station in central Anatolia. The contribution of particles with D>10 μm total particle number is 0.001% at the rural station and 0.003% at the suburban station. Numbers are small because such very large particles are not expected to contribute significantly to particle number, but there is a factor of three differences. With all uncertainties in mass computations, discussed previously, particles with D>10 μm accounts for 48% of particle mass at the suburban station and 27% of particle mass at our rural site. Particles of these large sizes do not remain in the atmosphere for long times. For 20 μm – 30 μm to be seen in our measurement channels they should be resuspended near the measurements point. Since our suburban area is in the middle of an arid environment dust resuspends everywhere around our measurement devices. Our rural station, on the other hand, is in the middle of a forest at 1000 m above sea level. There is no source for soil resuspensions near the station. This probably is the main difference between the two stations that affect concentrations of such very large particles.

4.3.2 Flow Climatology

Flow climatology calculations are frequently used to generate information on the transport of pollutants to receptors (Balcilar et al., 2014; Moody et al., 2013), but it is also useful to understand the probability and frequency of dust transport (Córdoba-Jabonero et al., 2011). In this study, air mass flow patterns in the region were calculated using the residence time analysis approach. For this, 5-day long back trajectories were calculated every day for 13 years. Each day, three different trajectories with different starting altitudes (100 m, 500 m, and 1500 m above sea level) were calculated using Hysplit, trajectory model (Draxler & Hess, 1998; Stein et al., 2015). Five-day-long back trajectories consisted of coordinates (x, y, z) of 120 1-hour segments. The study area, which extends from Siberia in the north to the

equator in the south and from the Caspian Sea in the east to the west of the UK in the west is divided into 1°x1° grids and number of trajectory segments at each grid was counted. Since each trajectory segment corresponds to one hour period in the history of the trajectory, total segment counts in grids give how long air masses remained in that grid (in hours), which is the residence time in that grid. Residence times of air masses in grids were mapped using GIS software (MapInfo - Pitney Bowes Software and MapInfo Corporation). Results for rural and suburban stations are depicted in Figure 4.3. All trajectory segments at all starting altitudes were combined to generate this figure. Corresponding figures for each starting altitude were also prepared and given in Figure A4 in the supplementary material. Distributions of residence times at different starting altitudes are not different from distributions depicted in Figure 4.3 for combined trajectory segments. Computations were performed for a 13-year period, which is longer than our study period to minimize year-to-year variations.

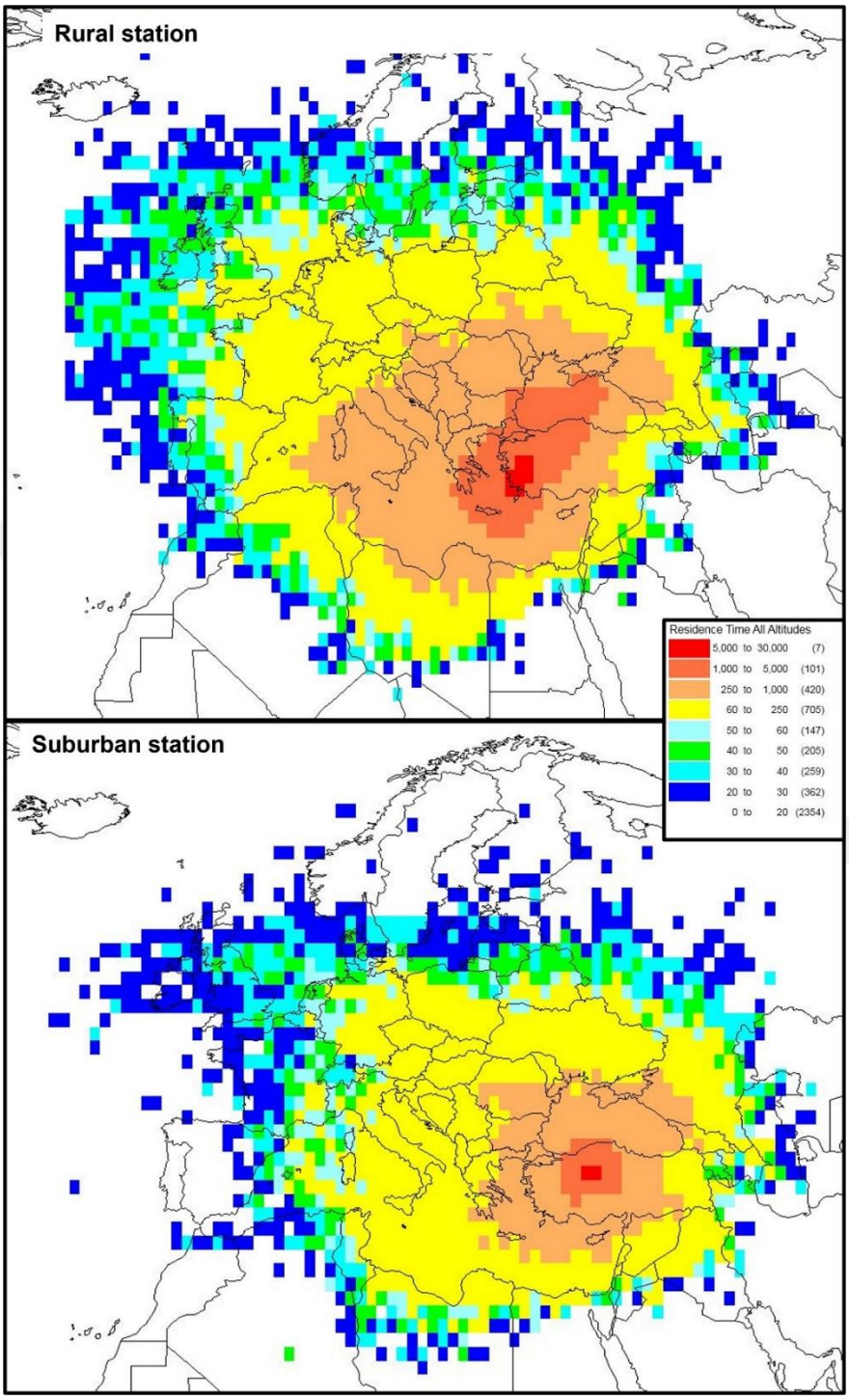

Figure 4.3 Residence times of back trajectories in each 1ºx1º grid in the study region computed for rural and suburban stations. Trajectory segments from trajectories with all starting altitudes were combined.

The highest residence times were observed near stations because every trajectory that advected to the station must go through those grids. However, distribution was not symmetrical and elongated on NW - SE axis. This is a general feature of climatology in this region. Seventy percent of the time air masses come in from the NW sector (Mehta & Yang, 2008).

The differences in upper atmospheric movements of air masses between the summer and winter months were also investigated at both stations. In this case, the number of trajectory segments counted in the winter season is subtracted from the number of segments counted in the summer season. This computation was performed for each grid separately. Results are presented in Figure 4.4 for the rural station and in Figure A5, in the supplementary material for the suburban station.

Yellow and green colored grids are the ones in which air masses spent more time in winter and grids with brown color and its different tones are the ones in which air masses spent more time during the summer season. Air masses that affect both stations have a longer residence time in the North and Northeast direction during summer and the South direction during winter.

Correlation between PM size fractions can provide information about similarities and differences in sources of particles in these size fractions. The correlation between PM_{10}, $PM_{2.5,}$ and PM_1 hourly concentrations in both stations is given in Figure 4.5. PM_{10} and $PM_{2.5}$ were correlated at both stations ($P(r,n)<0.01$) (Figures 4.5a and 4.5c). Please note that with large data sets such as this one, even the R^2 values as low as 0.1 and 0.2 become statistically significant, because "P" (probability of chance correlation) depends not only on the correlation coefficient (r) but also on the number of data points.

At the suburban station, PM_{10} was also correlated with PM_1 [$P(r,n)<0.05$] (Figure 4.5b); however a similar correlation between PM_{10} and PM_1 was not observed at the rural station (Figure 4.5e). The correlation between PM_{10} and PM_1 particles can be attributed to primary sources of PM_1 in our suburban station. Local anthropogenic sources, particularly traffic, generate primary submicron particles (Lin & Lee, 2004).

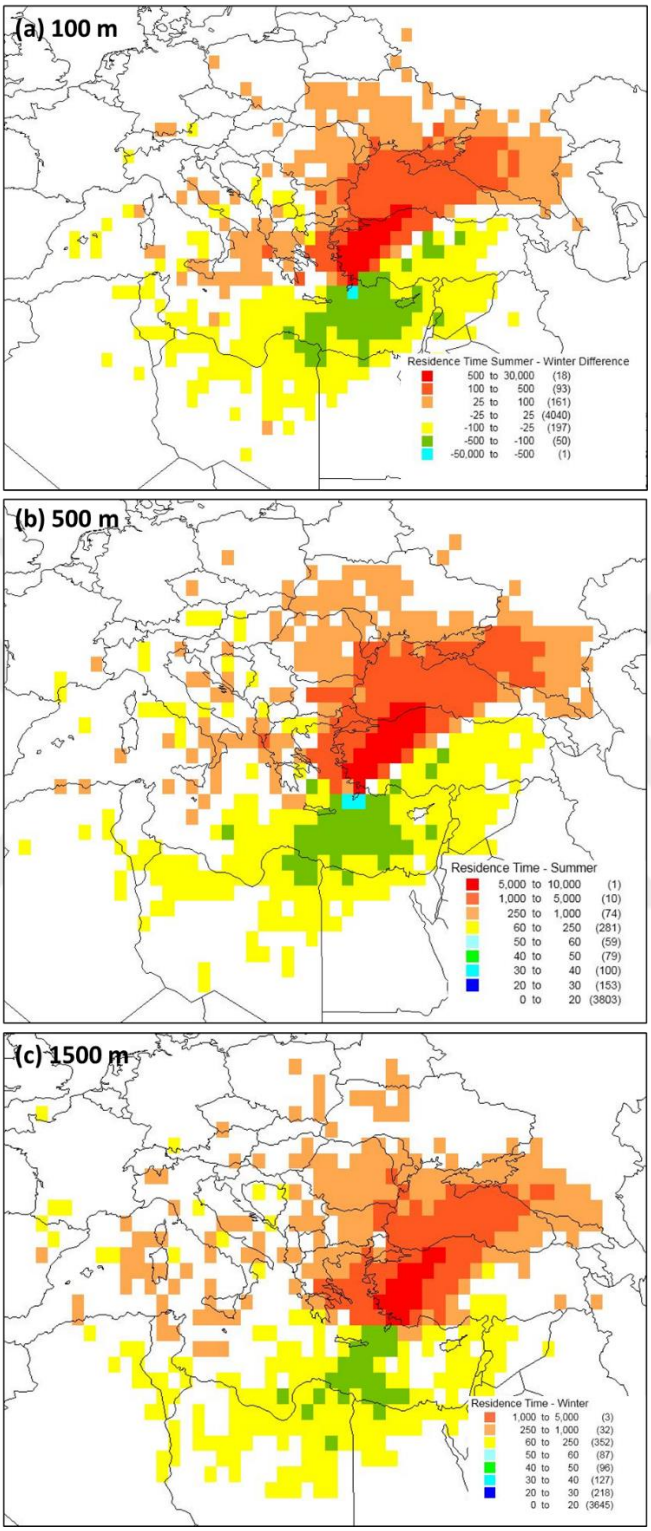

Figure 4.4 Summer – winter difference in residence times of air masses in the study domain at Marmaris station. (a) for 100 m starting altitude, (b) for 500 m starting altitude, and (c) for 1500 m starting altitude.

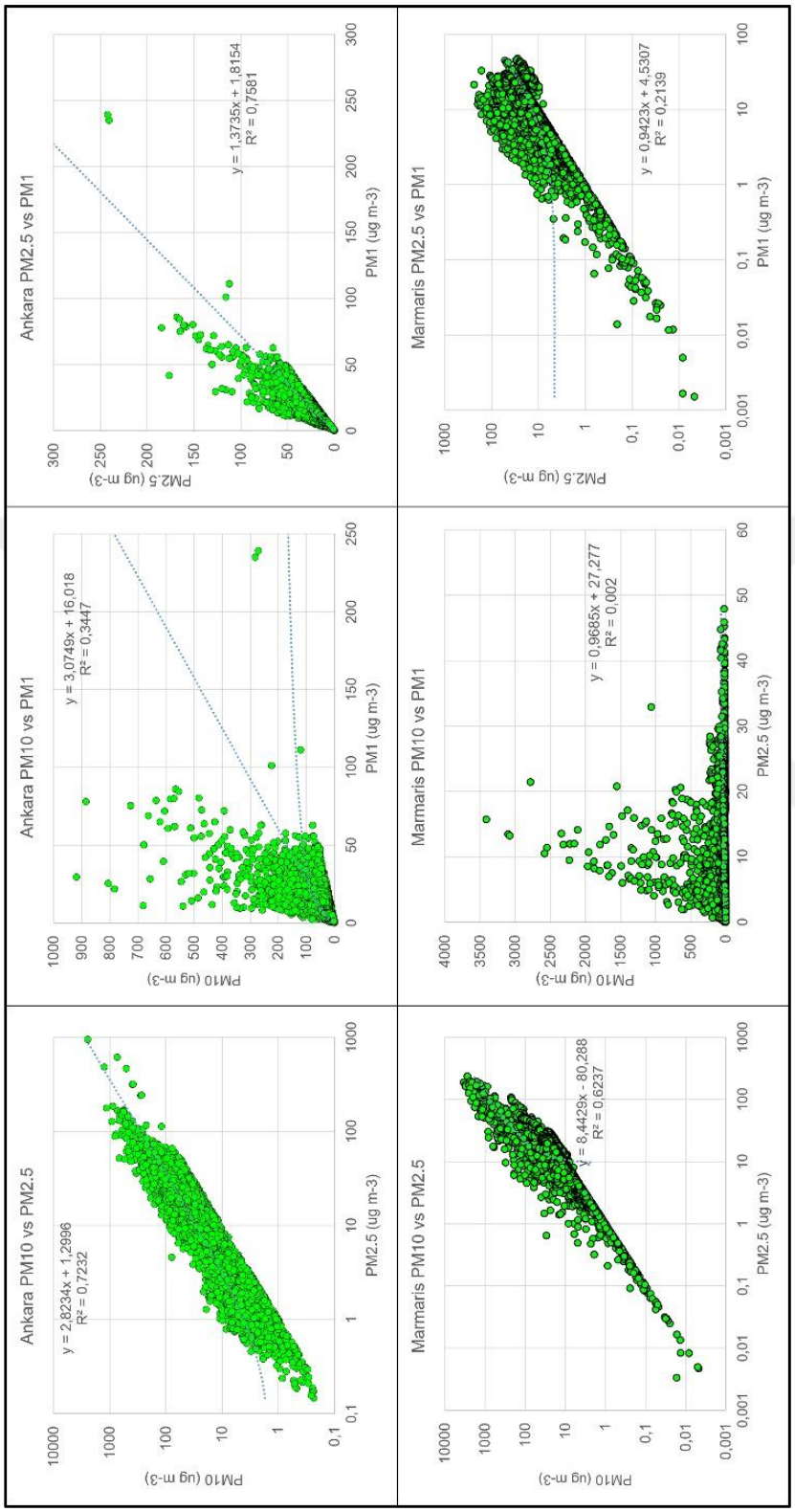

Figure 4.5 Binary correlations between hourly PM size fractions at both stations

Since the same sources also generate some of the PM_{10} particles, a weak correlation between these two size fractions should be expected. However, there is no primary PM_1 source at the rural station. The main source of particles measured in the PM_1 size range is the coagulation of secondary particles formed in the Aitken size range (Carnerero et al., 2021; Pey et al., 2009; Wang et al., 2021). Since sources of PM_{1-10} particles are entirely different (dust transported from Africa, local resuspended soil, sea salt, regionally transported anthropogenic particles), particle concentrations in these size fractions are not expected to be correlated at the rural site. Concentrations decrease with particle size in the lower size range of our measurement devices (see Figure 4.2) due to the secondary formation of smaller-sized particles and their subsequent coagulation into our measurable size range (> 0.26 μm).

There is a reasonably strong correlation between $PM_{2.5}$ and PM_1 at the suburban station [$R^2 = 0.75$, $P(r,n) < 0.01$], while it is not as strong at the rural site ($R^2 = 0.21$). The existence of a correlation between PM_1 and PM_{10} size fractions at suburban and the lack of similar correlation at Marmaris station suggest that primary particles are important contributors to PM_1 concentration at the Ankara station, whereas, coagulation of secondary particles that formed at Aitken range is the main PM_1 source in Marmaris station.

Temporal variations in concentrations of measured parameters were investigated in three steps as episodic events, seasonal variations, and weekday-weekend variations. Weekday-weekend variations are due to variations in anthropogenic source – strength between weekends and weekdays. Since there is no anthropogenic source around the rural station, weekday-weekend variations in number and mass concentrations were only discussed for the suburban station.

Short-term variations in PM_{10} size fraction are depicted in Figure 4.6. 1-minute, 1-hour, and 1-day averages of each particle size for April 2018 are presented as an example. Corresponding plots for $PM_{2.5}$ and PM_1 are given in Figures A6 and A7 in Supplementary Material, respectively. Time series plots from 1-minute measurements showed that PM_{10} concentrations could reach up to 3500 – 4000 μg

m^{-3} and maximum hourly averages were approximately 300 $\mu g/m^3$ at both stations. The maximum daily average concentration is 60 $\mu g/m^3$ at the rural station and 140 $\mu g/m^3$ at the suburban station. The coefficient of variation values for one-minute, hourly, and daily measurements were 93%, 67%, and 41%, respectively, for the suburban station, and 182%, 83%, and 43% for the rural station. The coefficient of variation values was higher for PM_{10} compared to $PM_{2.5}$ and PM_1 at both stations because the PM_{10} fraction is affected more by natural sources, such as dust or sea salt, which are highly episodic. Since both dust and sea salt affect the PM_{10} fraction more than $PM_{2.5}$ and PM_1 size fractions, higher coefficient of variation values at the PM_{10} fraction was not surprising.

Monthly median variations of PM_{10}, $PM_{2.5}$, and PM_1 mass concentrations in both stations are given in Figure 4.7. There is a clear, but different, seasonal pattern in particle mass concentrations in both stations. Summer concentrations are higher in the rural station, but they are comparable in the suburban station. Higher concentrations of secondary inorganic ions, such as SO_4^{2-}, NO_3^- and NH_4^+ during the summer season are frequently reported in the literature (Güllü et al., 1998; Koçak et al., 2004) and attributed to both more effective scavenging of particles in winter (Koçak et al., 2004) and enhanced photochemical particle formation during summer (Ma & Birmili, 2015; Zhang et al., 2012). Secondary inorganic particles are the most important component of particle mass, particularly in the $PM_{2.5}$ size range (Long et al., 2014; Vieno et al., 2014). The seasonal pattern observed in fine particle fraction is expected to be similar to that of SO_4^{2-} and NO_3^-. In the coarse fraction resuspended soil and dust transported from North Africa also contribute to the observed particle mass. Local soil has a higher contribution to particle mass during summer because in winter resuspension is limited due to the muddy surface (Güllü et al., 2005; Öztürk et al., 2012; Yatin et al., 2000). Similarly, dust transport from North Africa is more frequent in April and May (Israelevich et al., 2012; Varga, 2020). Please note that summer in this study starts in April and ends in September, and thus includes April and May as well.

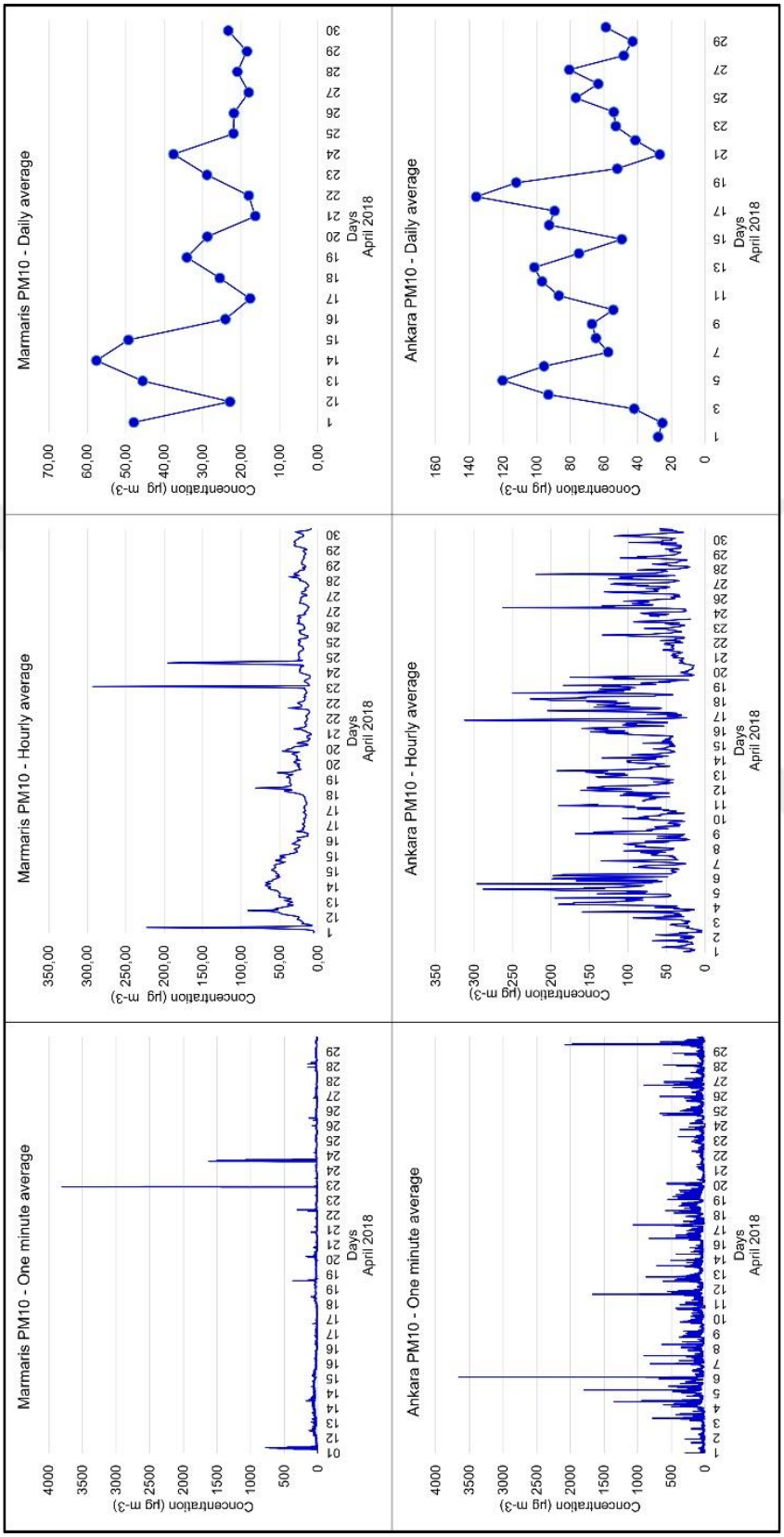

Figure 4.6 1-min, 1-hour, and 24-hour averaged PM_{10} concentrations at Marmaris and Ankara stations, in April 2018.

Seasonal variation is not significant in the suburban station, due to the combined effect of various factors; some favoring high summer and some favoring high winter concentrations. Higher emissions of combustion products in the winter season due to space heating favors high winter concentrations. This particularly affects PM_{10} and $PM_{2.5}$ size fractions. Traffic density is approximately 30% lower in the summer months due to the migration of some of the population to coastal areas in summer (Genc et al., 2010). This factor also favors higher winter concentrations, particularly in PM_1 and $PM_{2.5}$ fractions. Another factor that favors higher winter concentrations is the lower mixing height in winter, which affects all size fractions (Civan et al., 2015). In addition to these factors that favor high PM concentration in winter, there are also processes, which favor higher concentrations in the summer season. One of them is increased soil resuspension in summer (due to dry surface soil), which is effective in coarse fractions. Enhanced photochemistry and increased secondary particle formation in summer. As pointed out in previous sections, secondary particle formation occurs in sizes below our measurement range. However rapid coagulation of those Aitken-sized particles brings them to accumulation mode and into our measurement range. Consequently, seasonal variation in secondary particle formation affects particle number and mass concentration in PM_1 size fraction. Particle concentrations do not change much at our urban station owing to the combined effect of all these factors.

Particle number size distributions, which are shown in Figure A8 in supplementary material support the discussion presented for PM_{10}, $PM_{2.5}$, and PM_1 mass size fractions. In Ankara station, there is not much difference between summer and winter number size distributions for the reasons discussed in previous paragraphs. In the rural station, number concentrations are higher in summer in all sizes, but the summer-winter difference is more pronounced at the coarse fraction (D>2.5 um), due to enhanced local soil resuspension and more frequent dust transport in that period. Higher summer concentrations in the submicron range are due to enhanced secondary particle formation in summer.

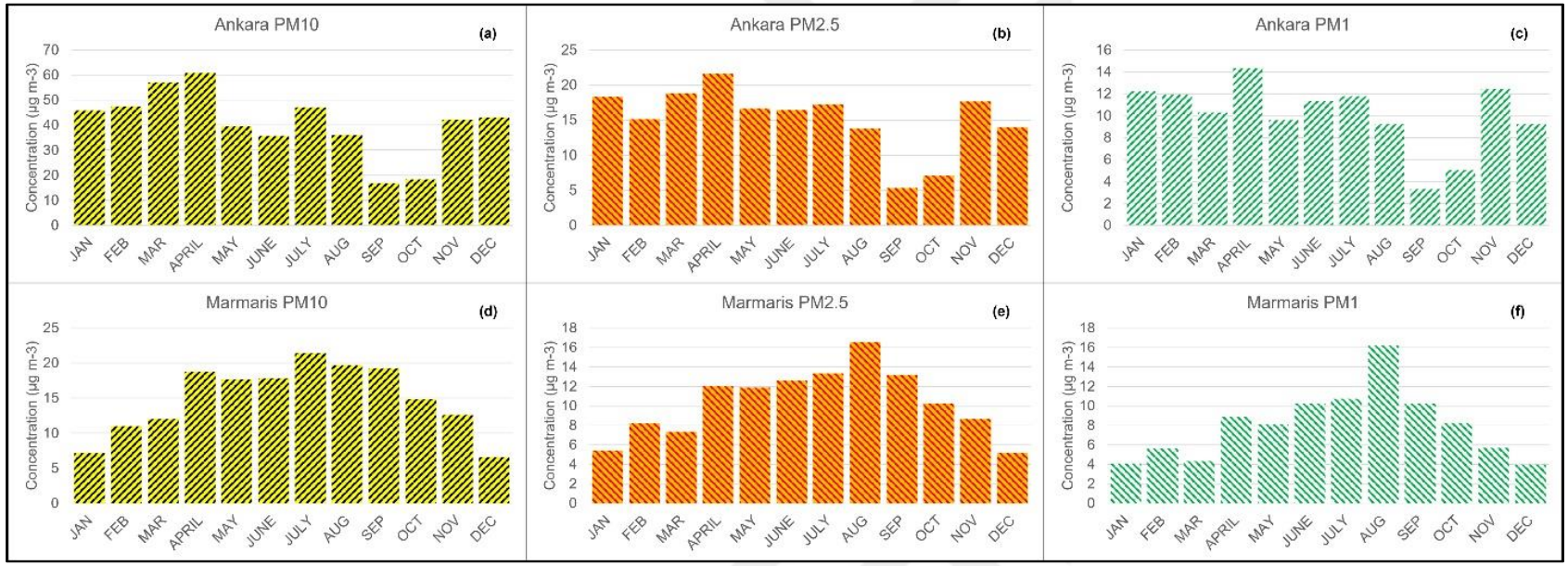

Figure 4.7 Monthly variations of particle size fractions at Marmaris and Ankara stations.

Unlike seasonal variations, particle number and mass concentrations do not show a clear diurnal pattern at the rural station but have a well-defined pattern in the suburban station. These diurnal variations in PM_1, $PM_{2.5,}$ and PM_{10} mass concentrations are depicted in Figure 4.8 along with the number concentrations in selected bins. Mass concentrations in PM size fractions and number concentrations in different size bins showed similar patterns. At the suburban station, mass and number concentrations are low at night, gradually increase, and reach a maximum between 9 and 11 hours, then concentrations decrease in the rest of the day. A slight increase was observed after 18 hours. This pattern resembles traffic emissions, except afternoon rush hour was not observed. The lack of afternoon rush hour peak in number and mass concentrations may be due to compensation of increased traffic emissions by higher mixing height in afternoon hours (Genc et al., 2010). Consequently, particle mass and number concentrations at our suburban station are dictated by traffic emissions.

Particle mass and number concentrations at the rural station did not show a significant diurnal pattern, which is not surprising because there are no primary particle sources around the measurement point. However, a slight increase in particle mass and number concentrations were observed in the afternoon hours, particularly in small size channels (0.265 μm and 1.45 μm). It was first suspected that afternoon increase in concentrations may be due to the transport of pollution-derived particles from low altitude sources to measurement sites by persistent afternoon winds, which is a situation observed in some other mountain-top stations in other parts of Turkey (Tuncel et al., 1994). However, the investigation of wind direction and speed at five automated meteorological stations around our site did not show any persistent wind system that can bring anthropogenic particles to our measurement point. The observed pattern was eventually attributed to enhanced particle formation in smaller sizes with increased solar flux at noon and growth of these particles to our small particle size range.

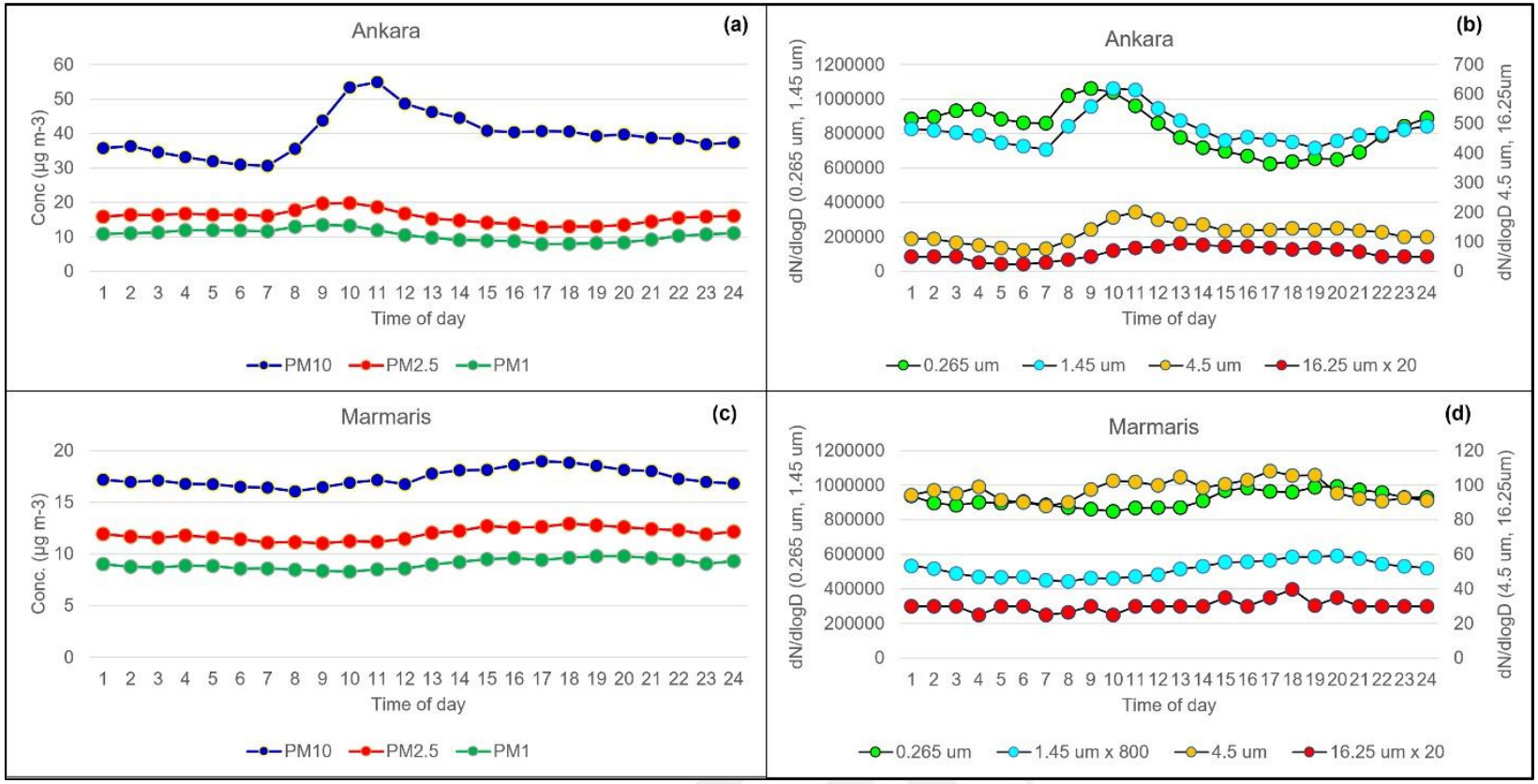

Figure 4.8 Diurnal variation in number and mass concentrations at different size fractions in both stations. PM_1, $PM_{2.5}$ and PM_{10} concentrations in Figures (a) and (c) are mass concentrations. The particle concentrations in different size bins in Figures (b) and (d) are number concentrations in (# L^{-1}).

Weekday – weekend differences in particle mass and number concentrations are expected only at locations that are under the influence of anthropogenic sources because there is no reason for natural sources to have different emissions on weekdays and weekends. Hence, in this study, weekday – weekend differences in particle concentrations are discussed only for the suburban station, which is under the influence of anthropogenic emissions in Ankara.

Weekday and weekend variations in number concentrations are given in Figure A9 for the suburban station. There is no weekend-weekday variation in the rural station as there are no sources that have different source strengths on weekdays and weekends. In the suburban station, the difference is more pronounced in coarse particles (D > 2.5 μm). Although fine particles have also higher concentrations during weekdays, the difference is not statistically significant. This is interesting because in the previous section importance of traffic particles on diurnal variation in particle concentrations was highlighted. Resuspended road dust, rather than primary particle emissions from vehicles determines the weekday-weekend difference in particle number concentrations.

This pattern was also observed at measured PM_{10}, $PM_{2.5}$, and PM_1 concentrations. Median PM_{10} concentrations were found to be 40 $\mu g/m^3$ and 35 $\mu g/m^3$ on weekdays and weekends, respectively. For $PM_{2.5}$, both weekday and weekend concentrations were 15 $\mu g/m^3$. Similarly, for PM_1, weekday and weekend median concentrations were 10 $\mu g/m^3$.

4.4 Conclusions

In this study, the size distribution of particles and the spatial and temporal variation of size distribution are investigated at two stations in Turkey. One of the stations was located in a rural area on the Mediterranean coast of Turkey. The other one was located at a suburban location in Ankara, which is the capital located in the middle of the Anatolian Plateau.

The QA/QC procedures demonstrated that two laser spectrometers that operate in our two stations generate comparable data when operated side-by-side. They also generated comparable data with conventional gravimetric samplers and beta-gauge. Data generated at our suburban station were in general agreement with data generated in 7 air quality monitoring stations in Ankara city. But some deviation in high PM mass concentrations was also observed.

The results obtained showed that there were differences between temporal variabilities recorded in rural and suburban stations. The results were also compatible with the data from national air monitoring stations. Suburban station PM concentrations were higher compared to the rural station at almost all size fractions. Although it is not under the influence of heavy traffic, the primary source of PM was identified as traffic at the suburban station. However, PM_1 sources were not identified. PM_1 contributed almost 70% of the $PM_{2.5}$ concentrations at the suburban station, and it was well correlated with PM_{10}. However, in the rural station, this was not the case as the primary source of PM_1 was secondary formation.

During the study period, the study region was dominantly under the influence of air masses coming from the Northwest. During the summer season, the North and Northeast directions became dominant. Winds from the South were dominant during the winter season. During dust events, the particle sizes shifted towards the smaller fractions. The effect of the seasonality was observed: the winter concentrations were higher at both stations compared to the summer concentrations, and the most significant difference was observed in the coarse size range. Diurnal variation was

not very significant at the rural station. At the suburban station, the variation supported the dominance of the traffic sources. Similarly, higher weekday concentrations of the coarse particles compared to weekend measurements were another confirmation of this observation. After these comparisons, it was clear that the local sources are more dominant at the suburban station compared to particle transport from the dust regions. The effect of dust transport was lost over 600 km distance between the stations.

During the evaluation of the data, both the mass and number concentration measurements were used. Both data provided valuable contributions at different stages of the data evaluation process. However, as mass concentrations were calculated from the number concentration measurements, the uncertainties should always be kept in mind.

CHAPTER 5

MODIFICATION OF SAHARAN DUST SIZE DISTRIBUTION DURING ITS TRANSPORT OVER THE ANATOLIAN PLATEAU

5.1 Introduction

Although PM levels in the atmosphere can be expressed as mass and number concentrations, mass concentration is more frequently used, because current standards are based on mass concentrations, and pollution monitoring to demonstrate compliance or incompliance with standards should include mass measurement. However, mass concentration ignores submicron particle concentrations as their contribution to mass measurements is very small. Sub-micron particles are expressed better using number concentrations (Greig, 2000; Saha et al., 2020). Particle number concentrations are important and are being used more and more frequently due to information it provides on particle sources (Hopke et al. 2022; Liang et al. 2021), new particle formation (Dinoi et al., 2021; Zhu et al., 2021), atmospheric transformations (Wegner et al., 2012), its effect on hydrological cycle (Guy et al., 2021; Merikanto et al., 2009), energy budget and climate (Schmale et al., 2018) and particularly information it provides on health effects of particles (Fuller et al., 2018; Yin et al., 2019). Mineral or desert dust particles mainly occur in regions having dry soil with little or no vegetation resulting in the mobilization of soil particles with the effect of strong winds. More than half of the global atmospheric aerosols originate from deserts in the form of mineral dust. Sahara, Gobi, and Taklamakan deserts are important contributors to such mineral dust emissions.

Desert dust particles, including Asian and Saharan dust, can travel long distances on continental scales in several weeks. Asian dust which becomes airborne from arid regions in Asia, particularly from the Gobi and Taklamakan deserts, is shown to affect air quality in Korea, Japan, and North America (Benedetti et al., 2019). The

influence of Asian dust on other regions such as the North Pacific is also well-documented (Holmes et al. 1997; Holmes and Zoller 1996; Husar et al. 2001; Parrington et al. 1983). The effect of Asian dust is becoming more serious as the concentrations of anthropogenic emissions from Asia are increasing. The increase in industrialization and desertification is the major cause of higher dust emissions in Asia (Benedetti et al., 2019).

Saharan dust can be considered the major producer of particulate matter globally. Dust emission from Africa, which is approximately 400 and 2200 Tg yr^{-1}, accounts for approximately 36% -70% of the global mineral dust emissions (Goudie & Middleton, 2006; Huneeus et al., 2011; Kok et al., 2021; Wu et al., 2020). Dust emitted from Sahara crosses the Atlantic Ocean (Prospero et al., 2021) and reaches the Caribbean (Huneeus et al., 2011; Prospero et al., 2021), different southern states in the US (Bozlaker et al., 2019; Hand et al., 2016), and South America (Kok et al., 2021; Prospero et al., 2020). The Mediterranean region is also under the strong influence of dust transport from North Africa due to the proximity of the source region. Approximately 5% of dust resuspended from the Sahara Desert (which corresponds to 20 – 110 Tg yr^{-1}) ends up in the Mediterranean basin (Calidonna et al. 2020; Rodriguez-Navarro et al. 2018). In addition to litophilic particles, the aerosol population in the Eastern Mediterranean also includes sea salt particles (Koçak et al., 2011; Theodosi et al., 2010), biogenic particles (Ganor et al. 2000; Kocak et al. 2009; Kouvarakis and Mihalopoulos 2002), biomass burning particles (Achilleos et al., 2015; Bossioli et al., 2016; Petroselli et al., 2018), oil combustion particles (Achilleos et al., 2015; Calzolai et al., 2015), urban particles (Achilleos et al., 2015), organic particles (Koulouri et al., 2008; Sciare et al., 2008) and secondary ions (Achilleos et al., 2015; Calzolai et al., 2015). Some of these source types are detected in most studies, and some are unique to certain locations.

In this study, the main goal was to determine the changes in dust particle size distribution during its 600 km-transport over the Anatolian Plateau from the Mediterranean coast to Central Anatolia. For this purpose, two sampling stations were established, one on the Mediterranean coast (a rural station on the Taurus

mountains) and the other one in central Anatolia (a suburban station in Ankara city). Both stations are approximately 1000 m from sea level. PM_1, $PM_{2.5,}$ and PM_{10} mass concentrations and number concentrations of particles in 31 size bins between 0.265 μm and 34 μm were measured at 1-min intervals in these two stations. The contribution of local sources and the effect of meteorological parameters, such as rain and wind speed, on the size distribution of particles, were also investigated. The areas, other than Sahara, that are responsible for crustal particle concentrations measured in our stations were investigated using trajectory clustering. Dust climatology and the contribution of the Middle East and Arabic Peninsula to events recorded in Eastern Mediterranean and central Anatolia are also discussed.

5.2 Materials and Methods

5.2.1 Stations

Particle concentrations were measured in two stations, one on the Mediterranean coast of Turkey (Marmaris station) and the other one in central Anatolia (Ankara station). Locations of stations are given in Figure 5.1. Ankara station was on the Middle East Technical University campus (39°53'13" N, 32°46'59"E). Since the university is in one of the suburbs of Ankara, the station is considered a "suburban station". The altitude of the station is 948 m above sea level (ASL).

The second station was on the premises of Marmaris meteorological radar, which is located approximately 10 km to the northeast of the city of Marmaris on the Mediterranean coast of Turkey (36º53'9" N, 28º19'57" E). It is a rural station because the radar is in the middle of a pine forest in the Taurus mountains. The nearest human activity is in the city of Marmaris. The altitude of the station is 935 m ASL.

For Ankara station, supplementary air quality data were obtained from seven stations in the national air quality monitoring (AQM) network operated by the Ministry of Environment and Urbanization. The AQM data was used to distinguish dust episodes

from anthropogenic episodes. For the rural station, surface meteorological data were obtained from the nearest five automated meteorological stations. Locations of AQM and Meteorological stations around our stations are also depicted in Figure 5.1.

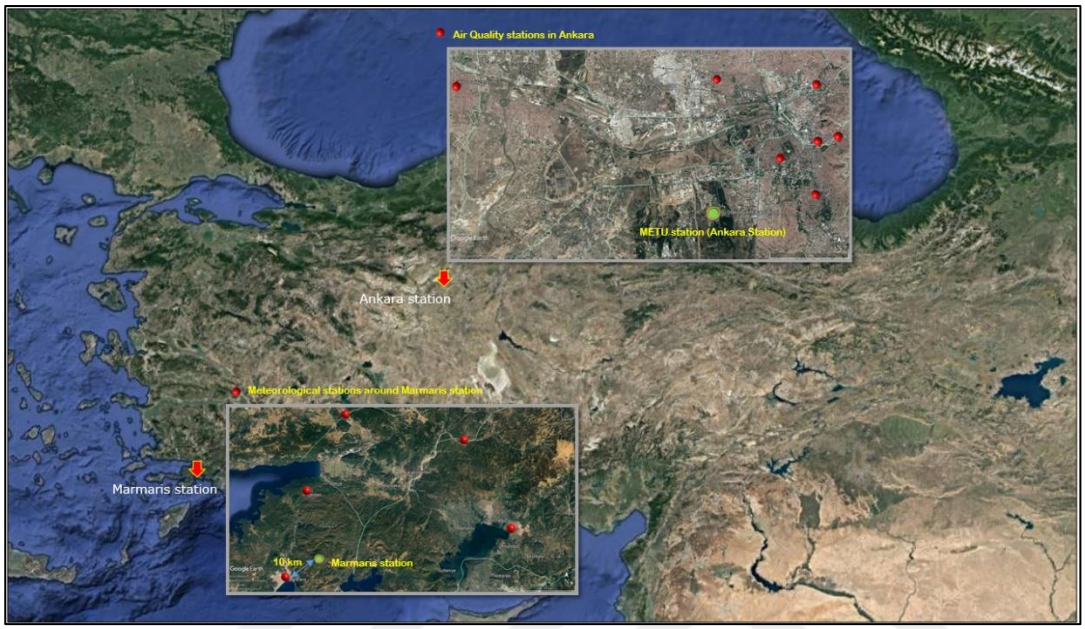

Figure 5.1 Locations of stations.

5.2.2 Instrumentation and Data Validation

In both stations, particle mass concentrations in PM_1, $PM_{2.5}$, and PM_{10} size fractions and number concentrations in 31 size bins between 0.26 and 34 μm size intervals were measured using a GRIMM, Model EDM 164 aerosol dust monitor. Stations were operated between April 1, 2017, and October 31, 2018. Measurement frequency was 1-min, but generally hourly averaged data were used in data treatment because data with one-minute intervals was difficult to handle and was not essential for data evaluation in this study.

Data validation studies were performed before the start of field operations. As part of the data validation exercise, both spectrometers were operated side by side at the suburban station for approximately one month between March 16, 2017, and April 12, 2017, to ensure that similar data (not different with > 99% statistical significance) is

generated in both stations. In addition to the comparison of two spectrometers, one of the aerosol spectrometers was operated side by side with gravimetric and beta-attenuation PM measurement devices to compare PM_1, $PM_{2.5}$, and PM_{10} data. Stations became operational only after ensuring that data generated by our aerosol spectrometers are comparable to corresponding data generated with conventional measurement techniques.

5.3 Results and Discussion

5.3.1 Data

Concentrations of PM_{10}, PM_1, and $PM_{2.5}$ along with Al and Si are summarized in Table 5.1. In both of our stations, daily particle samples were collected and the PM number concentrations were measured. Collected samples were analyzed using energy-dispersive x-ray fluorescence (ED-XRF) spectrometry for fifteen trace elements. Trace element data is not discussed in this manuscript. However, Al and Si data were used in confirming dust episodes as they are good markers for crustal material.

Since all PM fractions have right-skewed distributions (not necessarily lognormal), median concentrations of all parameters are more representative of the data population than average concentrations. Suburban PM_{10} measurements are significantly higher than the corresponding average and median PM_{10} concentration at the rural site. Higher average PM_{10} levels in Ankara station are due to different land cover in our two stations. Anatolian plateau, where our Ankara station is located, is an arid region, where soil can easily be resuspended. Marmaris station, on the other hand, is in the middle of the pine forest and the surface is covered by pine needles which limit the resuspension of soil, resulting in a lower average PM_{10} concentration at Marmaris station.

$PM_{2.5}$ concentrations are higher in the Ankara (suburban) station, which is not surprising because Ankara station is strongly affected by urban anthropogenic emissions. On the other hand, there is no significant anthropogenic activity in the close vicinity of Marmaris (rural) station. Please note that part of the PM_1 mass measured in both stations is from secondary particle formation (Chen et al., 2018; Khan et al., 2015; Niu et al., 2010). This issue will be discussed in more detail in later parts of the manuscript.

At Marmaris station, $PM_{2.5}$ and PM_1 accounted for 38% and 27% of PM_{10} mass concentration, respectively. This also means that PM_1 accounted for 71% of $PM_{2.5}$ mass. The contribution of $PM_{2.5}$ and PM_1 to PM_{10} mass concentration was not significantly different at the Ankara station ($PM_{2.5}$ accounted for 33% and PM_1 accounted for 22% of PM_{10} mass concentration). These are average contributions calculated for the entire measurement period. How they changed during dust episodes will be discussed later in the manuscript.

Table 5.1 Summary statistics of PM_1, $PM_{2.5}$, PM_{10}, Al, and Si concentrations measured in this work

	Average ± std	Median	Max	Min	N
Marmaris (μg m^{-3})					
PM_{10}	37 ± 136	17	3410	0.005	12232
$PM_{2.5}$	14 ± 13	12	237	0.003	12232
PM_1	10 ± 6	9	48	0.002	12230
PM_{10} – Al (ng m^{-3})	127 ± 177	72	1610	1.8	299
$PM_{2.5}$ – Al (ng m^{-3})	36 ± 94	7.9	902	0.08	307
PM_{10} – Si (ng m^{-3})	403 ± 490	258	3891	3.44	223
$PM_{2.5}$ - Si (ng m^{-3})	110 ± 257	29	2167	0.54	232
Ankara (μg m^{-3})					
PM_{10}	53 ± 66	38	2460	0.23	11248
$PM_{2.5}$	18 ± 18	16	948	0.14	11248
PM_1	12 ± 13	10	611	0.1	11248
PM_{10} – Al (ng m^{-3})	792 ± 903	454	6642	10	255
$PM_{2.5}$ – Al (ng m^{-3})	340 ± 494	172	4996	3.04	258
PM_1 – Al (ng m^{-3})	88.6 ± 151	36	1188	0.51	258
PM_{10} – Si (ng m^{-3})	2137 ± 2298	1304	15886	28.1	255
$PM_{2.5}$ – Si (ng m^{-3})	852 ± 1168	453	11642	8.1	258
PM_1 – Si (ng m^{-3})	223 ± 365	94	2712	0.9	254

5.3.2 Cluster Analysis

A cluster analysis was performed on 5-day long back trajectories calculated for every day during our measurement period. Saharan dust is not the only PM source at our stations. Dust from the Middle East, Arabic Peninsula, central Anatolia, sea salt even anthropogenic emissions can contribute to measured PM_{10}, $PM_{2.5,}$ and PM_1 mass and number concentrations.

Clustering trajectories depending on their length and curvature can provide, at least preliminary information on potential locations of PM sources. In cluster analysis, the number of clusters was changed between 2 and 20, and the total root mean square

deviation (TRMS) was calculated for each cluster number at each station, to decide on the total number of clusters to be included in the exercise. A 5% deviation between two consecutive cluster numbers was used as the indicator to select the last cluster number (Brankov et al. 1998).

Back trajectories were grouped into 9 clusters at Ankara and 6 clusters at Marmaris stations. Cluster centroids for both stations are given in Figure 5.2. Back-trajectory groups in each cluster are provided in Figures B1 and B2 in supplementary material, for Ankara and Marmaris stations, respectively. For Ankara station, Clusters 1, 2, and 6 have a moderate length (crossing Entire Europe in 5 days). They are all from W and NW wind sectors. These trajectories are expected to bring anthropogenic emissions from industrialized Western European countries to central Anatolia.

Clusters 3, 5, 7, and 8 consist of short trajectories, which can bring relatively local emissions from Turkey, other Balkan Countries, Ukraine, and the Middle East. Cluster 4 has the longest back-trajectories reaching North America in 5 days. Such very long trajectories extending to North America are reported frequently for different parts of Europe (Li et al., 2002; Markowicz et al., 2016; Trickl et al., 2015) including our previous studies in Eastern Mediterranean and Black Sea regions (Balcilar et al., 2014; Öztürk et al., 2012). These trajectories are reported to bring boreal fire emissions from Canada to Europe (Forster et al., 2001). Cluster 9 has a moderate length and its centroid spends most of its time over the Mediterranean Sea. It should be noted that determining potential source areas affecting a receptor using cluster centroids only may not be a good idea, because trajectories spent a significant period over regions around the centroid. Distributions of trajectories around cluster centroids, which are shown in Figure B1, demonstrate that Saharan Dust transport to Ankara station occurs with trajectories in clusters 6, 7, 9 and 3. Cluster 8, on the other hand, has potential to bring dust from Middle East.

Custer analysis resulted in 6 trajectory groups (clusters) in the Marmaris station. Back trajectories in clusters 1 and 4 were moderately long, crossing entire Europe before they were intercepted at our station. Trajectories in these two clusters are the

ones that are likely to bring anthropogenic emissions from western European countries to the Eastern Mediterranean. Clusters 1 and 4 in Marmaris station are like clusters 1 and 6 in Ankara station, in terms of their length, curvature and direction. Unlike in Ankara station, there is only one cluster consisting of short trajectories, namely cluster 2, which can bring relatively local emissions in Turkey and Balkan countries to the Eastern Mediterranean. Cluster 5 in Marmaris is like cluster 5 in Ankara, but trajectories in Marmaris cluster 5 are longer than trajectories in Ankara cluster 5. However, source areas from which these air masses can pick up and carry emissions to Eastern Mediterranean are not very different. Cluster 6 is very similar to cluster 9 in the Ankara cluster analysis. Trajectories in this cluster spent most of their time over the Mediterranean Sea. Cluster 6 is the one that is most likely to bring Saharan Dust to Eastern Mediterranean. Trajectories in cluster 2, on the other hand, can bring dust from deserts in the Middle East and Arabic Peninsula. However, it should be noted that very few dust events coming from the Middle East and Arabic Peninsula were identified at our Marmaris station. Cluster 3 in Marmaris station is identical to cluster 4 in Ankara station, consisting of very long trajectories extending to North America.

Clusters that are found for Marmaris station are not significantly different from clusters found for Ankara station. This conclusion can even be extended to other parts of Turkey and the Eastern Mediterranean because similar trajectory groups were identified in other studies performed in other parts of the Eastern Mediterranean (Öztürk et al., 2012) and the Black Sea (Genç Tokgöz et al., 2015). Similarities in air mass transport patterns observed in different parts of the Eastern Mediterranean and the Black Sea were also observed in flow climatology calculated in various studies (Balcılar, 2018; Dayan & Miller, 1989; Güllü et al., 1998; Kubilay & Saydam, 1995; Genç Tokgöz, 2013). This similarity in clusters and air mass flow patterns can explain why similar source areas were identified in PSCF calculations performed for different locations in the basin (Doğan et al., 2008; Koçak et al., 2009; Öztürk et al., 2012).

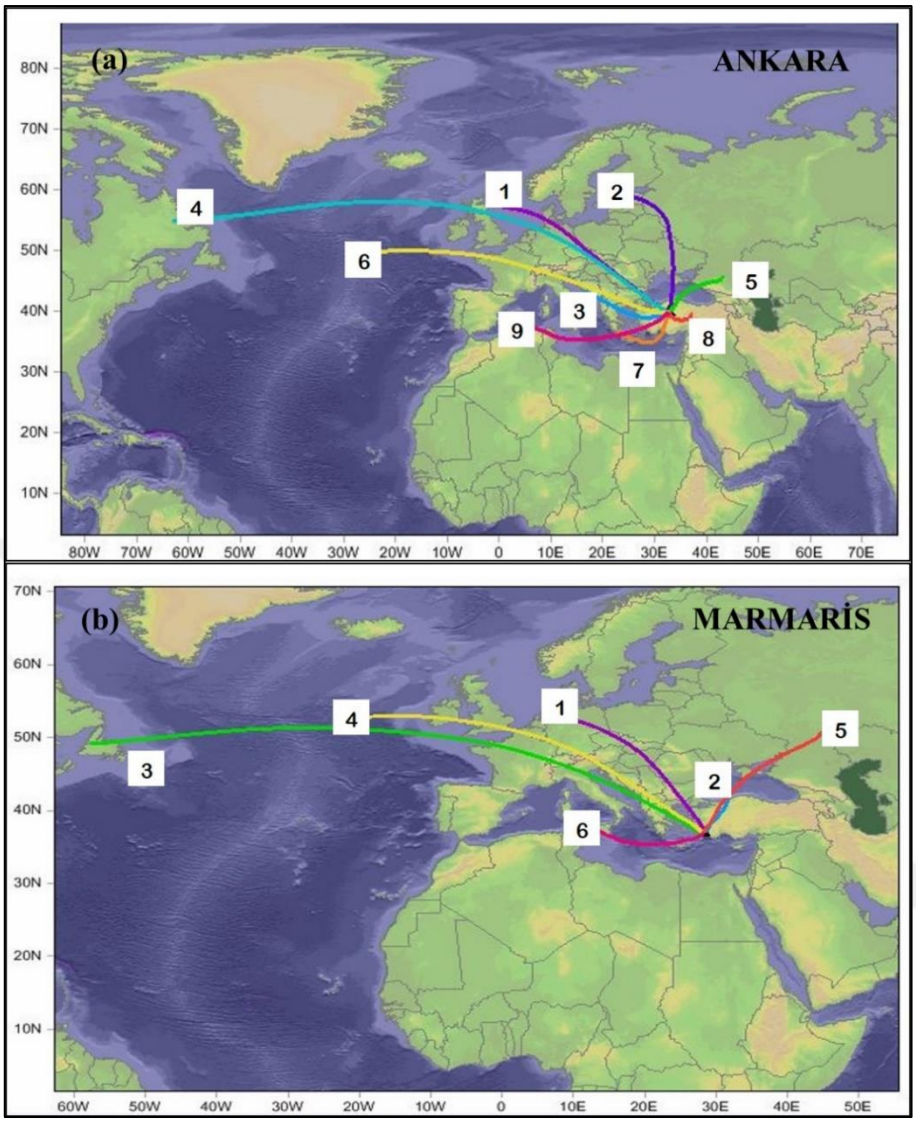

Figure 5.2 Cluster centroids at (a) suburban (Ankara) and (b) rural (Marmaris) stations

5.3.2.1 Particle Size Distribution in Clusters

Number size distributions of particles in each cluster are given in Figure 5.3 for both stations. Number concentrations in each size bin in the figure is the median concentration of particles in that size bin in all trajectories in that cluster. In the figure, logarithmic scaling is not used to highlight inter-cluster differences in small sizes. However, unfortunately, the difference between particle number

concentrations between small and large size bins is so large that all information in large size bins is masked. To avoid this, we also prepared log-scaled size distributions as an inner graph for both stations.

There is not a significant difference between particle number size distributions between clusters in Ankara station. The reason for this can be the masking effect of strong local urban emissions on the size distributions of particles. Inter-cluster differences in the size distribution of particles are larger in the Marmaris station, particularly in small-size bins. Clusters 5 and 2 have the highest and Cluster 3 has the lowest number concentrations in size bins with $D < 0.5$ μm. In coarse fraction, on the other hand, cluster 6 has the highest and cluster 5 has the lowest number concentrations in size bins with diameters between 1.8 and 10 μm. Please note that clusters 5 and 2 consist of trajectories that are expected to bring anthropogenic particles to the Eastern Mediterranean. Cluster 5 from Russia, Ukraine, and Central Turkey and Cluster 2 from Western Turkey and Balkan countries. This means that particles associated with trajectories in these clusters are expected to be smaller, which means that they have higher concentrations in small sizes and lower concentrations in large sizes. High concentration of cluster 6 particles in coarse sizes also makes sense, because Cluster 6 is the cluster that is most likely to bring coarse Saharan Dust to our site. We did not speculate about particles with $D>10$ μm, because concentrations reported for size bins with $D>10$ μm based on one-or-two very large particles counted in these channels, and average or median values generated from that data have high statistical uncertainties.

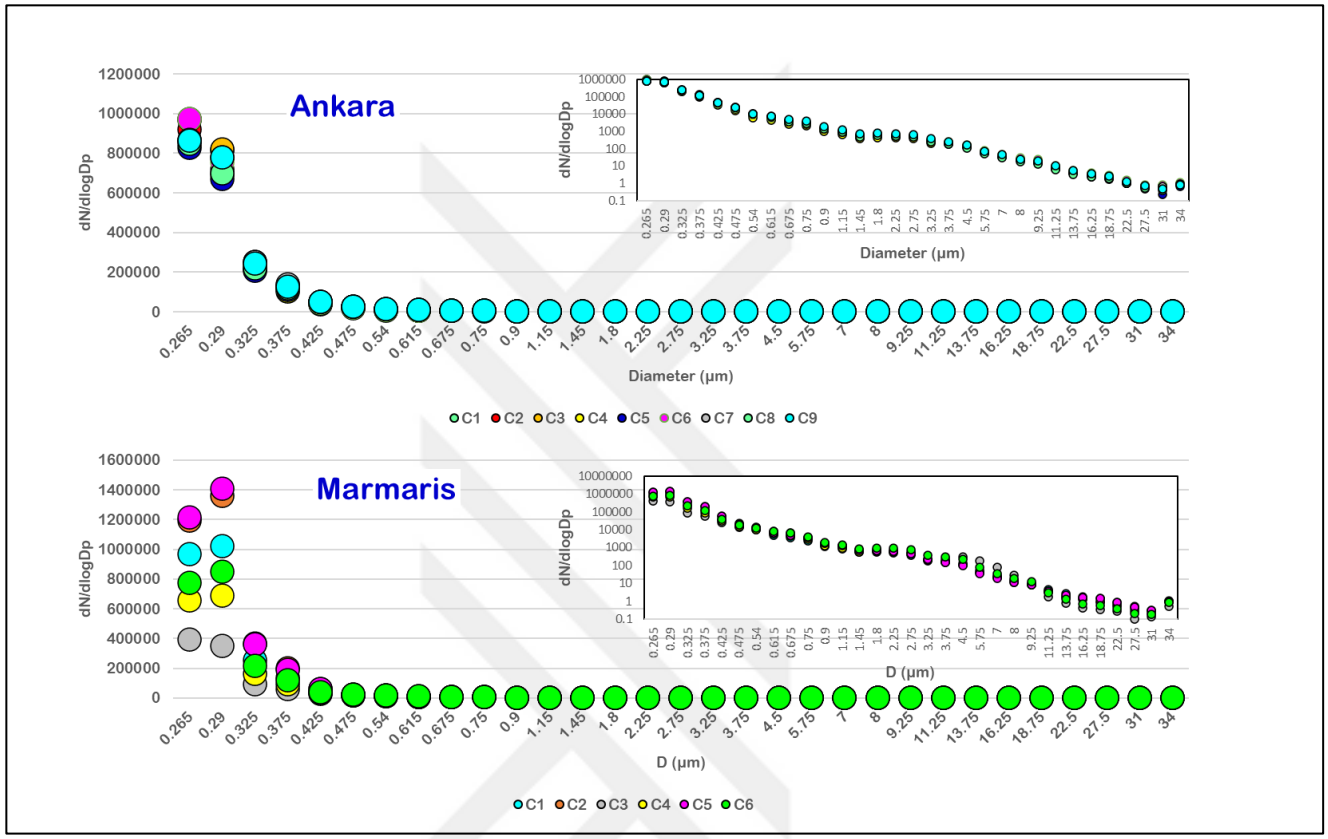

Figure 5.3 Average median particle mass size distributions in each cluster at (a) suburban (Ankara) and (b) rural (Marmaris) stations. Inner graphs are same plots prepared in logarithmic y-scale

5.3.2.2 Particulate Matter Concentrations in Clusters

Median concentrations of PM fractions in each cluster are given in Table 5.2 for both stations. PM_{10} concentrations in Ankara station do not show significant variations between clusters. The highest PM_{10} concentration was measured in Cluster 9, which is not surprising because trajectories in this cluster spent a significant period of their time over North Africa and were most likely to bring Saharan Dust to our Ankara station. Median PM_{10} concentrations were relatively low in Clusters 2 and 4. Low PM_{10} concentrations are expected in Cluster 4 because trajectories associated with this cluster correspond to fast-moving air masses arriving from North America in five days. Concentrations of PM_{10} are low in this cluster as coarse particles are scavenged out during such long-range transport. Trajectories in Cluster 2 have a reasonable length for scavenging coarse particles and there is no known source area for coarse crustal particles in that direction.

In Marmaris station, the lowest PM_{10} concentrations were associated with cluster 3 and the highest in Clusters 2, 5, and 6. The lowest PM_{10} concentration was found in this cluster because it included the longest trajectories crossing the Atlantic Ocean. Please note that the lowest PM_{10} concentrations in the Ankara station were also measured in the corresponding cluster with very long trajectories. High PM_{10} concentrations measured in Cluster 6 are also not surprising because Cluster 6 includes a trajectory group that most likely brings Saharan dust to the Eastern Mediterranean and our Marmaris station. High PM_{10} concentrations measured in Clusters 5 and 2 are interesting because in recent years we started to observe high PM concentrations originating from an emerging dust source area in Konya province in central Anatolia, which is attributed to the drying of a Salt Lake due to over-irrigation. Trajectories in Cluster 5 cross central Anatolia before they are intercepted at our Marmaris station.

In Ankara station, $PM_{2.5}$ and PM_1 median concentrations did not change significantly from one cluster to another. Both $PM_{2.5}$ and PM_1 have strong anthropogenic sources

in Ankara. The lack of inter-cluster differences in median $PM_{2.5}$ and PM_1 concentrations can be attributed to the masking effect of local sources on $PM_{2.5}$ and PM_1 concentrations arriving in the city by long-range transport.

In Marmaris station PM_1 and $PM_{2.5}$ concentrations also do not vary significantly from one cluster to another. The reason for similar PM_1 concentrations in all clusters is the local source for PM_1 particles. Most of the submicron particles measured in the Marmaris station are secondary and have a short atmospheric lifetime, which means they are local, and their concentration does not depend on trajectory groups. The lack of significant difference between clusters in $PM_{2.5}$ concentration is because this sized particle occurs in all sources. Transport of not only anthropogenic emissions, but also transport of soil or sea salt aerosol also brings $PM_{2.5}$ particles. Variation of $PM_{2.5}$ concentration during dust events is discussed later in the manuscript.

Table 5.2 Median concentrations of particle mass fractions in each cluster.

	N	**PM_{10}**	**$PM_{2.5}$**	**PM_1**
			(µg m^{-3})	
		Ankara		
Cluster 1	90	44.4	23.1	17.0
Cluster 2	73	38.5	22.3	15.8
Cluster 3	94	43.9	24.2	18.4
Cluster 4	26	37.6	18.9	13.9
Cluster 5	114	40.2	22.4	15.9
Cluster 6	91	46.3	23.1	16.1
Cluster 7	104	43.5	24.3	18.5
Cluster 8	128	47.7	23.5	17.2
Cluster 9	54	51.3	25.7	18.7
		Marmaris		
Cluster 1	85	14.0	11.0	10.0
Cluster 2	213	18.0	14.0	12.0
Cluster 3	39	11.0	9.2	4.9
Cluster 4	115	13.0	10.0	7.4
Cluster 5	78	19.0	14.0	12.0
Cluster 6	199	19.0	13.0	8.8

5.3.3 Dust Dynamics

Dust dynamics are discussed under four headings; (1) identification of dust episodes, (2) dust climatology (distribution of episodes in a year), (3) comparison of particle size distributions in dust and non-dust periods, and (4) modification of dust size distribution during transport of plume from the Mediterranean coast to Central Anatolia.

5.3.3.1 Identification of Dust Episodes

Detection of episodes is easy because PM_{10} increases to very high concentrations during episodes. However, identifying an episode as a dust episode requires validation, because the observed episode can be due to an incursion of sea salt or an anthropogenic plume to the station. In this study, a four-step validation procedure was used to identify an episode as a dust episode; (i) one of the five-day-long back trajectories, which were calculated every day at three starting altitudes (100 m, 500 m, and 1500 m) follows a path including north Africa, (ii) aerosol optical depth (AOD) and Aerosol index (AI) from Moderate Resolution Imaging Spectroradiometer (MODIS) onboard AQUA and TERRA satellites indicate presence of dust in the grids where our stations are located, (iii) output of the DREAM (Dust Regional Atmospheric Model), which is operated by Barcelona Super Computing Center (BSC) (Haustein et al., 2012; Pérez et al., 2011) predicts an episode in our area and (iv) Al and Si concentrations measured in stations increase significantly during observed events.

Aerosol Optical Depth, AI, back trajectories, and DREAM predictions were then used to assess if the observed lithophilic episode is from Sahara, local soil, or dust from elsewhere (we may receive dust from the Middle East and Arabic Peninsula). An example of the back-trajectories, AOD, AI, and the DREAM output for a day that corresponds to a Saharan Dust episode is given in Figure B3.

In the suburban station, data from regulatory air quality monitoring stations were also used to differentiate between anthropogenic episodes and dust episodes. Although these stations measure local emissions in general, in the case of regional dust transport, an increase in the PM concentrations is observed at all stations as can be seen in Figure B4.

5.3.3.2 Mass Concentrations of PM Size Fractions in Episodes

Dust transport affects the concentration, composition, and size distribution of particles in a region. During the study period, concentrations of particles increased when dust reached stations in all size fractions, except for the PM_1 fraction in the Marmaris station. Concentrations of PM size fractions for both stations, during dust and non-dust periods, are given in Table 5.3. Since dust data are outliers in our PM data set, this increase is more evident in mean concentrations, rather than median concentrations. The highest concentration change during dust events was in the PM_{10} size fraction, which increased by approximately 80% in Marmaris and 60% in Ankara stations during dust events. $PM_{2.5}$ concentrations have also increased, but not as much as the increase observed in the PM_{10} size fraction. PM_1 concentrations, on the other hand, increased approximately 40% in Ankara station but decreased in Marmaris station during dust events.

A significant fraction of PM_1 concentration comes from secondary particle formation (Bougiatioti et al., 2013; Cusack et al., 2013; Freney et al., 2018; Galindo et al., 2020; Perrone et al., 2006; Zhang et al., 2018) Our non-dust period is largely in summer when solar flux is high and secondary particle formation is enhanced. This probably is the main reason for higher PM_1 concentrations observed in the non-dust period in Marmaris. On the contrary, PM_1 concentrations increased during dust events in the suburban station. This is probably due to primary anthropogenic PM_1 emissions in Ankara. These conclusions are supported in Figure 5.4, where the PM_{10}-to-PM_1 ratio is plotted against PM_{10} concentration in both stations. If PM_1 and PM_{10} concentrations were related since both would increase and decrease together, the

PM_{10}-to-PM_1 ratio would not change and the PM_{10}-to-PM_1 ratio vs PM_{10} concentration plot would be a vertical line. However, as can be seen in the figure, the PM_{10}-to-PM_1 ratio is strongly correlated with PM_{10} concentration at Marmaris station, indicating that at our rural station PM_1 concentration is independent of PM_{10} concentration. In Ankara station, on the other hand, the correlation between PM_{10} and PM_{10}-to-PM_1 ratio is not as strong as it is in Marmaris station. There is a statistically significant correlation (in 95% confidence level), but R^2 is 0.25 indicating that the correlation is marginal. The statistical significance of the correlation between two parameters depends not only on the value of the correlation coefficient (r) but also on the number of data points. When there are > 13000 data points, very small r values can be statistically significant, but it does not mean that there is a strong correlation between the two parameters. This lack of strong correlation between PM_{10} and PM_{10}-to-PM_1 ratio in Ankara station is due to the complex relation between PM_{10} and PM_1 in our suburban station and the contribution of primary PM_1 sources, which also emit primary PM_{10} particles. This hypothesis is also supported by the lack of correlation between PM_{10} and PM_1 concentrations in the Marmaris station, which is depicted in Figure B5 in the supplementary material. There is a statistically significant (at 95% confidence level (or P[(r,n) < 0,05]) correlation between PM_{10} - $PM_{2.5}$ concentrations at Marmaris and between both PM_{10} - PM_1 and PM_{10} - $PM_{2.5}$ concentrations in the Ankara station. However, there is no statistically significant correlation between PM_{10} and PM_1 concentrations in Marmaris station, suggesting that most of the measured PM_1 concentration at our rural station originates from secondary particle formation and Saharan dust incursions has no contribution to measured PM_1 levels.

Table 5.3 Average PM_{10}, $PM_{2.5}$, and PM_1 concentrations at Ankara and Marmaris stations during dust and non-dust periods. Concentrations are in ($\mu g\ m^{-3}$)

	Dust			**No Dust**		
	PM_{10}	$PM_{2.5}$	PM_1	PM_{10}	$PM_{2.5}$	PM_1
			Marmaris			
Mean	113 ± 292	21.1 ± 25.2	7.7 ± 5.9	20.0 ± 51.2	12.6 ± 7.2	10.6 ± 6.2
Median	30	13.0	6.4	17.1	12.0	9.7
N	1851	1851	1850	9722	9722	9721
	$PM_{10}/PM_{2.5}$	**PM_{10}/PM_1**	**$PM_{2.5}/PM_1$**	**$PM_{10}/PM_{2.5}$**	**PM_{10}/PM_1**	**$PM_{2.5}/PM_1$**
	5.4	14.7	2.7	1.6	1.9	1.2
%	**$PM_{2.5}$ in PM_{10}**	**PM_1 in PM_{10}**	**PM_1 in $PM_{2.5}$**	**$PM_{2.5}$ in PM_{10}**	**PM_1 in PM_{10}**	**PM_1 in $PM_{2.5}$**
	19	6.8	36	63	53	84
			Ankara			
Mean	90.5 ± 97.4	27.9 ± 28.9	16.5 ± 17.8	33.1 ± 25.1	15.4 ± 8.7	9.7 ± 6.9
Median	64.5	22.7	13.3	30.9	13.2	8.9
N	2977	2977	2977	7737	7737	7737
	$PM_{10}/PM_{2.5}$	**PM_{10}/PM_1**	**$PM_{2.5}/PM_1$**	**$PM_{10}/PM_{2.5}$**	**PM_{10}/PM_1**	**$PM_{2.5}/PM_1$**
	3.2	5.5	1.7	2.5	3.4	1.4
%	**$PM_{2.5}$ in PM_{10}**	**PM_1 in PM_{10}**	**PM_1 in $PM_{2.5}$**	**$PM_{2.5}$ in PM_{10}**	**PM_1 in PM_{10}**	**PM_1 in $PM_{2.5}$**
	31	18	59	40	29	72

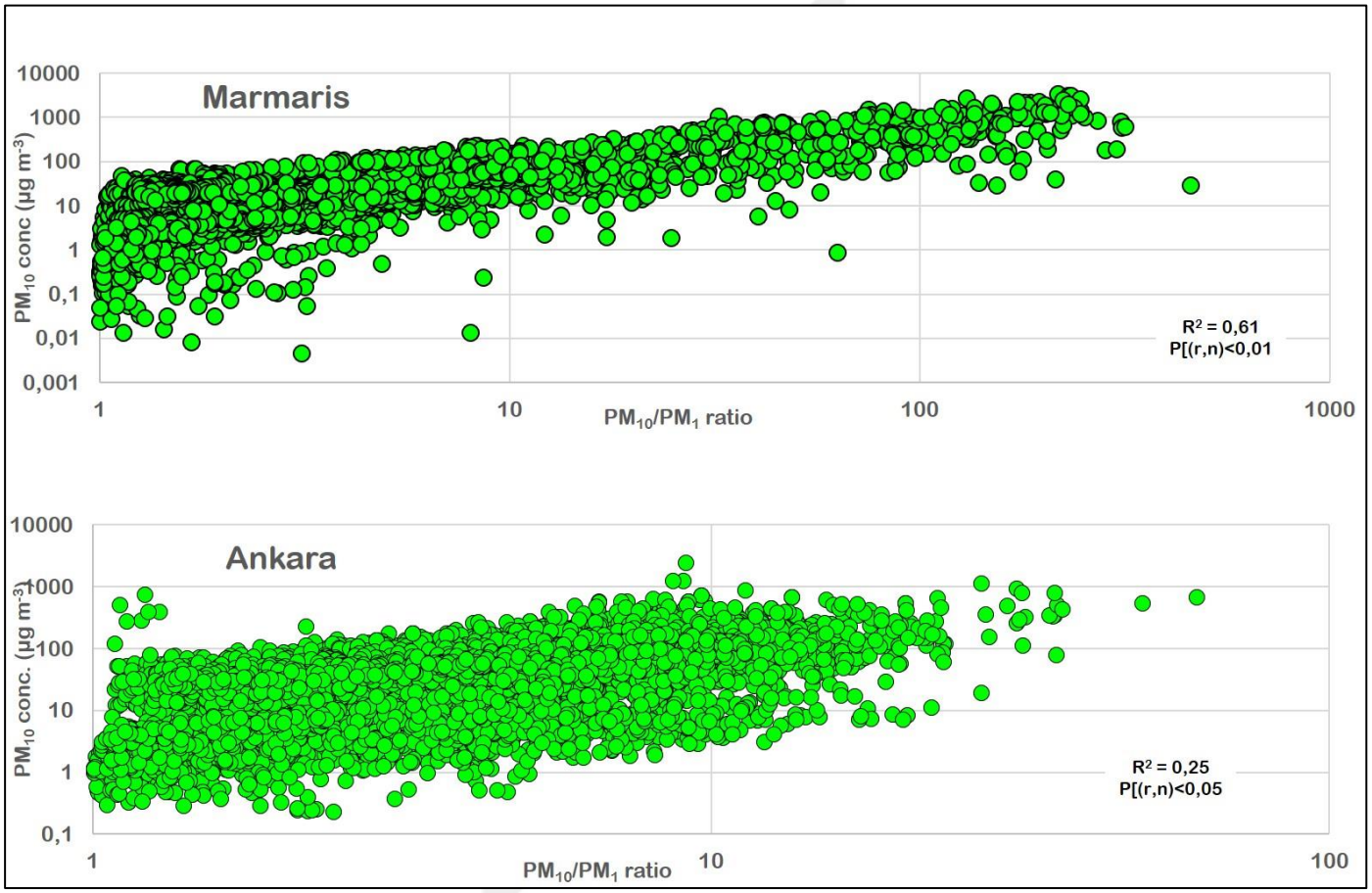

Figure 5.4 Variation of PM_{10}-to-PM_1 ratio with PM_{10} concentration in both stations.

5.3.3.3 Particle Number Size Distributions During Episodes

Number size distributions at both stations during episodes and non-episode days are given in Figure 5.5. Number concentrations at each size bin for the dust period were determined by taking the median value of number concentrations at each size bin in all dust hours. A similar calculation was done for non-dust hours to find the median number size distribution for the non-dust period.

In the Marmaris station, concentrations during the non-dust period are higher in the smallest five-size bins (D< 0.42 μm). The average dust-to-non-dust concentration ratio in this size range is 0.48 ± 0.11. This observation explains why PM_1 concentrations are high during the non-dust period, which was discussed in the previous section.

In Ankara station, there is no significant dust – the non-dust difference in particle number concentrations in this size range (D<0.42 μm), probably due to the contribution of anthropogenic primary PM_1 emissions (such as traffic emissions), which are not different in dust and non-dust periods of the study. Dust-to-nondust concentration ratio in Ankara for D < 0.425 μm is 1.44 ± 0.22.

Dust period concentrations are higher in all size bins between 0.5 μm < D < 15 μm. Since litophilic component in the Eastern Mediterranean aerosol population has a mass median diameter of approximately 3.1 μm (Kuloglu & Tuncel, 2005), it would be reasonable to consider this region as the size range impacted by dust. The average dust-to-non-dust concentration ratio in this size range is 2.2 ± 0.9 and 2.4 ± 0.3 at Marmaris and Ankara stations, respectively. It is obvious that dust doubles particle numbers between 0.5 μm and 15 μm in both stations.

For D > 15 μm there is not a significant difference between dust and non-dust periods in both stations. Dust-to-non-dust ratios in these size bins are 1.2 ± 0.5 at Marmaris and 1.2 ± 0.3 at Ankara stations. Since there are very few particles in D > 15 μm channels, averaging was carried out with these few particles.

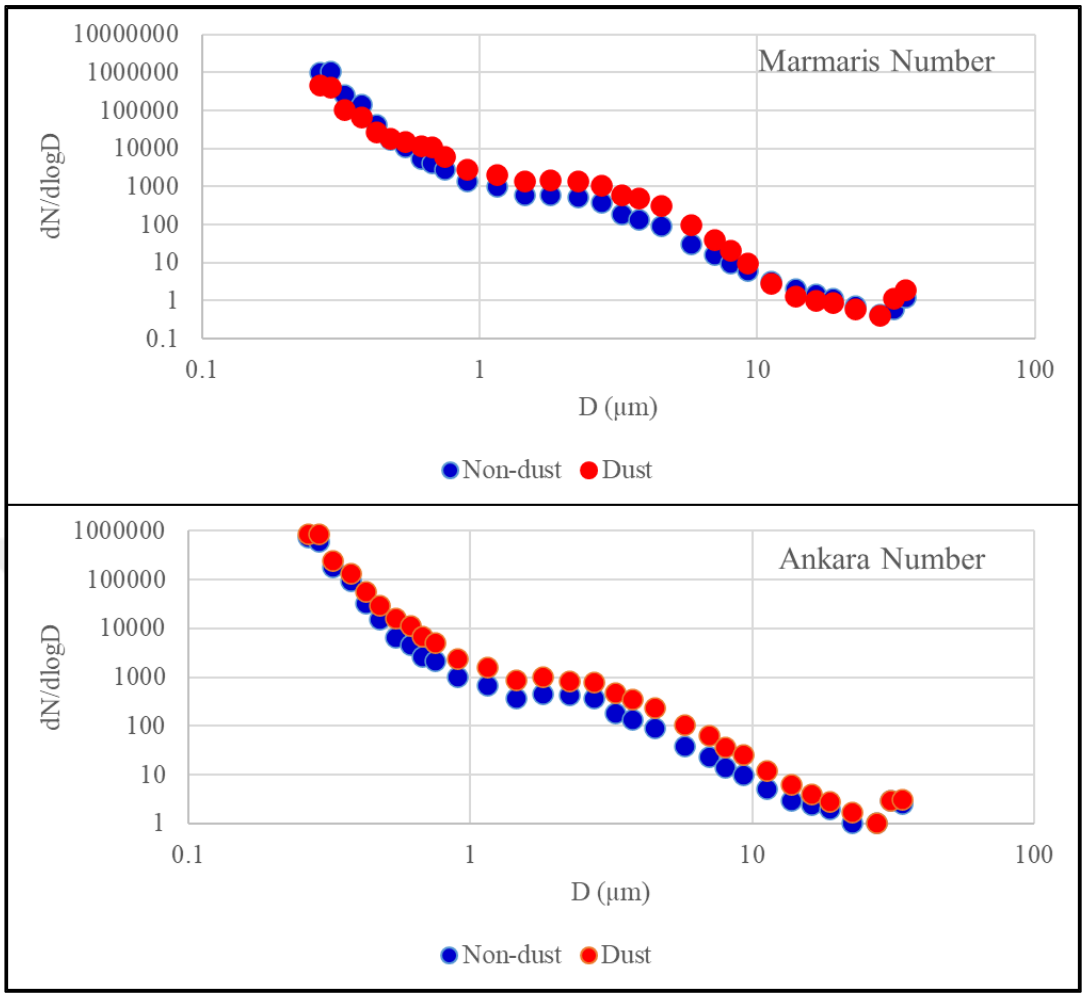

Figure 5.5 Particle number size distributions for dust and non-dust days at the suburban (Ankara) and the rural (Marmaris) stations

5.3.4 Dust Climatology

48 episodes in Marmaris and 42 episodes in Ankara stations were identified based on back trajectories, MODIS data, DREAM outputs, satellite pictures, and Al and Si concentrations, as discussed earlier in the manuscript. In Marmaris station, 26 of these 48 episodes were from Sahara, 6 were from the Middle East and Arabic peninsula and 16 were "non-dust" episodes. The concentration of PM was high in these non-dust episodes, but they were not validated as dust episodes originating from known dust source regions, based on criteria used in confirming dust episodes.

In Ankara station 18 episodes were from Sahara, 8 from the Middle East and 16 were non-dust episodes. Episodes were longer in Ankara station. The total duration of episodes during the study period is 721 hours in Marmaris and approximately 2000 hours in Ankara station, resulting in 20 and 48 hours per episode average duration in Marmaris and Ankara stations, respectively. The difference is not specific to an episode type but is observed in all episode groups. The reason for this difference is not clear, but plumes spread out during transport over the Anatolian plateau.

The seasonal distribution of episodes in both stations is given in Table 5.4. It is well documented that the transport of dust from North Africa to the Eastern Mediterranean is most frequent in Spring (Gkikas et al., 2015; Kaskaoutis et al., 2007; Masson-delmotte et al., 1998) and in some years in winter (Floutsi et al., 2016; López-Caravaca et al., 2021; Mărmureanu et al., 2019). The increase in winter episodes in recent years was also reported (Varga, 2020). Seasonal distribution of episodes in our stations followed this general pattern with certain modifications.

In Marmaris station, most of the events, occurred in the winter and spring months (76% of events occurred between November and May). Saharan dust events are more frequent in Spring, but some Saharan Dust events are also observed in winter months, as reported in the literature. There were too few events that originated from the Middle East to discuss their distribution. However, three out of 6 Middle East events occurred in October.

Non-dust events in Marmaris station depicted a well-defined seasonal pattern with significantly higher frequencies (73% of 16 non-dust episodes) occurring in winter. This pattern suggested that most of the non-dust episodes observed in Marmaris station are sea-salt episodes. Higher winter occurrences are due to the enhanced bubble bursting process with higher winds in the winter season. There are also other indications supporting our conclusion that non-dust episodes in Marmaris are sea salt episodes. During these episodes, $PM_{2.5}$ concentration did not increase significantly and PM_1 concentration did not change at all. If these episodes were anthropogenic fine particle concentration is expected to increase during the episode. Concentrations

of Na, which is a good marker for sea salt and measured at daily intervals during our measurements at Marmaris station were high in most (but not all) of the non-dust episodes. With all these indications we concluded that non-dust episodes in Marmaris station are sea salt episodes. Observed seasonal pattern in non-dust episodes also suggests that high frequencies of winter episodes reported in studies where the type of episode is not distinguished may be due to sea salt, rather than Saharan Dust transport.

In the Ankara station, episodes were observed mostly in spring (49% of episodes occurred in April, May, and June). A high frequency of episodes in winter was not observed in Ankara. Probably because, unlike in Marmaris, non-dust events in Ankara are not sea salt episodes and hence do not occur only in the winter season. The observed pattern in Ankara station is determined by the frequency of Saharan Dust transport. As in Marmaris station, Middle East dust events are too few to have a meaningful monthly distribution. Non-sea salt episodes in Ankara are mostly anthropogenic, because when PM_{10} concentration increases during a non-dust episode $PM_{2.5}$, PM_1 concentrations also increase, which was not the case in Marmaris station. In addition to fine particle mass concentrations, SO_2 and NO_2, which are good markers for local, anthropogenic emissions also increase during "no-dust" episodes.

Please note that the number of dust episodes was obtained from an 18 months-long study and the statistical uncertainty of results is expected to be high, particularly considering the high inter-annual variability of dust events reaching the eastern Mediterranean atmosphere (Kaskaoutis et al., 2007). Measurements are continuing both in Ankara and Marmaris stations. More extensive data will be available in the coming years to discuss dust climatology with better statistical uncertainty.

Table 5.4 Monthly distribution of episodes and their durations.

	Marmaris								Ankara							
	Total		Saharan Dust		Middle East Dust		Nondust		Total		Saharan Dust		Middle East Dust		Nondust	
	# of episodes	Duration Hr	# of episodes	Duration Hr	# of episodes	Duration Hr	# of episodes	Duration Hr	# of episodes	Duration Hr	# of episodes	Duration Hr	# of episodes	Duration Hr	# of episodes	Duration Hr
JAN	3	116	1	6	1	46	1	64	0	0	0	0	0	0	0	0
FEB	6	267	5	261			1	6	0	0	0	0	0	0	0	0
MAR	5	306	4	304			1	2	2	262	2	262	0	0	0	0
APR	6	172	2	33	1	49	3	90	8	869	3	348	3	245	2	276
MAY	6	187	4	150	1	35	1	2	6	569	6	569	0	0	0	0
JUN	2	31	1	26			1	5	7	329	3	191	0	0	4	138
JUL	4	52	1	46			3	6	4	453	2	169	1	114	1	170
AUG	0	0	0	0			0	0	2	97	0	0	0	0	2	97
SEP	1	66	1	66			0	0	4	597	2	282	2	315	0	0
OCT	6	140	3	9	3	131	0	0	4	168	0	0	1	39	3	129
NOV	3	185	1	61			2	124	2	126	0	0	1	37	1	89
DEC	6	333	3	220			3	113	3	208	0	0	0	0	3	208
Total	48	1855	26	1182	6	261	16	412	42	3678	18	1821	8	750	16	1107

5.3.5 Contribution of episodes on annual average PM_{10}, $PM_{2.5}$, and PM_1 concentrations

The contribution of Saharan dust to PM_{10} concentrations was discussed in several studies in the Eastern Mediterranean and the Black Sea basins and reported to be between 19% and 62% (Balcılar, 2018; Güllü et al., 1998; Liora et al., 2016; Öztürk et al., 2012; Scerri et al., 2016; Genç Tokgöz, 2013). The results are presented in Table B1. With few exceptions (Güllü et al., 1998; Scerri et al., 2016) Saharan dust is not differentiated from other dust sources, such as dust from the Middle East or local soil, in these studies. Since we were able to identify and separate Saharan Dust episodes from dust originating from the Middle East and Arabic peninsula and episodes which are not dust, we were able to calculate the contribution of different episode types on annual average PM_{10}, $PM_{2.5,}$ and PM_1 concentrations measured in Marmaris and Ankara stations. For this, data corresponding to episode hours was selectively deleted and average concentrations were recalculated. Results are given in Table 5.5.

All episodes, without differentiating the type accounted for 46% of the annual average PM_{10} concentration in Marmaris and 33% in Ankara. Episodes accounted for 10% of $PM_{2.5}$ concentration at Marmaris but 23% in Ankara, probably indicating the contribution of anthropogenic urban sources to fine particle concentrations in Ankara. Episodes accounted for 18% of PM_1 concentration in Ankara, which means the average PM_1 concentration decreased by 18% when episode data is removed from the data set. However, in Marmaris station, the average PM_1 concentration increased by 5% when episode PM_1 data is deleted. This is due to enhanced secondary particle formation in summer, with high solar flux, as discussed earlier in the manuscript. Similarly, higher concentrations of PM_1 during the non-episode period were not observed in Ankara, because there are strong sources of primary submicron particles, such as traffic, which emits both during the episode and non-episode periods.

Saharan dust episodes accounted for 32% and 8% of annual average PM_{10} and $PM_{2.5}$ concentrations in Marmaris station, respectively. However, PM_1 concentration increased 3% due to enhanced secondary particle formation in summer when there are few Saharan dust episodes. These contributions also indicate that, although Saharan dust plumes consist of coarse particles, there is a small $PM_{2.5}$ component as well.

In Ankara station, on the other hand, Saharan Dust plumes contributed 12%, 10%, and 7% of measured PM_{10}, $PM_{2.5,}$ and PM_1 concentrations, respectively. Saharan Dust has a smaller contribution to PM_{10} mass in Ankara. This is partly because the annual average PM_{10} concentration is higher and the number of Saharan Dust events is fewer (26 at Marmaris and 18 in Ankara) in Ankara station. The contribution of North African dust to $PM_{2.5}$ is comparable in both stations. Please note that when it comes to fine particles, it is difficult to differentiate how much $PM_{2.5}$ and PM_1 are from dust and how much from the high local, anthropogenic background in Ankara station.

The contribution of Middle East dust to annual average concentrations of all size fractions is small in both stations owing to the very small number of such events. The contribution of non-dust events to annual average concentrations of PM size fractions is also small (<10%) in both stations. As pointed before in the manuscript, non-dust Episodes have different sources in two stations. In Marmaris station, which is approximately 10 km from the coastline these episodes are due to sea salt. In Ankara station, on the other hand, non-dust episodes are due to anthropogenic emissions, which is supported by their covariance with SO_2 and NO_2 measured in the air quality monitoring network in Ankara. One would expect a higher contribution of non-dust episodes to $PM_{2.5}$ and PM_1 concentrations in Ankara station. However, the contribution of non-dust episodes was 4% to PM_{10}, 3% to $PM_{2.5,}$ and 4% to PM_1 concentration. This is attributed to the small number of non-dust episode events (16 events) and their shorter duration. The average duration of non-dust events was 69 hours, whereas the average length of Saharan Dust events was 101 hours in Ankara station.

Table 5.5 Contribution of episodes to PM_{10}, $PM_{2.5}$, and PM_{10} average concentrations

	Marmaris		Ankara	
	Avg ± σ µg m^{-3}	**Decrease %**	**Avg ± σ µg m^{-3}**	**Decrease %**
All data				
PM_{10}	37 ± 136		53 ± 50	
$PM_{2.5}$	14 ± 13		18 ± 52	
PM_1	10 ± 6		12 ± 17	
All episodes deleted				
PM_{10}	20 ± 50	46	35 ± 29	33
$PM_{2.5}$	12 ± 7	10	14 ± 30	23
PM_1	10 ± 6	-5	10 ± 9	18
Saharan Dust episodes deleted				
PM_{10}	25 ± 77	32	46 ± 42	12
$PM_{2.5}$	13 ± 9	8	16 ± 44	10
PM_1	10 ± 6	-3	11 ± 13	7
Middle East dust episodes deleted				
PM_{10}	35 ± 134	4	48 ± 44	9
$PM_{2.5}$	14 ± 12	2	17 ± 47	6
PM_1	10 ± 6	0	11 ± 16	5
Non-dust episodes deleted				
PM_{10}	35 ± 129	6	50 ± 49	4
$PM_{2.5}$	14 ± 12	0	17.6 ± 51	3
PM_1	10 ± 6	-2	11.5 ± 16	4

5.3.6 Variation of Particle Size Distribution During Transport

One of the objectives of this study was to determine if particle size distribution in dust plumes changes as the plume travels between the Marmaris station on the Mediterranean coast and Ankara station approximately at the center of Anatolia. Since there is approximately 600 km between the two stations, some modification in the size distribution of particles due to particle scavenging was expected. Such an evaluation cannot be done by combining dust period data in each station, because it

was demonstrated earlier in the manuscript that the two stations do not always intercept dust plumes from the same source regions. For this reason, episodes that affected both stations were selected based on back trajectories, DREAM model outputs, and satellite data and pictures. This information for the common episode intercepted on June 28, 2018, at Ankara station is given in Figure 5.6. Six such common episodes were identified. The time these dust episodes were intercepted at stations, their duration in each station, and the episode number they correspond to at Marmaris and Ankara stations are given in Table 5.6. Most common episodes are first measured in Marmaris station before they were detected in Ankara, as expected. There is no standard travel time between stations. Four of the six episodes arrived in Ankara 1 or 2 days after they were intercepted in Marmaris station. However, episode 2 was observed in both stations on the same day and episode 1 was observed in Ankara station four days after it was observed in Marmaris station. Typical travel time is 1 or 2 days, but there are frequent exceptions due to air mass velocity, which can be highly variable. The duration of episodes is approximately 48 hours in both stations. However, Episode 5 lasted 24 hours longer in Ankara station.

Table 5.6 Dates and durations of common episodes observed in both stations

Common	**Date observed at**		**Marmaris**	**Ankara**
Episode No	**Marmaris**	**Ankara**	**episode no**	**Episode No**
1	9.5.2017 (48 h)	13.5.2017 (48 h)	6	6
2	26.7.2017 (48 h)	26.7.2017 (50 h)	13	13
3	12.3.2018 (48 h)	14.3.2018 (60 h)	38	26
4	18.3.2018 (48 h)	19.3.2018 (48 h)	40	27
5	21.5.2018 (48 h)	23.5.2018 (72 h)	45	34
6	27.6.2018 (72 h)	28.6.2018 (72 h)	46	37

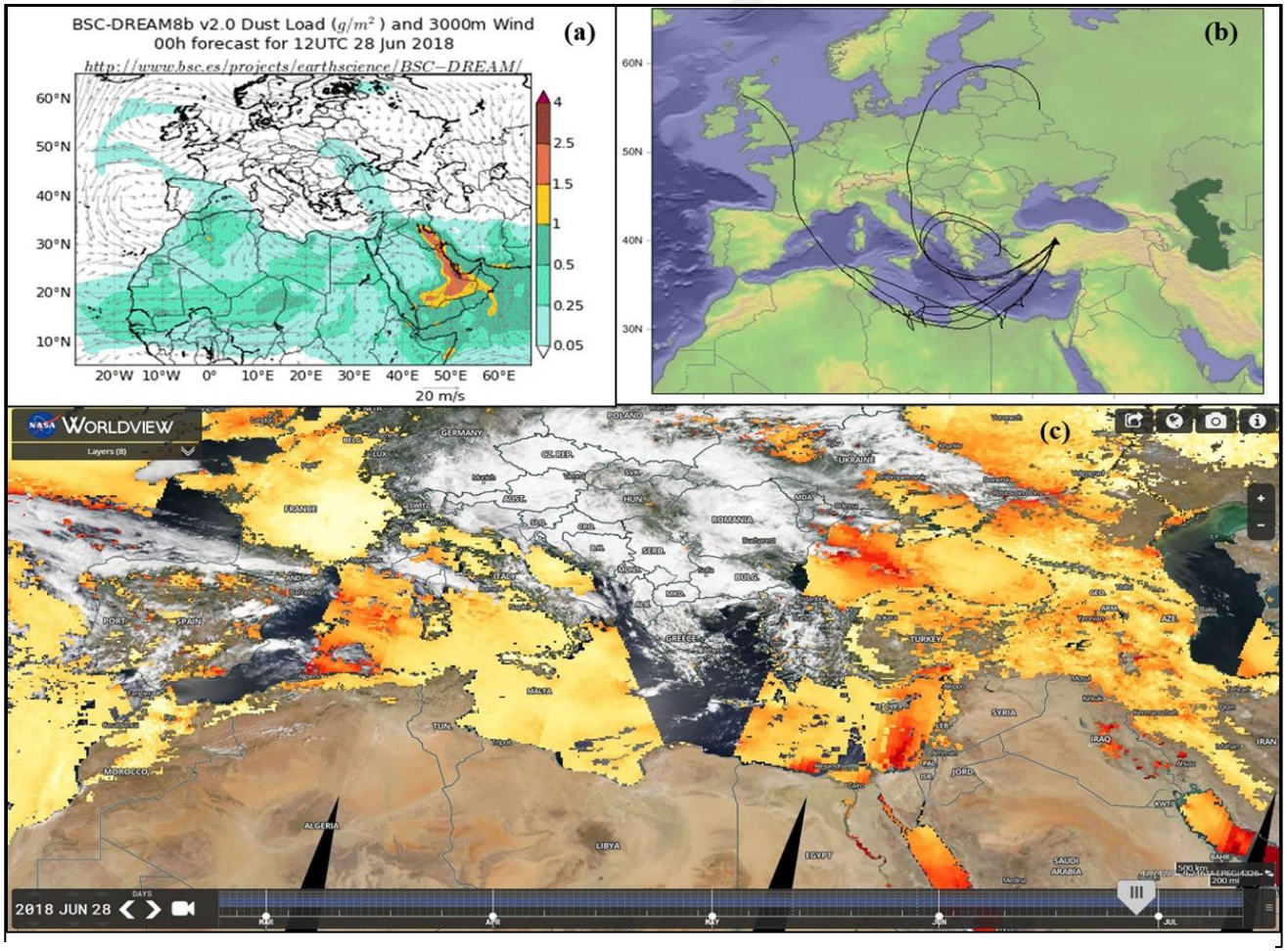

Figure 5.6 (a) DREAM model, (b) Back-trajectories, and (c) AOD for a common episode (June 28, 2018) as an example

The average size distribution in each common episode at Marmaris and Ankara stations is depicted in Figure 5.7. There is not a consistent trend in particle concentrations for D<1 μm. Number concentrations of PM_1 fraction were higher in Marmaris station for episodes 2, 4, and 6, and higher in Ankara station for episodes 1, 3, and 5. Concentrations of particles in size range between 1 μm and 10 μm are consistently high in all episodes in Ankara station. Various factors can affect the concentrations of submicron particles. These factors include meteorology, particularly solar flux, concentrations of precursors that affect secondary particle generation, presence, and absence of primary PM_1 sources. Since these factors are highly variable in space and time, differences in PM_1 number concentrations between stations change from one episode to another.

Particle number concentrations between 1 μm and 10 μm are less transient. Particle number concentrations in all channels in this size range are 54% - 82% higher in Ankara station. The only exception to this general trend is observed in episode 2, where concentrations in the 1 μm <D< 10 μm range are similar in both stations. Higher fine particle (D<2.5 μm) concentrations at Ankara station are not surprising due to the presence of anthropogenic sources in the city, but higher concentrations of coarse particles (2.5 μm <D< 10 μm) in Ankara during dust episodes was not expected. We expected to see a decrease in number concentrations, in coarse size fraction, owing to scavenging of coarse particles as dust plume travels from the Mediterranean coast to central Anatolia. Higher particle numbers in the 1 μm – 10 μm size range at Ankara station indicates that air masses pick up additional coarse particles as they travel between the Mediterranean coast and Ankara. This is possible because, the region between the Mediterranean coast and Ankara is arid and includes the Konya plain, which is an emerging dust source area.

5.3.7 Effect of meteorology (rain and wind) on the number size distribution of particles

Since particles of different sizes are affected by rain differently, we also investigated how rain modifies the size distributions of particles. The number size distributions of particles during rain and non-raining periods are given in Figure 5.8 for both stations. The average number of particles in each size bin is calculated by taking the median value for all rainy (or rainless) hours in the data set. The number of concentrations of particles with diameters smaller than 2.5 μm is not different in rain and non-raining periods. However, for D>2.5 μm, rainy period concentrations are smaller, indicating that, relatively large particles are scavenged by rain, but not fine and ultrafine particles. This observation cast doubt on the common saying that "rain clean the atmosphere" because particles that are removed from the atmosphere by rain are not the ones that we inhale.

The relationship between wind speed and the particle size distribution is given in Figure 5.9 in both stations. Patterns observed at Marmaris and Ankara stations are not the same. In Marmaris station, size distributions during low and high wind speeds are not significantly different from each other. However; in Ankara, station number concentrations during high and low wind speeds are not different for fine and ultrafine sizes (D< 2.5 μm), but for D> 2.5 μm, concentrations are higher during high wind speeds. This difference in size distributions of particles in Ankara and Marmaris stations is probably due to different land covers in these two regions. Marmaris station is in the middle of a pine forest where soil resuspension is limited, as the surface is covered with pine needles. In Ankara station, on the other hand, the region is arid and soil can easily become resuspended by wind action. The effect of increased local soil resuspension with increasing wind speed can be seen in particle size distribution in Ankara. Like rain, wind speed affects concentrations of coarse particles, rather than fine and ultrafine size fractions.

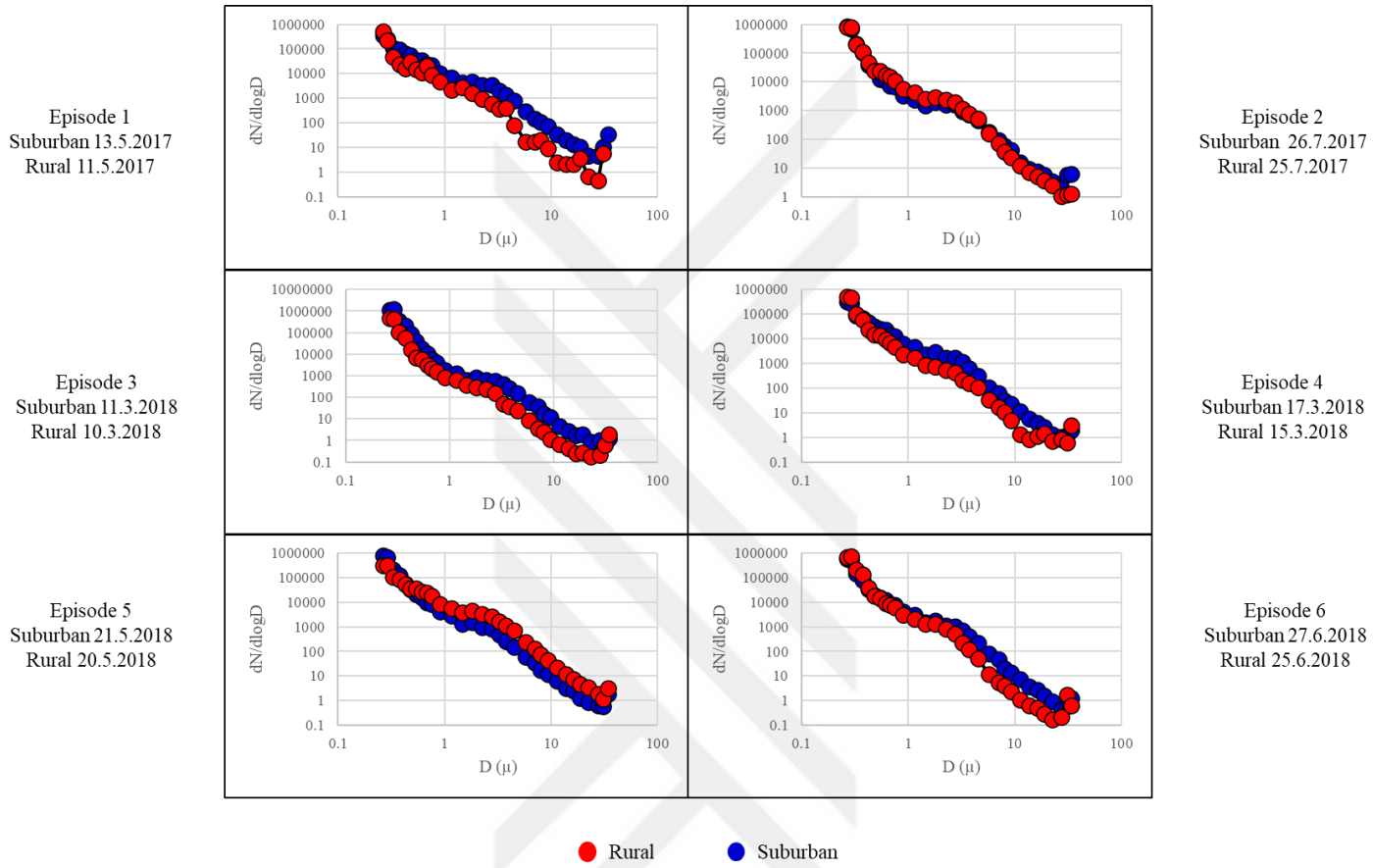

Figure 5.7 Particle number size distributions measured at rural and suburban stations in each of the common dust episodes (a-f)

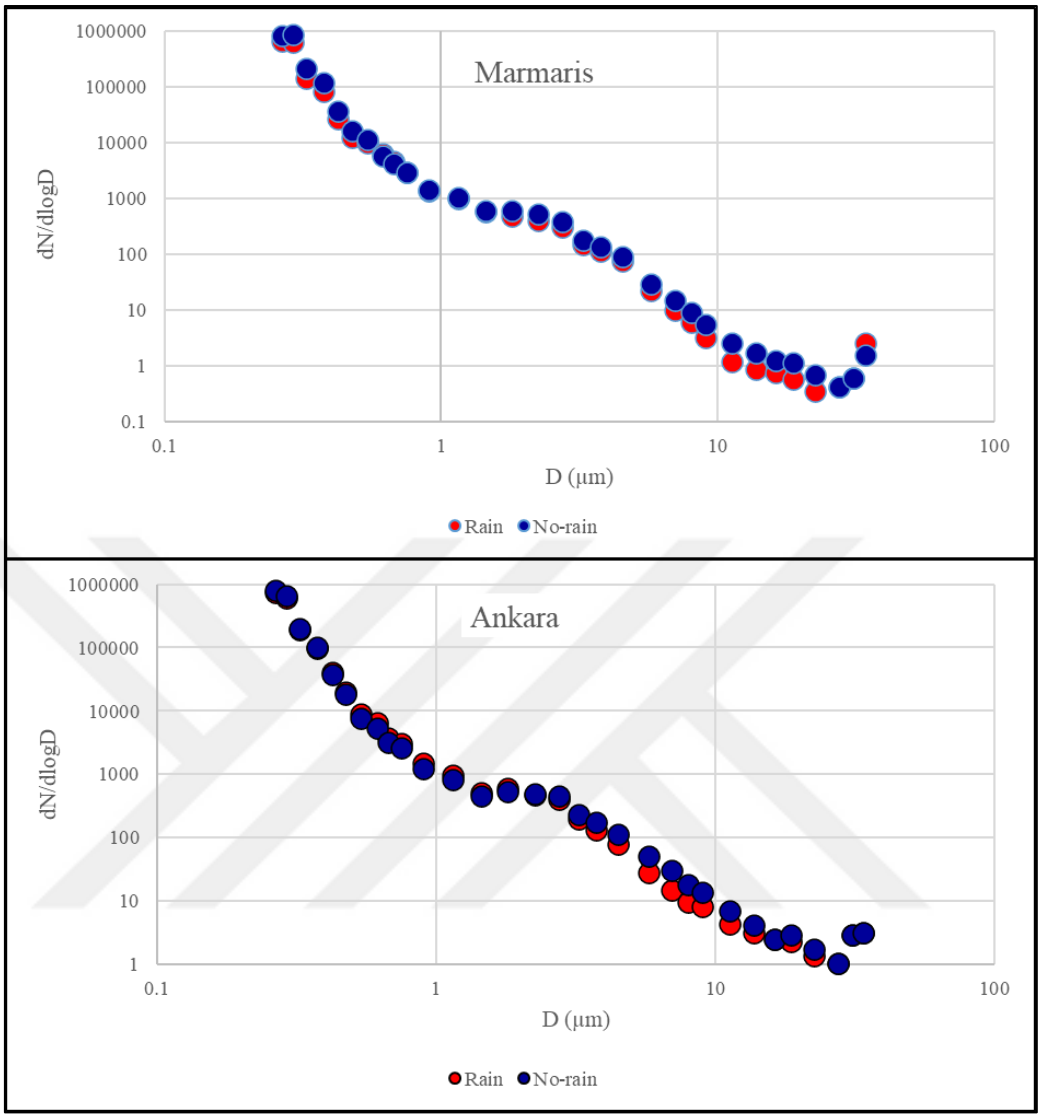

Figure 5.8 Effect of rain on the number size distribution of particles at the rural (Marmaris) and the suburban (Ankara) stations

The relationship between wind speed and the particle size distribution is given in Figure 5.9. With higher wind speeds, an increase in the concentrations of the particles above $PM_{2.5}$ is observed at both stations, indicating the resuspension of heavier particles (Figgis et al., 2018). This effect is more explicit at the suburban station than at the rural station. The size range ($D > 1$ µm), where the concentration increase is observed, is also broader compared to the rural station ($D > 2.5$ µm). Wind speeds,

as well as anthropogenic emissions (Chen et al., 2018), are generally higher during the winter months. Due to the lack of anthropogenic sources at the rural station, the effect of higher wind speeds on the particle concentrations is low. Since anthropogenic sources are dominant at the suburban station, this effect is more significant, and has a broader size range, as expected.

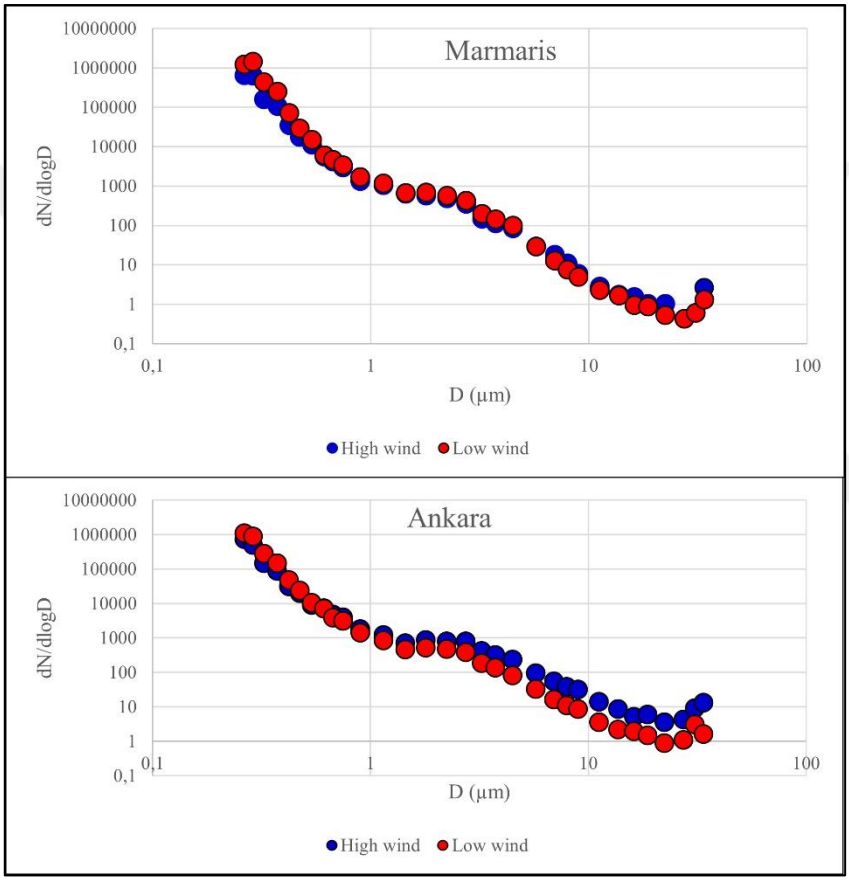

Figure 5.9 Effect of wind speed on the number size distribution of particles at the rural (Marmaris) and the suburban (Ankara) stations

5.4 Conclusions

Two stations were established to study the size distribution in dust episodes and how that size distribution is modified as dust plume travels on the Anatolian plateau. One of the stations was on the Mediterranean coast of Turkey (Marmaris station) and the

other one was in the middle of the Anatolian plateau (Ankara station). Marmaris station was a rural station in the middle of a pine forest in the Taurus mountains (approximately 1000 m ASL). Ankara station was on a university campus approximately 10 km from the city center of Ankara. It is a typical suburban station. It is also approximately 1000 m ASL.

In both stations PM_{10}, $PM_{2.5}$, and PM_1 mass concentrations and particle number concentrations in 31 size channels between 0.265 μm and 34 μ were measured between April 2017 and October 2018 using Grimm spectrometers. Supplementary data were also obtained from seven AQM stations in Ankara and five automated meteorology stations around Marmaris station.

Cluster analysis resulted in 6 trajectory groups in Marmaris and 9 trajectory groups in Ankara stations. Cluster 6 in Marmaris and Clusters 6, 7, and 9 in Ankara stations have the potential to bring Saharan Dust to our stations. Cluster 8 in Ankara station and 6 in Marmaris station have the potential to bring dust from the Middle East and the Arabic peninsula.

There is not a significant difference between particle number size distributions between clusters in Ankara station due to the masking of transported particles by strong local anthropogenic emissions. The difference is larger in Marmaris. Clusters that are expected to bring pollution-derived particles to Eastern Mediterranean have a higher concentration of fine particles and Cluster 6 which is likely to bring dust to Marmaris has a higher concentration of coarse particles.

The impact of dust episodes on the composition and size distribution of particles in the aerosol population in the Eastern Mediterranean was investigated. Dust episodes were identified based on the occurrence of PM_{10} peaks, satellite data, back trajectories, and DREAM outputs for the region, Al and Si concentrations.

When the dust was advected to our stations, PM_{10} concentrations increased 80% in Marmaris and 40% in Ankara stations. $PM_{2.5}$ concentration also increased in both stations, but not as much as PM_{10}. PM_1 concentrations, on the other hand, increased

approximately 40% in Ankara station but decreased 37% in Marmaris station, which is due to enhanced secondary particle formation in summer when dust transport is at its minimum.

Particle number size distributions during dust and non-dust periods demonstrated that in the Marmaris station number concentrations of particles with D<0.5 μm was higher in the non-dust period owing to the strong contribution of secondary particles to this size range. A similar difference was not observed in the Ankara station. Particle number concentrations in the size range between 0.5 μm and 15 μm was approximately a factor 2 higher during dust events. This region was identified as a dust-impacted size range.

Dust climatology was investigated for different episode types separately. In both stations, Saharan dust episodes were most frequent in the spring period. Dust transport from the Middle East was not frequent enough to discuss their monthly distribution. Non-dust episodes in Marmaris station were the most frequent in the winter season due to the arrival of sea salt to our station. Non-dust episodes in Ankara station, on the other hand, were anthropogenic and did not show a specific seasonal pattern.

Six Saharan Dust episodes that were sequentially intercepted in both Marmaris and Ankara stations were identified and how dust size distribution is modified as plume travels from the Mediterranean coast to central Anatolia was investigated. Travel time between the two stations is 1-2 days on average. There is not a consistent trend in particle concentrations for D<1 μm. However, particle number concentrations in the 1 μm <D<10 μm range were consistently high in Ankara station, indicating that local sources modify the number size distribution in the plume as it travels over the Anatolian plateau.

CHAPTER 6

CHEMICAL COMPOSITION OF FINE AND COARSE PARTICLES AT AN HIGH-ALTITUDE STATION IN EASTERN MEDITERRANEAN: ASSESSMENT OF AEROSOL COMPONENTS AND THEIR SOURCE REGIONS

6.1 Introduction

The Eastern Mediterranean basin is surrounded by natural and anthropogenic source areas that affect the composition of the aerosol population in the region. Anthropogenic and natural source areas are not distributed uniformly around the basin. Most of the anthropogenic source areas are located to the North of the basin whereas most of the crustal emissions are located to the South. This inhomogeneity in the distribution of sources around the basin resulted in a complex aerosol population in the Eastern Mediterranean atmosphere. The composition of the aerosol population changes considerably depending on the proximity of the sampling point to these source areas. Eastern Mediterranean aerosol consists of four main components, including crustal particles, sea salt and biogenic particles, which makes up the natural component, and pollution-derived particles from a variety of sources making up the anthropogenic component. Extensive effort was spent to find the contribution of these sources to the aerosol population and resolve anthropogenic components into individual source types, and find the locations of their source areas.

In this complex mixture, dust is the most studied component owing to its strong impact on ecosystems in the basin. The Mediterranean region is under the strong influence of Saharan Dust due to its proximity to source areas in North Africa. Approximately 15% of dust (120 Tg) resuspended in Sahara ends up in the Mediterranean basin (Huneeus et al., 2011). The reported contribution of the crustal component to PM_{10} mass in Eastern Mediterranean aerosol varies between 19% and 62% (Liora et al., 2016; Öztürk et al., 2012) and between 28% and 41% in the Black

Sea (Balcılar, 2018; Tokgöz, 2013). In a few source apportionment studies, multivariate receptor modeling techniques revealed two separate crustal components one of which is attributed to Saharan dust (Güllü et al., 1998; Scerri et al., 2016).

Recently, with increasing desertification in the Middle East, dust transport from arid areas in the Middle East and Arabic Peninsula to Eastern Mediterranean also attracted attention (Moridnejad et al., 2015a, 2015b). There had been some attempts to differentiate the contributions of Saharan and dust transported from the Middle East (Nisantzi et al., 2015; Scerri et al., 2016). However, the strength of the Middle East source and the magnitude of its impacts on the Eastern Mediterranean atmosphere needs more work. Various tracers, including rare earth elements (Öztürk et al., 2012), titanium (Nicolás et al., 2008), phosphorous (Avila et al., 1997; Bergametti et al., 1992), optical properties, particularly single scattering albedo Ångström exponent (Ealo et al., 2016), lidar ratio (Mamouri et al., 2016) and mineralogical composition of particles (Ganor et al., 2009; Taieb & Brahim, 2014) was used as tracers of dust. Among these, rare earth elements are particularly important as they are reported as specific Saharan dust markers in Eastern Mediterranean and elsewhere in several studies (Güllü et al., 1998; Muhs et al., 2007; Öztürk et al., 2012; Pey et al., 2009; Trapp et al., 2010).

Dust particles in such large quantities have a strong impact on life in the Eastern Mediterranean region. The dust has health effects (Goudie, 2014; Tobias et al., 2019). In addition, it affects boundary layer meteorology and, particularly rainfall amount (Tobias et al., 2019), affects radiative fluxes (Osipov et al., 2015), affects the chemistry of the atmosphere by providing an alkaline surface for heterogenous reactions (Athanasopoulou et al., 2016), affects marine productivity by providing nutrients, including soluble iron (Özsoy & Saydam, 2001; Ravelo-Pérez et al., 2016), affects air quality (Pandolfi et al., 2014; Querol et al., 2019), affects energy budget by modifying reflectivity of the atmosphere (Jandaghian & Akbari, 2020), affects water quality, by the input of bacteria to lakes and reservoirs (Reche et al., 2009), affects solar energy production (Sarver et al., 2013), affects hydrological cycle by

acting as cloud condensation nuclei (CCN) (Peng, 2015) and provides nutrients to forest areas where nutrient supply is limited (Louis et al., 2017).

Information on long-term variation in dust incursion to the Eastern Mediterranean atmosphere is contradictory. Some researchers reported decreasing trends based on aerosol optical depth (AOD) (Foltz & McPhaden, 2008) and litophilic element concentrations (Öztürk et al., 2012), whereas other researchers reported increasing trends (Avila & Peñuelas, 1999; Ganor et al., 2010) or no trend (Heimbürger et al., 2010). More data is needed on this issue.

Another natural component in the Eastern Mediterranean aerosol is sea salt. It is an important aerosol component because it cools the atmosphere by scattering radiation and hence increasing albedo (MÅrtensson et al., 2010), providing a surface for heterogeneous reactions, particularly involving H_2SO_4 and HNO_3 (Ghosh et al., 2020; Gonçalves et al., 2021), it also provides a surface for condensation of organic compounds (Chrit et al., 2018) and contributes to incompliance with regulatory standards in coastal cities. The contribution of sea salt to PM_{10} concentrations in the region is highly variable and depends on the proximity of the sampling location to the coastline. Approximately 7.5% - 14% sea salt contribution to PM_{10} mass concentration was reported for Istanbul (Koçak et al., 2011; Theodosi et al., 2010), 4.5% for Athens (Theodosi et al., 2011), 11% for Beirut, Lebanon (Jaafar et al., 2014), 42.5% for Erdemli (a rural site at Eastern Mediterranean) (Koçak et al., 2004), 8% at Torul (a rural site at Eastern Black Sea) (Balcılar, 2018), 9% for Derekoy (a rural site in Western Black Sea) (Genç Tokgöz et al., 2012) and 17% for Antalya (a rural site in Eastern Mediterranean) (Öztürk et al., 2012).

Natural biogenic sources in the Eastern Mediterranean are not characterized as much as sea salt and dust. The contribution of biogenic sulfur emissions from the Mediterranean Sea to the sulfur budget in the region was studied by a few researchers. Kouvarakis et al. (2002) reported that the contribution of biogenic SO_4^{2-} to nss-SO_4^{2-} is negligible in winter but can be as high as 26% in summer at Crete Island. Biogenic contribution between 6% and 22% to total SO_4^{2-} was reported on

the Israeli coast (Ganor et al., 2000). Koçak et al. (2009) reported that the contribution of biogenic SO_4^{2-} to PM_{10} mass is 12% annually but can be as high as 40% in summer. Approximately 26% contribution of biogenic emissions to total SO_4^{2-} concentration was reported for the Mediterranean coast of Turkey (Uzun, 2000). Biogenic emissions of other organic gases are also reported by several authors (Chrit et al., 2018; Peñuelas et al., 1999).

Eastern Mediterranean is also under the strong influence of anthropogenic sources. Pollution-derived particles identified in the basin reach the area both by long-range transport from strong source regions located to the north of the basin and from strong hot spots, such as Istanbul, Athens, and Cairo which are located within the basin. The anthropogenic component in Eastern Mediterranean aerosol is resolved to their sources in several source apportionment studies. These studies revealed a variety of sources and source regions, some of which are common in most studies and some unique for each study. Oil combustion sources were identified in most of the studies (Achilleos et al., 2015; Calzolai et al., 2015) generally attributed to emissions from shipping activities (Chrit et al., 2018). Traffic particles are identified in some of the studies where samples are collected close to urban areas (Achilleos et al., 2015). Biomass burning is another source of anthropogenic particles in the region, which is detected in several studies, particularly in studies where organic carbon is measured (Achilleos et al., 2015; Bossioli et al., 2016; Petroselli et al., 2018). Combustion-related particles (which are identified as either combustion particles or secondary sulfate and nitrate sources) are also commonly found in several studies (Achilleos et al., 2015; Calzolai et al., 2015). These combustion sources (secondary inorganic ions) have the highest contribution to PM_{10} mass, along with crustal particles.

Natural and anthropogenic organic component in Eastern Mediterranean aerosol is studied less frequently. The contribution of organic particles to PM_{10} mass is discussed in a few mass closure studies, which showed that organic particles accounted for 33% of fine mass at Beirut (Jaafar et al., 2014), 26% at Crete Island (Koulouri et al., 2008; Sciare et al., 2008).

Organic particles are shown to account for 58% of PM_1 mass in Ispra, Italy (Bressi et al., 2016) and %3% in Montseny, Spain (Minguillón et al., 2015). 15% of this organic contribution is shown to be from fossil fuel combustion and 23% from biomass burning (Bressi et al., 2016). Wood burning accounted for 33% of OC in winter, but only 3% in summer, whereas the contribution of secondary particle formation accounted for most of the OC (66%) in summer (Pietrogrande et al., 2016).

In this study, we attempted to characterize the aerosol population at a high-altitude site (approximately 1000 m above sea level) on the Mediterranean coast of Turkey. Daily aerosol samples were collected between March 2014 and January 2018. Collected samples were analyzed using energy-dispersive x-ray fluorescence (ED-XRF) spectrometer. Flow climatology, the elemental composition of trajectory clusters, seasonal patterns in concentrations of measured elements, the contribution of Saharan Dust to PM_{10} mass concentration, and concentrations of litophilic elements were discussed. Sources contributing to PM_{10} mass concentration and concentrations of measured elements were calculated using positive matrix factorization (PMF).

6.2 Materials and Methods

6.2.1 Sampling

The sampling station was located at the Doppler radar, which is operated by the General Directorate of Meteorology. The location of the sampling station is given in Figure C1 in the supplementary material. The radar is located approximately 8 km to the northeast of the Marmaris province of Mugla in the Taurus Mountains (36º53’13” N, 28º20’02” E). It was in the middle of a pine forest and at an altitude of 936 m above sea level (ASL). The nearest human-induced emissions can be from a highway that connects Marmaris to Mugla, which is approximately 5 km to the west of the station and from the town of Marmaris. Marmaris is a resort city, with

96 000 population. However, the population increases to 600 000 in the summer season. There is no significant industry in Marmaris that could affect our samples.

Sampling was started in March 2014 and completed in January 2018. It was not continuous there were several interruptions due to instrument malfunctions and lack of adequate funding. Only samples that have both coarse and fine fraction data were used in data treatment. A total of 408 samples (in each size fraction) fulfilled this requirement and were included in the data analysis.

Fine and coarse fraction samples were separately collected on polycarbonate (Nuclepore Co.) filters using a stack filter unit (SFU), The SFU was developed at Gent University, Belgium (Maenhaut et al., 1993) and is frequently used to collect fine and coarse particles (Alves et al., 2020; Humairoh et al., 2020; Santoso et al., 2020). Satisfactory particle cut-off characteristics and collection efficiency of SFU were reported in the literature (Hopke et al., 1997). We obtained technical drawings of the sampler, constructed them in our labs, and used them in several studies in the past (Balcılar et al., 2014; Yatin et al., 2000).

6.2.2 Analysis of Collected Samples

Since energy-dispersive x-ray fluorescence (ED-XRF) analysis does not require extensive processing of filters, sample preparation included only the weighting of filters before and after sampling. For this, filters were left in a homemade constant-humidity and constant-temperature chamber for 24 hours and weighted, to the nearest 1 µg, using a Sartorius, model MC-5 microbalance.

Samples were analyzed, in the Turkish Atomic Energy Agency, Sarayköy Nuclear Research and Training Center using an Oxford, ED-2000 energy dispersive X-Ray Fluorescence Spectrometer. Four different excitations conditions were used for different groups of elements. Details of ED-XRF analysis are given elsewhere (Öztürk et al., 2011). Fifteen elements, including Al, Si, Ca, Na, Mg, K, Ti, V, Mn. Ni, As, Cu, Pb, S, and Zn, were determined in collected samples.

6.2.3 Quality Assurance / Quality Control (QA/QC)

Since details of QA/QC protocol used in rural studies in our group are described in detail elsewhere (Balcılar et al., 2014; Öztürk et al., 2012) only a summary is presented here. The QA/QC protocol included routine counting of SRM filters, reanalysis of 5% of the filters in every batch, routine analysis of field and laboratory blanks, and computation of analytical parameters, such as precision and detection limits.

National Institute of Standards and Technology (NIST) reference filters (SRM 2783) were counted at the beginning of each analysis day to monitor variations in the sensitivity of the instrument. If the difference between certified and measured values of an element is > ± 10%, the instrument was recalibrated before resuming analysis. Similarly, 5% of the previously counted samples were resent to XRF laboratory, without informing laboratory personnel, with every sample batch to assess variation of repeatability in time. The precision of the analytical system was reasonably good, the relative standard deviation varied between 3.3% for Ca and Ti and 10% for Pb.

Blank filters were collected once every week at the beginning of sampling, once a month toward the end. Field blanks were one of the sample filters, which were loaded to the sampler and then removed after one-minute sampling. Twenty of the collected field blanks and numerous laboratory blanks were analyzed to assess and minimize sample contamination. Sample-to-blank ratios of elements varied between 1.1 for Zn and 150 for S. Concentrations of elements, V, Cu, Zn, As, and Pb in blank filters were between 16% to 40% of their concentrations in sample filters. High blank subtraction for these elements is reflected in their frequency of observances. Blank subtraction was <10% for the remaining elements.

6.3 Results and Discussion

6.3.1 Data

The average and median concentrations of elements measured in this study are given in Table 6.1. Fifteen elements were measured with ED-XRF and particle mass was measured gravimetrically. Since all elements and mass concentrations have right-skewed (not necessarily lognormal) distributions, the median is more representative of the data population in this study. Average and standard deviations are also included in the table to facilitate comparison with literature where average concentrations are frequently reported.

Table 6.1 Summary statistics for coarse, fine, and PM_{10} data. Numbers in parenthesis are median concentrations of elements. Concentrations are in ng m^{-3}.

	Coarse		Fine	PM_{10}
	X ± σ (median)	N	X ± σ (median)	X ± σ (median)
Mass	14000 ± 21000 (8500)	320	11000 ± 29000 (5800)	25000 ± 41000 (15000)
Al	93 ± 123 (50)	304	35 ± 95 (8,0)	129 ± 176 (71)
As	0,17 ± 0,19 (0,11)	63	0,17 ± 0,13 (0,13)	0,34 ± 0,24 (0,29)
Ca	344 ± 401 (220)	276	95 ± 223 (30)	440 ± 478 (332)
Cu	5,5 ± 6,0 (4,4)	183	5,5 ± 4,4 (4,0)	11 ± 7,8 (10)
K	56 ± 64 (34)	276	27 ± 48 (13)	83 ± 85 (56)
Mg	44 ± 57 (27)	290	14 ± 31 (3,8)	58 ± 69 (41)
Mn	6,2 ± 8,6 (2,0)	77	7,4 ± 9,3 (2,0)	14 ± 14 (4,2)
Na	102 ± 132 (59)	282	31 ± 70 (8,5)	132 ± 156 (89)
Ni	1,8 ± 2,1 (0,6)	120	2,1 ± 2,3 (0,8)	3,9 ± 3,6 (3,1)
Pb	4,4 ± 3,1 (3,9)	26	6,5 ± 9,6 (3,7)	10,9 ± 11,2 (9,0)
S	53 ± 54 (34)	275	178 ± 297 (78)	231 ± 309 (130)
Si	297 ± 361 (177)	224	110 ± 260 (29)	405 ± 489 (256)
Ti	9,0 ± 11,4 (5,2)	203	3,7 ± 8,0 (1,5)	13 ± 16 (8,2)
V	1,0 ± 0,77 (0,90)	95	1,1 ± 0,9 (1,0)	2,1 ± 1,2 (2,1)
Zn	6,2 ± 5,9 (7,9)	277	5,9 ± 5,3 (7,8)	12 ± 8,1 (11)

In this group of fifteen elements Al, Ca, and Si are litophilic elements for which the earth's crust is the main source. Atmospheric concentrations of chalchophilic elements, namely, As, Cu, Pb, S, and Zn are dominated by their emissions from anthropogenic sources. Atmospheric concentrations of remaining elements, namely K, Mn, Ni, Ti, V, Na, and Mg are determined by a mixture of sources. Resuspended soil particles in the atmosphere contribute strongly to their measured concentrations. However, they also have non-crustal sources. Potassium is emitted from biomass burning, Ni and V from oil combustion, Mn and Ti from the iron and steel industry, and Na and Mg from the sea. Treatment of elemental concentrations in different sections in this manuscript is based on this grouping.

Elemental concentrations in our data vary between 0.17 ng m^{-3} for coarse fraction As and 297 ng m^{-3} for coarse fraction Si. Please note that Sulfur is included as S, not as SO_4^{2-} in the table (also throughout the manuscript), because XRF measures S, not SO_4^{2-}. If it is converted to SO_4^{2-}, fine fraction SO_4^{2-} becomes the most abundant species in our data set (534 ng m^{-3}).

6.3.2 Coarse-to-Fine Ratio

Course-to-fine concentration ratios of elements and percent fine fraction concentrations in PM_{10} are given in Table 6.2. Coarse-to-fine concentration ratios for crustal and marine elements (Na, Mg, Al, Ca, and Si) varies between 5 – 7 indicating that 12 – 16% of their PM_{10} concentration is accounted for by fine fraction, which is typical for lithophilic elements.

Coarse-to-fine ratios of pollution-derived elements (As, Cu, Pb, S, and Zn) vary in a very narrow range between 0.9 for Cu and 1.04 for Zn. Indicating that 49 to 52% of PM_{10} concentrations of these elements can be accounted for by fine fraction. The only exception to this general pattern is for S (or SO_4^{2-}). For this element coarse-to-fine ratio is 0.4 indicating that 70% of S in PM_{10} is associated with fine fraction, which is significantly higher than fine fraction contribution in other anthropogenic

elements. This is probably due to the secondary nature of SO_4^{2-} particles. In earlier size distribution studies in the region SO_4^{2-} was shown to have a smaller mass median diameter than other anthropogenic elements (Kuloglu & Tuncel, 2005). Sulfate is a secondary ion and starts its atmospheric life in Aitken mode, but it quickly coagulates into accumulation mode. However, the coagulation rate decreases as particles grow and it can reach a certain diameter, which turns out to be approximately 1 μm in the Eastern Mediterranean atmosphere (Kuloglu & Tuncel, 2005). All other elements with anthropogenic sources have MMD between 1.5 μm and 2.0 μm (Kuloglu & Tuncel, 2005).

Table 6.2 Coarse-to-fine concentration ratios and enrichments of elements in coarse and fine fractions relative to soil composition

			Coarse		**Fine**	
	C/F ratio	**% Fine**	**% Element from soil**	**EF_c**	**% Element from soil**	**EF_c**
Mass	1,4	41				
Na	7	12	25,2	3,4	28,1	3,6
Mg	6	14	34,2	2,5	38,9	2,6
Al	5	16	100,0	0,8	100,0	1,0
Ca	7	13	7,2	11,8	8,3	12,1
Si	6	14	108,6	0,8	104,7	1,0
As	1,00	50	2,7	31,0	0,4	272,3
Cu	0,92	52	0,4	217,2	0,1	1457,4
Pb	1,00	50	0,3	315,3	0,05	2193,7
S	0,41	71	0,1	762,6	0,01	12800,0
Zn	1,04	49	0,5	161,5	0,1	1190,8
K	2,43	29	42,6	2,0	17,6	5,7
Mn	0,96	51	24,5	3,5	3,7	26,9
Ni	0,95	51	4,5	18,9	0,6	181,2
Ti	3,67	21	45,7	1,9	25,1	4,0
V	1,00	50	6,6	12,8	1,0	101,4

The third group of elements (K, Mn, Ni, Ti, and V) in our measurement protocol has mixed sources as discussed previously in this manuscript. Non-crustal contribution to concentrations of these elements depends on the proximity of the sampling point to their sources. Soil is their main source if the sampling point is not close to

anthropogenic emission sources. In our study, coarse-to-fine ratios for this group of elements are variable. The ratio is close to the anthropogenic ratio for Mn, Ni, and V, indicating that residual oil combustion and particles emitted from metallurgical industries are significant components in the Eastern Mediterranean aerosol population. Please note that oil combustion appeared as a separate component in the source apportionment exercise, which will be discussed later in the manuscript. The oil combustion factor was also reported in other source apportionment studies in the region (Achilleos et al., 2015). All these findings suggest that particles that are emitted from oil combustion are an important component of the Eastern Mediterranean aerosol population. Although we do not have conclusive evidence, heavy marine traffic can be an important contributor to this aerosol component. Similarly, high Mn concentrations in air masses coming from central Russia were reported for the Black Sea atmosphere (Dzubay et al., 1984).

Coarse-to-fine concentration ratios are between crustal and anthropogenic ratios for K and Ti, indicating that resuspended soil is the main source of their measured concentrations.

Anthropogenic elements in coarse fraction account for approximately half of their PM_{10} concentrations. Since most of these elements are known to be associated with fine particles, we expected to see a higher contribution of the fine fraction on their PM_{10} levels. This may be either due to a high concentration of litophilic particles in coarse fractions or the sticking of small anthropogenic particles onto coarse litophilic particles.

We calculated fractions of elements that can be accounted for by crustal particles and crustal enrichment factors of elements (EF_c) to understand if the relatively high contribution of coarse fraction anthropogenic elements can be due to their presence in litophilic particles. Results are also included in Table 6.2. Enrichment factors were calculated using Al as a crustal reference element and using the global crustal composition given in Rudnick and Gao (2003).

Results that are given in the table demonstrate that lithophilic components in concentrations of chalchophilic elements cannot account for a significant part of their observed concentrations. Sulfur is highly and As, Cu, Pb, and Zn are moderately enriched in coarse fraction. If litophilic particles affecting our samples have a similar composition to that given in Rudnick and Gao (2003), they account for 0.1 – 2.7 % of observed concentrations of pollution-derived elements in coarse fraction. The observed enrichment of anthropogenic elements in the coarse fraction is probably due to the sticking of fine anthropogenic particles onto coarse crustal particles as observed earlier in this region.

One other possibility is the difference in compositions of soil affecting our samples and global composition used in EF_c calculations. Although it is not likely to have two orders of magnitude difference in concentrations of chalchophilic elements between different soils, we prepared EF_c-Al plots for all elements to test this hypothesis. These are simple plots of EF_c's of elements against Al concentration. Since concentrations of elements with dominating crustal source will covary with Al concentration, which is our soil reference element, their EF_c will be unity in all Al concentrations and thus they define a horizontal line at $EF_c = 1.0$. Crustal enrichment factors of pollution-derived elements, on the other hand, are independent of Al concentration, and their EF_c decreases with increasing Al concentration. These patterns are given in Figure 6.1 for selected litophilic and chalchophilic elements.

The pattern shown for S is typical for anthropogenic elements. Sulfur has dominating anthropogenic source both in fine and coarse fractions and litophilic particles do not have a significant contribution to S concentrations at all Al concentrations. The behavior of Si and Ca in the figure is typical for most litophilic elements, with one exception. The EF_c of Ca does not define a horizontal line at $EF_c = 1.0$ but defines a horizontal line around $EF_c = 10$ in both coarse and fine fractions, indicating that the Ca/Al ratio in soil affecting our samples is approximately an order of magnitude higher than the corresponding ratio in global average soil given in Rudnick and Gao (2003) (median EF_c is 11.8 in coarse and 8.6 in fine fractions). The average Ca/Al

ratio in our samples, is 4.8 ± 3.9. Please note that the Ca-to-Al ratio found in soil samples collected from 100 separate locations in urban and rural Antalya, which is a city approximately 200 km to the east of our sampling point is 5.9 (Guvenç et al., 2003). This is not surprising, because the soil in the Eastern Mediterranean basin is highly alkaline (Al-Momani et al., 1995; Charron et al., 2000; Özsoy et al., 2007).

EF_c – Al plots for remaining pollution-derived elements (As, Cu, Pb) are not different. Concentrations of chalchophilic elements measured in this study depict a clear anthropogenic pattern with decreasing EF_c with increasing Al concentration in both coarse and fine fractions, indicating that observed enrichment of these elements in coarse fraction has nothing to do with soil composition and is due to the contribution of anthropogenic sources and most likely owing to the sticking of fine anthropogenic particles on coarse litophilic ones.

Elements K, Mn, Ni, Ti, and V are elements with mixed sources (crustal and anthropogenic) as pointed out earlier in the manuscript. In their EFc – Al diagrams Mn, Ni and V depict anthropogenic patterns, in both coarse and fine fractions, as suggested by their coarse-to-fine ratios. This is shown in Figure 6.1 for V, indicating that anthropogenic sources, namely residual oil combustion is influential on their observed concentrations at our station Potassium and Ti, on the other hand, showed a different pattern. EF_cs of these two elements showed decreasing trend with increasing Al concentration until a certain threshold Al concentration, which is approximately 50 ng m^{-3}, is reached. Beyond this threshold value, their EF_cs do not change with Al concentration anymore indicating that their non-crustal sources (biomass burning for K and metallurgical industry for Ti) have a strong influence on their measured concentrations at low concentrations of litophilic particles. However, beyond a certain loading of crustal particles in the atmosphere, their non-crustal sources are completely masked by crustal particles.

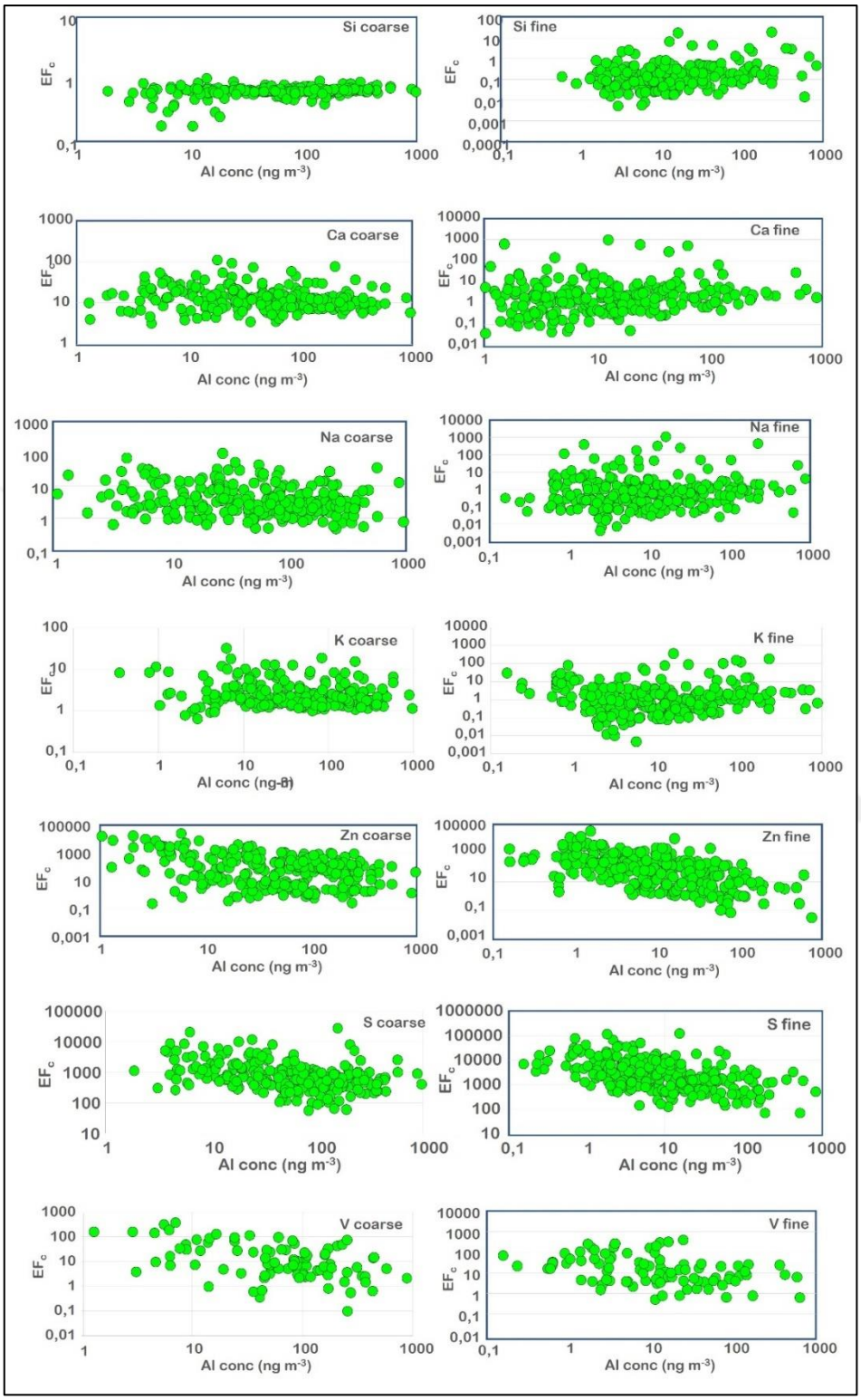

Figure 6.1 EF_c – Al diagrams for selected elements

6.3.3 Comparison with Literature

Concentrations of elements measured in this study are compared with corresponding data reported for other rural locations in Turkey in Figure 6.2. Concentrations measured at Marmaris are not significantly different from corresponding concentrations measured in other locations in Turkey. However, there are some minor categoric differences due to differences in proximity of the site to natural and anthropogenic sources, time samples were collected, and altitude.

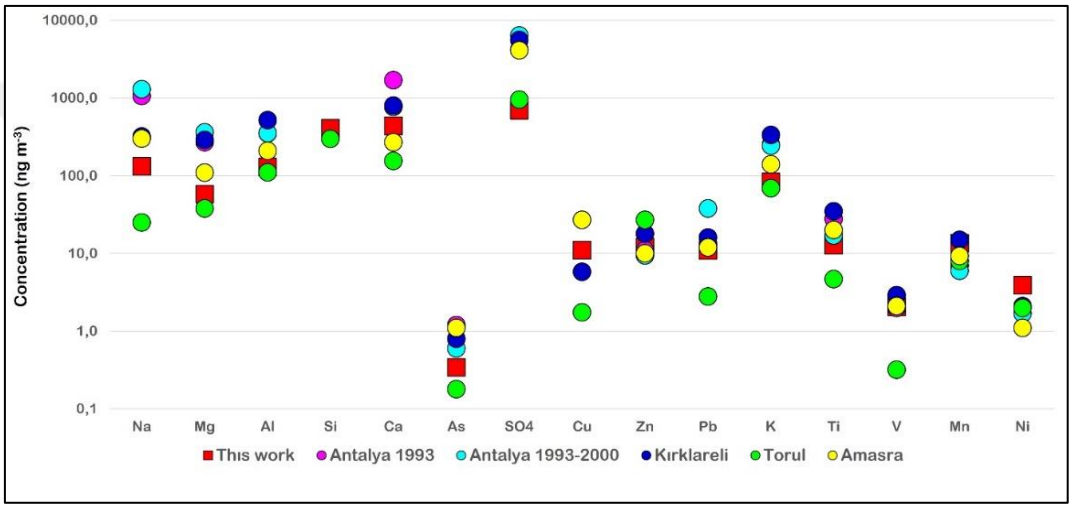

Figure 6.2 Concentrations of elements measured in this work and other locations in Turkey

Concentrations of marine elements (Na and Mg) depend strongly on the distance between the sampling point and the coast. The highest concentrations of these elements are measured at Antalya because the sampling point was immediately by the sea. Sodium and Mg concentrations measured in this study are low compared to concentrations reported at Antalya because the station is 8 km away from the coast and at an altitude of approximately 1000 m.

Concentrations of litophilic elements are also low compared to other locations, probably because the station is in the middle of a forest, where local soil resuspension is limited. Concentrations of chalchophilic elements depend on the time samples are

collected because the emission of pollution-derived particles is decreasing over time in entire Europe (Sun et al., 2021; Waldner et al., 2014). This is particularly true for SO_4^{2-}. The lowest SO_4^{2-} concentrations in the table are reported for Torul and this study. These are the two newest data sets. Torul data were generated between 2013 and 2015, and this study includes samples collected between 2014 and 2018. All other data sets are older. Data in Antalya were generated between 1993 and 2000, and samples at Amasra were collected in 1996, and at Kirklareli between 2006 and 2008.

Concentrations of other anthropogenic elements are relatively low in this study for the same reason. The only exception to this is Mn and Ni for which concentrations measured in this work are among the highest in the table.

6.3.4 Flow Climatology

Since particle sources are not homogeneously distributed around the Eastern Mediterranean basin flow climatology, which refers to the frequency of transport from different wind sectors, is important as it provides information on the probability of transport from source regions located in different directions to the receptor site.

Annual and seasonal residence times of air masses in each wind sector are given in Figure 6.3. Sector-based residence times are calculated by counting hourly segments of five-day-long back trajectories. Back trajectories were calculated using Hybrid Single-Particle Lagrangian Integrated Trajectory (HYSPLIT) model, (Draxler & Hess, 1998). Back trajectories and hence flow climatology were computed only for our study period (2014 – 2018).

Flow climatology in the Mediterranean and other parts of Turkey was investigated in several studies (Dayan & Miller, 1989; Güllü et al., 1998; Kubilay & Saydam, 1995). General features of flow climatology calculated in this study using data between 2014 and 2018 are not significantly different from those found in other studies. The main flow direction in the region is from SW, W, and NW. Air masses

spend a total of 77% of their time in these three sectors and 23% of the time in the remaining five sectors. This flow pattern suggests that anthropogenic emissions from developed Western European countries and Mediterranean countries have a higher probability of reaching the Eastern Mediterranean atmosphere than emissions from countries located to the south and east of the basin.

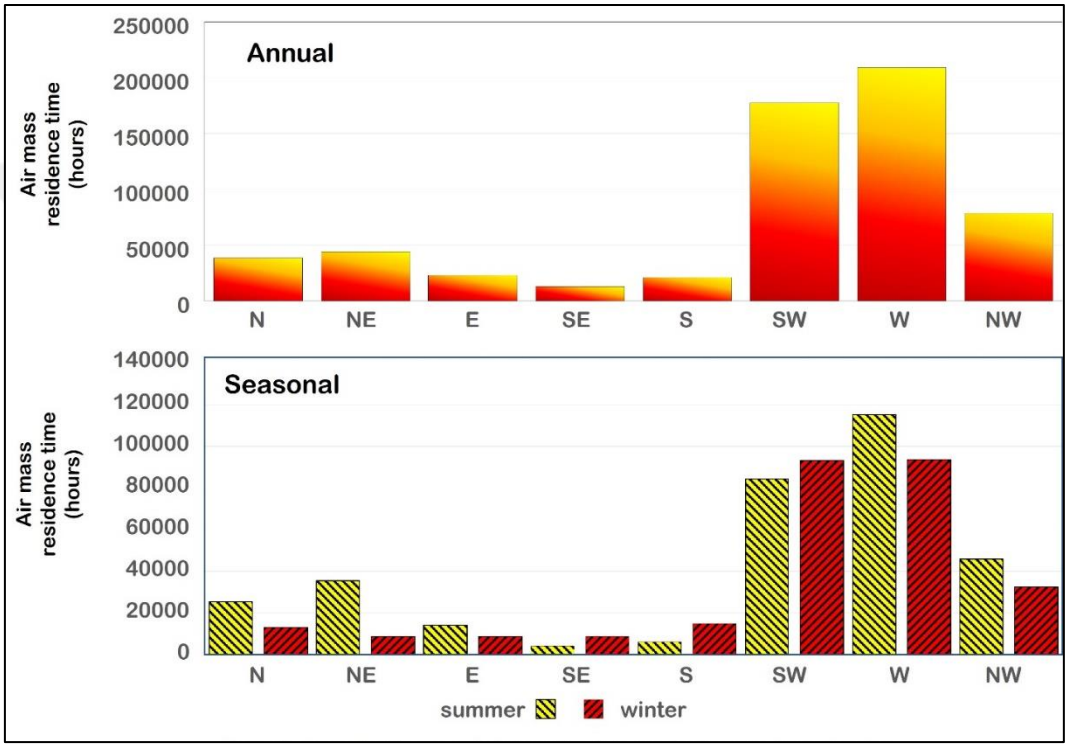

Figure 6.3 Annual and seasonal air mass flow frequencies from each wind sector

Flow frequencies show minor, but systematic differences between summer and winter seasons. Air masses spent more time in W, NW, N, NE, and E sectors during summer and spent more time in SE, S, SW, and W sectors during winter. Summer winter difference in residence times is not very different in SW and W sectors, which accounts for most of the air mass flow to the region. These patterns observed in this study indicate that flow climatology in our study period is not different from flow climatology for different periods reported in the literature.

6.3.5 Cluster Analysis

Back trajectories were grouped based on the length (transport speed) and curvature using cluster analysis (TrajStat software). The optimum number of clusters was determined by investigating variation in total root means square deviation (TRMSD) by increasing the number of clusters (Brankov et al., 1998).

TrajStat software generated seven clusters. Centroids of these clusters are given in Figure 6.4 and all trajectories in each cluster are depicted in Figure C2 in the supplementary material. Cluster 1 accounts for 28% of trajectories, which is followed by clusters 5 and 3, which include 19% and 17% of computed trajectories, respectively.

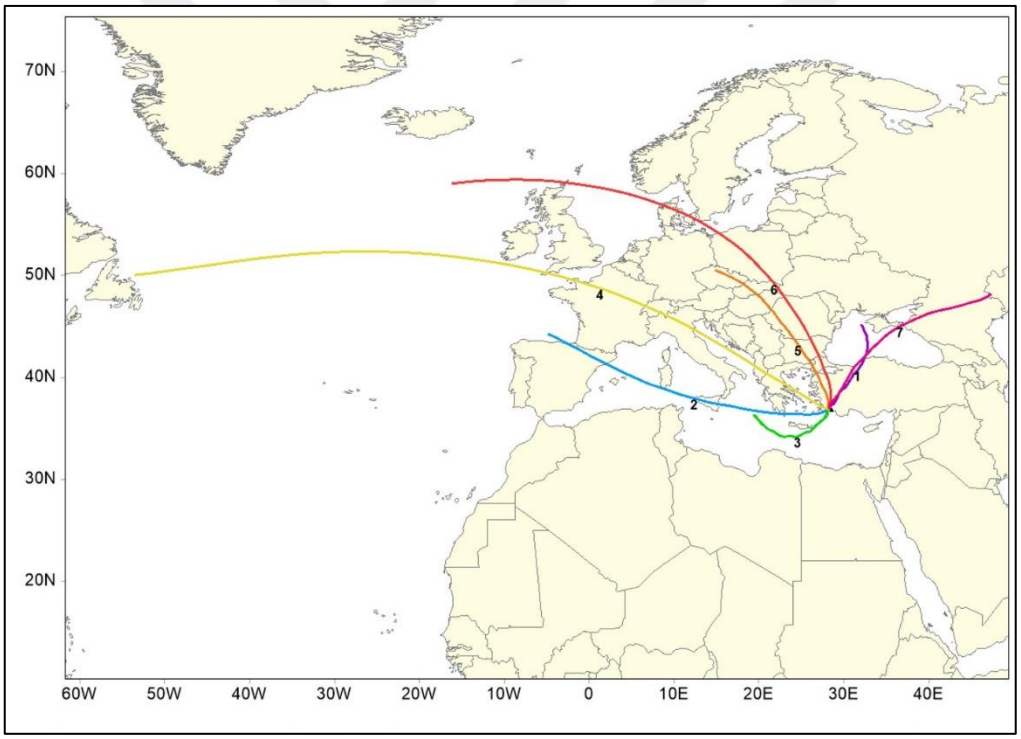

Figure 6.4 Centroids of back trajectory clusters arriving at Marmaris station. Trajectories calculated for the entire study period are used in cluster analysis

Two of the seven clusters (clusters 1 and 3) consist of short trajectories indicating that they carry emissions from local sources in western and central parts of Turkey and Balkan countries. However, trajectories in cluster 3 extend to the southern coast of the Eastern Mediterranean and thus have the potential to include dust transported via Egypt and Libya.

The rest of the clusters represent medium and long-range transport of particles. Trajectories in cluster 2 travel over the Mediterranean Sea bringing sea salt elements to our site. This trajectory group is also likely to bring Saharan dust because most of the trajectories in this cluster spent appreciable time over North Africa. Clusters 5, 6, and 7 are the trajectories that pass over industrial regions in Europe, Ukraine, and Russia and are likely to bring pollution-derived elements to Eastern Mediterranean. Cluster 4 consists of very long trajectories originating from North America and represents very fast-moving air masses. Transport of pollutants and radioactivity from boreal forest fires in Canada to Europe by fast-moving air masses was frequently reported in the literature (Forster et al., 2021; Kang et al., 2022).

Trying to relate particle sources to trajectory clusters using a two-dimensional treatment of trajectories has some limitations because trajectory segments close to the surface do not have the same probability of picking up particles from sources at the surface as trajectory segments at high altitudes. To be more realistic in this discussion, we investigated distributions of trajectory segments below 500 m in each cluster, assuming that these segments are the ones that have a higher probability of picking up particles from source regions and thus better indicators of source areas affecting our receptor site at Marmaris.

Distributions of low-lying segments in each cluster are given in Figure 6.5. Distributions of low-lying segments in general support our discussion with the two-dimensional treatment of trajectories in previous paragraphs, with few exceptions. Our earlier statement that clusters 1 and 3, which represent short trajectories are indicators of local effects on particle composition at Marmaris is supported because most of the low-lying trajectory segments in these two clusters occur in western and

central Turkey, Balkan Countries, and over the Eastern Mediterranean Sea. Air mass transport associated with clusters 2 and 3 is the one that brings Saharan dust to our site. Trajectories associated with clusters 5 and 7 are the ones that can be expected to bring anthropogenic particles to Eastern Mediterranean. Cluster 5 from Balkan countries and Italy and cluster 7 from Ukraine and Russia.

Clusters 4 and 6 include the longest trajectories. Air masses represented by these two cluster crosses entire Europe before they are intercepted at our station. However, distributions of low-lying trajectory segments in Figure 6.5 indicate that air mass transport in these two clusters occurs at high altitudes and the contribution of sources on air masses in these two clusters can be less than what we expect to see based on trajectory directions only.

Median concentrations of elements in each cluster are given in Table 6.3. The highest median concentrations of litophilic elements are observed in clusters 2, 3, and 7. High concentrations of these elements in clusters 2 and 3 are not surprising because these clusters are the ones that bring dust from North Africa to the eastern Mediterranean basin. However, the high contribution of cluster 7 on measured concentrations of litophilic elements was not expected, as low-lying trajectory segments in this cluster occurred in Ukraine and Russia. However, please note that all trajectories in cluster 7 must cross the Anatolian plateau before they are intercepted at Marmaris. The Anatolian plateau is an arid region and is a good source of crustal material. Konya plain is a particularly important regional dust source (Oğuz & Pekin, 2016). The same argument can also be extended to observed high concentrations of some of the litophilic elements in samples associated with cluster 1 because most of the low-lying segments in this cluster occur in central Anatolia.

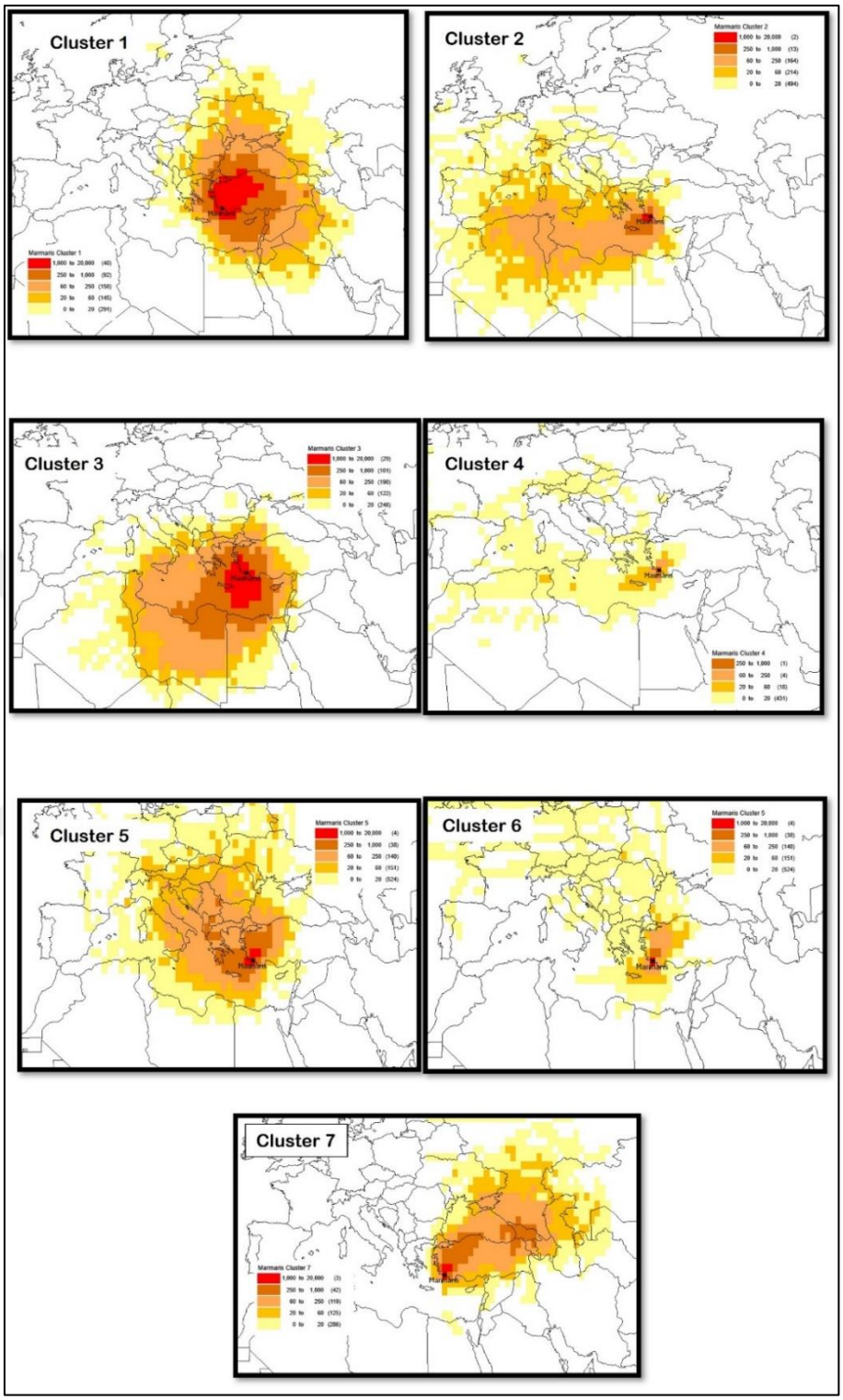

Figure 6.5 Distribution of trajectory segments with z < 500 m

Table 6.3 Median PM_{10} concentrations of elements in each cluster (concentrations of elements are in ng m^{-3}, except for mass which is in μg m^{-3})

Cluster	**1**	**2**	**3**	**4**	**5**	**6**	**7**
Mass	18	16	16	11	15	14	20
Al	67	96	71	29	66	35	131
As	0.36	0.22	0.23	0.21	0.6	0.46	0.49
Ca	350	403	404	214	247	217	501
Cu	9.3	7.8	8.4	8.8	14	11	11
K	65	63	73	30	50	46	80
Mg	47	40	47	21	37	23	54
Mn	19.0	4.0	5.0	19	3.8	4.2	4.0
Na	93	103	137	53	69	49	98
Ni	1.4	3.8	1.3	0.9	4.5	4.2	2.4
Pb	8.5	8.2	10	8.6	12	14	14
S	162	124	161	86	213	96	227
Si	235	258	336	106	262	155	358
Ti	9.0	6.9	8.4	4.5	8.6	4.6	12
V	1.9	2.5	2.5	1.0	2.1	1.7	2.0
Zn	11	11	11	9	11	11	11

This discussion of litophilic element concentrations in clusters suggests that crustal material measured in Eastern Mediterranean is contributed by both dusts transported from North Africa and local dust generated largely in the arid Anatolian Plateau. We did not see a significant contribution from dust generated in the Middle East and Arabic Peninsula, probably because the number of trajectories coming from the East was very limited.

Median concentrations of pollution-derived elements, namely, As, Cu, Pb, S, and Zn have higher median concentrations in clusters 5, 6, and 7, except for Zn. Zinc concentrations do not vary significantly from one cluster to another. High concentrations of anthropogenic elements in clusters 5, 6, and 7 are not surprising, because these three clusters are the ones that are expected to bring anthropogenic particles from Europe, Balkan countries, Ukraine and Russia.

Median concentrations of elements with mixed sources, namely K, Mn, Ni, V, and Ti, show different patterns. Concentrations of K, Ti, and V have patterns like crustal

elements with higher concentrations in Clusters 2, 3, and 7. Nickel, on the other hand, has higher median concentrations in Clusters 5, 6, and 7 like other anthropogenic elements.

6.3.6 Seasonal Variations

Monthly median concentrations of selected elements are given in Figure 6.6. Concentrations of litophilic elements, including Al, Ca, Si, Mg, K, and Ti are higher in the summer season. For these elements, the summer-to-winter median ratio varies between 1.9 for Mg, Ca, and 4.4 for Al. Higher summer season concentrations of these elements are attributed to more extensive wet scavenging of particles in winter and limited resuspension from the wet surface in winter. The summer-to-winter ratio in Na is not as large as those observed in other crustal elements (1.6) due to sea salt contribution to measured Na concentration, which is higher in the winter season.

Pollution-derived elements, including As, Cu, Pb, Zn, V, and Ni, do not show as well-defined seasonal patterns as observed in crustal elements. Their concentrations are slightly higher in summer, probably due to more extensive scavenging in winter, but the difference is not much (summer-to-winter ratios vary between 1.0 for Zn 1.2 for As and Cu). The only exception to this general behavior is observed in S concentration which is significantly higher in summer (summer-to-winter ratio is 1.6), due to enhanced photochemical oxidation of SO_2 to SO_4^{2-} during the summer season. The seasonal pattern observed in this study is not different from seasonal variations of elements reported in earlier studies in the Eastern Mediterranean (Glavas et al., 2008; Güllü et al., 1998; Öztürk et al., 2012).

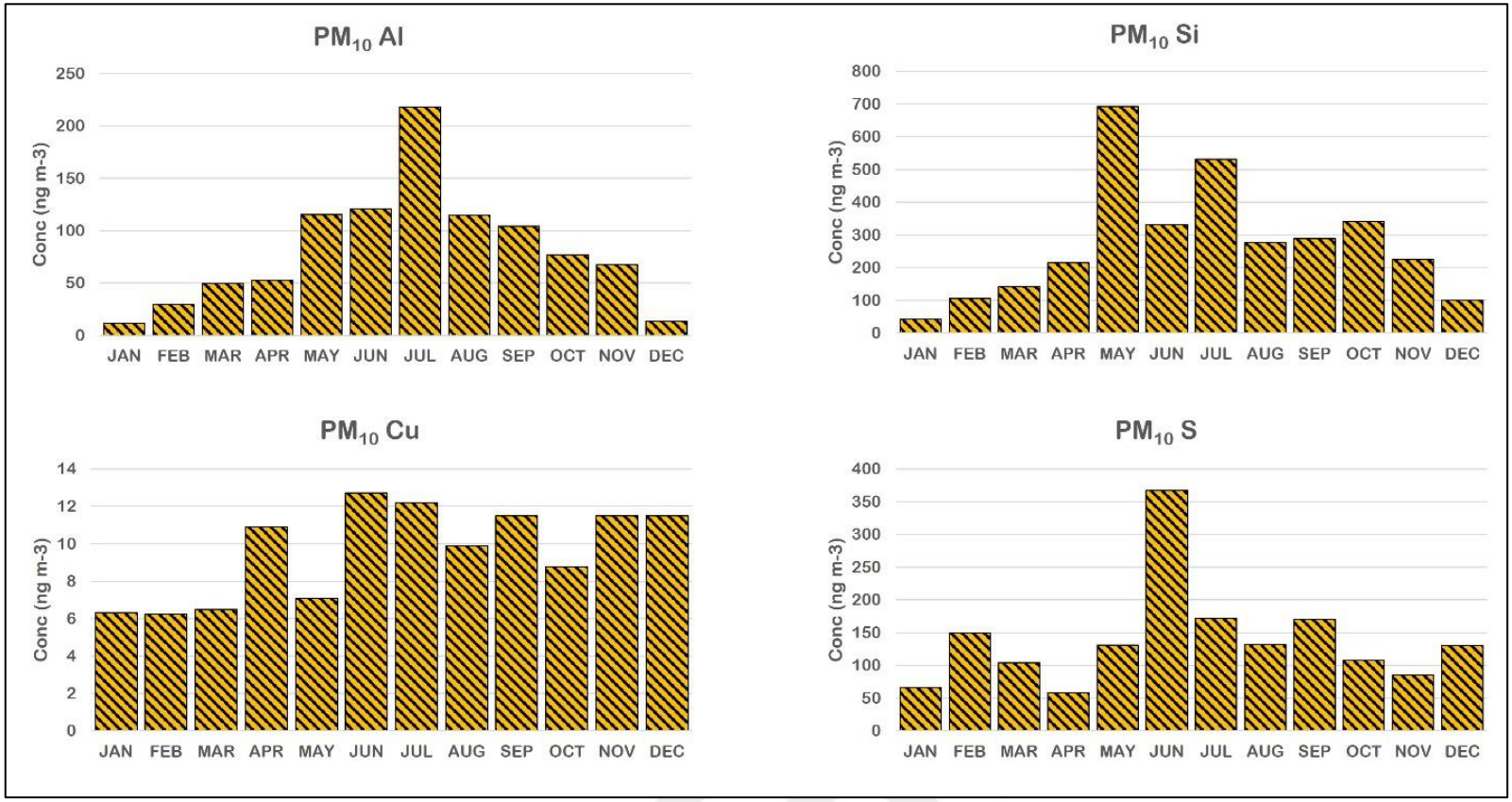

Figure 6.6 Monthly median concentrations of selected elements at Marmaris station

6.3.7 Positive Matrix Factorization

Positive matrix factorization (PMF) was used to determine aerosol components and how much each of these components contributes to PM_{10} mass concentration in the Eastern Mediterranean aerosol population. Five factors were found to be ideal after an optimization process that includes minimization of the difference between objection function Q_{robust} and $Q_{theoretical}$, by adjusting parameters F-peak, scale residuals for the different number of factors. After optimization, Q_{robust} and $Q_{theoretical}$ values for the five-factor solution were 550.5 and 825.7, respectively. Additional modeling uncertainty was assigned the value of 0 because Q values were sufficiently close without using it. The robustness of the five-factor solution was tested using bootstrapping with 100 iterations.

Diagnostic figures that helped us to identify the physical nature of factors are given in Figures 6.7 and 6.8, for factors 3 and 5, which are two anthropogenic factors. Corresponding figures for factors 1, 2, and 4 are given in Figures C3, C4, and C5 in the supplementary material.

Diagnostic figures for each factor include factor composition in ng m^{-3} (F loading), percentage of concentrations of each element explained by that factor, monthly median values of factor scores, and crustal enrichment factors of elements in that factor. Enrichment factors were calculated using composition data (F loading) for that factor, global soil composition given in Rudnick and Gao (2013), and Al as a soil reference element.

Diagnostic figures for Factor 1 are given in Figure C3. Factor 1 accounted for 70% of Na, 20% of Mg and > 10% of K concentrations. This factor represents the sea salt component in the aerosol population. This is supported by higher factor scores in winter due to more extensive bubble bursting and thus higher sea salt production in the winter months. Sodium is moderately and Mg, K, and Ca are weakly enriched in Factor 1. These are elements that have a relatively high concentration in seawater and thus in the marine aerosol. In addition to these elements with strong marine

contribution, chalchophilic elements, As, Cu, S, and Zn are strongly enriched relative to the soil, indicating the mixing of the marine component with anthropogenic during transport. Sea salt factor accounts for 18.2% of PM_{10} mass.

Diagnostic figures for factor 2 are depicted in Figure C4 in the supplementary material. Factor 2 accounts for 40- 80% of the concentrations of crustal elements. None of the elements are significantly enriched and factor scores are higher in summer. Factor 2 is a typical crustal factor and accounts for 25% of PM_{10} mass at our site.

Diagnostic figures for Factor 3 are depicted in Figure 6.7. The figure also includes the distribution of potential Source Contribution Function (PSCF) values in the study domain. The PSCF is a frequently used tool in trajectory statistics. We used back trajectories corresponding to the highest 30% of Factor 3 scores as polluted trajectories. The weighting method, developed by Zhao and Hopke (2006) was used to minimize the effect of grids with only a few trajectory segments in them at the edges of the study area. In addition to this, we also weighted trajectory segments depending on their altitude, to increase the significance of segments that are close to the surface, assuming that those segments have a higher probability of picking up particles from sources at the surface than segments at high altitudes (Malkaz, 2014; Yıkmaz, 2010). For this, segments with altitudes <500 m are multiplied by 1.0, segments between 500 and 1000 m are weighted by 0.5, and segments with z>1000 m are weighted by 0.3. Optimization of these weighting factors using well-defined marine factors in other studies will be discussed in another publication.

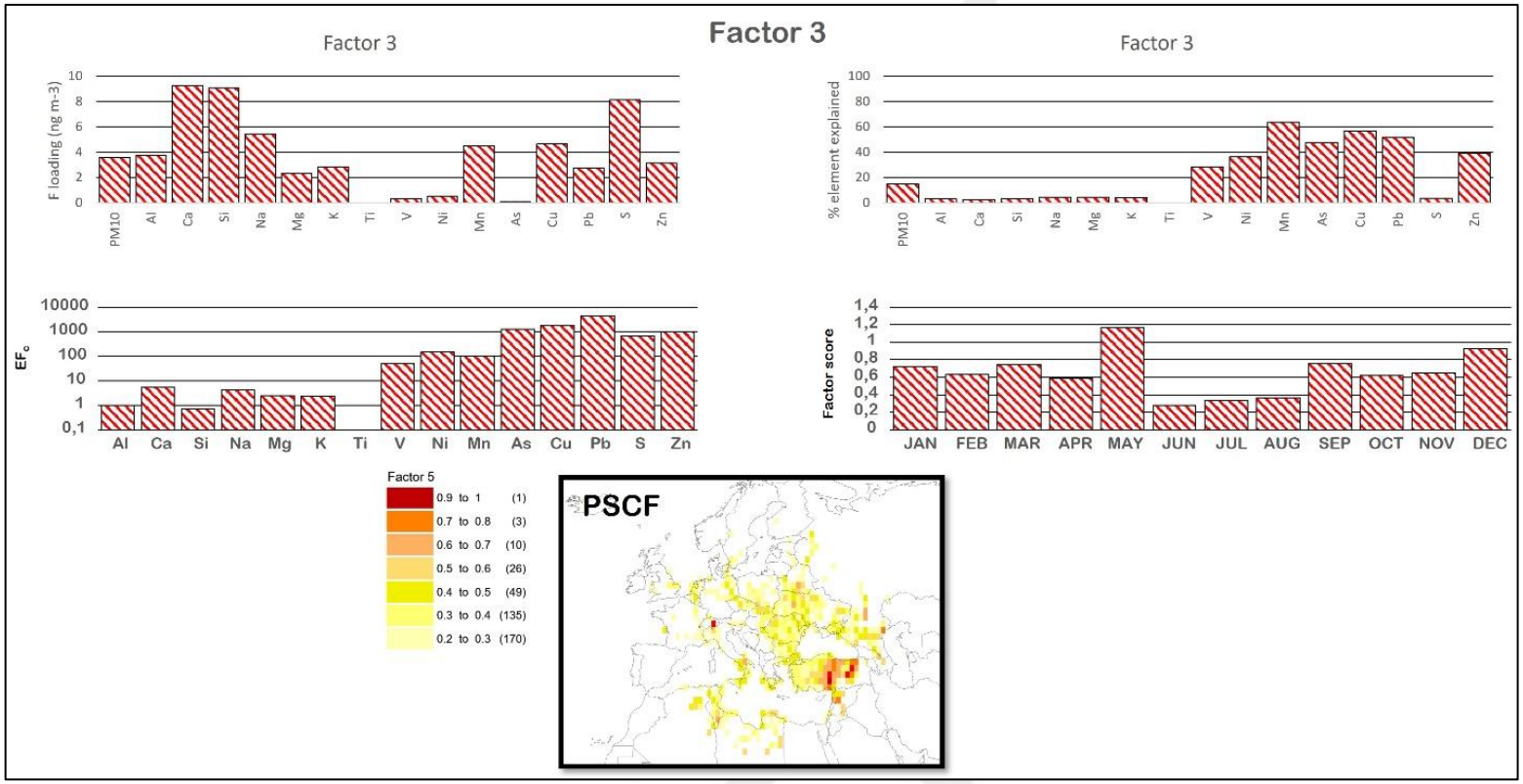

Figure 6.7 Factor composition, fractions of elements explained by each factor crustal enrichment factors of elements in factor, monthly average factor scores and distribution of PSCF values for Factor 3

Factor 3 is an anthropogenic factor. It explains 20- 60% of concentrations of Mn, As, Cu, Pb, and Zn. These elements are moderate to highly enriched relative to the earth's crust (Figure 6.7). Factor 3 scores are higher in the winter months (Figure 6.7). This is interesting and provides a clue about the sources of these chalchophilic elements. As pointed out before in this manuscript, the seasonal behavior of elements with the anthropogenic origin is at least partly determined by the scavenging of these particles during their transport to the Eastern Mediterranean basin. Since wet scavenging is more effective in winter, concentrations of anthropogenic elements are slightly higher in summer months as reported in earlier studies (Güllü et al., 1998; Öztürk et al., 2012). But in this case factor scores are higher in the winter season. This is possible only if sources of elements in this factor are close to the sampling point and they are not effectively scavenged during transport. We observed this phenomenon as in our earlier studies at Antalya, which is approximately 200 km to the east of our sampling point in this study, but not for other elements (Güllü et al., 1998; Öztürk et al., 2012). Relatively local sources for factor 3 are also supported by the distribution of PSCF values in Figure 6.7. The main source areas affecting concentrations of elements in Factor 3 are located in central Anatolia, which means particles emitted from these sources travel 400 to 600 km to reach our sampling location. This travel distance is significantly smaller than the distance traveled by particles emitted from regional sources outside the country. Factor 3 accounts for approximately 15% of measured PM_{10} mass concentration.

Diagnostic figures for Factor 4 are given in Figure C5 in the supplementary material. Factor 4 is another anthropogenic factor. It explains 20% of the concentrations of V, Ni, and Ca. Most of the anthropogenic elements, including, As, Cu, Pb, S, and Zn are highly enriched in Factor 4, Factor scores are higher during the summer season. Tracer species for factor 4 are V and Ni. Since both elements are well-documented indicator species for residual oil combustion, factor 4 was identified as the oil combustion factor. Oil combustion is a frequently reported source of V and/or Ni bearing particles in the Eastern Mediterranean (Achilleos et al., 2015; Calzolai et al., 2015) and is generally attributed to emissions from shipping activities (Chrit et al.,

2018). We do not have a clue about shipping activities as a source of observed Ni and V in this study, but factor 4 is an oil combustion factor. Factor 4 accounts for approximately 10% of PM_{10} mass concentration.

Diagnostic figures for factor 5 are given in Figure 6.8. It is the third anthropogenic component in the Eastern Mediterranean aerosol population. The factor explains approximately 80% of S concentration. Anthropogenic elements, other than S are enriched, but only moderately (EF_c around 100). Sulfur is highly enriched. This is a typical regional secondary sulfate factor, which is a combustion-related factor observed in most regional source apportionment studies (Kušan et al., 2020; Scotto et al., 2021). Factor scores in summer are slightly higher than scores in winter, due to both enhanced photochemistry in summer and more effective wet scavenging during winter months. The distribution of PSCF values in the study domain is given in Figure 6.8. Unlike distributions observed for factor 3, source areas for this factor are more diverse and include Western parts of Turkey, Balkan countries, Eastern Ukraine, and the Black Sea coast of Russia. Factor 5 accounts for 32% of PM_{10} mass concentration in the Eastern Mediterranean atmosphere.

The PMF analysis demonstrated that the aerosol population at our site consists of five components. Please note that the number and type of components found in the PMF exercise depend on the number and type of marker species included in the analysis. With a different set of marker elements, a different set of components could have been found in this study.

Three of the found factors included particles emitted from anthropogenic sources, one included litophilic particles from the crust and one included sea salt particles. One of the anthropogenic sources was relatively local in Central Anatolia, probably from cities with relatively high populations, like Konya, Sivas, Kayseri in that area, the second anthropogenic component (factor 5) is more regional and is related to coal combustion and probably an indicator of powerplants in the region. The last anthropogenic component included well-defined markers of oil combustion.

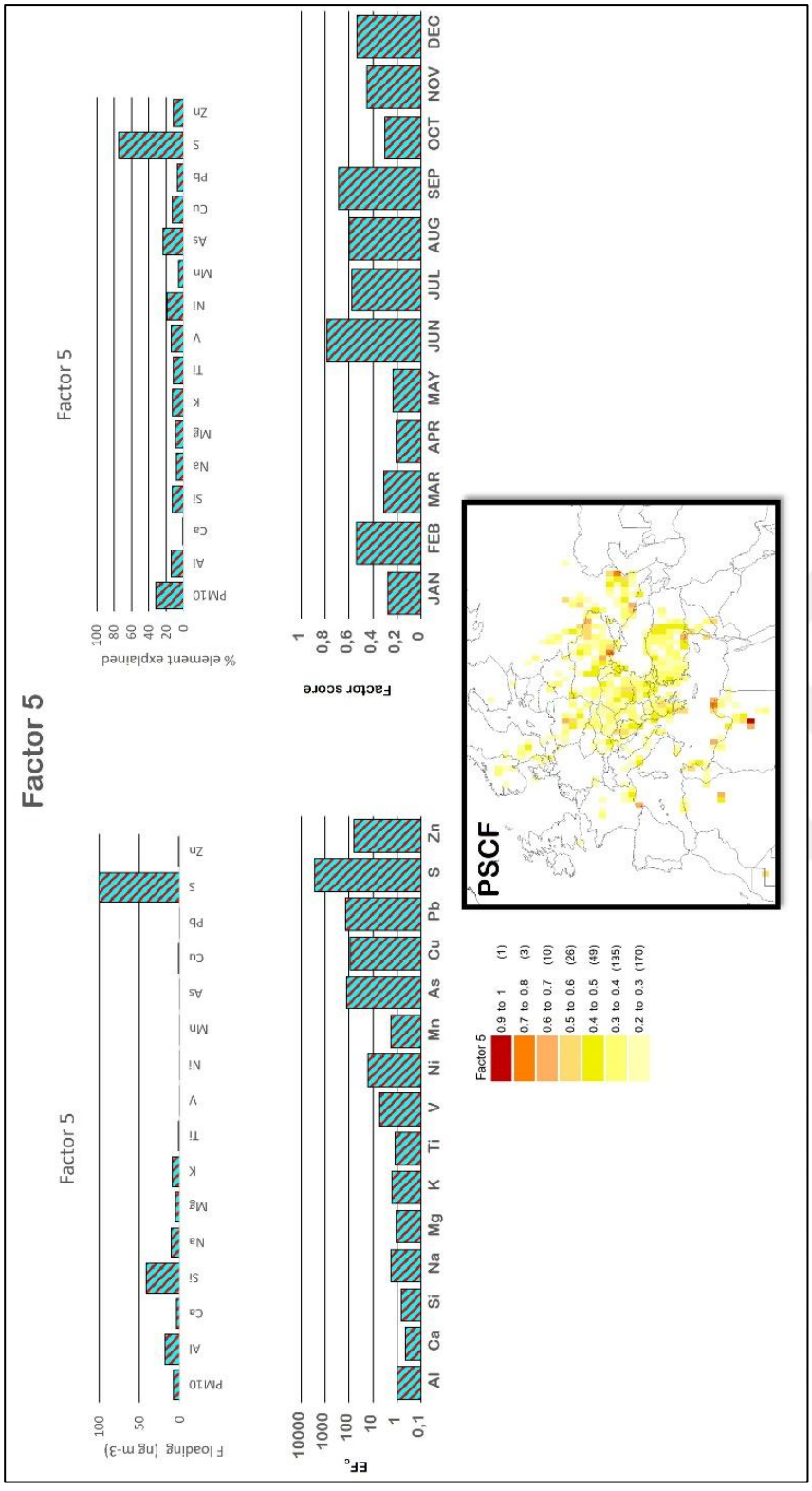

Figure 6.8 Factor composition, fractions of elements explained by each factor crustal enrichment factors of elements in factor, monthly average factor scores and distribution of PSCF values for Factor 5.

The crustal component and regional S component accounted for most of the PM_{10} mass measured at our site. These two sources together accounted for 57% of PM_{10} mass which is followed by the sea salt component. Please note that crustal contribution to PM_{10} mass included both contribution from resuspended local soil and Saharan dust contribution. To differentiate between the two, we identified Saharan dust episodes, using back trajectories, satellite pictures, dream model outputs, and concentrations of Al and Si (TUBITAK, 2019) and deleted these episode data from the data set. The difference between average concentrations of elements and PM_{10} mass with and without those episode data was considered as a contribution of dust transported from North Africa.

The contribution of episodes to concentrations of litophilic elements was 79% for Si and Al, 74% for Ti, 62% for Mg, 55% for Ca and K. Contributions of these dust episodes to concentrations of chalchophilic elements was less than 10%.

6.4 Conclusions

Atmospheric particles and sources contributing to their composition were investigated at a high-altitude station on the Mediterranean coast of Turkey. Daily coarse and fine aerosol samples were collected between 2014 and 2018 and analyzed for fifteen trace elements using ED-XRF.

Concentrations measured at Marmaris are comparable with corresponding data generated in other locations in Turkey. However, there are some minor categoric differences due to the different times samples were collected in different studies.

Coarse-to-fine concentration ratios were between 5 and 7 for litophilic and approximately unity for chalchophilic elements. Indicating that approximately 15% of concentrations of crustal and 50% of concentrations of anthropogenic elements were associated with fine fraction. Calculation EF_c and EF_c – Al diagrams suggested that unexpected enrichment of chalchophilic elements in the coarse fraction is likely

to be due to the sticking of fine pollution–derived particles on coarse crustal and sea salt particles.

Concentrations of elements measured in this study are not significantly different from corresponding concentrations reported for other parts of Turkey. Observed differences can be explained by different times at which samples were collected in different studies.

Dominant upper atmospheric flow directions are SW, W and NW. Air masses spent 77% of their time in these three sectors before they are intercepted at our station. Air masses spent more time in W, NW, N, NE, and E sectors during summer and spent more time in SE, S, SW, and W sectors during winter.

Cluster analysis revealed 7 trajectory clusters. Clusters 2 and 3 are the ones that can potentially bring dust to the Eastern Mediterranean basin. Clusters 5, 6, and 7 are the ones that can potentially bring pollution-derived particles. Clusters 4 and 6 are long trajectories that cross entire Europe before arriving at our site. However, an investigation of altitudes of trajectory segments showed that trajectories in these two clusters generally travel at high altitudes and do not have many low-lying segments that can pick up pollutants from the surface.

Concentrations of crustal elements were higher during the summer season due to easier resuspension of surface soil during summer. The concentration of S was also higher in summer owing to more active photochemistry in the summer months. Concentrations of pollution-derived elements, other than S, did not depict a significant seasonal variation.

A five-factor solution was found to be optimum in PMF exercise. Three of these factors, including factors 3, 4, and 5 represented anthropogenic components in the aerosol population, factors 1 and 2 were sea salt and crustal factors, respectively. One of the anthropogenic factors represented oil combustion component in aerosol population and the other one (factor 3) represented emissions from sources in central

Anatolia and the third one (factor 5) was secondary sulfate factor that has distributed source areas in Balkans, West of Turkey and North of Black Sea.

Crustal factor (F2) and secondary ions (F5) together accounted for approximately 60% of PM_{10} mass concentration. They are followed by sea salt contribution (18%). The crustal component in the aerosol population consisted of both particles from local soil resuspension and crustal particles transported from North Africa. A simple calculation demonstrated that Saharan dust accounts for 55% (K and Ca) – 79% (Al, Si) of concentrations of litophilic elements.

CHAPTER 7

CONCLUSIONS

The present study aimed to examine the relationship between particle sizes and processes in the atmosphere, such as wind and rain while demonstrating how size distributions of particles change during dust transport. The flow climatology of the Eastern Mediterranean region was examined. The sources and/or source regions contributing to PM_{10} concentrations at the rural station were also determined.

Number and mass measurement results showed that during non-dust periods, coarse particles were more dominant in the Ankara atmosphere while the Marmaris atmosphere contained relatively smaller-sized particles. When dust episodes reached the stations, concentrations of PM_{10} particles increase at Marmaris almost two times more than at Ankara station. The decrease in the PM_1 concentrations at the Marmaris station during dust episodes was explained by enhanced secondary particle formation in summer when dust transport is at its minimum.

The change in the general size distribution of the stations during dust transport was investigated through common dust episodes that were observed at both stations. During the 600 km journey of the dust from the Mediterranean coast to central Anatolia, the particle number concentrations in the PM_{10} range were consistently high in Ankara station. This observation suggested that local sources modified the number size distribution in the plume as it traveled over the Anatolian plateau. The effect of transported particulate matter, including dust, on the size distribution at Ankara station, could not be observed clearly due to the masking of transported particles by strong local anthropogenic emissions.

Dust dynamics during the study period showed that episodes last longer in the suburban station compared to the rural station. The influence of Eastern dust sources on the suburban station, as opposed to the rural station, was thought to be the reason

for this observation. However, the lack of sampling along this air pathway makes it hard to prove this deduction. The distribution of dust events showed an unexpected pattern at the rural station and occurred dominantly in the winter months as opposed to the expected summer season dominance. Similar observations were published in the literature previously. Hence, the results supported the seasonality shift in the Saharan dust events.

It was seen that the size distribution was also affected by meteorological events during the transport of the dust cloud from Africa to the receptor region. An increase in the concentration of coarse particles at high wind speeds was observed. In the case of rain, particle concentrations above $PM_{2.5}$ were decreased while there was no change in the concentrations below $PM_{2.5}$. Subsequently, it was deduced that rain events did not lower the effect of PM on human health, as particles below $PM_{2.5}$ are more hazardous to the human respiratory system.

As one of the aims of this study, the source region(s) contributing to PM_{10} concentrations at suburban and rural stations were analyzed. Both stations were under the influence of anthropogenic emissions from local sources, the European continent and North America, and dust emissions from the Sahara region. The heavy influence of the Balkans and West of Turkey's emission sources on the Mediterranean region was significant.

Trace element analysis of collected samples at the rural station showed that chalcophile elements were enriched in the coarse fraction, contrary to general expectation. This suggested the possibility of fine-sized pollution-derived particles to be sticking to coarse crustal and sea salt particles. Concentrations of crustal elements were higher during the summer season due to easier resuspension of surface soil during summer as a result of limited wet scavenging, when compared to the winter season. The effect of meteorological parameters on trace elements and their enrichment at different size ranges could be observed clearly.

PMF analysis of the trace element data obtained from the rural station revealed a total of five factors indicating both anthropogenic and natural origins. Oil

combustion was a very significant anthropogenic source. Although there was no conclusive evidence, heavy marine traffic could also be an important contributor to this factor. Analysis of the composition of the measured PM_{10} showed that the PM_{10} concentrations dominantly consisted of crustal elements and secondary sulfate formation. The contribution of Saharan dust to lithophilic element concentrations and the composition analysis showed the dominant effect of dust (both Saharan and resuspended) on the region.

CHAPTER 8

OVERVIEW

There were a number of points that made this study an interesting one. First, the measurement of submicron particles at two stations in Turkey for 18 months, by itself, is an important contribution to literature. Both are high altitude stations, at approximately 1000 m from sea level and data from such high-altitude locations in the Eastern Mediterranean atmosphere is rare. This was the only study in Turkey that focused on the measurement of particle size distributions between $0.26<D<34$ um. It was a good starting point for policymakers to understand the effects and contribution of these particles to air quality in the region and enable them to shift towards more science-based regulations. Generated data on PM1 concentrations is particularly important because this is the first piece of information on concentrations of submicron particles in Turkey.

In addition to these points, which reflect the novelty of the study due to experimental design, several points reflect the novelty of the study in terms of findings.

- Modification of particle size distribution during transport of dust plume is studied for the first time to our knowledge.

- Separate identification of Saharan dust, Middle East dust, sea salt, and anthropogenic episodes as well as assessment of their climatological features was also very scarce in the region.

- Our treatment of back trajectories was also highly novel. Trajectories are generally treated in two dimensions, but we treated them in three dimensions by weighting them with altitude. This approach was developed because air parcels have a higher probability of picking up pollutants if they are close to the surface. We applied this approach to trajectory clusters and PSCF calculations in the source apportionment part of the study where trace elements were used as source markers.

• The approach we used in investigating flow climatology, particularly in assessing the difference between summer and winter climatology was also not used before. In most of the previous studies, trajectories were assigned to one of the wind sectors depending on the time they spent in that wind sector. Although this approach is not entirely wrong and proved to be useful in earlier studies, most of the trajectories spent their time in more than one wind sector. In this study, we separated each 5-day-long trajectory into 105 hourly segments and counted these segments in each 1ºx1º grid and each wind sector, thus determining how many hours trajectories were spent in each grid and wind sector during the study period. The difference between summer and winter climatology was determined by subtracting the number of segments counted in summer months from a corresponding number of segments counted in winter months. Both approaches, to our knowledge, were not used before.

• In this study, it was found that median diameters of dust plumes increase as they travel from our Mediterranean coast station to Ankara station in central Anatolia. This was also an interesting finding because one would expect to see a decrease in mean particle size during transport due to the faster scavenging of coarse particles. What we observed was just the opposite and indicated that the plume picks up local soil during its 600 km long travel.

• Another interesting finding in this study was the influence of meteorology on particle size. The effect of wind speed and rain on particle size distribution was investigated. Particle concentrations decreased with wind speed as expected. However, the rain had an interesting influence on particle size distribution. Concentrations of particles with diameters between 2.5 and 10 μm decreased significantly during rain events, but concentrations of particles with D< 2.5 μm did not change with rain. Since fine particles with D < 2.5 μm are the one that has health effects, the common belief that "rain cleans the atmosphere" is shown to be wrong (at least for particles).

• Measurement of 16 trace elements using ED-XRF improved our trace element database in the country. Although trace element data is for a short period

between 2014 and 2018, comparison with earlier data suggested that concentrations of anthropogenic elements in the atmosphere are decreasing in time.

- An unexpected enrichment of chalchophilic elements in the coarse fraction was observed and attributed to the sticking of fine pollution-derived particles on coarse crustal and sea salt particles.

- Positive matrix factorization analysis revealed 5 factors at Marmaris. Four of these factors, including crustal, sea salt oil combustion, and secondary sulfate factors were common in all source apportionment studies performed in the Eastern Mediterranean basin. However, one factor, which is unique to this study was also found. This factor represented emissions in central Anatolia, particularly in Konya province.

- Cluster analysis in this study also showed an emerging dust source area in central Anatolia, owing to the drying of Salt Lake due to over-irrigation. Both findings are important for decision-makers and suggest that they should keep an eye on the Konya region in the coming years.

CHAPTER 9

RECOMMENDATIONS

The present study investigated the effect of both meteorological parameters and the transport on the measured concentrations and size distributions of the particulate matter at two stations for 18 months. During the study period some important observations and deductions were made that can act as a guideline for future studies:

- During the study, PM samples were collected for 18 months. This short period brings a relatively high statistical uncertainty to the measurement results. Increasing the duration of the sampling period and incorporating with results from this study will reduce the uncertainty in the observations.
- In the current study, dust could only be measured at the surface level. Incorporation of the sun photometer in future studies can enable the measurement of dust in the upper atmosphere and clarify the dust patterns in the region better.
- Since the rural station was located almost 1000 km above sea level, the comparison between the sea level concentrations and the measurements at the sampling station could not be made. Sea-level number and mass measurements of PM_1, $PM_{2.5}$, and PM_{10} can enable the investigation of the size distribution throughout a tropospheric vertical column.
- Since the trace element analysis of the samples was done with ED-XRF, only 16 trace elements could be identified in the collected samples. Some of the very important marker elements, such as rare earth elements used as Saharan dust tracers, could not be measured. Therefore, the use of ICP-MS analysis during the following studies could be a better option.
- Measurement of < 0.1 μm particulates can give information on the contribution of secondary particle formation on the total particulate matter concentration. Our minimum size range was 0.26 μm and this pattern could

not be observed clearly. We could only observe the results of the coagulation of the formed secondary particulate matter.

- The locations of the sampling stations can be arranged to cross the pathways of the air masses coming from both the Sahara and the Middle East and Arabian Peninsula. Dust sources in the Middle East and Arabian Peninsula are not as well-known as in the Sahara region. Thus, this setup can enable us to measure dust concentrations, determine their sources and observe the effects on other regions.

REFERENCES

Aalto, P., Hameri, K., Paatero, P., Kulmala, M., Bellander, T., Berglind, N., Bouso, L., Castaño-Vinyals, G., Sunyer, J., Cattani, G., Marconi, A., Cyrys, J., von Klot, S., Peters, A., Zetzsche, K., Lanki, T., Pekkanen, J., Nyberg, F., Sjövall, B., & Forastiere, F. (2005). Aerosol particle number concentration measurements in five European cities using TSI-3022 condensation particle counter over a three-year period during health effects of air pollution on susceptible subpopulations. *Journal of the Air & Waste Management Association*, *55*(8), 1064–1076. https://doi.org/10.1080/10473289.2005.10464702.

Abdurrahman, M. I., Chaki, S., & Saini, G. (2020). Stubble burning: Effects on health & environment, regulations and management practices. *Environmental Advances*, *2*(September), 100011. https://doi.org/10.1016/j.envadv.2020.100011

Achilleos, S., Ferguson, S., Kang, C.-M., Hadjimitsis, D., Hadjicharalambous, M., Achilleos, C., Christodoulou, A., Nisantzi, A., Papoutsa, C., Themistocleous, K., Athanasatos, S., Perdikou, S., & Koutrakis, P. (2015). Spatial variability of fine and coarse particle composition and sources in Cyprus. *Atmospheric Research*, *169*, 255–270. https://doi.org/10.1016/j.atmosres.2015.10.005

Agudelo-Castañeda, D. M., Teixeira, E. C., Schneider, I. L., Lara, S. R., & Silva, L. F. O. (2017). Exposure to polycyclic aromatic hydrocarbons in atmospheric PM1.0 of urban environments: Carcinogenic and mutagenic respiratory health risk by age groups. *Environmental Pollution*, *224*, 158–170. https://doi.org/10.1016/J.ENVPOL.2017.01.075

Aguilera, R., Corringham, T., Gershunov, A., & Benmarhnia, T. (2021). Wildfire smoke impacts respiratory health more than fine particles from other sources: observational evidence from Southern California. *Nature Communications*,

12(1). https://doi.org/10.1038/s41467-021-21708-0

Al-Momani, I. F., Momani, K. A., Jaradat, Q. M., Massadeh, A. M., Yousef, Y. A., & Alomary, A. A. (2008). Atmospheric deposition of major and trace elements in Amman, Jordan. *Environmental Monitoring and Assessment*, *136*(1–3), 209–218. https://doi.org/10.1007/s10661-007-9676-4

Al-Momani, I., Tuncel, S. G., Eler, Ü., Örtel, E., Gürol!^irin, & Tuncel, G. (1995). Major ion composition of wet and dry deposition in the eastern Mediterranean basin. *Science of The Total Environment*, *164*, 75–85.

Alves, D. D., Riegel, R. P., Klauck, C. R., Ceratti, A. M., Hansen, J., Cansi, L. M., Pozza, S. A., de Quevedo, D. M., & Osório, D. M. M. (2020). Source apportionment of metallic elements in urban atmospheric particulate matter and assessment of its water-soluble fraction toxicity. *Environmental Science and Pollution Research International*, *27*(11), 12202–12214. https://doi.org/10.1007/s11356-020-07791-8

Andreae, M. . (1995). Climate effects of changing atmospheric aerosol levels. *World Survey of Climatology*, *16*, 341–392.

Araujo, J. A., & Nel, A. E. (2009). *Particle and Fibre Toxicology Particulate matter and atherosclerosis: role of particle size, composition and oxidative stress*. https://doi.org/10.1186/1743-8977-6-24

Argyropoulos, G., Manoli, E., Kouras, A., & Samara, C. (2012). Concentrations and source apportionment of PM10 and associated major and trace elements in the Rhodes Island, Greece. *Science of The Total Environment*, *432*, 12–22. https://doi.org/10.1016/J.SCITOTENV.2012.05.076

Asgharian, B., Hofmann, W., & Bergmann, R. (2001). Particle deposition in a multiple-path model of the human lung. *Aerosol Science and Technology*, *34*(4), 332–339. https://doi.org/10.1080/02786820119122

Athanasopoulou, E., Protonotariou, A., Papangelis, G., Tombrou, M., Mihalopoulos,

N., & Gerasopoulos, E. (2016). Long-range transport of Saharan dust and chemical transformations over the Eastern Mediterranean. *Atmospheric Environment*, *140*, 592–604. https://doi.org/10.1016/j.atmosenv.2016.06.041

Avila, A., & Peñuelas, J. (1999). Increasing frequency of Saharan rains over northeastern Spain and its ecological consequences. *Science of The Total Environment*, *228*(2), 153–156. https://doi.org/https://doi.org/10.1016/S0048-9697(99)00041-8

Avila, A., Queralt, I., & Alarcón, M. (1997). Mineralogical composition of African dust delivered by red rains over North-Eastern Spain. *Journal of Geophysical Research*, *102*, 21977–21996. https://doi.org/10.1029/97JD00485

Baccini, M., Grisotto, L., Catelan, D., Consonni, D., Bertazzi, P. A., & Biggeri, A. (2015). Commuting-adjusted short-term health impact assessment of airborne fine particles with uncertainty quantification via Monte Carlo simulation. *Environmental Health Perspectives*, *123*(1), 27–33. https://doi.org/10.1289/ehp.1408218

Bagtasa, G., Cayetano, M. G., Yuan, C. S., Uchino, O., Sakai, T., Izumi, T., Morino, I., Nagai, T., Macatangay, R. C., & Velazco, V. A. (2019). Long-range transport of aerosols from East and Southeast Asia to northern Philippines and its direct radiative forcing effect. *Atmospheric Environment*, *218*(June), 117007. https://doi.org/10.1016/j.atmosenv.2019.117007

Baklanov, A., Aloyan, A., Mahura, A., Arutyunyan, V., & Luzan, P. (2011). Evaluation of source–receptor relationship for atmospheric pollutants using approaches of trajectory modelling, cluster, probability fields analyses and adjoint equations. *Atmospheric Pollution Research*, *2*(4), 400–408. https://doi.org/10.5094/APR.2011.045

Balcilar, I., Zararsiz, A., Kalayci, Y., Doğan, G., & Tuncel, G. (2014). Chemical composition of Eastern Black Sea aerosol-Preliminary results. *Science of the Total Environment*, *488–489*(1), 422–428.

https://doi.org/10.1016/j.scitotenv.2013.12.023

Balcılar, İ. (2018). *Chemical Composition of Atmospheric Particles as a Tool to Identify Sources Affecting Aerosol Population in the Eastern Black Sea Atmosphere* (Issue March). Middle East Technical University.

Balcılar, I., Zararsız, A., Kalaycı, Y., Doğan, G., & Tuncel, G. (2014). Chemical composition of Eastern Black Sea aerosol--preliminary results. *The Science of the Total Environment*, *488–489*, 422–428. https://doi.org/10.1016/j.scitotenv.2013.12.023

Balcılar, İ., Zararsız, A., Kalaycı, Y., Doğan, G., & Tuncel, G. (2014a). Chemical composition of Eastern Black Sea aerosol—Preliminary results. *Science of The Total Environment*, *488–489*, 422–428. https://doi.org/10.1016/j.scitotenv.2013.12.023

Balcılar, İ., Zararsız, A., Kalaycı, Y., Doğan, G., & Tuncel, G. (2014b). Chemical composition of Eastern Black Sea aerosol—Preliminary results. *Science of The Total Environment*, *488–489*, 422–428. https://doi.org/10.1016/J.SCITOTENV.2013.12.023

Beloconi, A., & Vounatsou, P. (2021). *Substantial Reduction in Particulate Matter Air Pollution across Europe during 2006 − 2019: A Spatiotemporal Modeling Analysis*. https://doi.org/10.1021/acs.est.1c03748

Benedetti, A., Di Giuseppe, F., Jones, L., Peuch, V. H., Rémy, S., & Zhang, X. (2019). The value of satellite observations in the analysis and short-range prediction of Asian dust. *Atmospheric Chemistry and Physics*, *19*(2), 987–998. https://doi.org/10.5194/acp-19-987-2019

Benkhalifa, J., Léon, J. F., & Chaabane, M. (2019). Aerosol vertical distribution, optical properties and dust transport in the Western Mediterranean basin (case study: Summer, 2012). *Atmospheric Pollution Research*, *10*(4), 1291–1298. https://doi.org/10.1016/j.apr.2019.02.013

Bergametti, G., Remoundaki, E., Losno, R., Steiner, E., Chatenet, B., & Buat-Menard, P. (1992). Source, transport and deposition of atmospheric phosphorus over the Northwestern Mediterranean. *Journal of Atmospheric Chemistry*, *14*, 501–513. https://doi.org/10.1007/BF00115254

Bergametti, Gi., Dutot, A.-L., Buat-MéNard, P., Losno, R., & Remoudaki, E. (1989). Seasonal variability of the elemental composition of atmospheric aerosol particles over the northwestern Mediterranean. *Tellus B: Chemical and Physical Meteorology*, *41*(3), 353–361. https://doi.org/10.3402/tellusb.v41i3.15092

Bonnefoy, A., Plumejeaud, S., Noack, Y., Robin, D., Doumenq, P., Chaspoul, F., Tassistro, V., & Orsière, T. (2017). Fine atmospheric particles emitted by industrial, traffic and urban sources in France: characterization and genotoxicity. *Toxicological and Environmental Chemistry*, *99*(2), 340–361. https://doi.org/10.1080/02772248.2016.1176169

Bossioli, E., Tombrou, M., Kalogiros, J., Allan, J., Bacak, A., Bezantakos, S., Biskos, G., Coe, H., Jones, B., Kouvarakis, G., Mihalopoulos, N., & Persival, C. J. (2016). Atmospheric composition in the Eastern Mediterranean: Influence of biomass burning during summertime using the WRF-Chem model. *Atmospheric Environment*, *132*. https://doi.org/10.1016/j.atmosenv.2016.03.011

Boucher, O., Randall, D., Artaxo, P., Bretherton, C., Feingold, G., Forster, P., Kerminen, V.-M., Kondo, Y., Liao, H., Lohmann, U., Rasch, P., Satheesh, S., Sherwood, S., Stevens, B., & Zhang, X. (2013). Clouds and Aerosols. In *Climate Change: The Physical Science Basis. Contribution of Working Group I to the Fifth Assessment Report of the Intergovernmental Panel on Climate Change*. Cambridge University Press.

Bougiatioti, A., Zarmpas, P., Koulouri, E., Antoniou, M., Theodosi, C., Kouvarakis, G., Saarikoski, S., Mäkelä, T., Hillamo, R., & Mihalopoulos, N. (2013).

Organic, elemental and water-soluble organic carbon in size segregated aerosols, in the marine boundary layer of the Eastern Mediterranean. *Atmospheric Environment*, *64*, 251–262. https://doi.org/10.1016/j.atmosenv.2012.09.071

Bozlaker, A., Prospero, J. M., Price, J., & Chellam, S. (2019). Identifying and Quantifying the Impacts of Advected North African Dust on the Concentration and Composition of Airborne Fine Particulate Matter in Houston and Galveston, Texas. *Journal of Geophysical Research: Atmospheres*, *124*(22), 12282–12300. https://doi.org/10.1029/2019JD030792

Brankov, E., Rao, S. T., & Porter, P. S. (1998). A trajectory-clustering-correlation methodology for examining the long-range transport of air pollutants. *Atmospheric Environment*, *32*(9), 1525–1534. https://doi.org/10.1016/S1352-2310(97)00388-9

Bressi, M., Cavalli, F., Belis, C. A., Putaud, J.-P., Fröhlich, R., dos Santos, S., Petralia, E., Prévôt, A. S. H., Berico, M., Malaguti, A., & Canonaco, F. (2016). Variations in the chemical composition of the submicron aerosol and in the sources of the organic fraction at a regional background site of the Po Valley (Italy). *Atmospheric Chemistry and Physics*, *16*(20), 12875–12896. https://doi.org/10.5194/acp-16-12875-2016

Byčenkiene, S., Dudoitis, V., & Ulevicius, V. (2014). The Use of Trajectory Cluster Analysis to Evaluate the Long-Range Transport of Black Carbon Aerosol in the South-Eastern Baltic Region. *Advances in Meteorology*, *2014*. https://doi.org/10.1155/2014/137694

Caggiano, R., Macchiato, M., & Trippetta, S. (2010). Levels, chemical composition and sources of fine aerosol particles (PM1) in an area of the Mediterranean basin. *Science of the Total Environment*, *408*(4), 884–895. https://doi.org/10.1016/j.scitotenv.2009.10.064

Caggiano, R., Sabia, S., & Speranza, A. (2019). Trace elements and human health

risks assessment of finer aerosol atmospheric particles (PM1). *Environmental Science and Pollution Research*, *26*(36), 36423–36433. https://doi.org/10.1007/s11356-019-06756-w

Calidonna, C. R., Avolio, E., Gullì, D., Ammoscato, I., De Pino, M., Donateo, A., & Feudo, T. Lo. (2020). Five years of dust episodes at the Southern Italy GAW regional coastal mediterranean observatory: Multisensors and modeling analysis. *Atmosphere*, *11*(5). https://doi.org/10.3390/ATMOS11050456

Calvo, A. I., Alves, C., Castro, A., Pont, V., Vicente, A. M., & Fraile, R. (2013). Research on aerosol sources and chemical composition: Past, current and emerging issues. *Atmospheric Research*, *120–121*, 1–28. https://doi.org/10.1016/j.atmosres.2012.09.021

Calzolai, G., Nava, S., Lucarelli, F., Chiari, M., Giannoni, M., Becagli, S., Traversi, R., Marconi, M., Frosini, D., Severi, M., Udisti, R., Di Sarra, A., Pace, G., Meloni, D., Bommarito, C., Monteleone, F., Anello, F., & Sferlazzo, D. M. (2015). Characterization of PM10 sources in the central Mediterranean. *Atmospheric Chemistry and Physics*, *15*(24), 13939–13955. https://doi.org/10.5194/acp-15-13939-2015

Cao, J., Chow, J. C., Lee, F. S. C., & Watson, J. G. (2013). Evolution of PM2.5 measurements and standards in the U.S. And future perspectives for China. *Aerosol and Air Quality Research*, *13*(4), 1197–1211. https://doi.org/10.4209/aaqr.2012.11.0302

Carnerero, C., Rivas, I., Reche, C., Perez, N., Alastuey, A., & Querol, X. (2021). Trends in primary and secondary particle number concentrations in urban and regional environments in NE Spain. *Atmospheric Environment*, *244*, 117982. https://doi.org/10.1016/j.atmosenv.2020.117982

Carter, W. P. L., & Seinfeld, J. H. (2012). Winter ozone formation and VOC incremental reactivities in the Upper Green River Basin of Wyoming. *Atmospheric Environment*, *50*(x), 255–266.

https://doi.org/10.1016/j.atmosenv.2011.12.025

Çelik, İ. (2014). *Source Apportionment of Trace Elements in Ankara* (Issue December). Middle East Technical University.

Charron, A., Plaisance, H., Sauvage, S., Coddeville, P., & J-C, G. (2000). A study of the source-receptor relationships influencing the acidity of precipitation collected at a rural site in France. *Atmospheric Environment*, *34*, 3665–3674. https://doi.org/10.1016/S1352-2310(00)00096-0

Chen, S., Jiang, N., Huang, J., Xu, X., Zhang, H., Zang, Z., Huang, K., Xu, X., Wei, Y., Guan, X., Zhang, X., Luo, Y., Hu, Z., & Feng, T. (2018). Quantifying contributions of natural and anthropogenic dust emission from different climatic regions. *Atmospheric Environment*, *191*(July), 94–104. https://doi.org/10.1016/j.atmosenv.2018.07.043

Chen, X., Wang, Z., Li, J., Yang, W., Chen, H., Wang, Z., Hao, J., Ge, B., Wang, D., & Huang, H. (2018). Simulation on different response characteristics of aerosol particle number concentration and mass concentration to emission changes over mainland China. *Science of The Total Environment*, *643*, 692–703. https://doi.org/10.1016/J.SCITOTENV.2018.06.181

Cheriyan, D., Khamraev, K., & Choi, J. ho. (2021). Varying health risks of respirable and fine particles from construction works. *Sustainable Cities and Society*, *72*(May), 103016. https://doi.org/10.1016/j.scs.2021.103016

Choi, E., Choi, K., & Yi, S.-M. (2011). Non-methane hydrocarbons in the atmosphere of a Metropolitan City and a background site in South Korea: Sources and health risk potentials. *Atmospheric Environment*, *45*(40), 7563–7573. https://doi.org/10.1016/j.atmosenv.2010.11.049

Cholakian, A., Colette, A., Coll, I., Ciarelli, G., Beekmann, M., Atmosphériques, S., & Cnrs, U. M. R. (2019). *Future climatic drivers and their effect on PM 10 components in Europe and the Mediterranean Sea*. 4459–4484.

Choobari, O. A., Zawar-Reza, P., & Sturman, A. (2014). The global distribution of mineral dust and its impacts on the climate system: A review. *Atmospheric Research*, *138*, 152–165. https://doi.org/10.1016/J.ATMOSRES.2013.11.007

Chow, J. C. (1995). Measurement methods to determine compliance with ambient air quality standards for suspended particles. *Journal of the Air and Waste Management Association*, *45*(5), 320–382. https://doi.org/10.1080/10473289.1995.10467369

Chrit, M., Sartelet, K., Sciare, J., Pey, J., Nicolas, J. B., Marchand, N., Freney, E., Sellegri, K., Beekmann, M., & Dulac, F. (2018). Aerosol sources in the western Mediterranean during summertime: a model-based approach. *Atmospheric Chemistry and Physics*, *18*(13), 9631–9659. https://doi.org/10.5194/acp-18-9631-2018

Civan, M. Y., Elbir, T., Seyfioglu, R., Kuntasal, Ö. O., Bayram, A., Doğan, G., Yurdakul, S., Andiç, Ö., Müezzinoğlu, A., Sofuoglu, S. C., Pekey, H., Pekey, B., Bozlaker, A., Odabasi, M., & Tuncel, G. (2015). Spatial and temporal variations in atmospheric VOCs, NO2, SO2, and O3 concentrations at a heavily industrialized region in Western Turkey, and assessment of the carcinogenic risk levels of benzene. *Atmospheric Environment*, *103*, 102–113. https://doi.org/10.1016/j.atmosenv.2014.12.031

Colette, A., & Ineris, L. R. (2020). *Air Quality Trends in Europe : 2000-2017* (Issue 2).

Córdoba-Jabonero, C., Sorribas, M., Guerrero-Rascado, J. L., Adame, J. A., Hernández, Y., Lyamani, H., Cachorro, V., Gil, M., Alados-Arboledas, L., Cuevas, E., & De La Morena, B. (2011). Synergetic monitoring of Saharan dust plumes and potential impact on surface: A case study of dust transport from Canary Islands to Iberian Peninsula. *Atmospheric Chemistry and Physics*, *11*(7), 3067–3091. https://doi.org/10.5194/acp-11-3067-2011

Cusack, M., Pérez, N., Pey, J., Alastuey, A., & Querol, X. (2013). Source

apportionment of fine PM and sub-micron particle number concentrations at a regional background site in the western Mediterranean: A 2.5 year study. *Atmospheric Chemistry and Physics*, *13*(10), 5173–5187. https://doi.org/10.5194/acp-13-5173-2013

Cvitešić Kušan, A., Kroflič, A., Grgić, I., Ciglenečki, I., & Frka, S. (2020). Chemical characterization of fine aerosols in respect to water-soluble ions at the eastern Middle Adriatic coast. *Environmental Science and Pollution Research*, *27*(10), 10249–10264. https://doi.org/10.1007/s11356-020-07617-7

Dayan, U., & Miller, J. M. (1989). *Meteorological and climatological data from surface and upper air measurements for the assessment of atmospheric transport and deposition of pollutants in the Mediterranean Basin : a review. Mediterranean Action Plan Part A.*

Dimitriou, K., & Kassomenos, P. (2019). Estimation of North African dust contribution on PM10 episodes at four continental Greek cities. *Ecological Indicators*, *106*(June), 105530. https://doi.org/10.1016/j.ecolind.2019.105530

Dinoi, A., Weinhold, K., Wiedensohler, A., & Contini, D. (2021). Study of new particle formation events in southern Italy. *Atmospheric Environment*, *244*(September 2020), 117920. https://doi.org/10.1016/j.atmosenv.2020.117920

Doğan, G., Güllü, G., & Tuncel, G. (2008). Sources and source regions effecting the aerosol composition of the Eastern Mediterranean. *Microchemical Journal*, *88*, 142–149. https://doi.org/10.1016/j.microc.2007.11.017

Doyi, I. N. Y., Strezov, V., Isley, C. F., Yazdanparast, T., & Taylor, M. P. (2020). The relevance of particle size distribution and bioaccessibility on human health risk assessment for trace elements measured in indoor dust. *Science of the Total Environment*, *733*, 137931. https://doi.org/10.1016/j.scitotenv.2020.137931

Draxler, R. R., & Hess, G. D. (1998). An overview of the HYSPLIT_4 modelling system for trajectories, dispersion and deposition. In *Australian Meteorological*

Magazine (Vol. 47, Issue 4).

Dzubay, T. G., Stevens, R. K., & Haagenson, P. L. (1984). Composition and origins of aerosol at a forested mountain in Soviet Georgia. *Environmental Science & Technology*, *18*(11), 873–883. https://doi.org/10.1021/es00129a012

Ealo, M., Alastuey, A., Ripoll, A., Pérez, N., Minguillón, M. C., Querol, X., & Pandolfi, M. (2016). Detection of Saharan dust and biomass burning events using near-real-time intensive aerosol optical properties in the north-western Mediterranean. *Atmospheric Chemistry and Physics*, *16*(19), 12567–12586. https://doi.org/10.5194/acp-16-12567-2016

EEA. (2012). *Particulate matter from natural sources and related reporting under the EU Air Quality Directive in 2008 and 2009*. https://www.eea.europa.eu/publications/particulate-matter-from-natural-sources/file

Elmes, M., & Gasparon, M. (2017). Sampling and single particle analysis for the chemical characterisation of fine atmospheric particulates: A review. In *Journal of Environmental Management*. https://doi.org/10.1016/j.jenvman.2017.06.067

Eneroth, K., Kjellström, E., & Holmén, K. (2003). A trajectory climatology for Svalbard; investigating how atmospheric flow patterns influence observed tracer concentrations. *Physics and Chemistry of the Earth, Parts A/B/C*, *28*(28–32), 1191–1203. https://doi.org/10.1016/J.PCE.2003.08.051

Figgis, B., Guo, B., Javed, W., Ahzi, S., & Rémond, Y. (2018). Dominant environmental parameters for dust deposition and resuspension in desert climates. *Aerosol Science and Technology*, *52*(7), 788–798. https://doi.org/10.1080/02786826.2018.1462473

Floutsi, A. A., Korras-Carraca, M. B., Matsoukas, C., Hatzianastassiou, N., & Biskos, G. (2016). Climatology and trends of aerosol optical depth over the Mediterranean basin during the last 12 years (2002–2014) based on Collection 006 MODIS-Aqua data. *Science of The Total Environment*, *551–552*, 292–303.

https://doi.org/10.1016/J.SCITOTENV.2016.01.192

Foltz, G. R., & McPhaden, M. J. (2008). Trends in Saharan dust and tropical Atlantic climate during 1980–2006. *Geophysical Research Letters*, *35*(20). https://doi.org/https://doi.org/10.1029/2008GL035042

Forster, C., Wandinger, U., Wotawa, G., James, P., Mattis, I., Althausen, D., Simmonds, P., O'Doherty, S., Jennings, S. G., Kleefeld, C., Schneider, J., Trickl, T., Kreipl, S., Jäger, H., & Stohl, A. (2001). Transport of boreal forest fire emissions from Canada to Europe. *Journal of Geophysical Research Atmospheres*, *106*(D19), 22887–22906. https://doi.org/10.1029/2001JD900115

Forster, P. M., Storelvmo, T., Armour, K., Collins, W., Dufresne, J. L., Frame, D., Lunt, D. J., Mauritsen, T., Palmer, M. D., Watanabe, M., Wild, M., & Zhang, H. (2021). Chapter 7: The Earth's Energy Budget, Climate Feedbacks, and Climate Sensitivity. *Climate Change 2021: The Physical Science Basis. Contribution of Working Group I to the Sixth Assessment Report of the Intergovernmental Panel on Climate Change*, *August*, in press.

Freney, E., Sellegri, K., Chrit, M., Adachi, K., Brito, J., Waked, A., Borbon, A., Colomb, A., Dupuy, R., Pichon, J. M., Bouvier, L., Delon, C., Jambert, C., Durand, P., Bourianne, T., Gaimoz, C., Triquet, S., Féron, A., Beekmann, M., … Sartelet, K. (2018). Aerosol composition and the contribution of SOA formation over Mediterranean forests. *Atmospheric Chemistry and Physics*, *18*(10), 7041–7056. https://doi.org/10.5194/acp-18-7041-2018

Friese, C. A., van der Does, M., Merkel, U., Iversen, M. H., Fischer, G., & Stuut, J. B. W. (2016). Environmental factors controlling the seasonal variability in particle size distribution of modern Saharan dust deposited off Cape Blanc. *Aeolian Research*, *22*, 165–179. https://doi.org/10.1016/j.aeolia.2016.04.005

Fuller, C. H., O'Neill, M. S., Sarnat, J. A., Chang, H. H., Tucker, K. L., & Brugge, D. (2018). Short-and medium-term associations of particle number concentration with cardiovascular markers in a Puerto Rican cohort.

Environmental Research, *166*(June), 595–601. https://doi.org/10.1016/j.envres.2018.06.042

Galindo, N., Yubero, E., Clemente, Á., Nicolás, J. F., Varea, M., & Crespo, J. (2020). PM events and changes in the chemical composition of urban aerosols: A case study in the western Mediterranean. *Chemosphere*, *244*, 125520. https://doi.org/10.1016/j.chemosphere.2019.125520

Ganor, E., Foner, H. A., Bingemer, H. G., Udisti, R., & Setter, I. (2000). Biogenic sulphate generation in the Mediterranean Sea and its contribution to the sulphate anomaly in the aerosol over Israel and the Eastern Mediterranean. *Atmospheric Environment*, *34*(20), 3453–3462. https://doi.org/10.1016/S1352-2310(00)00077-7

Ganor, Eliezer, Osetinsky, I., Stupp, A., & Alpert, P. (2010). Increasing trend of African dust, over 49 years, in the eastern Mediterranean. *Journal of Geophysical Research: Atmospheres*, *115*(D7). https://doi.org/https://doi.org/10.1029/2009JD012500

Ganor, Eliezer, Stupp, A., & Alpert, P. (2009). A method to determine the effect of mineral dust aerosols on air quality. *Atmospheric Environment*, *43*(34), 5463–5468. https://doi.org/https://doi.org/10.1016/j.atmosenv.2009.07.028

Gatti, A. M., & Montanari, S. (Eds.). (2015). Chapter 2 - A Very Brief History of Particulate Pollution. In *Case Studies in Nanotoxicology and Particle Toxicology* (pp. 7–11). Academic Press. https://doi.org/https://doi.org/10.1016/B978-0-12-801215-4.00002-9

Genc, D. D., Yesilyurt, C., & Tuncel, G. (2010). Air pollution forecasting in Ankara, Turkey using air pollution index and its relation to assimilative capacity of the atmosphere. *Environmental Monitoring and Assessment*, *166*(1–4), 11–27. https://doi.org/10.1007/s10661-009-0981-y

Ghosh, A., Roy, A., Das, S. K., Ghosh, S. K., Raha, S., & Chatterjee, A. (2020). Identification of most preferable reaction pathways for chloride depletion from

size segregated sea-salt aerosols: A study over high altitude Himalaya, tropical urban metropolis and tropical coastal mangrove forest in eastern India. *Chemosphere*, *245*, 125673. https://doi.org/https://doi.org/10.1016/j.chemosphere.2019.125673

Gini, M., Manousakas, M.-I., Karydas, A. G., & Eleftheriadis, K. (2022). Mass size distributions, composition and dose estimates of particulate matter in Saharan dust outbreaks. *Environmental Pollution*, 118768. https://doi.org/https://doi.org/10.1016/j.envpol.2021.118768

Ginoux, P., Prospero, J. M., Gill, T. E., Hsu, N. C., & Zhao, M. (2012). Global-scale attribution of anthropogenic and natural dust sources and their emission rates based on MODIS Deep Blue aerosol products. *Reviews of Geophysics*, *50*(3), 1–36. https://doi.org/10.1029/2012RG000388

Gkikas, A., Houssos, E. E., Lolis, C. J., Bartzokas, A., & Mihalopoulos, N. (2015). *Atmospheric circulation evolution related to desert-dust episodes over the Mediterranean*. *July*, 1634–1645. https://doi.org/10.1002/qj.2466

Glavas, S. D., Nikolakis, P., Ambatzoglou, D., & Mihalopoulos, N. (2008). Factors affecting the seasonal variation of mass and ionic composition of PM2.5 at a central Mediterranean coastal site. *Atmospheric Environment*, *42*(21), 5365–5373. https://doi.org/https://doi.org/10.1016/j.atmosenv.2008.02.055

Gonçalves, S. J., Weis, J., China, S., Evangelista, H., Harder, T. H., Müller, S., Sampaio, M., Laskin, A., Gilles, M. K., & Godoi, R. H. M. (2021). Photochemical reactions on aerosols at West Antarctica: A molecular case-study of nitrate formation among sea salt aerosols. *Science of The Total Environment*, *758*, 143586. https://doi.org/https://doi.org/10.1016/j.scitotenv.2020.143586

Goudie, A.S., & Middleton, N. J. (2006). *Desert Dust in the Global System*. Springer.

Goudie, Andrew S. (2014). Desert dust and human health disorders. *Environment International*, *63*, 101–113.

https://doi.org/https://doi.org/10.1016/j.envint.2013.10.011

Greig, A. J. (2000). Monitoring airborne particles as mass and number concentrations: Implications for air quality management and health. *International Journal of Environmental Studies*, *57*(6), 641–662. https://doi.org/10.1080/00207230008711302

Guevara, M. (2016). Emissions of Primary Particulate Matter. In R.M. Harrison, R. E. Hester, & X. Querol (Eds.), *Airborne Particulate Matter: Sources, Atmospheric Processes and Health* (pp. 1–34). The Royal Society of Chemistry. https://doi.org/10.1039/9781782626589-00001

Güllü, G., Doğan, G., & Tuncel, G. (2005). Atmospheric trace element and major ion concentrations over the eastern Mediterranean Sea: Identification of anthropogenic source regions. *Atmospheric Environment*, *39*(34), 6376–6387. https://doi.org/10.1016/J.ATMOSENV.2005.07.031

Güllü, G., Ölmez, I., Aygün, S., & Tuncel, G. (1998). Atmospheric trace element concentrations over the eastern Mediterranean Sea: Factors affecting temporal variability. *Journal of Geophysical Research: Atmospheres*, *103*(D17), 21943–21954. https://doi.org/https://doi.org/10.1029/98JD01358

Güllü, G., Ölmez, İ., & Tuncel, G. (2000). Temporal variability of atmospheric trace element concentrations over the eastern Mediterranean Sea. *Spectrochimica Acta Part B: Atomic Spectroscopy*, *55*(7), 1135–1150. https://doi.org/10.1016/S0584-8547(00)00206-8

Guvenç, N., Alagha, O., & Tuncel, G. (2003). Investigation of Soil Multi-element Composition in Antalya, Turkey. *Environment International*, *29*, 631–640. https://doi.org/10.1016/S0160-4120(03)00046-1

Guy, H., Brooks, I. M., Carslaw, K. S., Murray, B. J., Walden, V. P., Shupe, M. D., Pettersen, C., Turner, D. D., Cox, C. J., Neff, W. D., Bennartz, R., & Iii, R. R. N. (2021). *Controls on surface aerosol particle number concentrations and aerosol-limited cloud regimes over the central Greenland Ice Sheet*. 15351–

15374.

Hand, J. L., White, W. H., Gebhart, K. A., Hyslop, N. P., Gill, T. E., & Schichtel, B. A. (2016). Earlier onset of the spring fine dust season in the southwestern United States. *Geophysical Research Letters*, *43*(8), 4001–4009. https://doi.org/10.1002/2016GL068519

Harrison, Roy M., Allan, J., Carruthers, D., Heal, M. R., Lewis, A. C., Marner, B., Murrells, T., & Williams, A. (2021). Non-exhaust vehicle emissions of particulate matter and VOC from road traffic: A review. *Atmospheric Environment*, *262*(July), 118592. https://doi.org/10.1016/j.atmosenv.2021.118592

Haustein, K., Pérez, C., Baldasano, J. M., Jorba, O., Basart, S., Miller, R. L., Janjic, Z., Black, T., Nickovic, S., Todd, M. C., Washington, R., Tesche, M., Weinzierl, B., Esselborn, M., & Schladitz, A. (2012). Atmospheric dust modeling from meso to global scales with the online NMMB/BSC-Dust model-Part 2: Experimental campaigns in Northern Africa. *Atmos. Chem. Phys*, *12*, 2933–2958. https://doi.org/10.5194/acp-12-2933-2012

Heimbürger, L.-E., Migon, C., Dufour, A., Chiffoleau, J.-F., & Cossa, D. (2010). Trace metal concentrations in the North-western Mediterranean atmospheric aerosol between 1986 and 2008: seasonal patterns and decadal trends. *The Science of the Total Environment*, *408*(13), 2629–2638. https://doi.org/10.1016/j.scitotenv.2010.02.042

Heintzenberg, J., Covert, D. C., & Van Dingenen, R. (2000). Size distribution and chemical composition of marine aerosols: A compilation and review. *Tellus, Series B: Chemical and Physical Meteorology*, *52*(4), 1104–1122. https://doi.org/10.3402/tellusb.v52i4.17090

Herut, B., Nimmo, M., Medway, A., Chester, R., & Krom, M. D. (2001). Dry atmospheric inputs of trace metals at the Mediterranean coast of Israel (SE Mediterranean): Sources and fluxes. *Atmospheric Environment*, *35*(4), 803–

813. https://doi.org/10.1016/S1352-2310(00)00216-8

Hinds, W. C. (1999). Aerosol Technology: Properties, Behavior, and Measurement of Airborne Particles. In *International Journal of Prisoner Health* (2nd ed.). John Wiley & Sons, Inc. https://doi.org/10.1080/17449200600935521

Hobbs, P. V. (2000). *Introduction to Atmospheric Chemistry* (1st ed.). Cambridge University Press.

Holmes, J, Samberg, T., Mcinnes, L., Zieman, J., Zoller, W., & Harris, J. (1997). Long-term aerosol and trace acidic gas collection at Mauna Loa Observatory 1979-1991. *Journal of Geophysical Research: Atmospheres*, *102*(D15), 19007–19019.

Holmes, Jennifer, & Zoller, W. (1996). The elemental signature of transported Asian dust at Mauna Loa observatory. *Tellus, Series B: Chemical and Physical Meteorology*, *48*(1), 83–92. https://doi.org/10.3402/tellusb.v48i1.15669

Hopke, P. K., Feng, Y., & Dai, Q. (2022). Source apportionment of particle number concentrations: A global review. *The Science of the Total Environment*, *819*, 153104. https://doi.org/10.1016/j.scitotenv.2022.153104

Hopke, P. K., Xie, Y., Raunemaa, T., Biegalski, S., Landsberger, S., Maenhaut, W., Artaxo, P., & Cohen, D. (1997). Characterization of the Gent Stacked Filter Unit PM10 Sampler. *Aerosol Science and Technology*, *27*(6), 726–735. https://doi.org/10.1080/02786829708965507

Humairoh, G. P., Syafei, A. D., Santoso, M., Boedisantoso, R., Assomadi, A. F., & Hermana, J. (2020). Identification of Trace Element in Ambient Air Case Study: Industrial Estate in Waru, Sidoarjo, East Java. *Aerosol and Air Quality Research*, *20*(9), 1910–1921. https://doi.org/10.4209/aaqr.2019.11.0590

Huneeus, N., Schulz, M., Balkanski, Y., Griesfeller, J., Prospero, J., Kinne, S., Bauer, S., Boucher, O., Chin, M., Dentener, F., Diehl, T., Easter, R., Fillmore, D., Ghan, S., Ginoux, P., Grini, A., Horowitz, L., Koch, D., Krol, M. C., …

Zender, C. S. (2011). Global dust model intercomparison in AeroCom phase i. *Atmospheric Chemistry and Physics*, *11*(15), 7781–7816. https://doi.org/10.5194/acp-11-7781-2011

Husar, R. B., Tratt, D. M., Schichtel, B. A., Falke, S. R., Li, F., Jaffe, D., Gassó, S., Gill, T., Laulainen, N. S., Lu, F., Reheis, M. C., Chun, Y., Westphal, D., Holben, B. N., Gueymard, C., McKendry, I., Kuring, N., Feldman, G. C., McClain, C., … Malm, W. C. (2001). Asian dust events of April 1998. *Journal of Geophysical Research Atmospheres*, *106*(D16), 18317–18330. https://doi.org/10.1029/2000JD900788

Israelevich, P., Ganor, E., Alpert, P., Kishcha, P., & Stupp, A. (2012). Predominant transport paths of Saharan dust over the Mediterranean Sea to Europe. *Journal of Geophysical Research Atmospheres*, *117*(2), 1–11. https://doi.org/10.1029/2011JD016482

Jaafar, M., Baalbaki, R., Mrad, R., Daher, N., Shihadeh, A., & Saliba, N. (2014). Dust episodes in Beirut and their effect on the chemical composition of coarse and fine particulate matter. *The Science of the Total Environment*, *496C*, 75–83. https://doi.org/10.1016/j.scitotenv.2014.07.018

Jandaghian, Z., & Akbari, H. (2020). Effects of increasing surface reflectivity on aerosol, radiation, and cloud interactions in the urban atmosphere. *Theoretical and Applied Climatology*, *139*. https://doi.org/10.1007/s00704-019-03006-4

Jiang, Y., Yang, X. Q., Liu, X., Qian, Y., Zhang, K., Wang, M., Li, F., Wang, Y., & Lu, Z. (2020). Impacts of wildfire aerosols on global energy budget and climate: The role of climate feedbacks. *Journal of Climate*, *33*(8), 3351–3366. https://doi.org/10.1175/JCLI-D-19-0572.1

Kallos, G., Astitha, M., Katsafados, P., & Spyrou, C. (2007). Long-range transport of anthropogenically and naturally produced particulate matter in the Mediterranean and North Atlantic: Current state of knowledge. *Journal of Applied Meteorology and Climatology*, *46*(8), 1230–1251.

https://doi.org/10.1175/JAM2530.1

Kang, S., Zhang, Q., Zhang, Y., Guo, W., Ji, Z., Shen, M., Wang, S., Wang, X., Tripathee, L., Liu, Y., Gao, T., Xu, G., Gao, Y., Kaspari, S., Luo, X., & Mayewski, P. (2022). Warming and thawing in the Mt. Everest region: A review of climate and environmental changes. *Earth-Science Reviews*, *225*(July 2021), 103911. https://doi.org/10.1016/j.earscirev.2021.103911

Karaca, F., & Camci, F. (2010). Distant source contributions to PM10 profile evaluated by SOM based cluster analysis of air mass trajectory sets. *Atmospheric Environment*, *44*(7), 892–899. https://doi.org/10.1016/j.atmosenv.2009.12.006

Kaskaoutis, D. G., Kosmopoulos, P., Kambezidis, H. D., & Nastos, P. T. (2007). Aerosol climatology and discrimination of different types over Athens, Greece, based on MODIS data. *Atmospheric Environment*, *41*(34), 7315–7329. https://doi.org/10.1016/j.atmosenv.2007.05.017

Kaskaoutis, D. G., Rashki, A., Dumka, U. C., Mofidi, A., Kambezidis, H. D., Psiloglou, B. E., Karagiannis, D., Petrinoli, K., & Gavriil, A. (2019). Atmospheric dynamics associated with exceptionally dusty conditions over the eastern Mediterranean and Greece in March 2018. *Atmospheric Research*. https://doi.org/10.1016/J.ATMOSRES.2018.12.009

Khan, B., Stenchikov, G., Weinzierl, B., Kalenderski, S., & Osipov, S. (2015). Dust plume formation in the free troposphere and aerosol size distribution during the Saharan Mineral Dust Experiment in North Africa. *Tellus, Series B: Chemical and Physical Meteorology*, *6*(1). https://doi.org/10.3402/tellusb.v67.27170

Kim, J. W. (2006). The environmental impact of industrialization in East Asia and strategies toward sustainable development. *Sustainability Science*, *1*(1), 107–114. https://doi.org/10.1007/s11625-006-0006-5

Kim, K.-H., Jahan, S. A., & Kabir, E. (2013). A review on human health perspective of air pollution with respect to allergies and asthma. *Environment International*,

59, 41–52. https://doi.org/10.1016/j.envint.2013.05.007

Kittelson, D. B. (1998). Engines and nanoparticles: A review. *Journal of Aerosol Science*, *29*(5–6), 575–588. https://doi.org/10.1016/S0021-8502(97)10037-4

Kivekäs, N., Kerminen, V. M., Engler, C., Lihavainen, H., Komppula, M., Viisanen, Y., & Kulmala, M. (2007). Particle number to volume concentration ratios at two measurement sites in Finland. *Journal of Geophysical Research Atmospheres*, *112*(4). https://doi.org/10.1029/2006JD007102

Kocak, M., Mihalopoulos, N., & Kubilay, N. (2009). Origin and source regions of PM10 in the Eastern Mediterranean atmosphere. *Atmospheric Research*, *92*(4), 464–474. https://doi.org/10.1016/j.atmosres.2009.01.005

Koçak, M, Theodosi, C., Zarmpas, P., Im, U., Bougiatioti, A., Yenigun, O., & Mihalopoulos, N. (2011). Particulate matter (PM10) in Istanbul: Origin, source areas and potential impact on surrounding regions. *Atmospheric Environment*, *45*(38), 6891–6900. https://doi.org/https://doi.org/10.1016/j.atmosenv.2010.10.007

Koçak, Mustafa, Kubilay, N., & Mihalopoulos, N. (2004). Ionic composition of lower tropospheric aerosols at a Northeastern Mediterranean site: Implications regarding sources and long-range transport. *Atmospheric Environment*, *38*, 2067–2077. https://doi.org/10.1016/j.atmosenv.2004.01.030

Koçak, Mustafa, Mihalopoulos, N., & Kubilay, N. (2009). Origin and source regions of PM10 in the Eastern Mediterranean atmosphere. *Atmospheric Research*, *92*(4), 464–474. https://doi.org/10.1016/j.atmosres.2009.01.005

Kok, J. F., Adebiyi, A. A., Albani, S., Balkanski, Y., Checa-Garcia, R., Chin, M., Colarco, P. R., Hamilton, D. S., Huang, Y., Ito, A., Klose, M., Li, L., Mahowald, N. M., Miller, R. L., Obiso, V., Pérez García-Pando, C., Rocha-Lima, A., & Wan, J. S. (2021). Contribution of the world's main dust source regions to the global cycle of desert dust. *Atmospheric Chemistry and Physics*, *21*(10), 8169–8193. https://doi.org/10.5194/acp-21-8169-2021

Konishi, T., Yonemochi, S., & Murata, M. (2018). Chemical Composition and Sources Estimation of PM2.5 and Submicron Particles (PM1) in Urban Atmosphere Based on Chemical Components. *Bunseki Kagaku*, *67*, 363–368. https://doi.org/10.2116/bunsekikagaku.67.363

Koulouri, E., Saarikoski, S., Theodosi, C., Markaki, Z., Gerasopoulos, E., Kouvarakis, G., Mä Kelä, T., Hillamo, R., & Mihalopoulos, N. (2008). Chemical composition and sources of fine and coarse aerosol particles in the Eastern Mediterranean. *Atmospheric Environment*, *42*, 6542–6550. https://doi.org/10.1016/j.atmosenv.2008.04.010

Kouvarakis, G, Bardouki, H., & Mihalopoulos, N. (2002). Sulfur budget above the Eastern Mediterranean: relative contribution of anthropogenic and biogenic sources. *Chemical and Physical Meteorology*, *54*, 201–212. https://doi.org/10.3402/tellusb.v54i3.16661

Kouvarakis, Giorgos, & Mihalopoulos, N. (2002). Seasonal variation of dimethylsulfide in the gas phase and of methanesulfonate and non-sea-salt sulfate in the aerosols phase in the Eastern Mediterranean atmosphere. *Atmospheric Environment*, *36*, 929–938. https://doi.org/10.1016/S1352-2310(01)00511-8

Kubilay, N., & Saydam, A. C. (1995). Trace Elements in Atmospheric Particulates Over the Eastern Mediterranean; Concentrations, Sources, and Temporal Variability. *Pergamon Atmospheric Environment*, *29*(17), 2289–2300. https://ac.els-cdn.com/1352231095001014/1-s2.0-1352231095001014-main.pdf?_tid=3ffb24a6-f098-11e7-bb94-00000aab0f6b&acdnat=1514992416_e1fc4df2f145e456b1553661d802199b

Kulkarni, P., Chellam, S., Flanagan, J. B., & Jayanty, R. K. M. (2007). Microwave digestion—ICP-MS for elemental analysis in ambient airborne fine particulate matter: Rare earth elements and validation using a filter borne fine particle certified reference material. *Analytica Chimica Acta*, *599*(2), 170–176.

https://doi.org/10.1016/J.ACA.2007.08.014

Kuloglu, E., & Tuncel, G. (2005). Size Distribution of Trace Elements and Major Ions in the Eastern Mediterranean Atmosphere. *Water, Air, and Soil Pollution*, *167*, 221–241. https://doi.org/10.1007/s11270-005-8651-3.

Lagzi, I., Mészáros, R., Gelybó, G., & Leelőssy, Á. (2013). *Atmospheric Chemistry*. Eötvös Loránd University. http://elte.prompt.hu/sites/default/files/tananyagok/AtmosphericChemistry/ch09.html

Landrigan, P. J., Fuller, R., Acosta, N. J. R., Adeyi, O., Arnold, R., Basu, N. N., Baldé, A. B., Bertollini, R., Fuster, V., Greenstone, M., Haines, A., Hanrahan, D., Hunter, D., Khare, M., Krupnick, A., Lanphear, B., Lohani, B., Martin, K., Mathiasen, K. V, … Steiner, A. (2017). *The Lancet Commissions The Lancet Commission on pollution and health*. *6736*(17). https://doi.org/10.1016/S0140-6736(17)32345-0

Lazaridis, M, Latos, M., & Aleksandropoulou, V. (2008). *Contribution of forest fire emissions to atmospheric pollution in Greece*. 143–158. https://doi.org/10.1007/s11869-008-0020-0

Lazaridis, Mihalis, & Drossinos, Y. (2014). Aerosol Dynamics. In Mihalis Lazaridis & I. Colbeck (Eds.), *Aerosol Science: Technology and Applications* (1st ed., pp. 15–44). John Wiley and Sons, Ltd.

Li, Q., Jacob, D. J., Bey, I., Palmer, P. I., Duncan, B. N., Field, B. D., Martin, R. V., Fiore, A. M., Yantosca, R. M., Parrish, D. D., Simmonds, P. G., & Oltmans, S. J. (2002). Transatlantic transport of pollution and its effects on surface ozone in Europe and North America. *Journal of Geophysical Research Atmospheres*, *107*(13), ACH 4-1-ACH 4-21. https://doi.org/10.1029/2001JD001422

Liang, C. S., Yue, D., Wu, H., Shi, J. Sen, & He, K. Bin. (2021). Source apportionment of atmospheric particle number concentrations with wide size range by nonnegative matrix factorization (NMF). *Environmental Pollution*,

289(March), 117846. https://doi.org/10.1016/j.envpol.2021.117846

Lin, Y., Ye, Z. (2017). Pollution level and source apportionment of atmospheric particles PM1 in downtown area of chengdu. *Environmental Science*, *37*(9), 3220–3226.

Lin, J. J., & Lee, L. C. (2004). Characterization of the concentration and distribution of urban submicron (PM1) aerosol particles. *Atmospheric Environment*, *38*(3), 469–475. https://doi.org/10.1016/j.atmosenv.2003.09.056

Liora, N., Poupkou, A., Giannaros, T. M., Kakosimos, K. E., Stein, O., & Melas, D. (2016). Impacts of natural emission sources on particle pollution levels in Europe. *Atmospheric Environment*, *137*, 171–185. https://doi.org/10.1016/j.atmosenv.2016.04.040

Liu, X., Gu, J., Li, Y., Cheng, Y., Qu, Y., Han, T., Wang, J., Tian, H., Chen, J., & Zhang, Y. (2013). Increase of aerosol scattering by hygroscopic growth: Observation, modeling, and implications on visibility. *Atmospheric Research*, *132–133*, 91–101. https://doi.org/10.1016/j.atmosres.2013.04.007

Long, S., Zeng, J., Li, Y., Bao, L., Cao, L., Liu, K., Xu, L., Lin, J., Liu, W., Wang, G., Yao, J., Ma, C., & Zhao, Y. (2014). Characteristics of secondary inorganic aerosol and sulfate species in size-fractionated aerosol particles in Shanghai. *Journal of Environmental Sciences (China)*, *26*(5), 1040–1051. https://doi.org/10.1016/S1001-0742(13)60521-5

López-Caravaca, A., Castañer, R., Clemente, A., Yubero, E., Galindo, N., Crespo, J., & Nicolás, J. F. (2021). The Impact of Intense Winter Saharan Dust Events on PM and Optical Properties at Urban Sites in the Southeast of the Iberian Peninsula. *Atmosphere*, *12*(11). https://doi.org/10.3390/atmos12111469

Louis, J., Gazeau, F., & Guieu, C. (2017). Atmospheric nutrients in seawater under current and high pCO2 conditions after Saharan dust deposition: Results from three minicosm experiments. *Progress In Oceanography*, *163*. https://doi.org/10.1016/j.pocean.2017.10.011

Lu, Z., & Sokolik, I. N. (2018). The impacts of smoke emitted from boreal forest wildfires on the high latitude radiative energy budget-A case study of the 2002 Yakutsk wildfires. *Atmosphere*, *9*(10). https://doi.org/10.3390/atmos9100410

Ma, N., & Birmili, W. (2015). Estimating the contribution of photochemical particle formation to ultrafine particle number averages in an urban atmosphere. *The Science of the Total Environment*, *512–513*, 154–166. https://doi.org/10.1016/j.scitotenv.2015.01.009

Maenhaut, W., Ducastel, G., Hillamo, R. E., Pakkanen, T. A., & Pacyna, J. M. (1993). Atmospheric aerosol studies in southern Norway using size-fractionating sampling devices and nuclear analytical techniques. *Journal of Radioanalytical and Nuclear Chemistry*, *167*(2), 271–281. http://inis.iaea.org/search/search.aspx?orig_q=RN:24068643

Mahowald, N., Albani, S., Kok, J. F., Engelstaeder, S., Scanza, R., Ward, D. S., & Flanner, M. G. (2014). The size distribution of desert dust aerosols and its impact on the Earth system. *Aeolian Research*, *15*, 53–71. https://doi.org/10.1016/j.aeolia.2013.09.002

Malkaz, Z. (2014). *Variation of Sulphate Source Regions Affecting Sulphate Concentrations in the Eastern Mediterranean Atmosphere*. Middle East Technical University.

Malm, W. C. (1999). *Introduction to Visibility*. https://www.epa.gov/sites/production/files/2016-07/documents/introvis.pdf

Mamouri, R.-E., Ansmann, A., Nisantzi, A., Solomos, S., Kallos, G., & Hadjimitsis, D. G. (2016). Extreme dust storm over the eastern Mediterranean in September 2015: satellite, lidar, and surface observations in the Cyprus region. *Atmospheric Chemistry and Physics*, *16*(21), 13711–13724. https://doi.org/10.5194/acp-16-13711-2016

Manigrasso, M., Protano, C., Martellucci, S., Mattei, V., Vitali, M., & Avino, P. (2019). Evaluation of the submicron particles distribution between mountain

and urban site: Contribution of the transportation for defining environmental and human health issues. *International Journal of Environmental Research and Public Health*, *16*(8). https://doi.org/10.3390/ijerph16081339

Markowicz, K., Chilinski, M. T., Lisok, J., Zawadzka-Manko, O., Stachlewska, I., Janicka, L., Rozwadowska, A., Makuch, P., Pakszys, P., Zielinski, T., Petelski, T., Posyniak, M., Pietruczuk, A., Szkop, A., & Westphal, D. L. (2016). Study of aerosol optical properties during long-range transport of biomass burning from Canada to Central Europe in July 2013. *Journal of Aerosol Science*, *101*. https://doi.org/10.1016/j.jaerosci.2016.08.006

Mărmureanu, L., Marin, C. A., Andrei, S., Antonescu, B., Ene, D., Boldeanu, M., & Levei, E. (2019). Orange snow-A saharan dust intrusion over romania during winter conditions. *Remote Sensing*, *11*(21). https://doi.org/10.3390/rs11212466

MÅrtensson, M., Tunved, P., Korhonen, H., & Nilsson, D. (2010). The role of sea-salt emissions in controlling the marine Aitken and accumulation mode aerosol: a model study. *Tellus B: Chemical and Physical Meteorology*, *62*(4), 259–279. https://doi.org/10.1111/j.1600-0889.2010.00465.x

Masson-delmotte, V., Moulin, C., Lambert, C. E., Dayan, U., Masson, V., Ramonet, M., Bousquet, P., Legrand, M., Balkanski, Y. J., Guelle, W., Marticorena, B., & Bergametti, G. (1998). *Satellite climatology of African dust transport in the Mediterranean atmosphere Satellite climatology of African dust transport in the Mediterranean atmosphere Faibles Radioactivit • s , Centre National de la Recherche depth • Laboratoire d ' Optique Atmo*. *June*. https://doi.org/10.1029/98JD00171

Mehta, A. V., & Yang, S. (2008). Precipitation climatology over Mediterranean Basin from ten years of TRMM measurements. *Advances in Geosciences*, *17*(June 2008), 87–91. https://doi.org/10.5194/adgeo-17-87-2008

Merikanto, J., Spracklen, D. V, Mann, G. W., Pickering, S. J., & Carslaw, K. S. (2009). *and Physics Impact of nucleation on global CCN*. 8601–8616.

Minguillón, M. C., Ripoll, A., Pérez, N., Prévôt, A. S. H., Canonaco, F., Querol, X., & Alastuey, A. (2015). Chemical characterization of submicron regional background aerosols in the western Mediterranean using an Aerosol Chemical Speciation Monitor. *Atmospheric Chemistry and Physics*, *15*(11), 6379–6391. https://doi.org/10.5194/acp-15-6379-2015

Moatti, J., & Thiébault, S. (2016). Sub-chapter 1.4.4. Impact of atmospheric chemistry on the regional climate. In IRD Éditions (Ed.), *In The Mediterranean region under climate change : A scientific update*. https://doi.org/10.4000/books.irdeditions.23379

Molinaroli, E., Guerzoni, S., & Rampazzo, G. (1993). Contribution of Saharan dust to the Central Mediterranean Basin. In M. J. Johnsson & A. Basu (Eds.), *Processes Controlling the Composition of Clastic Sediments* (Vol. 284, p. 0). Geological Society of America. https://doi.org/10.1130/SPE284-p303

Moody, J., Keene, W., Cooper, O., Voss, K., Aryal, R., Eckhardt, S., Holben, B., Maben, J., Izaguirre, M., & Galloway, J. (2013). Flow climatology for physicochemical properties of dichotomous aerosol over the western North Atlantic Ocean at Bermuda. *Atmospheric Chemistry and Physics Discussions*, *13*. https://doi.org/10.5194/acpd-13-22383-2013

Morawska, L. and Zhang, J. (2002). Combustion Sources of Particles. 1. Health Relevance and Source Signatures. *Chemosphere*, *49*, 1045–1058. https://doi.org/https://doi.org/10.1016/S0045-6535(02)00241-2

Morawska, L., Johnson, G., Ristovski, Z. D., & Agranovski, V. (1999). Relation between particle mass and number for submicrometer airborne particles. *Atmospheric Environment*, *33*(13), 1983–1990. https://doi.org/10.1016/S1352-2310(98)00433-6

Moridnejad, A., Karimi, N., & Ariya, P. (2015a). A new inventory for middle east dust source points. *Environmental Monitoring and Assessment*, *187*, 4806. https://doi.org/10.1007/s10661-015-4806-x

Moridnejad, A., Karimi, N., & Ariya, P. A. (2015b). Newly desertified regions in Iraq and its surrounding areas: Significant novel sources of global dust particles. *Journal of Arid Environments*, *116*, 1–10. https://doi.org/https://doi.org/10.1016/j.jaridenv.2015.01.008

Muhs, D. R., Budahn, J. R., Prospero, J. M., & Carey, S. N. (2007). Geochemical evidence for African dust inputs to soils of western Atlantic islands: Barbados, the Bahamas, and Florida. *Journal of Geophysical Research F: Earth Surface*, *112*(2). https://doi.org/10.1029/2005JF000445

Müller, R., Trentmann, J., Träger-Chatterjee, C., Posselt, R., & Stökli, R. (2011). The Role of the Effective Cloud Albedo for Climate Monitoringand Analysis. *Remote Sensing*, *3*, 2305–2320. https://doi.org/10.3390/rs3112305

Nava, S., Becagli, S., Calzolai, G., Chiari, M., Lucarelli, F., Prati, P., Traversi, R., Udisti, R., Valli, G., & Vecchi, R. (2012). Saharan dust impact in central Italy: An overview on three years elemental data records. *Atmospheric Environment*, *60*, 444–452. https://doi.org/10.1016/j.atmosenv.2012.06.064

Nenes, A., Murray, B., & Bougiatioti, A. (2014). *Mineral dust in microphysical interactions with clouds. In Mineral Dust: A key Player in the Earth System* (P. Knippertz & J. . Stuut (Eds.)). Springer.

Nicolás, José, García-Orellana, I., & Nava, S. (2008). *Quantification of Saharan and local dust impact in an arid Mediterranean area by the positive matrix factorization (PMF) technique*. https://doi.org/10.1016/j.atmosenv.2008.09.018

Nicolás, Jose, Lucarelli, F., Galindo, N., Yubero, E., Crespo, J., Calzolai, G., & Nava, S. (2020). Impact of traffic flows and meteorological events on the hourly elemental composition of fine and coarse particles at an urban site. *Aerosol and Air Quality Research*, *20*(5), 991–1001. https://doi.org/10.4209/aaqr.2019.09.0437

Nisantzi, A., Mamouri, R. E., Ansmann, A., Schuster, G. L., & Hadjimitsis, D. G.

(2015). Middle East versus Saharan dust extinction-to-backscatter ratios. *Atmospheric Chemistry and Physics*, *15*(12), 7071–7084. https://doi.org/10.5194/acp-15-7071-2015

Niu, J., Rasmussen, P. E., Wheeler, A., Williams, R., & Chénier, M. (2010). Evaluation of airborne particulate matter and metals data in personal, indoor and outdoor environments using ED-XRF and ICP-MS and co-located duplicate samples. *Atmospheric Environment*, *44*(2), 235–245. https://doi.org/10.1016/J.ATMOSENV.2009.10.009

NOAA. (2019). *HYSPLIT Trajectory Model*. https://www.ready.noaa.gov/HYSPLIT_traj.php

Norris, G., Duvall, R., & Brown, S. (2014). *EPA Positive Matrix Factorization (PM F) 5.0 Fundamentals and User Guide*. https://www.epa.gov/sites/production/files/2015-02/documents/pmf_5.0_user_guide.pdf

Oberdorster, G., Ferin, J., & Lehnert, B. E. (1994). Correlation between particle size, in vivo particle persistence, and lung injury. *Environmental Health Perspectives*, *102*(SUPPL. 5), 173–179. https://doi.org/10.1289/ehp.102-1567252

Oberdörster, G., Oberdörster, E., & Oberdörster, J. (2005). Nanotoxicology: An emerging discipline evolving from studies of ultrafine particles. *Environmental Health Perspectives*, *113*(7), 823–839. https://doi.org/10.1289/ehp.7339

Oğuz, K., & Pekin, M. (2016). Determination of dust emissive areas in Turkey. *Journal of the Faculty of Engineering and Architecture of Gazi University*, *31*, 933–940. https://doi.org/10.17341/gummfd.65383

Osipov, S., Stenchikov, G., Brindley, H., & Banks, J. (2015). Diurnal cycle of the dust instantaneous direct radiative forcing over the Arabian Peninsula. *Atmospheric Chemistry and Physics*, *15*(16), 9537–9553. https://doi.org/10.5194/acp-15-9537-2015

Ozdemir, E., Tuna Tuygun, G., & Elbir, T. (2020). Application of aerosol classification methods based on AERONET version 3 product over eastern Mediterranean and Black Sea. *Atmospheric Pollution Research*, *11*(12), 2226–2243. https://doi.org/10.1016/j.apr.2020.06.008

Özsoy, T., & Saydam, C. (2001). Iron Speciation in Precipitation in the North-Eastern Mediterranean and Its Relationship with Sahara Dust. *Journal of Atmospheric Chemistry*, *40*, 41-. https://doi.org/10.1023/A:1010602026579

Özsoy, T., Türker, P., & Ornektekin, S. (2007). Precipitation Chemistry as an Indicator of Urban Air Quality in Mersin, North-Eastern Mediterranean Region. *Water Air and Soil Pollution*, *189*. https://doi.org/10.1007/s11270-007-9557-z

Öztürk, F., Zararsz, A., Dutkiewicz, V. A., Husain, L., Hopke, P. K., & Tuncel, G. (2012). Temporal variations and sources of Eastern Mediterranean aerosols based on a 9-year observation. *Atmospheric Environment*, *61*, 463–475. https://doi.org/10.1016/j.atmosenv.2012.07.051

Öztürk, F., Zarasız, A., Kırmaz, R., & Tuncel, G. (2011). A new approach for the characterization of aerosols using EDXRF. *Talanta*, *83*(3), 823–831.

Pacitto, A., Stabile, L., Russo, S., & Buonanno, G. (2020). Exposure to submicron particles and estimation of the dose received by children in school and non-school environments. *Atmosphere*, *11*(5), 1–16. https://doi.org/10.3390/ATMOS11050485

Pandolfi, M., Tobias, A., Alastuey, A., Sunyer, J., Schwartz, J., Lorente, J., Pey, J., & Querol, X. (2014). Effect of atmospheric mixing layer depth variations on urban air quality and daily mortality during Saharan dust outbreaks. *Science of The Total Environment*, *494–495*, 283–289. https://doi.org/https://doi.org/10.1016/j.scitotenv.2014.07.004

Park, S. S., & Kim, Y. J. (2005). Source contributions to fine particulate matter in an urban atmosphere. *Chemosphere*, *59*(2), 217–226. https://doi.org/10.1016/j.chemosphere.2004.11.001

Park, S. U., Choe, A., & Park, M. S. (2010). Estimates of Asian dust deposition over the Asian region by using ADAM2 in 2007. *Science of the Total Environment*, *408*(11), 2347–2356. https://doi.org/10.1016/j.scitotenv.2010.02.001

Parrington, J. R., Zoller, W. H., & Aras, N. K. (1983). Asian Dust: Seasonal Transport to the Hawaiian Islands. *Science*, *220*(4593), 195–197. https://doi.org/10.1126/science.220.4593.195

Pateraki, S., Asimakopoulos, D. N., Bougiatioti, A., Maggos, T., Vasilakos, C., & Mihalopoulos, N. (2014). Assessment of PM 2.5 and PM 1 chemical profile in a multiple-impacted Mediterranean urban area: Origin, sources and meteorological dependence. *Science of the Total Environment, The*, *479–480*, 210–220. https://doi.org/10.1016/j.scitotenv.2014.02.008

Peng, J. (2015). Tentative discussion on the impact of aerosol on cloud and precipitation over Shanghai and its surrounding areas. *Torrential Rain Disasters*, *34*, 324–334. https://doi.org/doi:10.3969/j.issn.1004-9045.2015.04.005

Peñuelas, J., Llusià, J., & Gimeno, B. S. (1999). Effects of ozone concentrations on biogenic volatile organic compounds emission in the Mediterranean region. *Environmental Pollution*, *105*(1), 17–23. https://doi.org/10.1016/S0269-7491(98)00214-0

Pérez, C., Haustein, K., Janjic, Z., Jorba, O., Huneeus, N., Baldasano, J. M., Black, T., Basart, S., Nickovic, S., Miller, R. L., Perlwitz, J. P., Schulz, M., & Thomson, M. (2011). Atmospheric dust modeling from meso to global scales with the online NMMB/BSC-Dust model – Part 1: Model description, annual simulations and evaluation. *Atmospheric Chemistry and Physics*, *11*(24), 13001–13027. https://doi.org/10.5194/acp-11-13001-2011

Perrone, M. R., Turnone, A., Buccolieri, A., & Buccolieri, G. (2006). Particulate matter characterization at a coastal site in south-eastern Italy. *Journal of Environmental Monitoring*, *8*(1), 183–190. https://doi.org/10.1039/b513306h

Petroselli, C., Crocchianti, S., Moroni, B., Castellini, S., Selvaggi, R., Nava, S., Calzolai, G., Lucarelli, F., & Cappelletti, D. (2018). Disentangling the major source areas for an intense aerosol advection in the Central Mediterranean on the basis of Potential Source Contribution Function modeling of chemical and size distribution measurements. *Atmospheric Research*, *204*. https://doi.org/10.1016/j.atmosres.2018.01.011

Pey, J., Querol, X., Alastuey, A., Forastiere, F., & Stafoggia, M. (2013). African dust outbreaks over the Mediterranean Basin during 2001-2011: PM10 concentrations, phenomenology and trends, and its relation with synoptic and mesoscale meteorology. *Atmospheric Chemistry and Physics*, *13*(3), 1395–1410. https://doi.org/10.5194/acp-13-1395-2013

Pey, Jorge, Querol, X., & Alastuey, A. (2009). Variations of levels and composition of PM10 and PM2.5 at an insular site in the Western Mediterranean. *Atmospheric Research*, *94*, 285–299. https://doi.org/10.1016/j.atmosres.2009.06.006

Pey, Jorge, Querol, X., Alastuey, A., Rodríguez, S., Putaud, J. P., & Van Dingenen, R. (2009). Source apportionment of urban fine and ultra-fine particle number concentration in a Western Mediterranean city. *Atmospheric Environment*, *43*(29), 4407–4415. https://doi.org/10.1016/j.atmosenv.2009.05.024

Pietrogrande, M. C., Bacco, D., Ferrari, S., Ricciardelli, I., Scotto, F., Trentini, A., & Visentin, M. (2016). Characteristics and major sources of carbonaceous aerosols in PM2.5 in Emilia Romagna Region (Northern Italy) from four-year observations. *The Science of the Total Environment*, *553*, 172–183. https://doi.org/10.1016/j.scitotenv.2016.02.074

Piñero-García, F., Ferro-García, M. A., Chham, E., Cobos-Díaz, M., & González-Rodelas, P. (2015). A cluster analysis of back trajectories to study the behaviour of radioactive aerosols in the south-east of Spain. *Journal of Environmental Radioactivity*, *147*, 142–152. https://doi.org/10.1016/j.jenvrad.2015.05.029

Pope, C. A. (2016). International Conference on Atmospheric Optics: Aerosols, Visibility, and the Radiative Balance. *A 1960's Copper Smelter Strike and Increased Visibility: Natural Experiment of Reduced Sulfate Particle Pollution on Regional Mortality.*, 130–136.

Prospero, J.M. (1996). Saharan Dust Transport Over the North Atlantic Ocean and Mediterranean: An Overview. In S. Guerzoni & R. Chester (Eds.), *The Impact of Desert Dust Across the Mediterranean* (pp. 133–151). Springer Netherlands. https://doi.org/10.1007/978-94-017-3354-0_13

Prospero, Joseph M., Barkley, A. E., Gaston, C. J., Gatineau, A., Campos y Sansano, A., & Panechou, K. (2020). Characterizing and Quantifying African Dust Transport and Deposition to South America: Implications for the Phosphorus Budget in the Amazon Basin. *Global Biogeochemical Cycles*, *34*(9), 1–24. https://doi.org/10.1029/2020GB006536

Prospero, Joseph M., Delany, A. C., Delany, A. C., & Carlson, T. N. (2021). The discovery of african dust transport to the western hemisphere and the Saharan air layer: A history. *Bulletin of the American Meteorological Society*, *102*(6), E1239–E1260. https://doi.org/10.1175/BAMS-D-19-0309.1

Querol, X., Alastuey, A., Ruiz, C. R., Artiñano, B., Hansson, H. C., Harrison, R. M., Buringh, E., Ten Brink, H. M., Lutz, M., Bruckmann, P., Straehl, P., & Schneider, J. (2004). Speciation and origin of PM10 and PM2.5 in selected European cities. *Atmospheric Environment*, *38*(38), 6547–6555. https://doi.org/10.1016/j.atmosenv.2004.08.037

Querol, X., Pérez, N., Reche, C., Ealo, M., Ripoll, A., Tur, J., Pandolfi, M., Pey, J., Salvador, P., Moreno, T., & Alastuey, A. (2019). African dust and air quality over Spain: Is it only dust that matters? *Science of the Total Environment*, *686*, 737–752. https://doi.org/10.1016/j.scitotenv.2019.05.349

Querol, X., Tobías, A., Pérez, N., Karanasiou, A., Amato, F., Stafoggia, M., Pérez García-Pando, C., Ginoux, P., Forastiere, F., Gumy, S., Mudu, P., & Alastuey,

A. (2019). Monitoring the impact of desert dust outbreaks for air quality for health studies. *Environment International*, *130*(May), 104867. https://doi.org/10.1016/j.envint.2019.05.061

Raes, F., Dingenen, R. Van, Vignati, E., Wilson, J., Putaud, J.-P., Seinfeld, J. H., & Adams, P. (2000). Formation and cycling of aerosols in the global troposphere. *Atmospheric Environment*, *34*(25), 4215–4240. https://doi.org/10.1016/S1352-2310(00)00239-9

Rai, P., Chakraborty, A., Mandariya, A., & Gupta, T. (2016). Composition and source apportionment of PM1 at urban site Kanpur in India using PMF coupled with CBPF. *Atmospheric Research*, *178–179*, 506–520. https://doi.org/10.1016/j.atmosres.2016.04.015

Rajput, P., Izhar, S., & Gupta, T. (2019). Deposition modeling of ambient aerosols in human respiratory system: Health implication of fine particles penetration into pulmonary region. *Atmospheric Pollution Research*, *10*(1), 334–343. https://doi.org/10.1016/j.apr.2018.08.013

Rasch, P. J., Crutzen, P. J., & Coleman, D. B. (2008). Exploring the geoengineering of climate using stratospheric sulfate aerosols: The role of particle size. *Geophysical Research Letters*, *35*(2), 1–6. https://doi.org/10.1029/2007GL032179

Ravelo-Pérez, L. M., Rodríguez, S., Galindo, L., García, M. I., Alastuey, A., & López-Solano, J. (2016). Soluble iron dust export in the high altitude Saharan Air Layer. *Atmospheric Environment*, *133*, 49–59. https://doi.org/https://doi.org/10.1016/j.atmosenv.2016.03.030

Reche, C., Querol, X., Alastuey, A., Viana, M., Pey, J., Moreno, T., Rodríguez, S., González, Y., Fernández-Camacho, R., De La Campa, A. M. S., De La Rosa, J., Dall'Osto, M., Prévôt, A. S. H., Hueglin, C., Harrison, R. M., & Quincey, P. (2011). New considerations for PM, Black Carbon and particle number concentration for air quality monitoring across different European cities.

Atmospheric Chemistry and Physics, *11*(13), 6207–6227. https://doi.org/10.5194/acp-11-6207-2011

Reche, I., Ortega-Retuerta, E., Romera, O., Pulido-Villena, E., Morales-Baquero, R., & Casamayor, E. O. (2009). Effect of Saharan dust inputs on bacterial activity and community composition in Mediterranean lakes and reservoirs. *Limnology and Oceanography*, *54*, 869–879. https://doi.org/10.4319/lo.2009.54.3.0869

Reff, A., Eberly, S. I., & Bhave, P. V. (2007). Receptor modeling of ambient particulate matter data using positive matrix factorization: Review of existing methods. *Journal of the Air and Waste Management Association*, *57*(2), 146–154. https://doi.org/10.1080/10473289.2007.10465319

Reicher, N., Budke, C., Eickhoff, L., Raveh-Rubin, S., Kaplan-Ashiri, I., Koop, T., & Rudich, Y. (2019). Size-dependent ice nucleation by airborne particles during dust events in the eastern Mediterranean. *Atmospheric Chemistry and Physics*, *19*(17), 11143–11158. https://doi.org/10.5194/acp-19-11143-2019

Rodriguez-Navarro, C., Lorenzo, D., & Elert, K. (2018). Mineralogy and physicochemical features of Saharan dust wet deposited in the Iberian Peninsula during an extreme red rain event. *Atmos. Chem. Phys*, *18*, 10089–10122. https://doi.org/10.5194/acp-18-10089-2018

Rodriguez, S., Cuevas, E., Gonzalez, Y., Ramos, R., Romero, P. M., Perez, N., Querol, X., & Alastuey, A. (2008). Influence of sea breeze circulation and road traffic emissions on the relationship between particle number, black carbon, PM1, PM2.5 and PM2.5-10 concentrations in a coastal city. *Atmospheric Environment*, *42*, 6523–6534. https://doi.org/10.1016/j.atmosenv.2008.04.022.

Rolph, G., Stein, A., & Stunder, B. (2017). Real-time Environmental Applications and Display sYstem: READY. *Environmental Modelling and Software*, *95*, 210–228. https://doi.org/10.1016/j.envsoft.2017.06.025

Rudnick, R., & Gao, S. (2003). Composition of the Continental Crust. Treatise Geochem 3:1-64. *Treatise on Geochemistry*, *3*, 1–64.

https://doi.org/10.1016/B0-08-043751-6/03016-4

Saha, P. K., Sengupta, S., Adams, P., Robinson, A. L., & Presto, A. A. (2020). Spatial Correlation of Ultrafine Particle Number and Fine Particle Mass at Urban Scales: Implications for Health Assessment. *Environmental Science and Technology*, *54*(15), 9295–9304. https://doi.org/10.1021/acs.est.0c02763

Saltzman, E. S. (2013). Marine Aerosols. *Surface Ocean-Lower Atmosphere Processes*, 17–35. https://doi.org/10.1029/2008GM000769

Sanderson, P., Delgado-Saborit, J. M., & Harrison, R. M. (2014). A review of chemical and physical characterisation of atmospheric metallic nanoparticles. *Atmospheric Environment*, *94*, 353–365. https://doi.org/10.1016/j.atmosenv.2014.05.023

Sannigrahi, S., Pilla, F., Maiti, A., Bar, S., Bhatt, S., Zhang, Q., Keesstra, S., & Cerda, A. (2022). Examining the status of forest fire emission in 2020 and its connection to COVID-19 incidents in West Coast regions of the United States. *Environmental Research*. https://doi.org/10.1016/j.envres.2022.112818

Santoso, M., Lestiani, D. D., Damastuti, E., Kurniawati, S., Kusmartini, I., Dwi Atmodjo, D. P., Sari, D. K., Muhtarom, T., Permadi, D. A., & Hopke, P. K. (2020). Long term characteristics of atmospheric particulate matter and compositions in Jakarta, Indonesia. *Atmospheric Pollution Research*, *11*(12), 2215–2225. https://doi.org/https://doi.org/10.1016/j.apr.2020.09.006

Sarver, T., Al-Qaraghuli, A., & Kazmerski, L. L. (2013). A comprehensive review of the impact of dust on the use of solar energy: History, investigations, results, literature, and mitigation approaches. *Renewable and Sustainable Energy Reviews*, *22*, 698–733. https://doi.org/https://doi.org/10.1016/j.rser.2012.12.065

Scerri, M. M., Kandler, K., & Weinbruch, S. (2016). Disentangling the contribution of Saharan dust and marine aerosol to PM10 levels in the Central Mediterranean. *Atmospheric Environment*, *147*, 395–408.

https://doi.org/https://doi.org/10.1016/j.atmosenv.2016.10.028

Schmale, J., Henning, S., Decesari, S., Henzing, B., Keskinen, H., Sellegri, K., Ovadnevaite, J., Pöhlker, M., Brito, J., Bougiatioti, A., Kristensson, A., Kalivitis, N., Stavroulas, I., Carbone, S., Jefferson, A., Park, M., Schlag, P., Iwamoto, Y., Aalto, P., … Gysel, M. (2018). Long-term cloud condensation nuclei number concentration, particle number size distribution and chemical composition measurements at regionally representative observatories. *Atmospheric Chemistry and Physics*, *18*(4), 2853–2881. https://doi.org/10.5194/acp-18-2853-2018

Sciare, J., Oikonomou, K., Favez, O., Liakakou, E., Markaki, Z., Cachier, H., & Mihalopoulos, N. (2008). Long-term measurements of carbonaceous aerosols in the Eastern Mediterranean: evidence of long-range transport of biomass burning. *Atmospheric Chemistry and Physics*, *8*(18), 5551–5563. https://doi.org/10.5194/acp-8-5551-2008

Scotto, F., Bacco, D., Lasagni, S., Trentini, A., Poluzzi, V., & Vecchi, R. (2021). A multi-year source apportionment of PM2.5 at multiple sites in the southern Po Valley (Italy). *Atmospheric Pollution Research*, *12*(11), 101192. https://doi.org/https://doi.org/10.1016/j.apr.2021.101192

Seinfeld, J. H., & Pandis, S. N. (2006). *Atmospheric Chemistry and Physics: From Air Pollution to Climate Change* (2nd ed.). John Wiley and Sons, Inc.

Shepherd, G. (2016). *Global Assessment of Sand and Dust Storms*.

Sparks, C., Reponen, T., Ryan, P., Yermakov, M., Simmons, M., Alam, M., & Howard, L. (2014). Concentration gradient patterns of traffic and non-traffic generated fine and coarse aerosol particles. *Journal of Environmental Health*, *76*(6), 122–129. https://doi.org/10.1016/j.physbeh.2017.03.040

Spurny, K. R. (2000). *Aerosol Chemichal Processes in the Environment* (1st ed.). CRC Press.

Stein, A. F., Draxler, R. R., Rolph, G. D., Stunder, B. J. B., Cohen, M. D., & Ngan, F. (2015). Noaa's hysplit atmospheric transport and dispersion modeling system. *Bulletin of the American Meteorological Society*, *96*(12), 2059–2077. https://doi.org/10.1175/BAMS-D-14-00110.1

Su, L., & Toon, O. B. (2009). Numerical simulations of asian dust storms using a coupled climate-aerosol microphysical model. *Journal of Geophysical Research Atmospheres*, *114*(14), 1–17. https://doi.org/10.1029/2008JD010956

Sun, J., Hermann, M., Yuan, Y., Birmili, W., Collaud Coen, M., Weinhold, K., Madueño, L., Poulain, L., Tuch, T., Ries, L., Sohmer, R., Couret, C., Frank, G., Brem, B. T., Gysel-Beer, M., Ma, N., & Wiedensohler, A. (2021). Long-term trends of black carbon and particle number concentration in the lower free troposphere in Central Europe. *Environmental Sciences Europe*, *33*(1), 47. https://doi.org/10.1186/s12302-021-00488-w

Szkop, A., Pietruczuk, A., & Posyniak, M. (2016). Classification of Aerosol over Central Europe by Cluster Analysis of Aerosol Columnar Optical Properties and Backward Trajectory Statistics. *Acta Geophysica*, *64*(6), 2650–2676. https://doi.org/10.1515/acgeo-2016-00112

Tai, A. Y. C., Chen, L. W. A., Wang, X., Chow, J. C., & Watson, J. G. (2017). Atmospheric deposition of particles at a sensitive alpine lake: Size-segregated daily and annual fluxes from passive sampling techniques. *Science of the Total Environment*, *579*, 1736–1744. https://doi.org/10.1016/j.scitotenv.2016.11.117

Taieb, D., & Brahim, A. (2014). Chemistry and mineralogy studies of PM10 atmospheric aerosols in the Gulf of Gabès, South Tunisia. *International Journal of Energy Technology and Policy*, *10*, 125–144. https://doi.org/10.1504/IJETP.2014.066329

Taiwo, A. M., Harrison, R. M., & Shi, Z. (2014). A review of receptor modelling of industrially emitted particulate matter. *Atmospheric Environment*, *97*, 109–120. https://doi.org/10.1016/j.atmosenv.2014.07.051

Tecer, L. H., Tuncel, G., Karaca, F., Alagha, O., Süren, P., Zararsız, A., & Kırmaz, R. (2012). Metallic composition and source apportionment of fine and coarse particles using positive matrix factorization in the southern Black Sea atmosphere. *Atmospheric Research*, *118*, 153–169. https://doi.org/10.1016/J.ATMOSRES.2012.06.016

Tegen, I., Werner, M., Harrison, S. P., & Kohfeld, K. E. (2004). *Relative importance of climate and land use in determining present and future global soil dust emission*. *31*. https://doi.org/10.1029/2003GL019216

Theodosi, C., Grivas, G., Zarmpas, P., Chaloulakou, A., & Mihalopoulos, N. (2011). Mass and chemical composition of size-segregated aerosols (PM1, PM2.5, PM10) over Athens, Greece: local versus regional sources. *Atmospheric Chemistry and Physics*, *11*(22), 11895–11911. https://doi.org/10.5194/acp-11-11895-2011

Theodosi, C., im, ulas, Bougiatioti, A., Zarmpas, P., Yenigün, O., & Mihalopoulos, N. (2010). Aerosol chemical composition over Istanbul. *The Science of the Total Environment*, *408*, 2482–2491. https://doi.org/10.1016/j.scitotenv.2010.02.039

Thorpe, A., & Harrison, R. M. (2008). *Sources and properties of non-exhaust particulate matter from road traffic: A review*. https://doi.org/10.1016/j.scitotenv.2008.06.007

Titos, G., Lyamani, H., Pandolfi, M., Alastuey, A., & Alados-Arboledas, L. (2014). Identification of fine (PM 1) and coarse (PM 10-1) sources of particulate matter in an urban environment. *Atmospheric Environment*, *89*, 593–602. https://doi.org/10.1016/j.atmosenv.2014.03.001

Tobias, A., Karanasiou, A., Amato, F., Roqué, M., & Querol, X. (2019). Health effects of desert dust and sand storms: a systematic review and meta-analysis protocol. *BMJ Open*, *9*(7), e029876. https://doi.org/10.1136/bmjopen-2019-029876

Tokgöz, Deniz D. Genç, Doğan, G., İlhan, A. İ., Balta, T., & Tuncel, G. (2015). Ionic composition of aerosols at Northwestern Turkey. *International Journal of Global Warming*, *7*(2), 161. https://doi.org/10.1504/ijgw.2015.067747

Tokgöz, Derya Deniz Genç. (2013). *Temporal variation in aerosol composition at Northwestern Turkey*. Middle East Technical University.

Tokgöz, Derya Deniz Genç, Tuncel, G., & Doğan, G. (2012). Temporal variation in chemical composition of lower tropospheric aerosols at northwestern Turkey. *Air Quality Management at Urban, Regional and Global Scales, 4th International Symposium and IUAPPA Regional Conference, Book of Proceedings*, 294–301.

Trapp, J., Millero, F., & Prospero, J. (2010). Temporal variability of the elemental composition of African dust measured in trade wind aerosols at Barbados and Miami. *Marine Chemistry*, *120*, 71–82. https://doi.org/10.1016/j.marchem.2008.10.004

Trickl, T., Vogelmann, H., Flentje, H., & Ries, L. (2015). Stratospheric ozone in boreal fire plumes-the 2013 smoke season over central Europe. *Atmos. Chem. Phys*, *15*, 9631–9649. https://doi.org/10.5194/acp-15-9631-2015

Tsai, J. H., Lin, K. H., Chen, C. Y., Ding, J. Y., Choa, C. G., & Chiang, H. L. (2007). Chemical constituents in particulate emissions from an integrated iron and steel facility. *Journal of Hazardous Materials*, *147*(1–2), 111–119. https://doi.org/10.1016/j.jhazmat.2006.12.054

Tsoar, H., & PYE, K. (1987). Dust transport and the question of desert loess formation. *Sedimentology*, *34*(1), 139–153. https://doi.org/10.1111/j.1365-3091.1987.tb00566.x

U.S. EPA. (2011). *Particulate Matter Emissions* (Issue 1). https://cfpub.epa.gov/roe/indicator_pdf.cfm?i=19

U.S. EPA. (2014). *Particulate Matter Emissions*.

Uzun, B. (2000). *Investigation of biogenic sulfur in Eastern Mediterranean basin*. Middle East Technical University.

Vallero, D. (2014). Fundamentals of air pollution. In D. Vallero (Ed.), *Academic Press Publ./N.Y./: Vol. $14.95* (5th ed.). Elsevier Inc. https://doi.org/10.2307/2403263

Vallius, M. (2005). *Characteristics and sources of fine particulate matter in urban air* (Vol. A6). National Public Health Institute. http://www.ktl.fi/attachments/suomi/julkaisut/julkaisusarja_a/2005/2005a6.pdf .

Valotto, G., Squizzato, S., Masiol, M., Zannoni, D., Visin, F., & Rampazzo, G. (2014). Elemental characterization, sources and wind dependence of PM 1 near Venice, Italy. *Atmospheric Research*, *143*, 371–379. https://doi.org/10.1016/j.atmosres.2014.03.007

Varga, G. (2020). Changing nature of Saharan dust deposition in the Carpathian Basin (Central Europe): 40 years of identified North African dust events (1979–2018). *Environment International*, *139*(March), 105712. https://doi.org/10.1016/j.envint.2020.105712

Viana, M., Kuhlbusch, T. A. J., Querol, X., Alastuey, A., Harrison, R. M., Hopke, P. K., Winiwarter, W., Vallius, M., Szidat, S., Prévôt, A. S. H., Hueglin, C., Bloemen, H., Wåhlin, P., Vecchi, R., Miranda, A. I., Kasper-Giebl, A., Maenhaut, W., & Hitzenberger, R. (2008). Source apportionment of particulate matter in Europe: A review of methods and results. *Journal of Aerosol Science*, *39*(10), 827–849. https://doi.org/10.1016/J.JAEROSCI.2008.05.007

Vieno, M., Heal, M. R., Hallsworth, S., Famulari, D., Doherty, R. M., Dore, A. J., Tang, Y. S., Braban, C. F., Leaver, D., Sutton, M. A., & Reis, S. (2014). The role of long-range transport and domestic emissions in determining atmospheric secondary inorganic particle concentrations across the UK. *Atmospheric Chemistry and Physics*, *14*(16), 8435–8447. https://doi.org/10.5194/acp-14-

8435-2014

Waheed, A., Li, X., Tan, M., Bao, L., Liu, J., Zhang, Y., Zhang, G., & Li, Y. (2011). Size distribution and sources of trace metals in ultrafine/fine/coarse airborne particles in the atmosphere of Shanghai. *Aerosol Science and Technology*, *45*(2), 163–171. https://doi.org/10.1080/02786826.2010.528079

Wåhlin, P., Berkowicz, R., & Palmgren, F. (2006). Characterisation of traffic-generated particulate matter in Copenhagen. *Atmospheric Environment*, *40*(12), 2151–2159. https://doi.org/10.1016/j.atmosenv.2005.11.049

Waldner, P., Marchetto, A., Thimonier, A., Schmitt, M., Rogora, M., Granke, O., Mues, V., Hansen, K., Pihl Karlsson, G., Žlindra, D., Clarke, N., Verstraeten, A., Lazdins, A., Schimming, C., Iacoban, C., Lindroos, A.-J., Vanguelova, E., Benham, S., Meesenburg, H., … Lorenz, M. (2014). Detection of temporal trends in atmospheric deposition of inorganic nitrogen and sulphate to forests in Europe. *Atmospheric Environment*, *95*, 363–374. https://doi.org/https://doi.org/10.1016/j.atmosenv.2014.06.054

Wang, S., Wang, L., Wang, N., Ma, S., Su, F., & Zhang, R. (2021). Formation of droplet-mode secondary inorganic aerosol dominated the increased PM2.5 during both local and transport haze episodes in Zhengzhou, China. *Chemosphere*, *269*, 128744. https://doi.org/10.1016/j.chemosphere.2020.128744

Wanger, A., Peleg, M., Sharf, G., Mahrer, Y., Dayan, U., Kallos, G., Kotroni, V., Lagouvardos, K., Varinou, M., Papadopoulos, A., & Luria, M. (2000). Some observational and modeling evidence of long-range transport of air pollutants from Europe toward the Israeli coast. *Journal of Geophysical Research Atmospheres*, *105*(D6), 7177–7186. https://doi.org/10.1029/1999JD901060

Wegner, T., Hussein, T., Hämeri, K., Vesala, T., Kulmala, M., & Weber, S. (2012). Properties of aerosol signature size distributions in the urban environment as derived by cluster analysis. *Atmospheric Environment*, *61*, 350–360.

https://doi.org/10.1016/j.atmosenv.2012.07.048

WHO. (2016). *WHO releases country estimates on air pollution exposure and health impact*. https://www.who.int/en/news-room/detail/27-09-2016-who-releases-country-estimates-on-air-pollution-exposure-and-health-impact

Wilson, W. ., & Suh, H. H. (1997). Fine Particles and Coarse Particles: Concentration Relationships Relevant to Epidemiologic Studies. *Journal of the Air and Waste Management Association*, *47*(12), 1238–1249. https://doi.org/10.1080/10473289.1997.10464074

Woodward, S., Roberts, D. L., & Betts, R. A. (2005). *A simulation of the effect of climate change – induced desertification on mineral dust aerosol*. *32*, 2–5. https://doi.org/10.1029/2005GL023482

Wu, C., Lin, Z., & Liu, X. (2020). Global dust cycle and uncertainty in CMIP5 models. *Atmospheric Chemistry and Physics Discussions*, *5*, 1–52.

Wu, Y., Liu, J., Zhai, J., Cong, L., Wang, Y., Ma, W., Zhang, Z., & Li, C. (2018). Comparison of dry and wet deposition of particulate matter in near-surface waters during summer. *PLoS ONE*, *13*(6), 1–15. https://doi.org/10.1371/journal.pone.0199241

Yao, L., Yang, L., Yuan, Q., Yan, C., Dong, C., Meng, C., Sui, X., Yang, F., Lu, Y., & Wang, W. (2016). Sources apportionment of PM2.5 in a background site in the North China Plain. *Science of The Total Environment*, *541*, 590–598. https://doi.org/10.1016/J.SCITOTENV.2015.09.123

Yatin, M., Tuncel, S., Aras, N. K., Olmez, I., Aygun, S., & Tuncel, G. (2000). Atmospheric trace elements in Ankara, Turkey: 1. factors affecting chemical composition of fine particles. *Atmospheric Environment*, *34*(8), 1305–1318. https://doi.org/10.1016/S1352-2310(98)00297-0

Yin, G., Liu, C., Hao, L., Chen, Y., Wang, W., Huo, J., Zhao, Q., Zhang, Y., Duan, Y., Fu, Q., Chen, R., & Kan, H. (2019). Associations between size-fractionated

particle number concentrations and COPD mortality in Shanghai, China. *Atmospheric Environment*, *214*, 116875. https://doi.org/10.1016/j.atmosenv.2019.116875

Yıkmaz, R. F. (2010). *Development of GIS based trajectory statistical analysis method to identify potential sources of regional air pollution*. Middle East Technical University.

Yücel, G. (2019). *IONIC COMPOSITION OF PRECIPITATION IN MARMARIS STATION*. *May*.

Zender, C. S., Miller, R. L., & Tegen, I. (2004). Quantifying Mineral Dust Mass Budgets: Terminology, Constraints, and Current Estimates. *Eos*, *85*(48), 509–512. https://doi.org/10.1029/2003JD003483

Zhang, Yanyun; Lang, Jianlei; Cheng, Shuiyuan; Li, Shengyue; Zhou, Ying; Chen, Dongsheng; Zhang, Hanyu; Wang, H. (2018). Chemical composition and sources of PM1 and PM2.5 in Beijing in autumn. *Science of The Total Environment*, *630*, 72–82. https://doi.org/10.1016/j.scitotenv.2018.02.151

Zhang, X., Liu, Z., Hecobian, A., Zheng, M., Frank, N. H., Edgerton, E. S., & Weber, R. J. (2012). Spatial and seasonal variations of fine particle water-soluble organic carbon (WSOC) over the southeastern United States: Implications for secondary organic aerosol formation. *Atmospheric Chemistry and Physics*, *12*(14), 6593–6607. https://doi.org/10.5194/acp-12-6593-2012

Zhao, H., Che, H., Zhang, X., Ma, Y., Wang, Y., Wang, H., & Wang, Y. (2013). Characteristics of visibility and particulate matter (PM) in an urban area of Northeast China. *Atmospheric Pollution Research*, *4*(4), 427–434. https://doi.org/10.5094/APR.2013.049

Zhao, W., & Hopke, P. (2006). Source investigation for ambient PM 2.5 in Indianapolis, IN. *Aerosol Science and Technology*, *40*(10), 898–909. https://doi.org/10.1080/02786820500380297

Zhu, Y., Shen, Y., Li, K., Meng, H., Sun, Y., Yao, X., Gao, H., Xue, L., & Wang, W. (2021). Investigation of Particle Number Concentrations and New Particle Formation With Largely Reduced Air Pollutant Emissions at a Coastal Semi-Urban Site in Northern China. *Journal of Geophysical Research: Atmospheres*, *126*(17), e2021JD035419. https://doi.org/https://doi.org/10.1029/2021JD035419

Zwozdziak, A., Sówka, I., Willak-Janc, E., Zwozdziak, J., Kwiecińska, & K., & Balińska-Miśkiewicz, W. (2016). Influence of PM 1 and PM 2.5 on lung function parameters in healthy schoolchildren—a panel study. *Environmental Science and Pollution Research*, *23*, 23892–23901. https://doi.org/10.1007/s11356-016-7605-1

APPENDICES

A. Factors Affecting Particle Number Size Distributions at An Urban and A High-Altitude Rural Site at The Anatolian Plateau

Table A1. PM_{10}, $PM_{2.5}$ and PM_1 mass concentrations measured by two laser spectrometers operated side by side

		$x \pm \sigma$ ($\mu g\ m^{-3}$)	Median ($\mu g\ m^{-3}$)
PM_{10}	Spectrometer 1	14 ± 10	10
	Spectrometer 2	13 ± 10	9.4
$PM_{2.5}$	Spectrometer 1	10 ± 5.6	8.0
	Spectrometer 2	10 ± 5.9	8.0
PM_1	Spectrometer 1	8.9 ± 4.6	7.0
	Spectrometer 2	9.2 ± 5.0	7.2

Table A2. PM_{10}, $PM_{2.5}$ and PM_1 concentrations measured with collocated samplers.

PM_{10}	
SFU	21 ± 10
Cyclone	22 ± 9 (24)
164	26 ± 11 (27)
$PM_{2.5}$	
SFU	11 ± 4 (11)
Cyclone	12 ± 4 (12)
164	13 ± 4 (13)
Hi-Vol 1	14 ± 4 (14)
Hi-Vol 2	13 ± 4 (12)
PM_1	
Cyclone	9 ± 3 (7)
164	10 ± 4 (10)

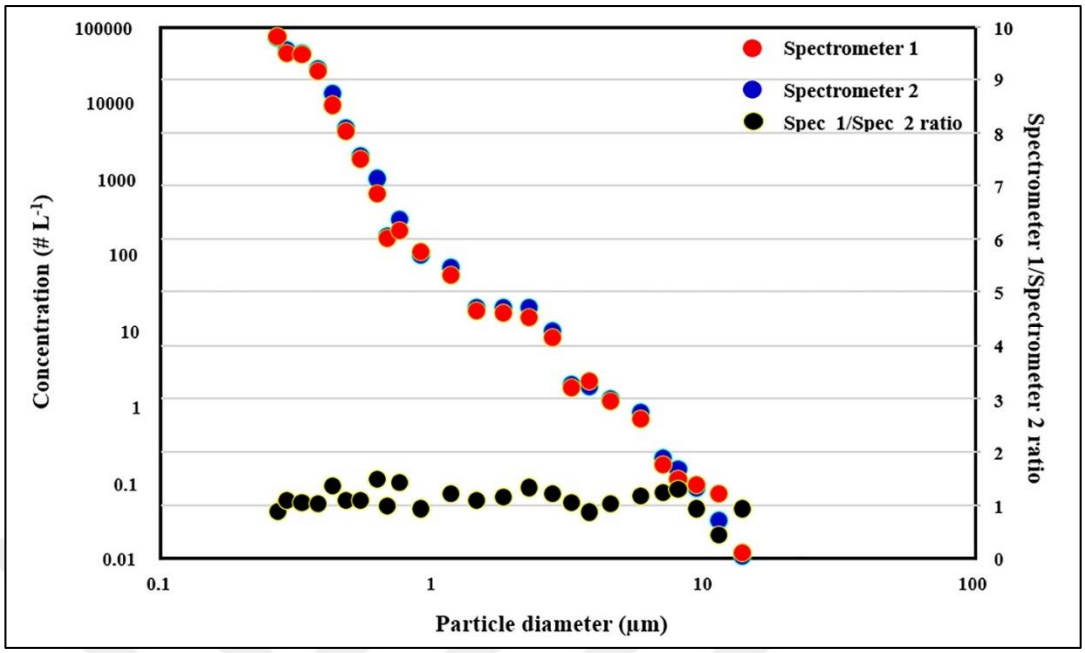

Figure A1. Particle number size distribution measured by two co-located laser spectrometers.

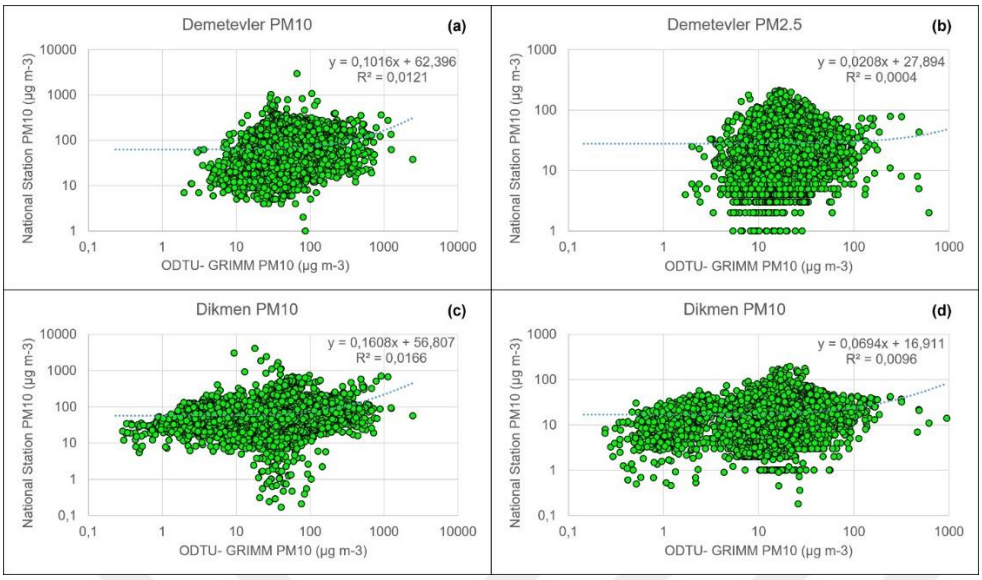

Figure A2. Correlations between PM_{10} and $PM_{2.5}$ concentrations measured at Ankara station and those measured at Demetevler and Dikmen air quality stations.

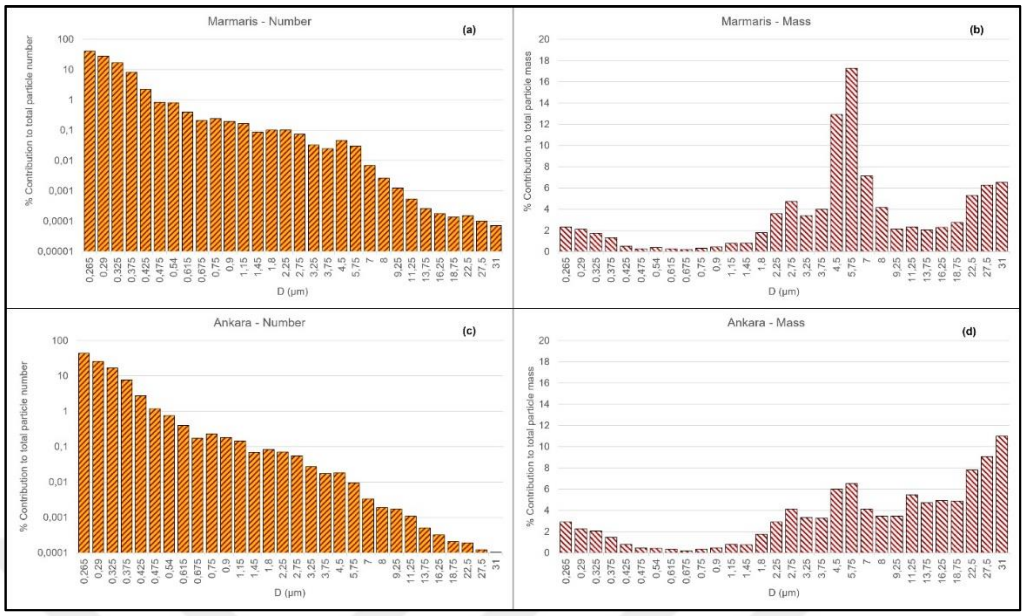

Figure A3. Contribution of each size bin to total particle number and mass

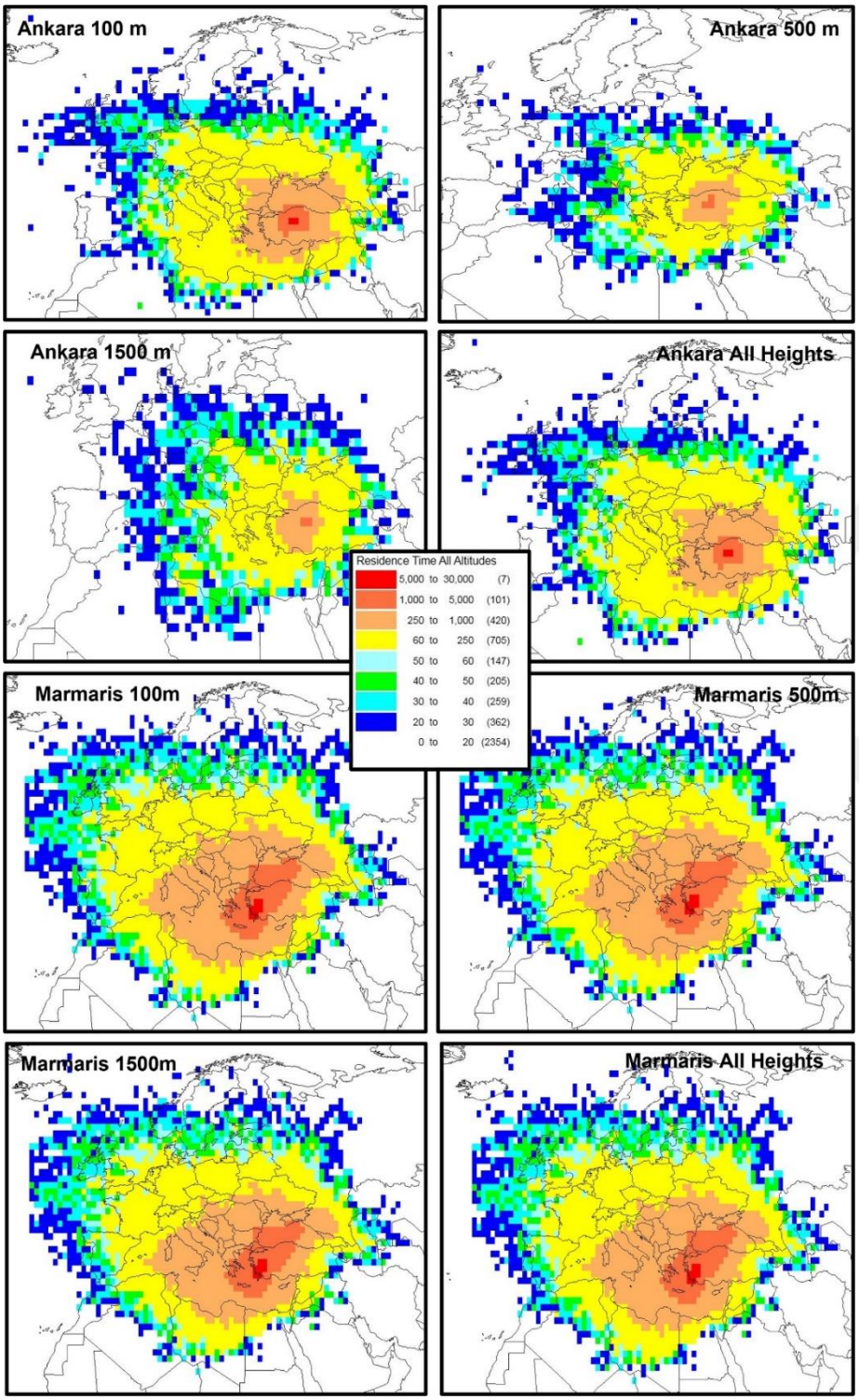

Figure A4. Residence times of trajectories with different starting altitudes at Ankara and Marmaris stations.

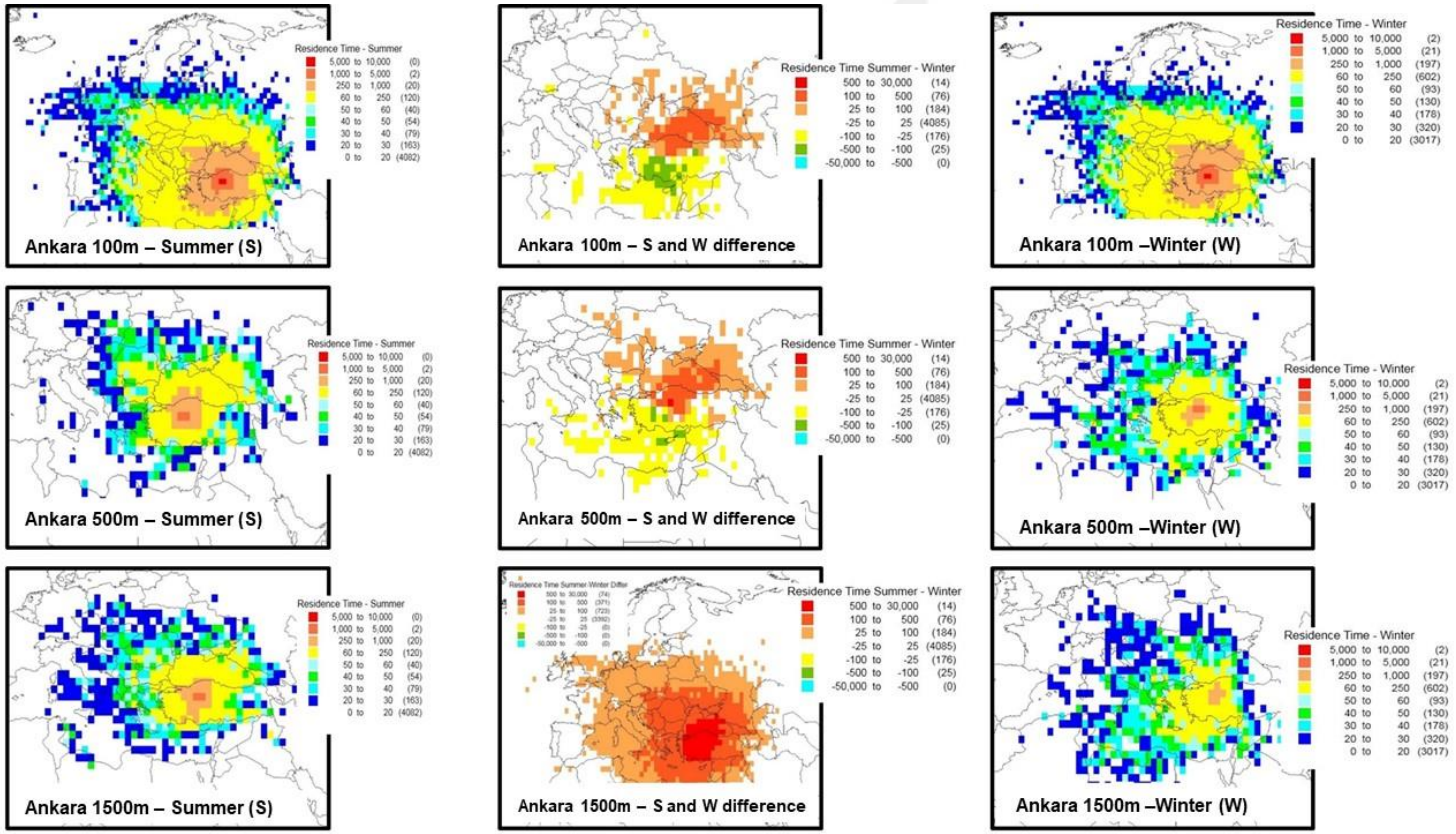

Figure A5. Summer – Winter difference in residence times of air masses around Ankara station.

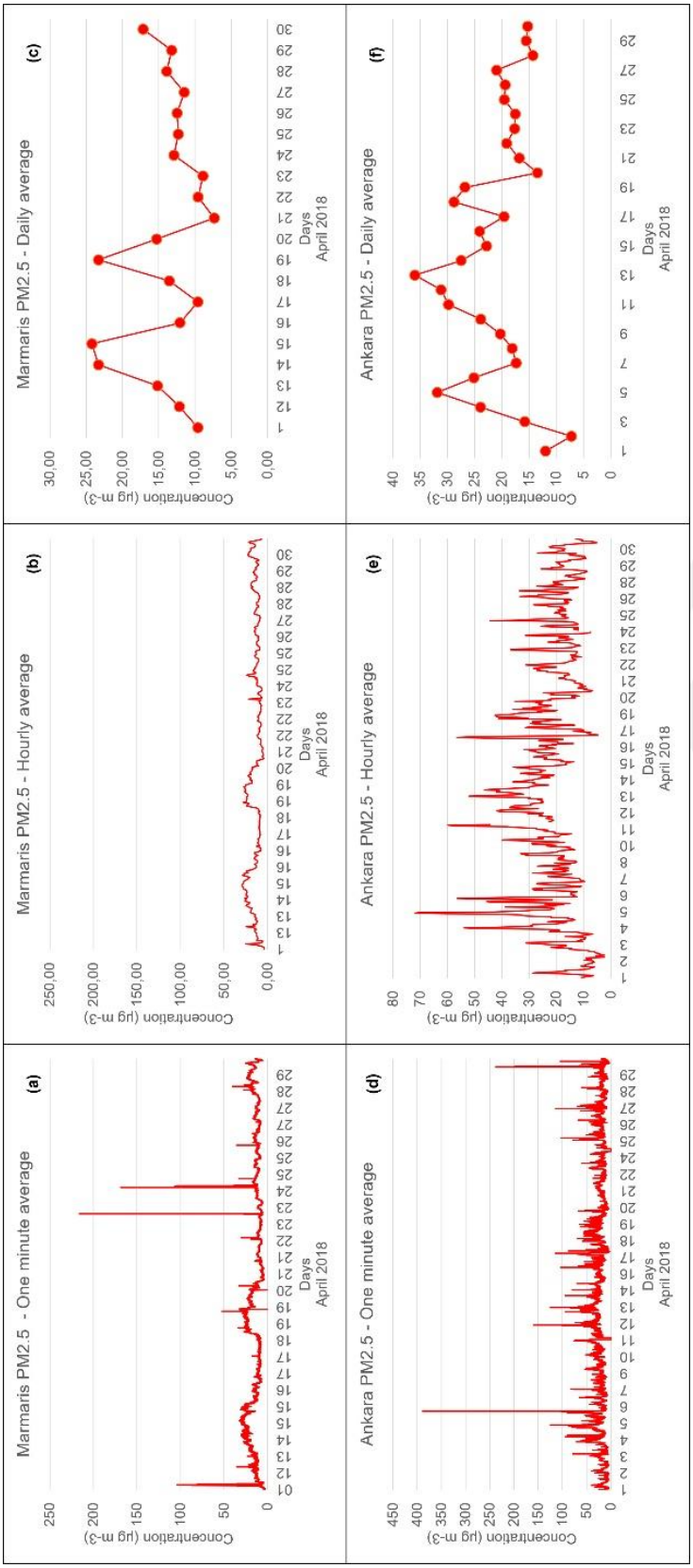

Figure A6. 1-min, 1-hour and 24-hour averaged PM2.5 concentrations at Marmaris and Ankara Stations, in April 2018.

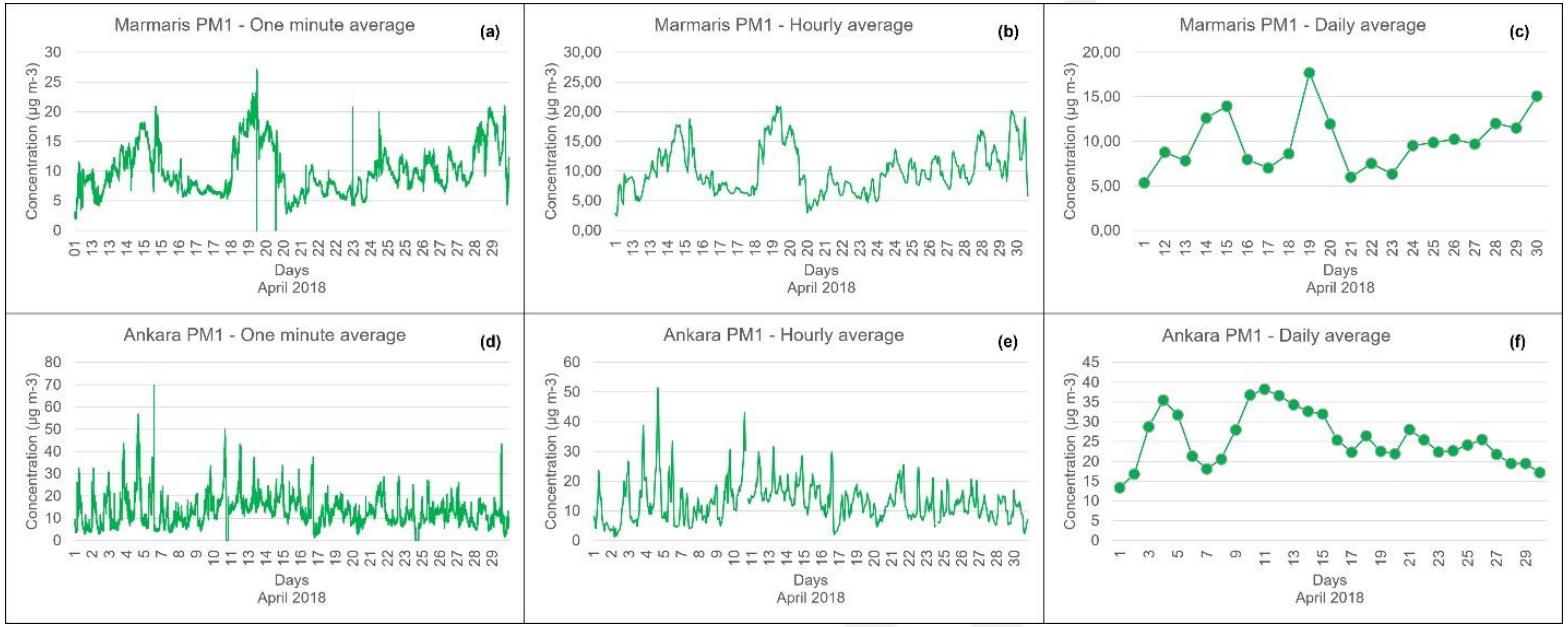

Figure A7. 1-min, 1-hour and 24-hour averaged PM1 concentrations at Marmaris and Ankara Stations in April 2018

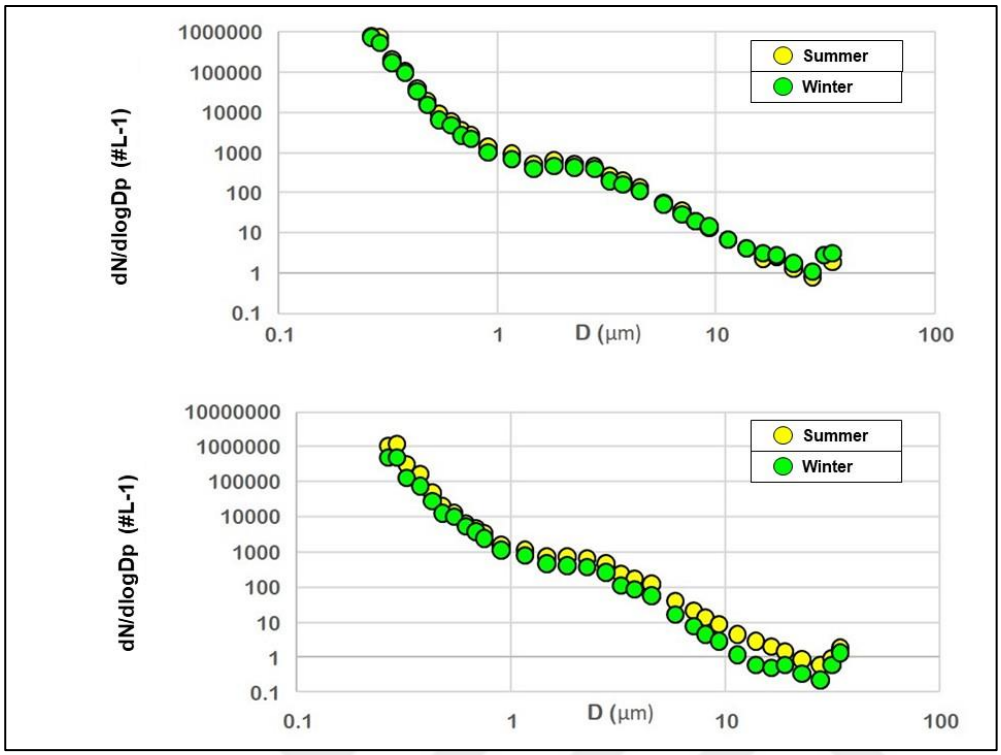

Figure A8. Summer and winter particle size distributions at Marmaris and Ankara stations.

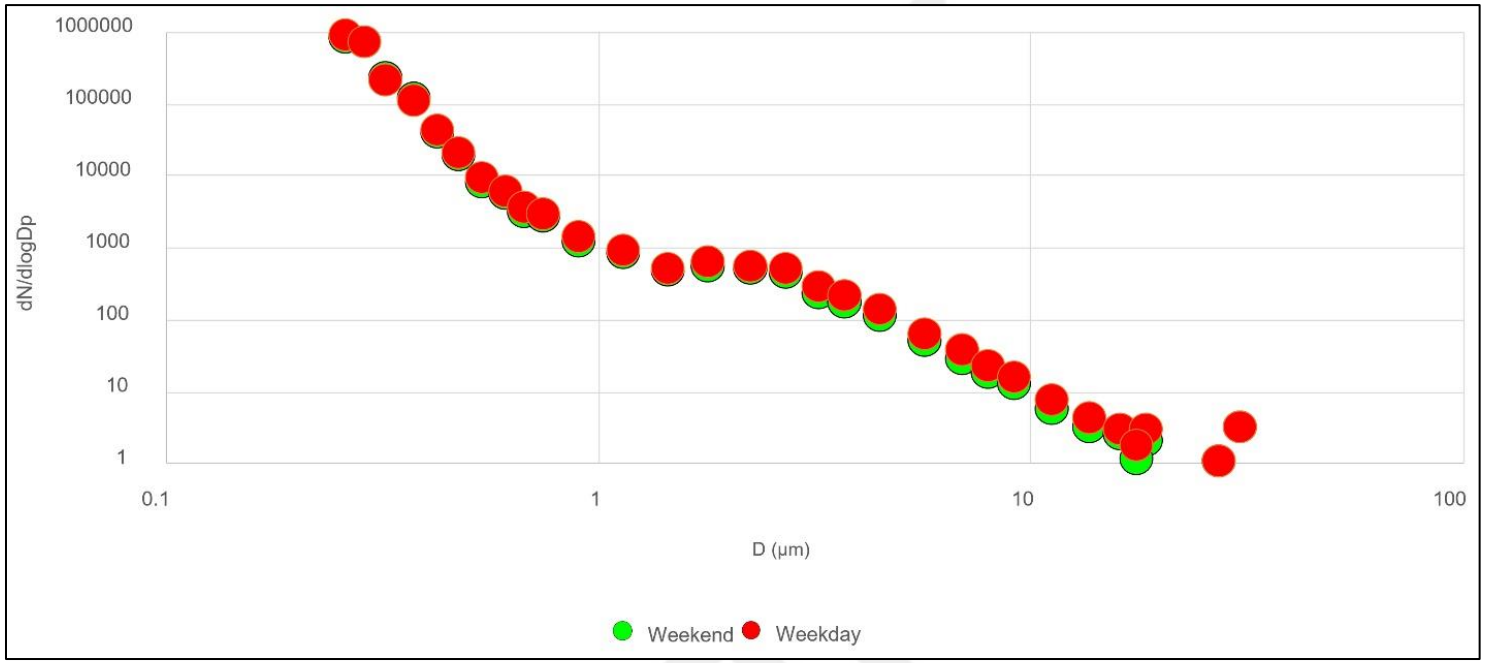

Figure A9. Weekend-Weekday difference in number and mass size distributions at Ankara station

B. Modification of Saharan Dust Size Distribution during Its Transport over the Anatolian Plateau

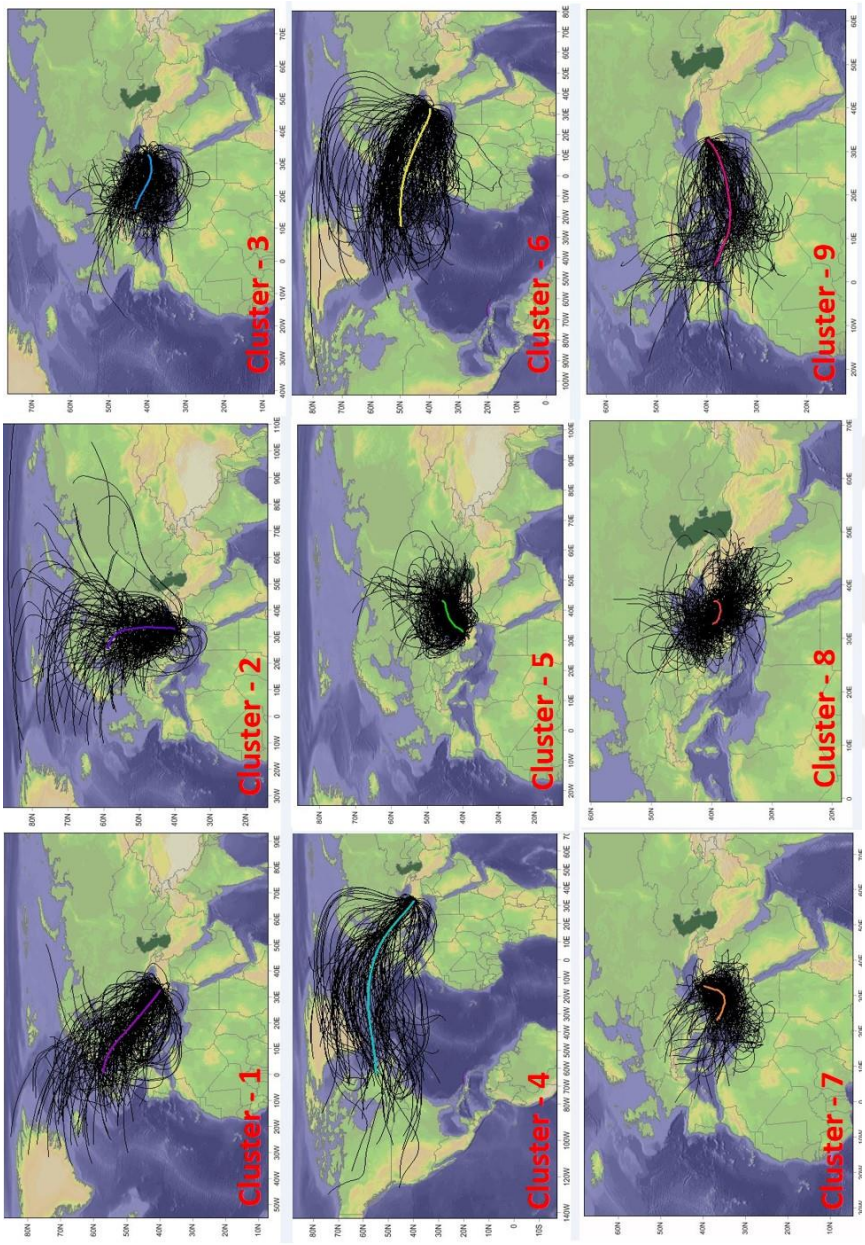

Figure B1. Back trajectories in each Cluster – Ankara station

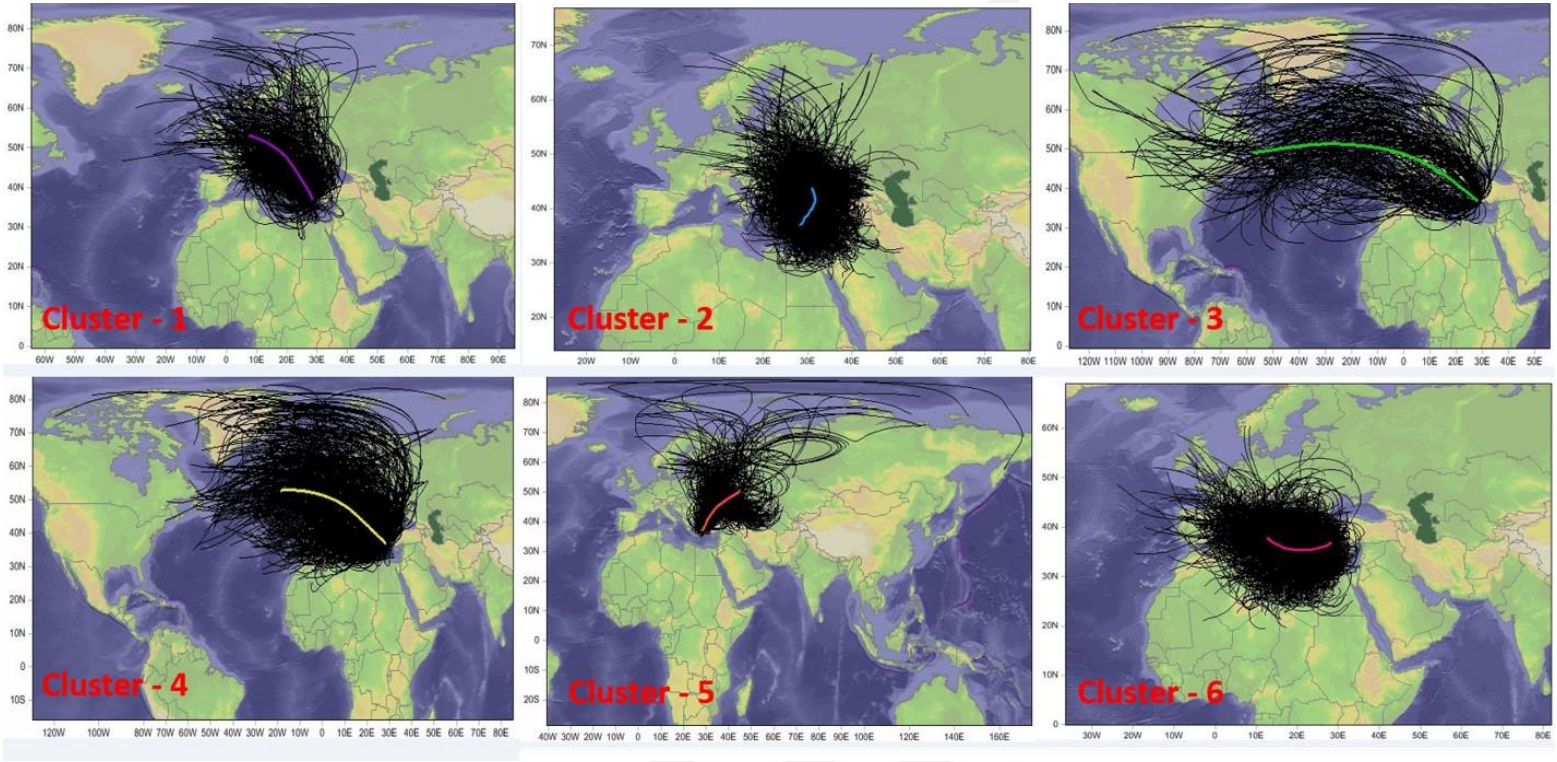

Figure B2. Back trajectories in each Cluster – Marmaris station

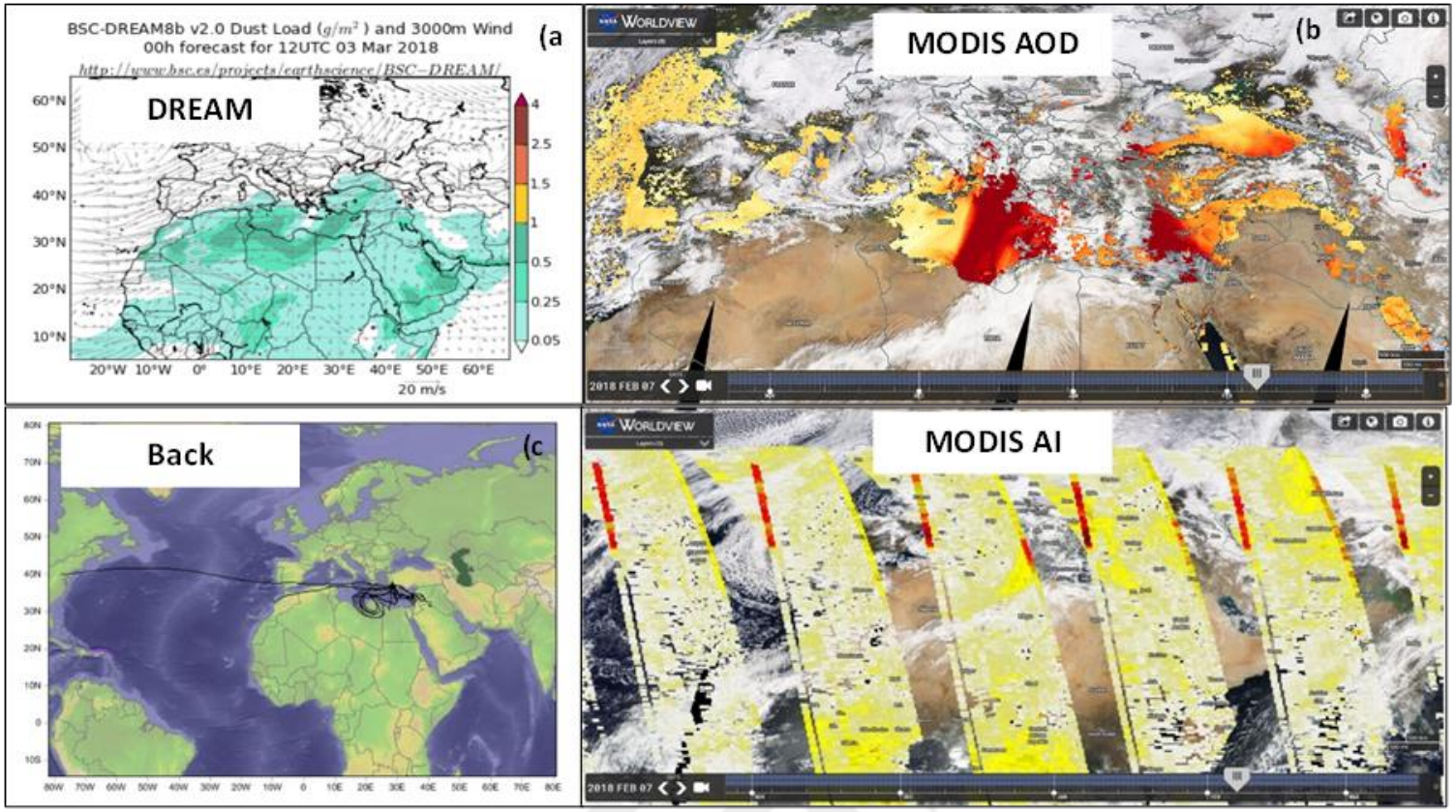

Figure B3. Dream model output, (b) Aerosol optical depth (AOD), (c) Back-trajectories, and (d) Aerosol index image for a dust episode at the rural (Marmaris) station (March 3, 2018)

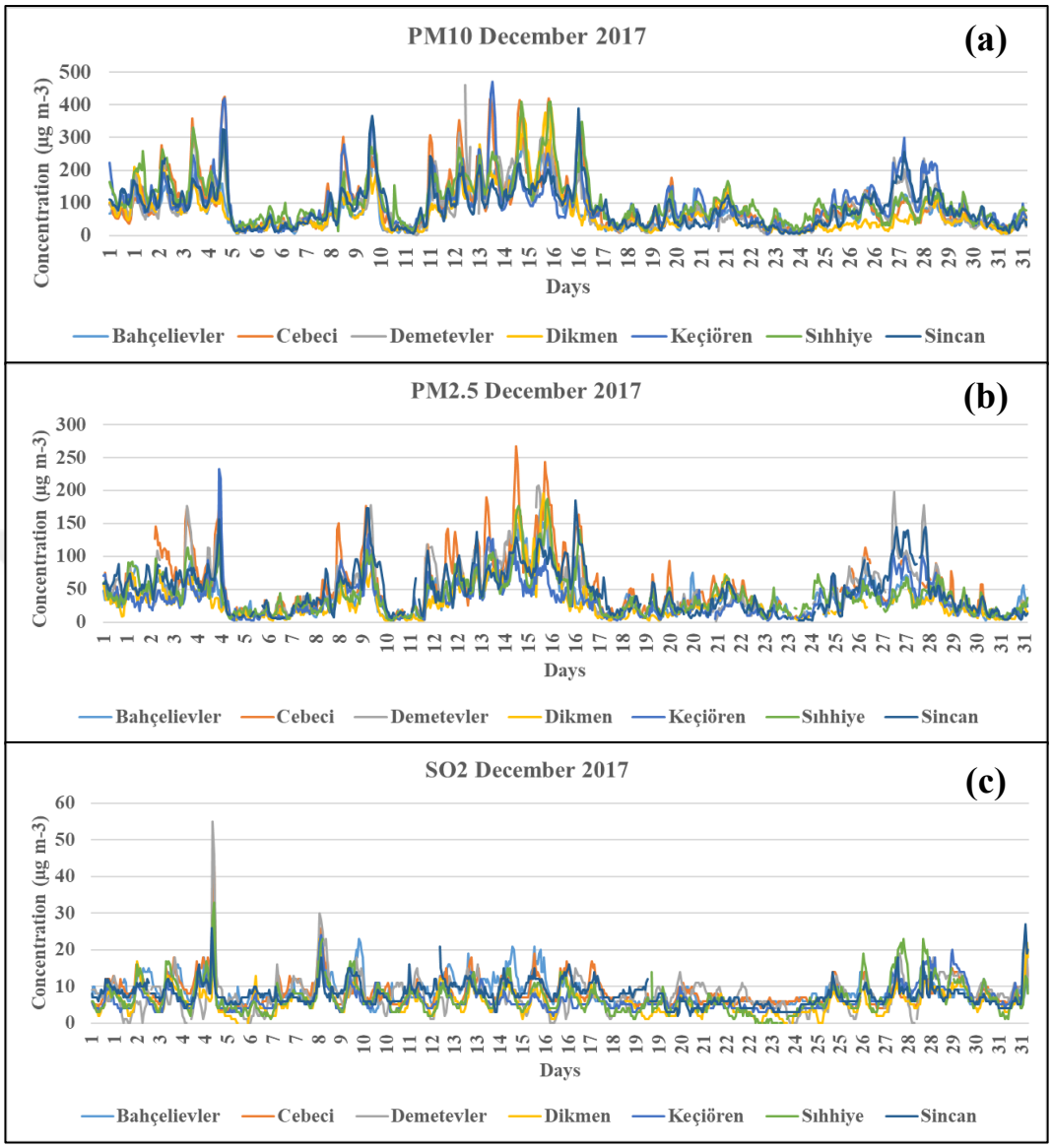

Figure B4. (a) PM_{10}, (b) $PM_{2.5}$, and (c) SO_2 data from seven regulatory monitoring stations at Ankara in December 2017

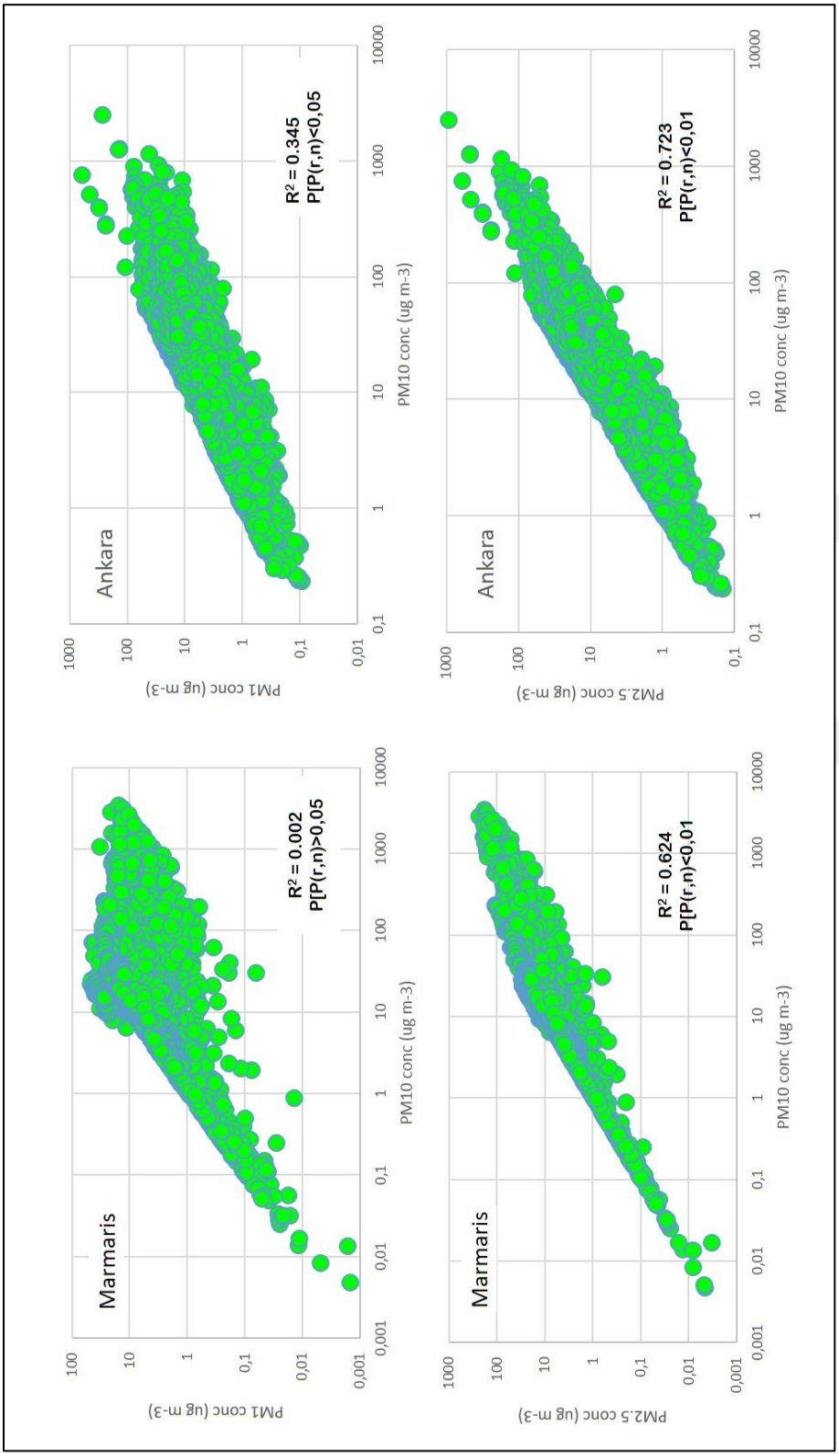

Figure B5. Scatterplots between PM_{10} and PM_1, PM_{10} and $PM_{2.5}$ concentrations in Ankara and Marmaris stations.

Table B1. Comparison of the dust contribution to PM_{10} concentrations with the literature

	Contribution of dust events to PM_{10} concentration
This study (Marmaris)	32%
This study (Ankara)	12%
Balcılar (2018)	62%
Liora et al. (2016)	20%
Öztürk et al. (2012)	19%
Genç Tokgöz (2013)	41%

C. Chemical Composition of Fine And Coarse Particles at An High-Altitude Station In Eastern Mediterranean: Assessment Aerosol Components and Their Source Regions.



Figure C1. Location of the sampling station

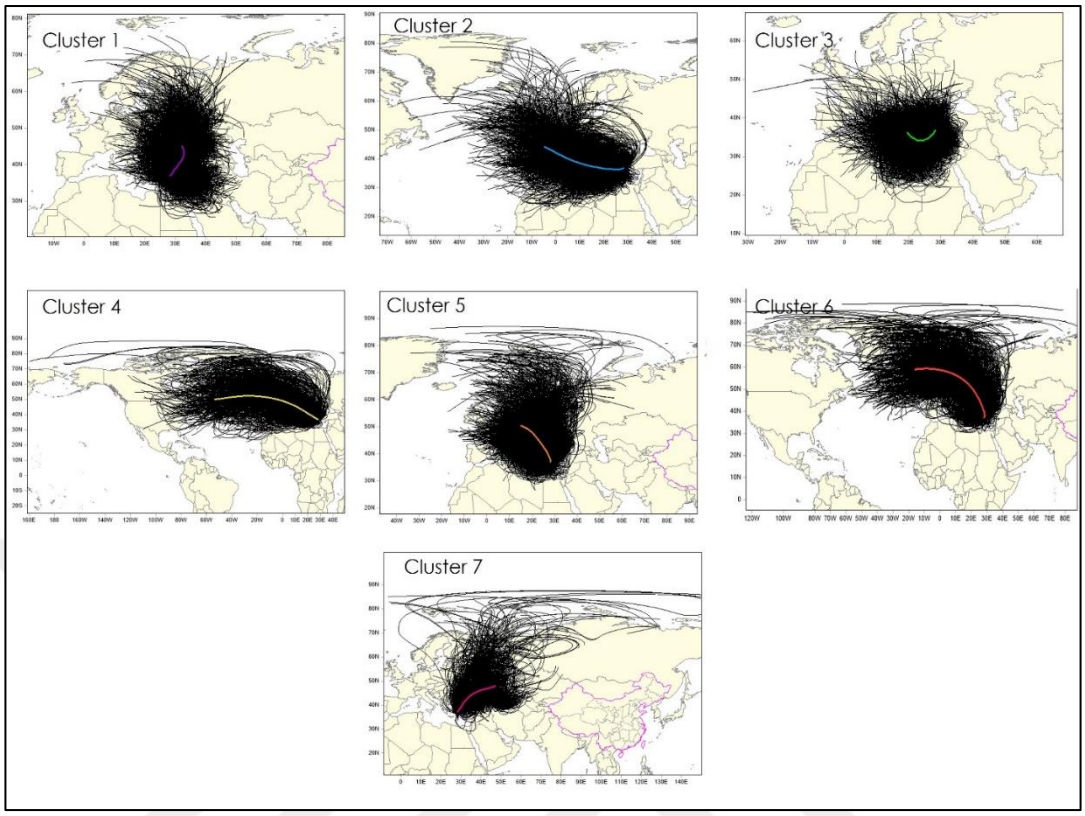

Figure C2. Trajectories in each cluster

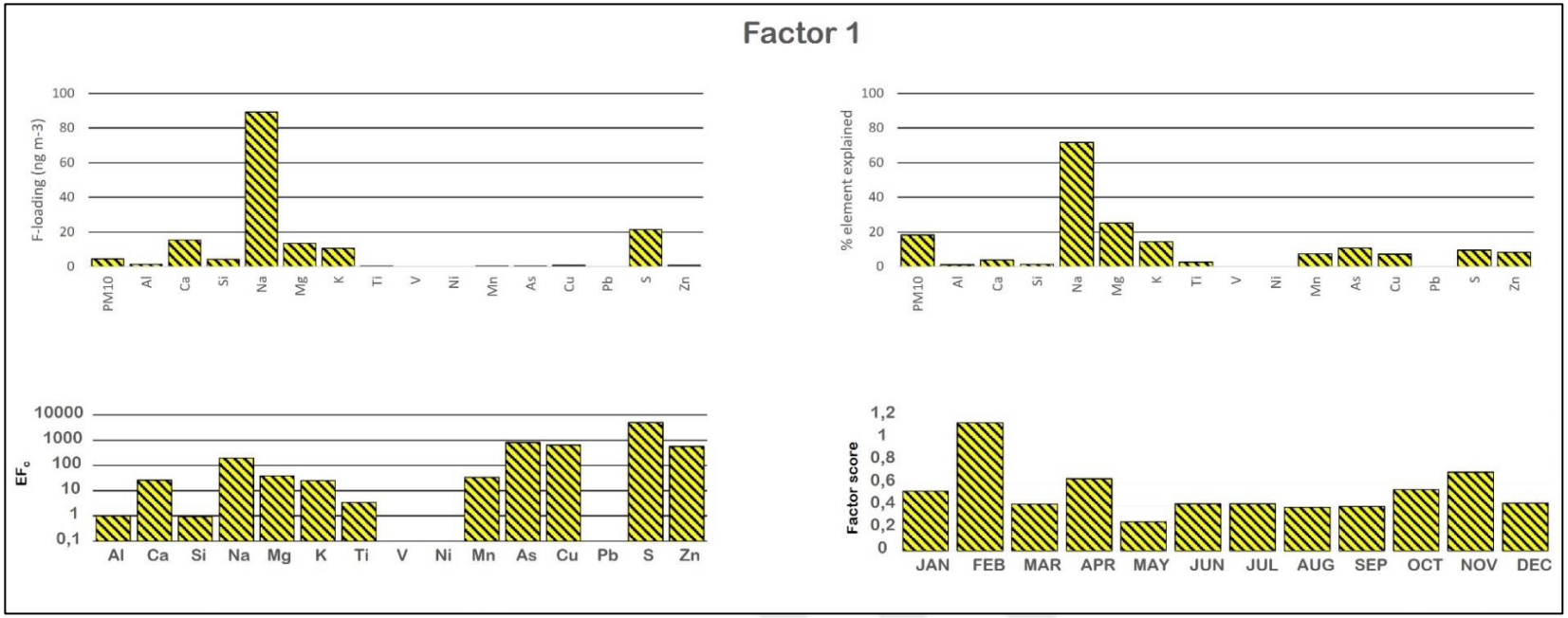

Figure C3. Factor composition, fractions of elements explained by each factor, crustal enrichment factors of elements in factor and monthly average factor scores for Factor 1

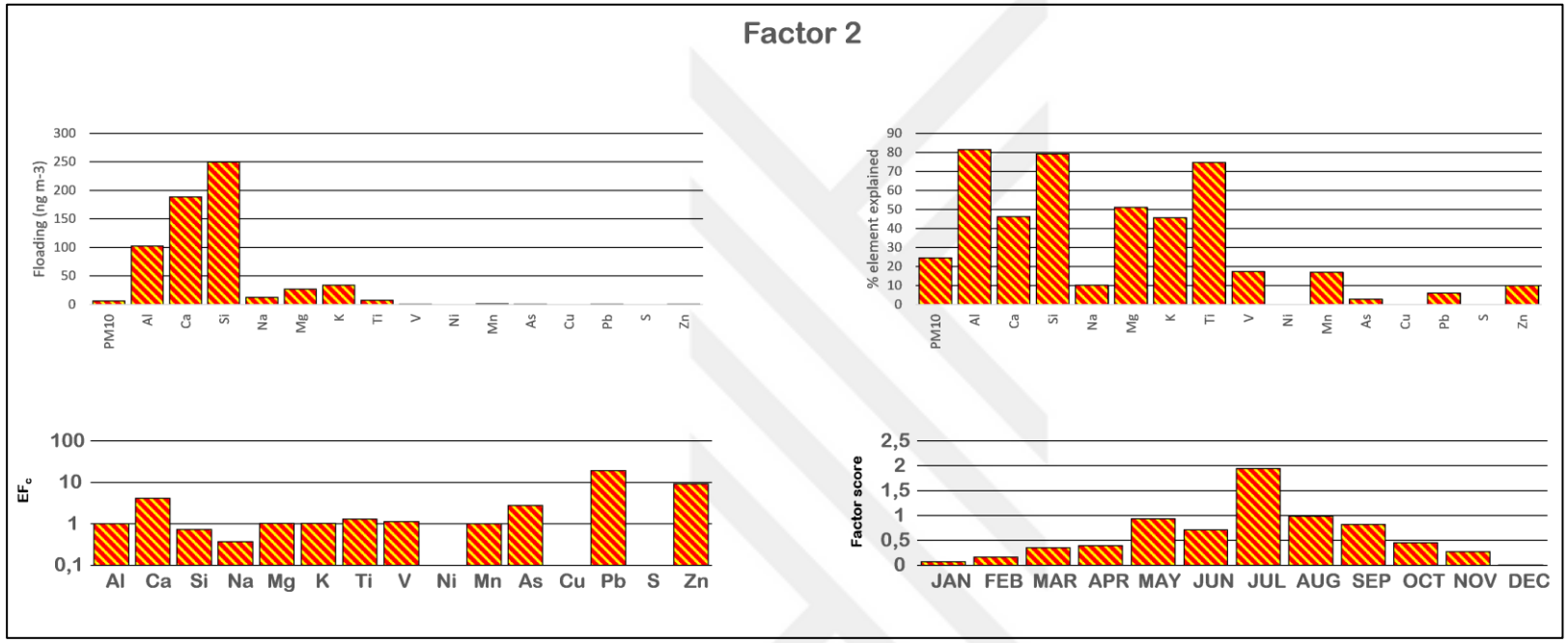

Figure C4. Factor composition, fractions of elements explained by each factor, crustal enrichment factors of elements in factor and monthly average factor scores for Factor 2

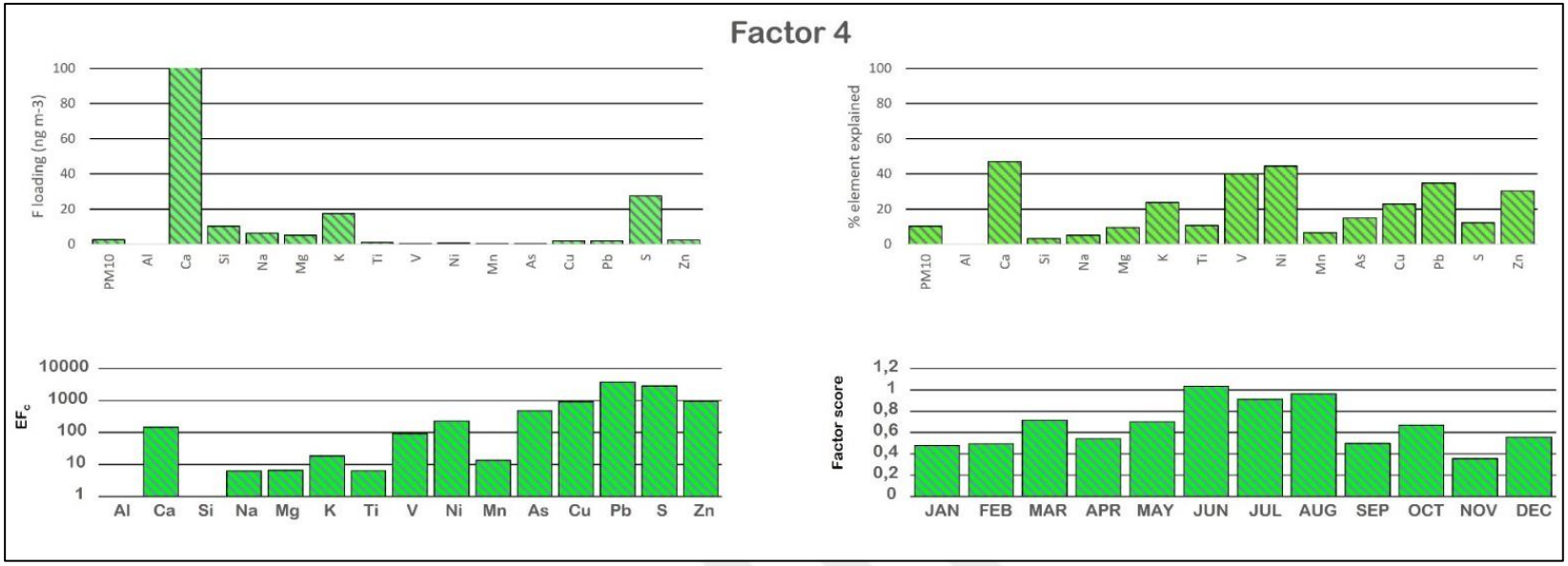

Figure C5. Factor composition, fractions of elements explained by each factor, crustal enrichment factors of elements in factor and monthly average factor scores for Factor 4

D. Summary Statistics of the Measured Data

Table D1. Summary statistics of PM (μg m^{-3}) and trace element (ng m^{-3}) concentrations for the sampling period

Marmaris					
	Avg ± STD	**Median**	**Max**	**Min**	**N**
PM_{10}	37 ± 136	17	3410	0.005	12232
$PM_{2.5}$	14 ± 13	12	237	0.003	12232
PM_1	10 ± 6	9	48	0.002	12230
	Coarse	**Fine**	**PM_{10}**	**N**	
	X ± σ (median)	**X ± σ (median)**	**X ± σ (median)**		
Mass	14000 ± 21000 (8500)	11000 ± 29000 (5800)	25000 ± 41000 (15000)	320	
Al	93 ± 123 (50)	35 ± 95 (8,0)	129 ± 176 (71)	304	
As	0,17 ± 0,19 (0,11)	0,17 ± 0,13 (0,13)	0,34 ± 0,24(0,29)	63	
Ca	344 ± 401 (220)	95 ± 223 (30)	440 ± 478 (332)	276	
Cu	5,5 ± 6,0 (4,4)	5,5 ± 4,4 (4,0)	11 ± 7,8 (10)	183	
K	56 ± 64 (34)	27 ± 48 (13)	83 ± 85 (56)	276	
Mg	44 ± 57 (27)	14 ± 31 (3,8)	58 ± 69 (41)	290	
Mn	6,2 ± 8,6 (2,0)	7,4 ± 9,3 (2,0)	14 ± 14 (4,2)	77	
Na	102 ± 132 (59)	31 ± 70 (8,5)	132 ± 156 (89)	282	
Ni	1,8 ± 2,1 (0,6)	2,1 ± 2,3 (0,8)	3,9 ± 3,6 (3,1)	120	
Pb	4,4 ± 3,1 (3,9)	6,5 ± 9,6 (3,7)	10,9 ± 11,2 (9,0)	26	
S	53 ± 54 (34)	178 ± 297 (78)	231 ± 309 (130)	275	
Si	297 ± 361 (177)	110 ± 260 (29)	405 ± 489 (256)	224	
Ti	9,0 ± 11,4 (5,2)	3,7 ± 8,0 (1,5)	13 ± 16 (8,2)	203	
V	1,0 ± 0,77 (0,90)	1,1 ± 0,9 (1,0)	2,1 ± 1,2 (2,1)	95	
Zn	6,2 ± 5,9 (7,9)	5,9 ± 5,3 (7,8)	12 ± 8,1 (11)	277	

Ankara					
	Avg ± STD	**Median**	**Max**	**Min**	**N**
PM_{10}	53 ± 66	38	2460	0.23	11248
$PM_{2.5}$	18 ± 18	16	948	0.14	11248
PM_1	12 ± 13	10	611	0.1	11248
PM_{10} Al	792 ± 903	454	6642	10	255
$PM_{2.5}$ Al	340 ± 494	172	4996	3.04	258
PM_1 Al	88.6 ± 151	36	1188	0.51	258
PM_{10} Si	2137 ± 2298	1304	15886	28.1	255
$PM_{2.5}$ Si	852 ± 1168	453	11642	8.1	258
PM_1 Si	223 ± 365	94	2712	0.9	254

CURRICULUM VITAE

Surname, Name: Uzunpınar, Elif Sena

EDUCATION

Degree	Institution	Year of Graduation
MS	METU Environmental Engineering	2015
BS	METU Environmental Engineering	2012
High School	Çağrıbey Anadolu High School, Ankara	2007

FOREIGN LANGUAGES

Advanced English, Basic Spanish

PUBLICATIONS

Accepted for Publication – Uzunpınar, E.S., Imamoglu, I., Rahmani, A., Tuncel, G., (2022)

"Factors Affecting Particle Number Size Distributions at an Urban and a High-altitude Rural Site at the Anatolian Plateau" *Atmospheric Pollution Research.*

Under Review – Uzunpınar, E.S., Balcilar, I., Imamoglu, I., Zararsız, A., Kalayci, Y., Tuncel, G., (2022)

"Chemical Composition of Fine and Coarse Particles at a High-Altitude Station in Eastern Mediterranean: Assessment Aerosol Component and Their Source Regions" *Atmospheric Environment.*

Conference Proceeding — Uzunpınar E. S., Dündar C., İmamoğlu İ., Tuncel G.

"Modification of Particle Number Size Distribution in Saharan Dust Events as They Travel Over the Anatolian Plateau", *18th World Clean Air Congress (WCAC'19) İstanbul/Turkey (2019)*

Journal Article — Uzunpınar E. S., Sert, E., Kılavuz S., İmamoğlu İ., Tuncel G. (2018)

"Source Identification of VOCs in METU Campus Through Factor Analysis" *Global NEST Journal, 20(1), 109-114.*

Conference Proceeding — Uzunpınar E. S., Sert, E., Kılavuz S., İmamoğlu İ., Tuncel G. "Diurnal Variation of Volatile Organic Compound Concentrations in Suburban Ankara Atmosphere", 8th International Atmospheric Sciences Symposium İstanbul/Turkey (2017) Conference Proceeding — Sert, E., Uzunpınar E. S., Kılavuz S., İmamoğlu İ., Tuncel G. "Ankara'da Kırsal ve Kentsel Alanda Uçucu Organik Bileşik Konsantrasyonlarının Belirlenmesi ve Karşılaştırılması", *12th National Chamber of Environmental Engineers Congress Ankara/Turkey (2017)*

Conference Proceeding — Uzunpınar E. S., Sert E., Kılavuz S., İmamoğlu İ., Tuncel G. "Source Identification of VOCs in METU Campus through Factor Analysis", *1st International Black Sea Congress on Environmental Sciences (IBCESS) Giresun / Turkey (2016)*

National Refereed Journal — Uzunpınar E. S., Kılavuz S., İmamoğlu İ., Sert E., Tuncel G. "Source Apportionment of Volatile Organic Compounds in Ankara Atmosphere" (In Turkish), *Çevre Bilim ve Teknoloji, 1(2), 89 – 105, (2016)*

Conference Proceeding — Uzunpınar E. S., Kılavuz S., İmamoğlu İ., Sert E., Tuncel G. "Source Apportionment of Volatile Organic Compounds in Ankara Atmosphere", *11th National Chamber of Environmental Engineers Congress Bursa/Turkey (2015)*